The role of Hedgehog signalling in the homeostasis and differentiation of gammadelta and alphabeta T cells.

by

Konstantinos Mengrelis

A thesis submitted to University College London for the Degree of Doctor of Philosophy

February 2016

Institute of Child Health
Infection, Immunity, Inflammation and Physiological Medicine
University College London

This is a declaration that the worked presented on this thesis is mine unless otherwise clearly stated

Konstantinos Mengrelis

The author declares that the research was conducted in the absence of any commercial or financial relationships that could be construed as a potential conflict of interest.

Abstract

The Hedgehog (Hh) signalling pathway is an important mediator of many mammalian developmental processes and mutations in Hh genes cause serious developmental disorders and birth defects in both mice and humans. The role of Hh signalling in the development of αβTCR$^+$ cells has been, and continues to be, explored by our and other laboratories. However, the impact of Hh signalling on unconventional T cells is not well characterised.

Here, we aim to investigate the effect of Hh signalling on thymic and peripheral γδ T cells, both in mice and humans. Our study reveals that key components of the Hh pathway are present in the murine thymus and spleen and that γδ T cells are responsive to Hh signalling. Furthermore, flow cytometry of mutant mice revealed that Sonic (Shh) and Desert (Dhh) hedgehog affect γδ T cell biology in distinct ways. Our research detected numerous changes in cell numbers, key cytokine production, subtype differentiation, peripheral localization in both fetal and adult tissues and in a LPS-induced disease model. In humans, we expanded γδ thymocytes and assessed their responsiveness to Hh signalling.

Furthermore, we investigated the role of Indian hedgehog (Ihh) in the transition from CD4$^-$CD8$^-$ double negative (DN) to CD4$^+$CD8$^+$ double positive (DP) stage during αβ T cell development. Analysis of mice with conditional deletion of Indian hedgehog showed that Ihh negatively regulates DN to DP transition of αβTCR$^+$ cells. Crossing of this conditional knockout (KO) to the male-specific antigen HY indicated that this effect is related to TCR rearrangement and signalling and thymic selection. Analysis of fetal and adult thymi also demonstrated that Ihh plays a role in DP to single positive (SP) transition too. Analysis of hydrocortisone (HC)-treated heterozygous Ihh and RagKO conditional Ihh mice further elucidated the role of Ihh in αβ T cell development.

Oh sancta simplicitas! In what strange simplification and falsification man lives! One can never cease wondering once one has acquired eyes for this marvel! How we have made everything around us clear and free and easy and simple! How we have been able to give our senses a passport to everything superficial, our thoughts a divine desire for wanton leaps and wrong inferences! How from the beginning we have contrived to retain our ignorance in order to enjoy an almost inconceivable freedom, lack of scruple and caution, heartiness, and gaiety of life, in order to enjoy life! And only on this now solid, granite foundation of ignorance could knowledge rise so far, the will to knowledge on the foundation of a far more powerful will, the will to no knowledge, to uncertainty, to the untruth! Not as its opposite, but rather—as its refinement! Even if *language*, here as elsewhere, will not get over its awkwardness, and will continue to talk of opposites where there are only degrees and many subtleties of gradation; even if the inveterate Tartuffery of morals, which now belongs to our unconquerable "flesh and blood," infects the words even of those of us who know better: here and there we understand it and laugh at the way in which precisely science at its best seeks most to keep us in this *simplified*, thoroughly artificial, suitably constructed and suitably falsified world, at the way in which, willy-nilly, it loves error, because, being alive—it loves life![1]

[1] Friedrich Nietzsche, *Beyond Good and Evil: The free spirit*. 1886. 25-26

Acknowledgments

It is impossible to express my gratitude to my primary supervisor, Tessa, for all her support over the last three and a half years for I would need the writing skills of a Pushkin or a Wilde. I will restraint myself to a humble Thank You. I sincerely wish myself the exceptional luck to meet a few more people like you in my life.

Kenth's contribution has been important both in terms of advice with the human γδ stuff but also due to all the breaks we took from chatting γδ antigen presentation and δ/αβ T cell-mediated antigen recognition to delve into conversations about the future of Europe, the immigration crisis (that coincided with this write up) and what it means to be young and feel responsible in a neoliberal world.

Of course, I would like to express my gratitude to all the beautiful creatures in the lab with whom we spent around a thousand days together; Amal, Sonia, Hemant, Anisha, Rain, Eleutheria, Diana, Anna, Jose, Alessandro, Sue, made the ICH a great place to work and live in. They are all bright with endless prospects and I feel blessed that I was given the chance to work alongside them.

I would like to thank Chris and Anastasia for the provision of E.coli, LP broth, coffee, bananas, a couch to crash on at midnight, bike parts and good times. Daniel allowed me to use his UV chamber and introduced me to Chopin concertos. I am obliged to my old friend Sofoklis for spending two days of his holidays designing the figures for the introduction of this thesis. Ayad and Stephanie have helped me with their cool attitude and expertise on the LSRII and cell sorting - it's a miracle that the LSRII still

functions after so many blockages! I would also like to thank Mona for providing plenty of LPS.

Finally, I would like to thank my London-based friends for their stimulating company and my family in Athens for all the unconditional love from day zero and for respecting my choice to be absent in these turbulent times.

Table of Contents

Abstract **4**

Acknowledgments **6**

Table of Figures **12**

Abbreviations **17**

Introduction **20**

1.1 Murine T cell biology **21**

1.1.1 The thymus 21

1.1.2 $\alpha\ \beta$ T cell development 21

1.1.3 TCR Rearrangement 23

1.1.4 Positive and negative Selection 24

1.1.5 $\alpha\ \beta$ T cell activation 26

1.1.6 $\gamma\ \delta$ T cell lineage commitment 31

1.1.7 Murine $\gamma\ \delta$ thymic subtypes and effector fate 36

1.2 Human $\gamma\ \delta$ T cell subtypes and effector fate **41**

1.3 The Hedgehog (Hh) signalling pathway **46**

1.3.1 The Hedgehog proteins 46

1.3.2 Hh signalling 46

1.3.3 The regulation of Hh activity 49

1.3.4 The role of Shh in T cell development 52

1.3.5 The role of Ihh in T cell development 53

1.3.6 The role of Dhh in T cell development 54

Material and methods **55**

2.1 Mice **56**

2.2 Antibodies and Flow Cytometry **56**

2.2.1 Cell surface staining 56

2.2.2 Annexin-V apoptosis staining assay 57

2.2.3 Propidium iodide (PI) staining 58

2.2.4 Intracellular stain (ic) for cytokines 58

2.2.4.1 Activation Assay 58

2.2.4.2 Intracellular stain 58
2.2.5 Cell Sorting 58
2.3 Fetal Thymic Organ Cultures (FTOCs) 59
2.4 Skin digestion 59
2.5 RNA extraction and cDNA synthesis 59
2.6 Quantitative Reverse Transcribed-Polymerase Chain Reaction (QRT-PCR) 60
2.7 DNA extraction and genotyping of mutant mice by PCR 60
2.8 Lipopolysaccharide (LPS) injection 63
2.9 Hydrocortisone (HC) injection 64
2.10 Human γ δ analysis 64
2.10.1 Human γ δ selection 64
2.10.2 Human γ δ expansion culture 65
2.10.3 Irradiation 65
2.10.4 Human γ δ recombinant hedgehog (rHh) cultures 65
2.11 Cell Counts 66
2.12 Experimental Data Analysis 66
Results 67
3. Murine and human γ δ cells can transduce Hh signals 68
3.1. Introduction 68
3.2 Results 70
3.2.1 Hh signalling components are expressed in thymic γ δ T cells 70
3.2.2 Hh signalling components are expressed in splenic γ δ T cells 71
3.2.3 Hh-reporter mice show active Hh-mediated transcription in γ δ T cell populations in vivo 71
4. The function of the Hh family proteins in γ δ T cell development in the thymus 77
4.1 Introduction 77
4.2 Results 77
4.2.1 The role of Shh in γ δ T cell development in the thymus 77
4.2.2 Adult γ δ T cell populations in the $Shh^{+/-}$ thymus 78
4.2.3 $Shh^{+/-}$ γ δ thymocytes show reduced Hh-mediated transcription in vivo 78
4.2.4 Conditional deletion of Shh from TEC 79
4.2.5 Shh-treatment of WT FTOC 79
4.2.6 Ihh signalling in γ δ T cell development in the thymus 80
4.2.7 The role of Dhh in γ δ T cell development 81

4.2.8 The adult Dhh-deficient thymus 81
4.2.9 γ δ thymocytes in the fetal Dhh-deficient thymus 81
4.2.10 Treatment of WT FTOC with rDhh and rHHip 82
4.2.11 The effect of Shh and Dhh double deficiency on γ δ T cells 82
4.3 Discussion 91
5. Modulation of Hh signalling during γ δ T cell development in the thymus ..92
5.1 Introduction 92
5.2 Results 92
5.2.1 The role of Gli3 in γ δ T cell development in the thymus 92
5.2.2 The role of Kif7 in γ δ thymocyte development 93
5.2.3 The adult Kif7$^{+/-}$ thymus 94
5.2.4 The fetal Kif7-mutant thymus 94
5.2.5 Inhibition of Hh-mediated transcription in γ δ thymocytes 94
5.2.6 Constitutive activation of Hh-mediated transcription in γ δ thymocytes 95
5.3 Discussion 102
6. Modulation of Hh signalling influences the homeostasis of γ δ T cell populations in the periphery 103
6.1 Introduction 103
6.2 Results 103
6.2.1 The influence of the Gli2N2 transgene on peripheral γ δ T cell biology 103
6.2.2 Inhibition of physiological Hh-mediated transcription in peripheral γ δ T cells 104
6.2.3 Dhh signalling in peripheral γ δ T cells 105
6.2.4 Peripheral γ δ T cell populations in Shh$^{+/-}$ mice 107
6.2.5 Peripheral γ δ T cell populations in ShhkoCO mice 108
6.2.6 Peripheral γ δ T cell populations in ShhcoKODhhKO double knockout mice 108
6.2.7: Peripheral γ δ T cells in Kif7$^{+/-}$ mice 109
6.2.8: Impact of Gli3-heterozygosity on peripheral γ δ T cells 110
7. The effect of Hedgehog signalling on γ δ T cells in an LPS mouse model.... 135
7.1 Introduction 135
7.2 Results 136
7.2.1 The effect of Gli2N2 on γ δ cells from LPS-injected young adult mice 136
7.2.2 The effect of Shh on γ δ cells from LPS-infected young adult mice 144
8. The role of Hh signalling in human γ δ T cells 149
8.1 Introduction 149
8.2 Results 150
8.2.1 γ δ expansion cultures from human thymocytes 150

8.2.2 The effect of Hh signalling on cell surface markers....150
8.2.3 The effect of Hh signalling on proliferation of human γ δ T cells....151
8.2.4 Expression analysis of key Hh components....151
8.3. Discussion....157
9. The Investigation of an Ihh-mediated feedback loop that controls thymus size....160
9.1 Introduction....160
9.2 Results....162
9.2.1 Conditional deletion of Ihh from thymocytes....162
9.2.2 Introduction of a transgenic TCR....163
9.2.3 The impact of Ihh deficiency on thymocyte differentiation in the fetal thymus....164
9.2.4 Recovery of DP and SP populations following Hydrocortisone (HC) treatment in Ihh deficient thymus....165
9.2.5 Reconstitution of DP and SP populations following anti-CD3 treatment in Ihh deficient $Rag^{-/-}$ thymus....166
9.3 Discussion....186
9.3.1 Transition from DN to DP stage of development....186
9.3.2 Transition from DP to SP stage of development....188
9.3.3 Effect of Ihh in periphery....189
Discussion....190
10.1 Murine γ δ T cells....191
10.1.1 Effect of Hh signalling on γ δ cell numbers....191
10.1.2 The effect of Hh signalling on the $CD27^{+}CD44^{+}$ γ δ subset....192
10.1.3 The effect of Hh signalling on the $CD44^{+}$ $CD27^{-}$ γ δ subset....195
10.1.4 The effect of Hh signalling on splenic γ δ T cells....196
10.1.5 The effect of Hh signalling on cytokine production of splenic γ δ cells....196
10.1.6 The effect of Hh signalling on CD24 expression of γ δ cells....196
10.1.7 The effect of Hh signalling on γ δ cells residing the murine lymph nodes....198
10.2 The effect of Hh signalling on γ δ cells upon LPS infection....198
Summary....200
Future directions....204
Publications arising from this work....206
REFERENCES....207

Table of Figures

Figure 1.1: α β T cell development in murine thymus 30
Figure 1.2: Murine γ δ T CR ontogeny 35
Figure 1.3: Mouse γ δ T cell subsets in the thymus and periphery 40
Figure 1.4: Human V δ 2 T cells 45
Figure 1.5 The mammalian Hedgehog signaling pathway 51
Figure 3.1: Expression of key Hh components in γ δ T cells of murine WT thymus 73
Figure 3.2: Expression of key Hh components and γ δ -specific markers in γ δ T cells of murine WT thymus 74
Figure 3.3: Expression analysis of Hh signaling components in the murine spleen 75
Figure 3.4: Gli Binding Site (GBS) GFP expression in the thymus and the spleen of 3 week old mice 76
Figure 4.1: Development of γ δ T cell subtypes in the adult $Shh^{+/-}$ thymus 83
Figure 4.2: Percentages of γ δ T cells in Shhfl/fl FoxN1-Cre thymus, spleen and lymph nodes 84
Figure 4.3: Numbers of γ δ T cells and surface expression of key markers in E14.5 fetal thymus organ cultures (FTOC) 85
Figure 4.4: Numbers of γ δ T cells and surface expression of key markers in E16.5 FTOC 86
Figure 4.5: The role of Ihh in thymic γ δ T cells 87
Figure 4.6: The effect of Dhh in γ δ T thymocytes 88
Figure 4.7: The effect of Dhh in E17.5 γ δ T cell development in the thymus and the spleen 89
Figure 4.8: The effect of double KO ($Dhh^{-/-}$-Shhfl/fl $FoxN1Cre^{+}$) on γ δ thymocytes 90
Figure 5.1: The effect of $Gli3^{+/-}$ on the expression of CD24 in γ δ T cells 96
Figure 5.2: The effect of $Kif7^{+/-}$ on γ δ T cells from the thymus 97

Figure 5.3 The effect of Kif7 on γ δ T cells from the thymus of E17.5 littermates 98
Figure 5.4: The effect of Gli2C2 on the γ δ T cell expression of CD4, CD24, CD27, CD44 and CD122 99
Figure 5.5: The effect of Gli2N2 on CD27 and CD44 expression on γ δ TCR+ thymocytes 100
Figure 5.6: The effect of Gli2N2 on CD24 and CD122 expression on γ δ TCR+ cells from thymus, spleen and lymph nodes 101
Figure 6.1: The effect of Gli2N2 on γ δ T cell splenocytes 113
Figure 6.2: The effect of Gli2N2 on CD4 and CD122 expression of γ δ T cell splenocytes 114
Figure 6.3: The effect of Gli2N2 on γ δ T lymphocytes 115
Figure 6.4: The effect of Gli2N2 on CD24 and CD122 expression of γ δ T cell lymphocytes 116
Figure 6.5: The effect of Gli2C2 on γ δ T lymphocytes 117
Figure 6.6: The role of Dhh in γ δ T cells from the LN 118
Figure 6.7: The role of Dhh in γ δ T splenocytes 120
Figure 6.8: The effect of Dhh on γ δ T cell production of IFN γ and IL-17 in the lymph nodes and the spleen of 4 week old mice 121
Figure 6.9: Reconstitution of γ δ T cell populations in the spleen of 3 week old mice, 14 days after irradiation in WT and Dhh-/- littermates 122
Figure 6.10: γ δ T cell subtypes in adult lymph nodes of Shh+/- and WT mice 123
Figure 6.11: Development of γ δ T cell subtypes in the adult spleen Shh+/- and WT mice 124
Figure 6.12: Expression of GBS-GFP in Shh+/- and WT spleen on major γ δ T cell populations according to CD27 and CD44 cell surface expression 125
Figure 6.13: The effect of Shh in the production of key cytokines IFN γ and IL-17 in γ δ T cells 126
Figure 6.14: The effect of conditional deletion of Shh on peripheral γ δ T cells 127

Figure 6.15: The effect of double Shh and Dhh KO on γ δ splenocytes 128
Figure 6.16: The effect of double Shh and Dhh KO on LN γ δ 129
Figure 6.17: Development of γ δ T cell subtypes in the adult Kif7$^{+/-}$ spleen....130
Figure 6.18: The influence of Gli3 on peripheral γ δ populations of young adult mice.....131
Figure 6.19: The effect of Gli3 on γ δ populations in the peritoneal cavity and the lungs of young adult mice.....132
Figure 6.20: Hedgehog reporter transgenic (GBS-GFP-Tg) show reduced Hh pathway activation in γ δ cells from Gli3$^{+/-}$ mice. 133
Figure 6.21: The role of Gli3 in the production of key γ δ T cell cytokines.....134
Figure 7.1: The effect of transgenic expression of Gli2N2 in LPS-treated γ δ thymocytes.....138
Figure 7.2: The effect of transgenic expression of Gli2N2 on LPS-injected γ δ subsets.....139
Figure 7.3: The effect of transgenic expression of Gli2 on LPS-treated γ δ splenocytes 140
Figure 7.4: The effect of transgenic expression of Gli2 on LPS-treated γ δ cells in lymph nodes 141
Figure 7.5: The effect of transgenic expression of Gli2 on LPS-treated γ δ T cells from the blood and the skin of young mice. 142
Figure 7.6: The effect of transgenic expression of Gli2 on LPS-treated γ δ thymocytes.....143
Figure 7.7: Activation of murine γ δ T cells with LPS causes important changes in the percentage, cell count and surface expression of key γ δ markers in the thymus of Shh FoxN1 KO mice after 4 days of LPS treatment.....145
Figure 7.8: The effect of Shh FoxN1 coKO on subtype populations of γ δ thymocytes after 4 days of LPS treatment.....146
Figure 7.9: The effect of Shh FoxN1 KO on several subsets of γ δ T cells in the spleen and lymph nodes after 4 days of LPS treatment. 147
Figure 7.10: The effect of conditional Shh KO on IL-17 secretion on LPS-treated spleens. 148

Figure 8.1: Positive selection of $\gamma\ \delta$ TCR$^+$ cells prior to expansion culture 152
Figure 8.2: Hh signalling and the effector fate of expanded human $\gamma\ \delta$ thymocytes.....153
Figure 8.3: Hh signalling and the effector fate of expanded human $\gamma\ \delta$ thymocytes.....154
Figure 8.4: The effect of Hh signalling on the cell cycle and apoptosis of human expanded $\gamma\ \delta$ thymocytes 155
Figure 8.5: The effect of Hh signalling on the transcription of several components of the Hh pathway as assessed by mRNA expression analysis from expanded human $\gamma\ \delta$ cells, treated with rHhip or rShh over the course of 6 days.....156
Figure 9.1: The effect of conditional Ihh deletion (CD4Cre$^+$) on thymocytes of young adult mice 167
Figure 9.2: The effect of conditional Ihh deletion (CD4-Cre+) on DN thymocytes of young adult mice 168
Figure 9.3: The effect of conditional Ihh deletion (CD4-Cre+) on T splenocytes of young adult mice 169
Figure 9.4: The effect of conditional Ihh deletion (CD4-Cre+) on T cells from the lymph nodes of young adult mice 170
Figure 9.5: The effect of conditional Ihh deletion on intracellular TCR β expression in DN cells.....171
Figure 9.6: The effect of conditional Ihh deletion on thymocytes of young adult male mice crossed with the male-specific HY TCR.....172
Figure 9.7: The effect of conditional Ihh deletion on thymic T3.70 expression in young adult male mice crossed with the male-specific HY TCR.....173
Figure 9.8: The effect of conditional Ihh deletion on T cells from the spleen and lymph nodes of young adult male mice crossed with the male-specific HY TCR.....174
Figure 9.9: The effect of conditional Ihh deletion on thymocytes of young adult female mice crossed with the male-specific HY TCR.....175
Figure 9.10: The effect of conditional Ihh deletion on T cells from the spleen of young adult female mice crossed with the male-specific antigen HY.....176

Figure 9.11: The effect of Ihh on E16.5 FTOC + 6 days in culture.....177
Figure 9.12: The effect of conditional Ihh deletion on HY^+ E18.5 thymocytes in male mice.....178
Figure 9.13: The effect of conditional Ihh deletion on HY^+ E18.5 thymocytes in male mice.....179
Figure 9.14: The effect of conditional Ihh HY^+ on E18.5 thymocytes in male mice 180
Figure 9.15: Thymocyte recovery of DP and SP populations 4 days after HC injection on $Ihh^{+/-}$ 4 weeks old mice.....181
Figure 9.16: Thymocyte recovery of DN populations 4 days after HC injection on Ihh+/- 4 weeks old mice.....182
Figure 9.17: Thymocyte recovery 6 days after HC injection on $Ihh^{+/-}$ 4 weeks old mice.....183
Figure 9.18: Thymocyte recovery in HC-injected $Ihh^{+/-}$ and conditional Ihh KO mice.....184
Figure 9.19: Thymocyte populations 7 days after α-CD3 stimulation on $Rag^{-/-}$ conditional Ihh KO FTOCs.....185
Figure 10.1: The effect of Hh signalling on murine γ δ T cell biology.....203

Abbreviations

-/-	Knockout
+/-	Heterozygote
+/+	Wild type
Ag	Antigen
Aire	Autoimmune regulator
APC	Antigen presenting cell
au	Arbitary unit
BCC	Basal cell carcinoma
BMP	Bone morphogenetic protein
bp	Base pair
BSA	Bovine serum albumin
c-Myc	Avian myelocytomatosis virus oncogene cellular homolog
CCR	Chemokine receptor
CD	Cluster of differentiation
cDNA	Complementary DNA
CKI	Casein Kinase I
CM	Central memory
CO_2	Carbon dioxide
coKO	Conditional knockout
Cos2	Costal 2
CTLA	Cytotoxic T-lymphocyte associated protein 4
CXCR	CXC chemokine receptor
Dhh	Desert hedgehog
DN	Double negative
DNA	Deoxyribonucleic acid
dNTPs	Deoxynucleotide triphosphate
DP	Double positive
E	Embryonic day
EDTA	Ethylenediaminetetraacetic acid
EGR	Early growth repsonse
EM	Effector memory
ER	Endoplasmic reticulum
ERK	Extracellular signal related kinsae
ETP	Early thymic progenitors
FACS	Fluorescence activated cell sorter
FCS	Fetal calf serum
FITC	Fluorescein isothiocyanate
fl	Floxed

FoxN1	Forkhead box N1
FoxP3	Forkhead box P3
FSC	Forward scanner
FTOC	Fetal thymic organ culture
Fu	Fused
Gata	Gata binding protein 3
GBS	Gli binding site
GFP	Green fluorescent protein
Gli	Glioma associated oncogene
GSK3	Glycogen synthase kinase 3
Gy	Gray unit
HBB-PP	E-4-hydroxy-3-methyl-but-2-enylpyrophosphate
HC	Hydrocortisone
Hh	Hedgehog
Hhip	Hedgehog-interacting protein
HMG	High motility gene
HPRT	Hypoxanthiine guanine phosphoribosyl transferase
HSA	Heat-stable antigen
ic	Intracellular
IEL	Intestinal intraepithilial lymphocytes
IFNγ	interferon gamma
Ihh	Indian Hedgehog
IL	Interleukin
IPP	Isopentenyl Pyrophosphate
kb	Kilobase
Kif7	Kinesin family member 7
KO	Knockout
Lck	Lymphocyte protein tyrosine kinase
LN	Lymph nodes
LPS	Lipopolysaccharide
MAP	Mitogen-activated protein
mg	Milligram
MHC	Major histocompatibility complex
mL	Milliliter
mm	Millimeter
mRNA	Messenger RNA
n	Naïve
NFAT	Nuclear factor of activated T cell
NfκB	Nuclear factor kappa B
ng	Nanogram
NK	Natural killer cell
p	p-value
PAMP	Pathogen associated molecular patterns

PBS	Phosphate buffer saline
PCR	Polymerase chain reaction
PE	Phycoerythrin
PI	Propidium iodide
PKA	Protein kinase A
PKC	Protein kinase C
PLCγ	Phospholipase gamma
PMA	Phorbol myristate acetate
PRR	Patern recognition receptors
PS	Penicillin / Streptomycin
Ptch	Patched
pTα	Pre T alpha chain
qPCR	quantitative PCR
r	Recombinant
Rag	Recombinase activating gene
RNA	Ribonucleic acid
RORγt	Retinoic acid receptor-related orphan receptor gamma
SCID	Severe combined immunodeficiency
SD	Standard deviation
Shh	Sonic Hedgehog
Smo	Smoothened
SOX13	SRY-like box
SP	Single positive
SRY	Sex-determining region Y
SSC	Side scatter
Tbx	T box protein
TCR	T cell receptor
Td	Terminally differentiated
TGFβ	Tumor growth factor beta
Th	T helper
TLR	Toll-like receptor
TNFα	Tumor necrosis factor
Treg	T regulatory cell
U	Units
Vγ	gamma chain
Vδ	delta chain
w/v	Weight / volume
Wnt	Wingless
WT	Wild type
αβ	alpha beta
γδ	gamma delta
µg	Microgram
µl	Miligram

Introduction

1.1 Murine T cell biology

1.1.1 The thymus

T lymphocytes are central players of the adaptive immune system. They take their name from the site of maturation, the primary lymphoid organ called the thymus, where the majority of T cells develop. Blood borne progenitors migrate to the thymus from the bone marrow (or fetal liver during embryonic development) (Moore and Zlotnik 1995), (Kawamoto, Wada et al. 2010). This thymic seeding begins at around embryonic day (E) 11 in mice and continues throughout adult life (Scollay, Smith et al. 1986) (Jotereau, Heuze et al. 1987).

The thymus provides a unique microenvironment with all the necessary cytokines, extra-cellular matrix components and cell-surface ligands needed to produce a functional repertoire of non-self reactive T cells.

The thymus is a flat, bilobed organ situated just above the heart, in the upper right thorax. Each lobe is surrounded by a capsule and divided into lobules, separated from each other by connective tissue called trabeculae. Each lobule is organised into two compartments, the cortical region, which is densely packed with immature T cells and the inner medullary region. Embryologically, the tissue derives from the gut endoderm of the third pharyngeal pouch (Carpenter and Bosselut 2010). For T cells to develop successfully, thymocytes must dynamically relocate within the different microenvironments of the thymus during different developmental stages (Petrie and Zuniga-Pflucker 2007).

1.1.2 αβ T cell development

In adults, progenitors from the bone marrow enter the thymus through a narrow region of the perimedullary cortex, the cortico-medullary junction,

to give rise to the early thymic progenitor (ETP) population (Prockop and Petrie 2000). These progenitors do not express CD4 or CD8 and are referred to as Double Negative (DN). Based on the expression of the cell adhesion protein CD44 and IL-2 receptor chain CD25, the DN population can be subdivided into four sequential phenotypic subsets. DN1 is the earliest thymic subset and is characterised by expression of CD44 but not CD25. These pluripotent cells also express CD117 and steadily migrate towards the outer subcapsular region. Upon acquisition of CD25, thymocytes enter the DN2 stage. DN2 cells are more restricted in their differentiation potential and are thought to have lost their ability to develop into B cells but can still differentiate into NK cells and thymic dendritic cells (Wu, Li et al. 1996). Cells then lose CD44 expression to become DN3 cells. By this stage, developing cells are fully committed to the T cell lineage. The last DN stage, DN4, is marked by a $CD25^-$ and $CD44^-$ phenotype. DN4 cells proliferate rapidly and differentiate into Double Positive cells (DP), expressing both CD4 and CD8 co-receptors often via a CD8+ single positive intermediate (ISP) (MacDonald, Budd et al. 1988). DN cells account for only 1-3% of all thymocytes whereas around 80% of the adult thymus consists of cells in the DP stage (Takahama 2006). The final step of T cell development involves downregulating either CD4 or CD8. Fully functional and mature $CD4^+CD8^-$ or $CD4^-CD8^+$ T cells have now been produced (Godfrey, Kennedy et al. 1993), ready to leave the thymus and migrate to the peripheral lymphoid organs via the circulatory system. About twice as many CD4 as CD8 cells will leave the thymus. Details and possible explanations regarding this phenomenon will be provided later in this chapter. These unprimed, naïve T cells that have not encountered an antigen and are not activated, are in G_0 stage, contain little cytoplasm and show basic, low level transcriptional activity (Kindt T 2007b).

1.1.3 TCR Rearrangement

TCR rearrangement is critical for developing thymocytes and only cells which have undergone a successful in-frame TCRβ rearrangement will proceed to the following stages of development, while the rest undergo apoptosis (Petrie, Pearse et al. 1990). This process, also called ''β-selection'', takes place during the DN3 stage of development. Rag1 and Rag2 genes are transiently expressed, leading to the rearrangement of the TCRβ chain locus (Godfrey, Kennedy et al. 1993), (Mallick, Dudley et al. 1993). Rag1 and Rag2 deficient mice show a profound arrest at the DN3 stage, indicating how essential TCRβ rearrangement is for differentiation to subsequent stages of development (Mombaerts, Iacomini et al. 1992), (Oettinger, Schatz et al. 1990), (Shinkai, Rathbun et al. 1992). The rearranged TCRβ interacts on the cell surface with the 33-kDa pre-TCRα chain (pre-Tα) and associates with CD3, forming the pre-TCR complex. Succesfull formation of the pre-TCR complex supresses further rearrangment of the TCRβ chain, leading to allelic exclusion, and signals progression to the DP stage. The pre-TCR complex on developing cells shows considerable structural resemblance to the TCRαβ complex on mature T cells, as both rely on CD3 chains to transmit signals from the cell surface to the nucleus. On treatment with anti-CD3 antibody, $Rag^{-/-}$ thymocytes can reverse arrest at the DN3 stage and resume differentiation to form DP cells, highlighting the importance of crosslinking between CD3 chains for the pre-TCR signal (Shinkai and Alt 1994). The notion that unlike TCRαβ, pre-TCR mediated signaling does not require a ligand (Irving, Alt et al. 1998) is currently under controversy (Mallis, Bai et al. 2015). Importantly, cells lacking ligand-independent pre-TCR signalling fail to progress to the DP stage. Thymocytes entering the DP stage immediately undergo rapid proliferation but rearrangement of the TCRα chain occurs only after proliferation has stopped and Rag2 protein levels have increased. This mechanism allows the production of an extremely

diverse population because each clone of cells with a single TCRβ chain rearrangement can rearrange a different TCRα chain gene. Overall, this random TCR germ-line rearrangement can generate more than 10^{15} different αβ receptors, able to recognize a great variety of antigens and major histocompatibility complex (MHC) molecules, both self and non-self (Robey and Fowlkes 1994).

1.1.4 Positive and negative Selection

Thymic selection reassures that only T cells, whose TCR recognizes a foreign antigen coupled to a self MHC molecule, will survive to leave the thymus. T cell selection is an extremely selective process with just 1-3% of all T cells managing to reach the last stage of development (Egerton, Scollay et al. 1990).

Positive selection occurs in the thymic cortex and refers to the elimination of those developing T cells which fail to bind a self-MHC class I or class II molecule, resulting in MHC restriction (Jameson, Hogquist et al. 1995). The DP cells that recognize a MHC class I will develop into CD8 T cells whereas DP cells recognizing a MHC class II will develop into CD4 T cells. CD4/CD8 lineage commitment is a topic of intense scientific interest and several hypotheses have been put forward in an attempt to explain the mode of action (Singer, Adoro et al. 2008). The TCR signal strength hypothesis suggests that recognition of either class I or class II MHC molecules and commitment to its subsequent cell fate is influenced by TCR signal strength. A stronger TCR signal favours commitment to the CD4 lineage and a weaker TCR signal favoring commitment to the CD8 lineage (Robey, Fowlkes et al. 1991). Another hypothesis implicates the duration rather than the strength of TCR signaling in the cell fate decision, where TCR signals of longer duration appears to terminate CD8 transcription. Alternatively, the stochastic model suggests that termination of transcription of one of the co-receptors occurs randomly and is followed

by a TCR-dependent rescue step in order to allow only SP thymocytes with appropriate co-receptors for their MHC restriction to survive (Chan, Cosgrove et al. 1993), (Davis, Killeen et al. 1993), (Itano, Kioussis et al. 1994), (Leung, Thomson et al. 2001). Further research on this demanding topic will shed light on the details of lineage commitment. It is important to mention that DP $TCR^{int}CD5^{hi}$ cells are asymmetric in their death rates, such that Class I MHC restricted cells undergo higher apoptosis, compared to Class II-restricted cells, despite similar levels of both cell types being initiated for development (Sinclair, Bains et al. 2013). This finding could explain why there is a 2:1-3:1 bias of CD4 to CD8 cells leaving the thymus.

Positively selected thymocytes will migrate to the thymic medulla where negative selection occurs. Negative selection refers to the elimination of self-reactive T cells bearing high affinity TCRs for self-molecules, either antigens or MHC. It is a process that requires thymocyte-epithelium crosstalk. During negative selection, antigen presenting cells (APCs) - macrophages and dendritic cells (DCs) - bearing class I and class II MHC molecules interact with developing thymocytes, exposing them to a wide range of antigenic products. Negative selection results in self-tolerance by clearing out potentially self-reactive T cells (Jameson, Hogquist et al. 1995), (Goldrath and Bevan 1999).

Early evidence for the elimination of self-reactive thymocytes came from experiments using the HY-TCR transgenic mouse model. The transgenic HY-TCR recognizes the Smcy gene-deriving, male-specific HY peptide in association with class I MHC H-$2D^b$. In male HY-TCR transgenic severe combined immunodeficiency (SCID) mice, all transgenic CD8-expressing T cells were deleted (including DP cells), while in females where the HY peptide is not present, single positive CD8 cells survived (Kisielow, Bluthmann et al. 1988), (Markiewicz, Girao et al. 1998).

Presentation of self-peptides to developing thymocytes is a key

requirement for negative selection of self-reactive thymocytes. The Autoimmune Regulator (Aire) transcription factor has been identified to be the master-switch in the regulation of several ectopic peripheral proteins in medullary epithelial and monocyte populations (Anderson, Venanzi et al. 2002), (Kogawa, Nagafuchi et al. 2002), (Liston, Lesage et al. 2003).

1.1.5 αβ T cell activation

Immune responses, either humoral or cell-mediated, require T cell activation and clonal expansion. The first necessary step for T cell activation is the interaction of the TCR-CD3 complex of an unprimed T cell with a processed antigen bound to the MHC class I or class II molecule on the surface of an APC. Antigen recognition is a necessary but not sufficient event for T cell activation. For full T cell activation, T cells require subsequent antigen-nonspecific co-stimulatory signals, provided primarily by interactions between CD28 on the T cell surface and members of the B7 family on APCs (June, Bluestone et al. 1994). The two members of the B7 family of protein receptors, glycoproteins CD80 and CD86, are constitutively expressed in dendritic cells and activated macrophages and B cells. Their ligands are CD28, which delivers a stimulatory signal to the T cell and promotes activation and proliferation and CTLA-4, also known as CD152, which shows the opposite effect and strongly inhibits T cell activation (Linsley, Brady et al. 1991). Only CD28 is present on the cell surface of resting T cells. CTLA-4, the expression of which interestingly relies on CD28 co-stimulatory signals, is detectable about 24h after T cell activation and peaks 2-3 days later. CTLA-4 shows a higher affinity to CD80 and CD86 than CD28. Therefore, in direct proportion to CD28 stimulation, CTLA-4 provides a regulatory brake on T cell expansion (Azuma, Ito et al. 1993, Hathcock, Laszlo et al. 1993). CTLA-4 knockout (KO) mice show lymphadenopathy, splenomegaly and die 3-4 weeks after death (Kindt T 2007b). Clearly, the production of inhibitory signals by

engagement of CTLA-4 is important for lymphocyte homeostasis. T cells that experience antigen recognition but do not recieve the co-stimulatory signal via CD28 fail to activate properly and exhibit a state of nonresponsiveness, named clonal anergy (Chen and Flies 2013).

T cell activation triggers several signal transduction pathways that result in gene transcription, proliferation and differentiation into memory or effector phenotypes. The most important of these cascades of biochemical events involve Phospholipase γ (PLCγ), Protein Kinase C (PKC), the Ras/MAP Kinase pathway, NfκB and calcium (Ca^{2+}), whose release from the endoplasmic reticulum (ER) results in the phosphorylation of the transcription factor NFAT which promotes T cell growth and proliferation by supporting transcription of cytokine genes (Kindt T 2007b).

During T cell activation, changes in gene transcription can be grouped according to their detection time upon antigen recognition. *Immediate genes*, expressed within 30 minutes after the initial interaction, encode mostly transcription factors such as c-Fos, c-Myc and Nf-κB. *Early genes*, expressed no more than two hours after antigen recognition, encode Interleukin 2 (IL-2), IL-3, IL-6, IL-2R and Interferon gamma (IFN-γ). Last, the so called *late genes*, whose expression is detected no earlier than two days after antigen recognition, involve mostly adhesion molecules (Kindt T 2007b).

The number of ligands a T cell must recognise for sufficient activation has been a very active research area for many years. Finally, experiments using antigenic compounds bound to biotin molecules, which emit light when a streptavidin-phycoerythrin conjugate is added, revealed that as little as 10 TCR-MHC interactions are sufficient in both CD4 and CD8 cells for T cell activation (Irvine, Purbhoo et al. 2002).

Activated CD4 T cells differentiate into T helper (Th) effector cells and CD8

T cells into cytotoxic T cells. Activated CD8+ T cells particularly express tumor necrosis factor (TNF) and secrete IFNγ. CD4 Th cells are subdivided into several types according to cytokine production and function. More specifically, Th1 cells, whose differentiation is promoted by APC-secreted IL-12 and the transcription factor Tbx21, also known as Tbet, secrete IFNγ, IL-2 and tumor necrosis factor alpha (TNFα) which support pro-inflammatory immunity against viral and intracellular bacterial pathogens. On the other hand, Th2 cells are promoted by IL4 and Gata3 and produce IL-4, IL-5, IL-9 and IL-13 (Constant and Bottomly 1997). Th2 cells play a key role in allergic inflammation as well as the protection against extracellular parasites. Not surprisingly, Th17 cells mainly produce IL-17 and modulate protection against extracellular bacteria and fungi while also playing an important role in autoimmunity (Korn, Bettelli et al. 2009). Regulatory T (Treg) cells, with the distinct $CD4^{+}CD25^{+}FoxP3^{+}CD122^{-}$ phenotype, negatively regulate immune responses and are therefore critical in maintaining lymphocyte homeostasis. Two major groups of Tregs have been identified, natural Tregs (nTregs) and inducible (iTregs), with the former differentiating in the thymus and the latter in the periphery (Curotto de Lafaille and Lafaille 2009).

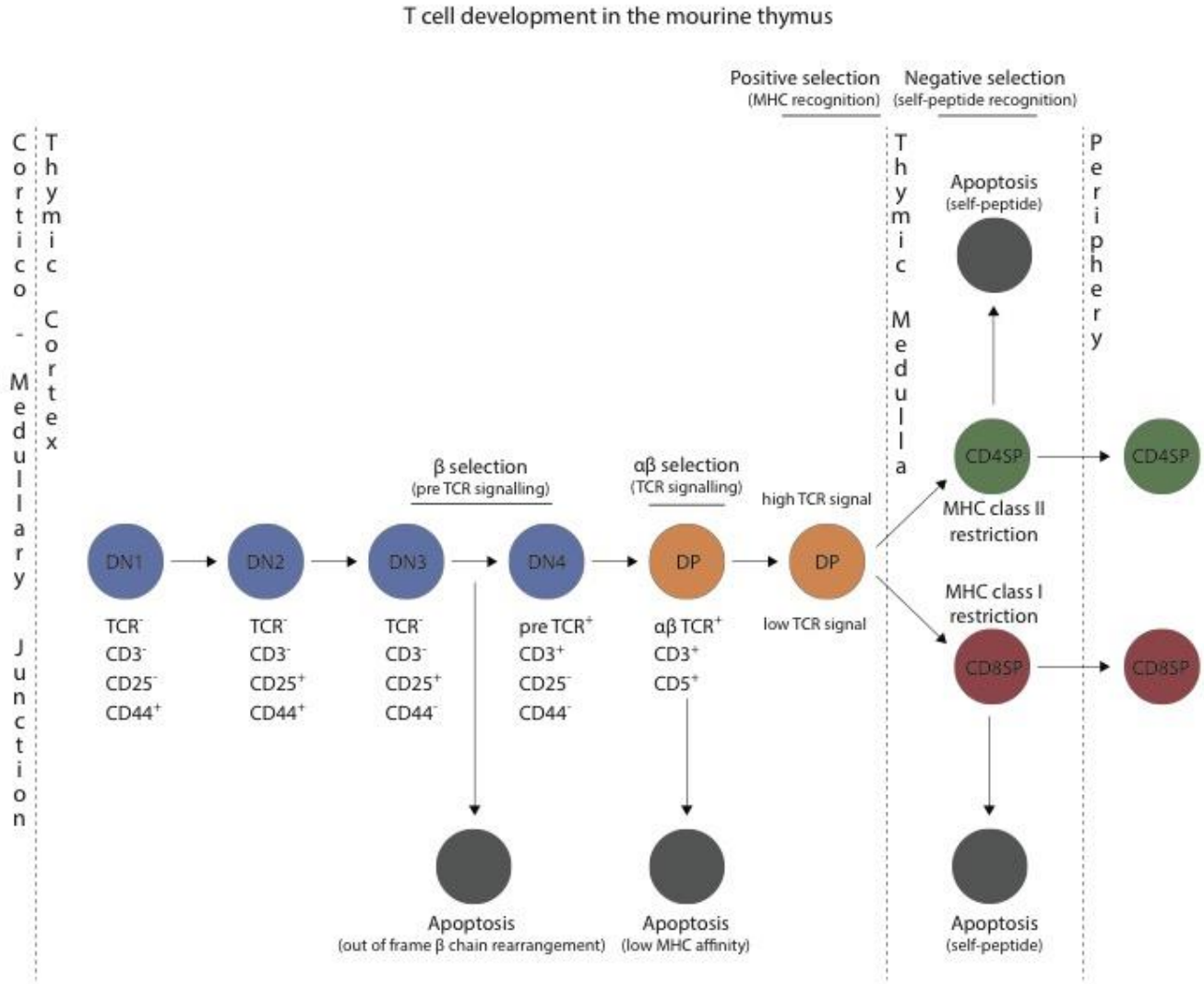
T cell development in the mourine thymus
Positive selection
(MHC recognition)
Negative selection
(self-peptide recognition)
Cortico - Medullary Junction
Thymic Cortex
Thymic Medulla
Periphery
β selection
(pre TCR signalling)
αβ selection
(TCR signalling)
high TCR signal
DN1
DN2
DN3
DN4
DP
DP
TCR- CD3- CD25- CD44+
TCR- CD3- CD25+ CD44+
TCR- CD3- CD25+ CD44-
pre TCR+ CD3+ CD25- CD44-
αβ TCR+ CD3+ CD5+
low TCR signal
Apoptosis
(out of frame β chain rearrangement)
Apoptosis
(low MHC affinity)
Apoptosis
(self-peptide)
CD4SP
MHC class II
restriction
CD4SP
MHC class I
restriction
CD8SP
CD8SP
Apoptosis
(self-peptide)

Figure 1.1: αβ T cell development in murine thymus

Blood borne lymphoid progenitors enter the thymus at the cortico-medullary junction and undergo a series of developmental stages and selection processes as they move to different thymic micro-environments. Different developmental stages can be classified according to expression of cell surface markers. Proliferation occurs at the DN2 stage and after pre-TCR signaling at the DN to DP stage. Selection takes place at several checkpoint stages; β selection occurs at the DN3 stage as the pre-TCR is formed by joining a rearranged β chain with a pTa, αβ selection occurs at the DP stage as the TCR is formed by joining a β chain with a rearranged α chain, positive selection occurs at the DP stage as only cells with moderate MHC affinity progress to further developmental stages and negative selection occurs at the final SP stage when self-reactive cells are eliminated. Cells that fail any of the above selection steps undergo apoptosis. Thymocytes that have completed their thymic development successfully will leave the thymus to migrate to primary lymphoid organs in the periphery.
DN – double negative, DP – double positive, SP – single positive, TCR – T cell receptor, MHC – major histocompatibility complex

1.1.6 γδ T cell lineage commitment

Both αβ and γδ T cells derive from common thymic precursors. The timing of lineage divergence however is not well defined, largely due to the lack of definitive markers that allow cells commited to a γδ lineage to be distinguished prior to γδTCR expression (Ciofani and Zuniga-Pflucker 2010). It appears that DN1 cells are uniformly bipotent, giving rise to both αβ and γδ lineage T cells (Ciofani, Knowles et al. 2006). In contrast, only half of DN2 cells retain bipotency, whereas by the DN3 stage, almost all cells appear to be lineage committed (Ciofani, Knowles et al. 2006).

The mechanisms that regulate γδ cell fate commitment are also poorly understood. TCR signaling plays an important role in this stage but existing data does not support a deterministic role because the type of TCR initially produced by the T cell does not absolutely determine the lineage, and the presence of a γδTCR or a premature αβTCR can lead to either αβ or γδ lineage commitment (Garbe, Krueger et al. 2006). Support for the non-deterministic role of the TCR was provided by two studies in which αβ and γδ T cell lineage fate was mediated exclusively by a γδTCR transgene (Hayes, Li et al. 2005) (Haks, Lefebvre et al. 2005). It seems that TCR signal strength, rather than type of TCR, is crucial for lineage commitment, with a strong TCR signal promoting a γδ T cell fate and a weak signal an αβ T cell fate (Hayes, Li et al. 2005). A stronger TCR signal is associated with strong activation of the extracellular signal-regulated kinase (ERK), early growth response (EGR) and inhibitor of DNA binding 3 (ID3) pathway (Haks, Lefebvre et al. 2005). In support of the signal strength hypothesis, γδ T lineage cells express higher levels of EGR1, EGF2 and EGR3 transcription factors and also induce higher expression levels of ID3 compared to β-selected thymocytes. It is worth noting that TCRα and

TCRδ share the same gene locus and therefore, expression of rearranged segments is mutually exclusive (Satyanarayana, Hata et al. 1988).

Other factors can also contribute to αβ versus γδ lineage determination. In IL-7Rα deficient mice, development of γδ cells is completely abolished as a result of TCRγ chain absence as IL-7 is known to stimulate rearrangement and expression of the TCR γ genes (Perumal, Kenniston et al. 1997). Importantly, It has been shown that DN2 ($CD25^{+}C44^{+}$c-$Kit^{+}TCR^{-}$) thymocytes expressing high levels of IL-7R give rise to γδ T cells more frequently than thymocytes lacking or expressing low levels of IL-7R (Kang, Volkmann et al. 2001). IL-$7R^{hi}$ DN2 cells showed a fivefold greater potential to develop into γδ T cells, indicating that a proportion of early DN thymocytes can be biased towards a γδ linage commitment before β-selection and fully independently of TCR-mediated signals.

In addition, the presence of the transcription factor SOX13 promotes a γδ T cell (Melichar, Narayan et al. 2007). Indeed, in a 2007 screen for transcription factors that are differentially expressed between αβ and γδ thymocytes, SOX13 was found to be the only γδ-specific gene. SOX13-deficient mice produced normal functional mature αβ T cells yet γδ T cell development was severely impaired (Melichar, Narayan et al. 2007). It is believed that SOX13, whose expression precedes and is independent of TCR rearrangement, interacts with the developmentally important Wnt signaling pathway. This is possibly mediated by the antagonizing T cell factor (TCF), a high motility gene (HMG) transcription factor, which is induced by Wnt and seems to promote an αβ lineage by repressing TCRγ gene expression (Melichar, Narayan et al. 2007).

Finally, the Notch pathway has also been implicated in γδ lineage specificity, although its contribution appears to be less crucial. It is worth

noting, however, that although Notch signaling promotes the formation of γδ T cells in humans (Van de Walle, De Smet et al. 2009), in contrast, it promotes the αβ T cell lineage in mice (Washburn, Schweighoffer et al. 1997).

γδ TCR ontogeny

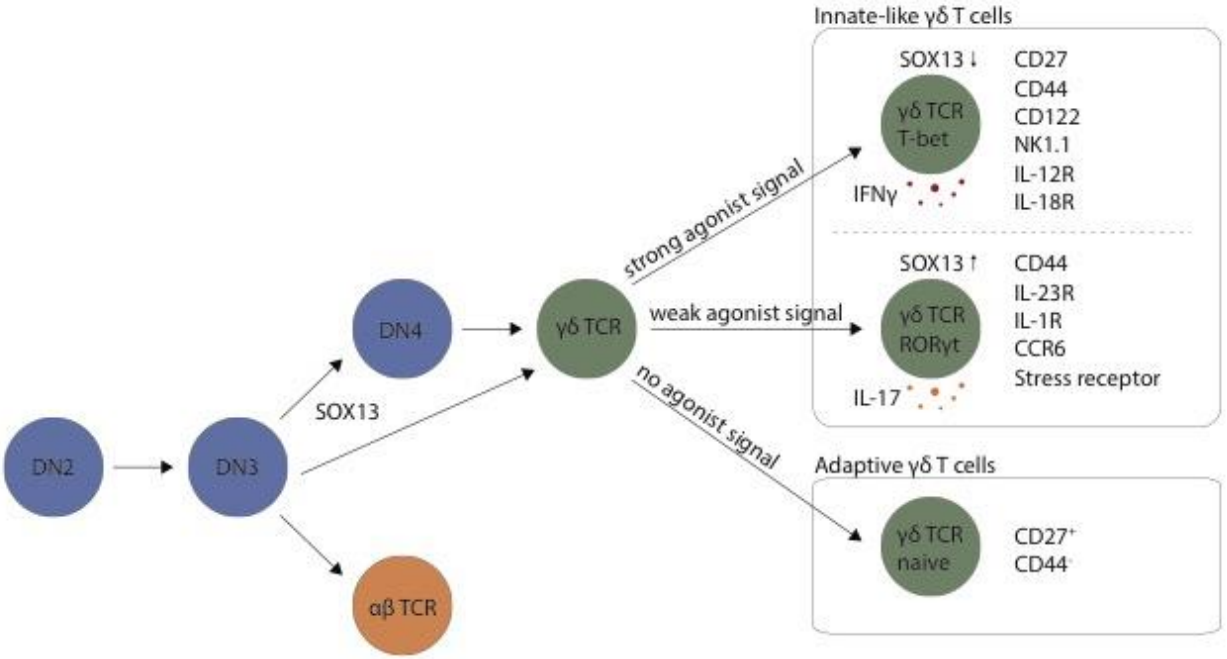

Figure 1.2: Murine γδ TCR ontogeny

In the murine thymus, DN cells can rearrange γδ TCR at the DN3 or the DN4 stage under the influence of the γδ-specific transcription factor SOX13 and γδ T cells acquire their final functional fate according to the presence of an agonist signal. In the prenatal thymus, fetus-derived γδ cells that produce IFNγ express CD27 and IL-17-producing γδ cells fail to express CD27. In the postnatal thymus, γδ development relies on a pool of bone marrow progenitors that give rise predominantly to naïve cells that do not show functional pre-programming, however some postnatally-developed γδ cells that engage agonists are believed to give rise to intestinal intraepithelial lymphocytes (IEL), not shown here. It is also believed that IL-17-producing γδ cells cannot be generated from bone marrow progenitors, indicating that γδ development of IL-17-producing cells is restricted in prenatal, fetus-derived thymocytes.
DN – Double Negative, DP – double positive, SOX13 - SRY-related HMG-box, NK – natural killer, IL – interleukin, IFNγ – Interferon gamma, RORγt - Retinoid-Acid Receptor-related Orphan Receptor gamma

1.1.7 Murine γδ thymic subtypes and effector fate

The murine TCRγ chain was discovered in 1984 (Saito, Kranz et al. 1984) and its human counterpart just two years later (Brenner, McLean et al. 1986). Nevertheless, many aspects regarding the ontogeny, function and diversity of γδ T cells remain unclear.

Despite the presence of a TCR, it is difficult to categorize γδ cells as adaptive or innate because, depending on the particular context, γδ cells can share features of one or the other system. In fact, γδ cells are increasingly being classified as a third branch of the immune system altogether (Hayday 2000).

In mice, the first wave of γδ T cell development appears in E14 and precedes aβ cells (Strominger 1989). Importantly, α and δ chains share the same locus and therefore expression of rearranged αTCR and δTCR are mutually exclusive (Satyanarayana, Hata et al. 1988). In the postnatal murine thymus and peripheral blood, γδ T cells constitute only a small population, rarely more than 3% of nucleated cells. Yet, the percentage rises dramatically in peripheral tissues, especially the epithelium (Hayday 2009). Five distinct γδ cell populations can be identified by expression of markers CD27, CD25, CD24 and CD44 markers (Ribot, deBarros et al. 2009), (Prinz, Sansoni et al. 2006). The most immature γδTCR cells are $CD27^{+}CD25^{+}CD24^{+}CD44^{-}$ with high proliferative potential (Ribot, deBarros et al. 2009), (Prinz, Sansoni et al. 2006) and express low TCR. These progenitors downregulate CD25 to become $CD27^{+}CD25^{-}CD24^{+}CD44^{-}$ cells that make up the majority of thymic γδ cells and can possibly already colonise the periphery (Tough and Sprent 1998). They probably also represent precursors for three mature γδ thymocyte populations that lack surface expression of CD24. The $CD27^{-}CD44^{+}$ subset (Haas, Gonzalez et al.

2009) is already committed to IL-17 expression (Ribot, deBarros et al. 2009). By contrast, mature $CD27^{+}CD44^{-}$ γδ T cells have the potential to secrete IFN-γ and can be subdivided into the $CD122^{+}$ and $CD122^{-}$ subsets. The former are largely $NK1.1^{+}$ (Haas, Gonzalez et al. 2009) and express γδTCR poorly, exhibiting common characteristics and functional overlap with natural killer (NK) cells (Stewart, Walzer et al. 2007). Overall, the thymus generates distinct γδ T cell populations with clear phenotypic links to peripheral γδ subsets.

Although conventional αβ T cells differentiate into effector subsets after encountering pathogens in peripheral tissues, the function of γδ T cell subtypes seems to be programmed in the thymus (Azuara, Levraud et al. 1997), (Jensen, Su et al. 2008), (Ribot, deBarros et al. 2009). Jensen et al. introduced the concept that thymic TCR ligation determines the differentiation of γδ T cells into antigen-experienced IFN-γ-producing and antigen-naive IL-17-producing cells. The signals, however, that actually promote proinflammatory IL-17 or IFN-γ production by effector γδ T cells are poorly understood. It is known that they can produce IL-17 in response to IL-23 (Lockhart, Green et al. 2006) and IFN-γ in response to cooperative activation with IL-12 and IL-18 (Qureshi, Zhang et al. 1999).

It is important to mention that a functional dichotomy between IFN-γ and IL-17-producing cells also exists in the spleen and lymph nodes of adult mice and has been largely attributed to thymic developmental preprogramming as opposed to peripheral plasticity (Jensen, Su et al. 2008). Interestingly, however, the underlying mechanisms remain unresolved.

Apart from cell surface markers, murine γδ T cell development can be classified according to Vγ and Vδ chains, where different subtypes migrate

to and populate different tissues and body surfaces (Prinz, Silva-Santos et al. 2013). For example, CD44$^+$ Vγ6 T cells and CD44+ Vγ4 T cells are highly concentrated at the peritoneal cavity and the dermis respectively. CD27$^+$CD44$^+$ Vγ1 cells, able to secrete both IFNγ and IL-4 upon activation, are localized in the liver and the spleen. The first wave of γδ T cells to leave the thymus is believed to be CD44$^+$ Vγ5 cells, detected by flow cytometry in the murine epidermis already by E15.

Unlike αβ T cells, there is thymus-independent γδ T cell development. Patients with DiGeorge syndrome suffer from severe thymic hypoplasia and lack functional αβ T cell, yet they have normal γδ T cells (Borst and van Dongen 1990). The human fetal liver is one site of γδ T cell development, where Vγ9Vδ2 cells develop even before thymic formation (Wucherpfennig, Liao et al. 1993) (McVay and Carding 1996).

Notably, intraepithelial γδ lymphocytes, mainly gut CD27$^+$ Vγ7 T cells, exhibit strong cytolytic and immunoregulatory capacities and seemingly lack peptide–MHC restriction, indicating that they bypass the complex medullary developmental progression of DP cells (Hayday and Gibbons 2008). Evidence that supports the concept of extrathymic γδ T cell development includes the rescue of intestinal γδ T cell development in IL-7 KO mice by gut epithelium-specific IL-7 expression (Laky, Lefrancois et al. 2000) as well as detection of gut γδ T cell in athymic mice (Hayday, Theodoridis et al. 2001).

γδ T cells recognize a plethora of molecules in a wide variety of contexts and understanding the different settings in which these ligands are presented to γδ T cells is essential to comprehend the range of functions carried out by γδ T cells. Phosphorylated isoprenoid precursors, collectively called phosphoantigens, are recognized by γδ TCR via TCR

binding. Phosphoantigens constitute the first description of a non-peptide T cell antigen (Tanaka, Sano et al. 1994). It is not clear yet how phosphoantigens are presented to γδ T cells. Soluble phosphoantigens fail to activate γδ T cells, and MHC class I or II, as well as cell-surface expression of CD1 are not required for successful presentation (Morita, Beckman et al. 1995). It is also known that γδ T cells can present phosphoantigens to other γδ T cells (Morita, Beckman et al. 1995). Some γδ T cells recognize proteins directly, without being processed. Examples include viral proteins (Sciammas, Johnson et al. 1994) and heat shock proteins (O'Brien, Happ et al. 1989). Some evidence suggests that γδ T cells can also recognize lipids (Azuara, Levraud et al. 1997).

The main function of γδ T cells is not the recognition of MHC complexes (Strominger 1989). Instead, γδ T cells have been proposed to constitute a first line of defense against pathogens (Allison and Havran 1991, Hayday 2000). In a study involving infection with *Listeria,* γδ T cells peaked 3 days after injection and αβ T cells 5 days later, suggesting that γδ T cells block the infection before αβ cells clear it at a later stage (Ohga, Yoshikai et al. 1990). However, some γδ T cells in the lymph nodes and the spleen have been described to express CD8, exhibiting lytic activity *in vivo*, hence being called $CD8^+$ cytotoxic γδ T cells (Lake, Pierce et al. 1991). Other γδ T-cells (1-4% of all peripheral T cells) co-express CD4 and secrete IL-4 (Wen, Barber et al. 1998). Finally, the existence of γδ regulatory T cells (Treg) has been proposed (Traxlmayr, Wesch et al. 2010). Taken together, it becomes clear that γδ T cells constitute a diverse arm of the immune system with different subsets playing distinct roles in immune responses.

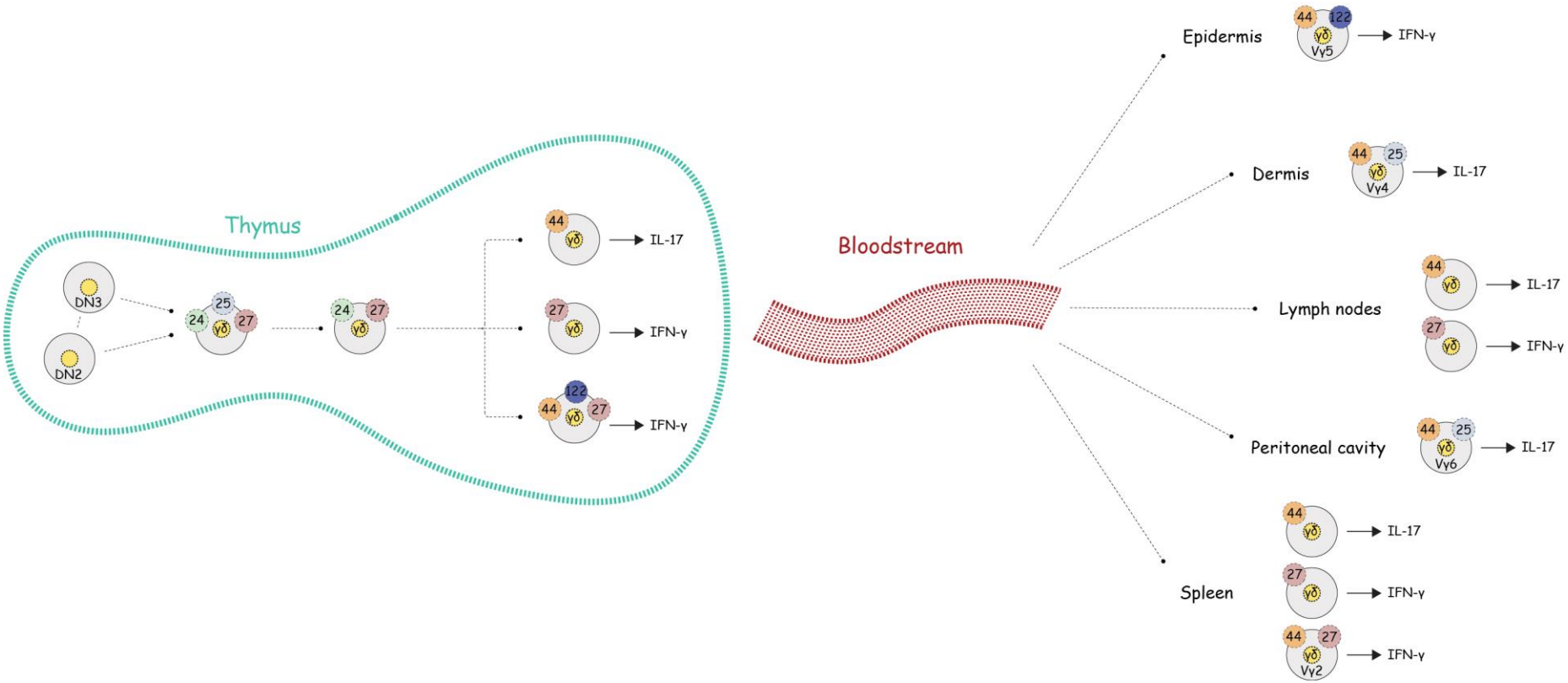

Figure 1.3: Mouse γδ T cell subsets in the thymus and periphery

Proposed developmental relationships between Vγ subsets, cell surface expression of key markers, potential for cytokine secretion and tissue localization are shown. IL-17 – interleukin 17; IFN-γ – interferon-γ

1.2 Human γδ T cell subtypes and effector fate

In humans, γδ T cells are also a minor population in peripheral blood with numbers more predominant in epithelial layers. The current view suggests that although γδ T cell function is associated with Vγ chains in the mouse, it correlates with Vδ usage in humans (Pang, Neves et al. 2012). For identification purposes, human γδ T cells are divided into three major categories according to their Vδ chain; Vδ1, Vδ2, or nonVδ1-nonVδ2 chain (Hayday 2000).

Vδ1 and nonVδ1-nonVδ2 are more abundant in mucosal surfaces such as the skin and intestine and can combine with several Vγ chains (Deusch, Luling et al. 1991, Ebert, Meuter et al. 2006). The most common Vδ1 T cell population in adult blood shows a CD45RA+ phenotype, which can be subdivided virtually evenly between two populations, IL-2-secreting $CD27^{+}CD11a^{-}$ and IFNγ-secreting $CD27^{-}CD11a^{+}$ (De Rosa, Andrus et al. 2004).

Unlike Vδ2 cells, Vδ1 cells frequently express CD8 and show considerable cytotoxic activity, found to respond to a broad range of antigenic compounds including autologous and endogenous phospholipids (Russano, Bassotti et al. 2007), cytomegalovirus (Dechanet, Merville et al. 1999), HIV (De Maria, Ferrazin et al. 1992), malaria (Hviid, Kurtzhals et al. 2001) and a range of epithelial tumors (Maeurer, Martin et al. 1996). This is mediated possibly through recognition of the stress-induced MHC class I – related molecules MICA and MICB (Groh, Rhinehart et al. 1999). The percentage of Vδ1 cells circulating in the peripheral blood remains relatively constant until late middle age, suggesting a constant thymic production (De Rosa, Andrus et al. 2004).

On the other hand, Vδ2, which are almost exclusively Vγ9, dominate the peripheral blood (Strauss, Quertermous et al. 1987) and characteristically show substantial expansion during certain bacterial and parasitic infections - to the point they can become the majority of circulatory leukocytes (Morita, Jin et al. 2007). The investigation of Vγ9Vδ2 cells is largely problematic because this population is only shared between higher primates with the absence of murine counterparts making them a difficult population to study.

Vγ9Vδ2 cells are unique in their recognition of non-peptide phosphoantigens such as (E)-4-hydroxy-3-methyl-but-2-enylpyrophosphate (HBB-PP) and isopentenyl pyrophosphate (IPP) (Tanaka, Morita et al. 1995), (Wang, Sarikonda et al. 2011), both intermediate metabolites of microbial isoprenoid biosynthesis and human mevalonate pathway of isoprenoid synthesis, respectively. The mechanism of activation and the nature of the molecules that present phosphoantigens to γδ T cells remain unclear as MHC I or II and CD1 expression are not required for successful phosphoantigen presentation and soluble, unprocessed phosphoantigens fail to activate γδ T cells (Morita, Beckman et al. 1995).

The Vγ9Vδ2 can be further subdivided according to CD27 and CD45RA cell surface expression. Unlike mice, however, CD27 expression in humans does not signify capacity for robust IFNγ production and secretion. These two markers identify four distinct populations: $CD27^{+}CD45RA^{+}$ naïve (T_{naive}), $CD27^{+}CD45RA^{-}$ central memory (T_{CM}), $CD27^{-}CD45RA^{-}$ memory (T_{EM}) and $CD27^{-}$ $CD45RA^{+}$ effector memory (T_{EMRA}) γδ T cells (Pang, Neves et al. 2012).

Naïve γδ T cells, the only Ag-inexperienced phenotype, are also $CCR7^+$ and $CD62L^+$, indicating migratory ability to lymph nodes. They can also proliferate rapidly upon IPP activation and do not secrete IFNγ (Dieli, Poccia et al. 2003), lacking cytotoxic function. Central memory cells retain the phenotype of naïve cells but switch expression of CD45RA for CD45RO. In healthy individuals, T_{CM} cells account for ≤50% of γδ cells in peripheral blood and around 25% in lymph nodes. T_{CM} cells can become activated in very low concentrations of IPP and secrete low levels of IFNγ (Dieli, Poccia et al. 2003). Approximately 2 weeks after IPP activation, T_{CM} cells give rise to T_{EM}, with a distinct phenotype $CD45RO^+CCR7^-CD62L^-$ and positive for the tissue-associated chemokine receptors CCR2, CCR5, CCR6 and CXCR3. These cells show reduced proliferative capacity compared to $CD62L^+$ Vγ9Vδ2 subtypes, but upon IPP activation can secrete abundant IFNγ as well as TNFα. IL-15 is believed to upregulate CD45RA in T_{EM} cells, generating T_{EMRA} γδ cells (Caccamo, Meraviglia et al. 2005) which are unresponsive to further TCR engagement and show little proliferative capacity. Nevertheless, T_{EMRA} cells, although minor contributor of IFNγ, exhibit strong cytolytic activity due to ample production of perforin and granulysin (Pang, Neves et al. 2012). T_{EM} and T_{EMRA} γδ cells strongly express the adhesion molecule CD11α, aiding their migration into sites of inflammation (Angelini, Borsellino et al. 2004).

It is noteworthy that one study has shown evidence of extrathymic selection for the Vδ2 T cell subset (Parker, Groh et al. 1990). More specifically, they showed that the percentage of Vδ2 cells was higher in the periphery than the thymus whereas Vδ1 cells declined. The change increased proportionally with age of donors and it was not accompanied by a similar change in the thymus, strongly suggesting peripheral selection. Another interesting finding is that different human populations show preference for different Vδs. For example, Vδ1 cells predominate in West African communities (Hviid, Akanmori et al. 2000) whereas Vδ2 cells

are more prominent in people living in Europe and the US, including African Americans in the US (De Rosa, Andrus et al. 2004).

The functional plasticity of Vγ9Vδ2 does not stop here. Expression of FoxP3 and regulatory activity has been demonstrated in Vδ2Vγ6 cells treated with IL-15 and TGFβ1 (Casetti, Agrati et al. 2009) whereas several studies report antigen-presenting activity either to other γδ cells *in vivo* (Morita, Beckman et al. 1995) or to αβ T cells *in vitro* (Brandes, Willimann et al. 2005), along with surface expression of MHC class II, CD80 and CD86. Unlike all other adaptive lymphocytes, γδ T cells can acquire pseudopodia similarly to myeloid cells when, for example, they engulf *E.coli* (Wu, Wu et al. 2009). Opsonization of γδ cells seems to be one means by which they become professional APCs (Himoudi, Morgenstern et al. 2012).

There are considerable differences between murine γδ T cells and human Vδ2 T cells beyond their cell surface markers. One example is IL-17 production, which is usually abundant in mice within inflamed tissues but very difficult to demonstrate in humans. The only IL-17-producing human Vγ9Vδ2 γδ T cells which form a subtype of non-cytotoxic $CD45RA^{+}CD27^{-}$ T_{EMRA} cells have been identified in psoriasis (O'Brien and Born 2015). Furthermore, as described above, murine γδ T cells are believed to acquire their effector fate during development in the thymus whereas human Vδ2Vγ6 γδ T cells show remarkable plasticity upon activation.

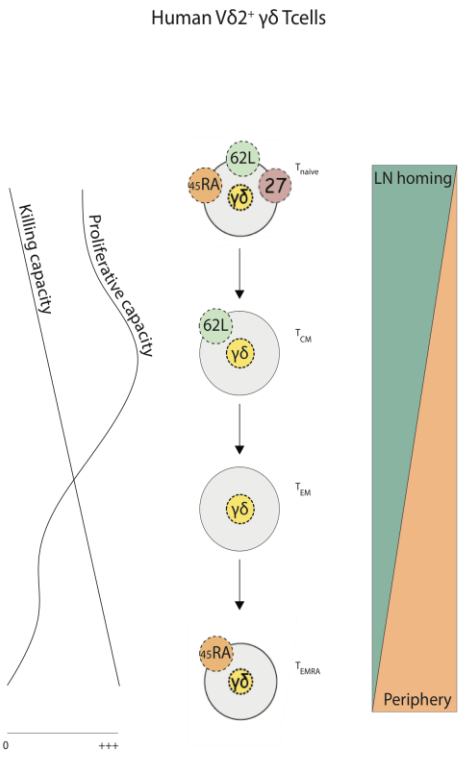

Figure 1.4: Human Vδ2 T cells

Vδ2Vγ9 cells are divided into four distinct subtypes according to cell surface expression of CD45RA and CD27. Naïve Vδ2 γδ cells, expressing CCR7, are the major subtype in the lymph nodes, capable of robust proliferation upon IPP activation. Naïve cells that downregulate CD27 become Central Memory cells that can be found in virtually equal numbers in the lymph nodes and peripheral blood. These cells, which are also able to proliferate extensively, show low IFNγ-secreting capacity. Downregulation of CD62L gives rise to Effector Memory cells, positive for CCR2, CCR5 and CCR6. These cells are absent from the lymph nodes and abundant in peripheral blood and inflammatory sites. They show decreased proliferative capacity and secrete ample IFNγ and TNFα. Finally, IL-15-induced activation of Effector Memory cells gives rise to a CD45RA Effector Memory subset that expresses CCR5 and shows strong killing capacity by robust production of perforin and granulysin and little IFNγ. These cells show minimal proliferative capacity and are unresponsive to TCR signaling.

1.3 The Hedgehog (Hh) signalling pathway

1.3.1 The Hedgehog proteins

In 1980, a large scale phenotype-driven screening was conducted to identify mutations that impair development in Drosophila melanogaster (fruit flies) (Nusslein-Volhard and Wieschaus 1980). The hedgehog gene was identified revealing its role in controlling the development of the larval body plan (Nusslein-Volhard and Wieschaus 1980). In Hh mutants, each larvae segment was entirely covered by spikes, hence the name. Later studies revealed that Hh genes are conserved in all vertebrates and that the family of Hh proteins affect a wide variety of functions in embryonic development including cell differentiation, survival and cell fate (Jiang and Hui 2008).

Three mammalian Hh proteins have been discovered, sharing about 90% homology to each other (Shimeld 1999): Sonic (Shh), Indian (Ihh) and Desert (Dhh) hedgehog. All three hedgehogs share the same canonical pathway although different expression patterns result in non-redundant roles during development (Ingham and McMahon 2001).

1.3.2 Hh signalling

The crucial receptor for the mammalian Hh pathway is known as Patched (Ptch), a 12-span transmembrane protein. Two Ptch homologues exist in mammals, Ptch1 and Ptch2 (Goodrich, Johnson et al. 1996),(Stone, Hynes et al. 1996), (Motoyama, Takabatake et al. 1998).

In the absence of Hh proteins, Ptch suppresses Smoothened (Smo), a 7-span transmembrane protein, disabling any downstream transcriptional activity (Alcedo, Ayzenzon et al. 1996). The exact mechanism of inhibition is unclear although recent evidence suggests that Ptch inhibits the

synthesis of Phosphatidylinsositol-4-phosphate, an essential protein for Smo activation (Yang and Lin 2010).

Binding of Hh with Ptch results in Ptch relieving its inhibitory effect on Smo, which then acts as the central transducer of the Hh signaling pathway and activates the gliomablastoma-associated (Gli1, Gli2 and Gli3) protein family of transcription factors (Matise and Joyner 1999) (Crompton, Outram et al. 2007). Gli proteins are then transported to the nucleus to promote target gene transcription. Gli proteins bind defined DNA consensus sequences, with Gli1 and Gli3 recognizing GACCACCCA and Gli2 recognizing GAAACCACCCA (Tanimura, Dan et al. 1998), (Vortkamp, Gessler et al. 1995).

Interestingly, Gli transcription factors are found even in the most primitive metazoan and thus seem to predate Hh itself (Srivastava, Simakov et al. 2010).

Gli1 lacks the N-terminal repressor domain and acts as a constitutive activator of Hh target genes (Marigo, Johnson et al. 1996). Gli1 is also a target gene of the Hh signaling pathway, so that detection of its transcription levels indicates the degree of Hh signaling in a population of cells (Crompton, Outram et al. 2007). By contrast, Gli2 and Gli3 can function as both transcriptional activators and transcriptional repressors, if they undergo cleavage of their C-terminal activation domain (Sasaki, Nishizaki et al. 1999) (Aza-Blanc, Lin et al. 2000). The ratio of the Gli activator to Gli repressor forms of the protein is affected by the Hh signal gradient received by the target cell. Cells closer to the Hh source will increase the amount of activator forms of Gli protein whereas the repressor forms of Gli proteins will be inhibited and vice versa (Stamataki, Ulloa et al. 2005) (Crompton, Outram et al. 2007).

On the contrary, if Hh signalling is completely absent, kinase recognition

motifs near the C- termini of Gli proteins are phosphorylated by Protein Kinase-A (PKA), Glycogen Synthase Kinase-3 (GSK3) and Casein Kinase-I (CKI) (Pan, Wang et al. 2009), (Pan, Wang et al. 2009), (Price and Kalderon 2002) marking them for ubiquitylation, catalyzed by Btrcp proteins (Zhang, Zhao et al. 2005, Tempe, Casas et al. 2006). For ubiquitylation to occur, the above proteins must associate with the scaffolding protein Kif7, which together with a serine/threonine kinase called Fused (Fu), form the hedgehog signaling complex. The mode of action of Kif7, the orthologue of fruit fly's Costal2 (Cos2) suggests that the hedgehog signalling complex regulates the processing of Gli proteins by controlling intracellular localization (Endoh-Yamagami, Evangelista et al. 2009), (Sisson, Ho et al. 1997), (Zhang, Zhao et al. 2005). Another important cell surface receptor, Hedgehog-interacting protein (Hhip) inhibits the Hh pathway by sequestering the Hh ligand, although it does not seem to have an active role in signal transduction itself (Beachy, Hymowitz et al. 2010).

Mutant mice studies have revealed that the three Gli proteins possess individual and partially overlapping functions. Gli1 KO are viable (Park, Bai et al. 2000), however, Gli2 and Gli3 KO mice are both embryonic lethal (Bai, Auerbach et al. 2002). The Gli2 KO embryos are small in size, suffer from teeth defects, cleft palate, flattened head and craniofacial abnormalities (Mo, Freer et al. 1997) while Gli3 KO have polysyndactyly (extra toes) and severe skeletal defects (Bai, Auerbach et al. 2002). Double mutants of Gli1 and Gli2 or Gli2 and Gli3 show more severe phenotypes. Gli1 expression under the control of Gli2 promoter can partially rescue Gli2KO mice, indicating functional redundancies (Bai and Joyner 2001).

In humans, loss of Gli2 results in serious defects in anterior pituitary formation and pan-hypopituitarism with or without cleft-palate (Roessler, Du et al. 2003), whereas mutations in Gli3 lead to severe skeletal and lung abnormalities, including Greig's Cephalopolysyndactyly (Vortkamp,

Gessler et al. 1991), (Hui and Joyner 1993).

Hedgehog signalling is also implicated in a number of cancers. Ptch mutations have been identified in the aetiology of a number of childhood cancers including medulloblastoma (Wolter, Reifenberger et al. 1997), rhabdomyosarcoma (Endoh-Yamagami, Evangelista et al. 2009). Ptch mutations are also the main cause of Gorlin syndrome, which increases pre-disposition to Basal Cell Carcinoma (BCC) (Gorlin 1995). An abnormally steep increase in Gli1 and Gli2 expression is found in nearly all cases of BCC (Dahmane, Lee et al. 1997), (Regl, Neill et al. 2002). Moreover, abnormal Hh signalling is involved in many malignant tumours such as pancreatic, prostate and lung cancer (Thayer, di Magliano et al. 2003), (Karhadkar, Bova et al. 2004), (Chi, Huang et al. 2006).

1.3.3 The regulation of Hh activity

Hh proteins act as morphogens. Studies have confirmed that the Hh-induced effect is regulated in a concentration-dependent manner, allowing responding cells to be exposed to different concentrations of Hh proteins during different stages of development (Harfe, Scherz et al. 2004) (Varjosalo and Taipale 2008). Hh also acts in a duration-dependent method, where duration of signal influences outcome (Briscoe and Ericson 1999). Thus, Hh controls cellular development dependent on the responding cell type, the concentration and the duration of exposure to Hh by target cells.

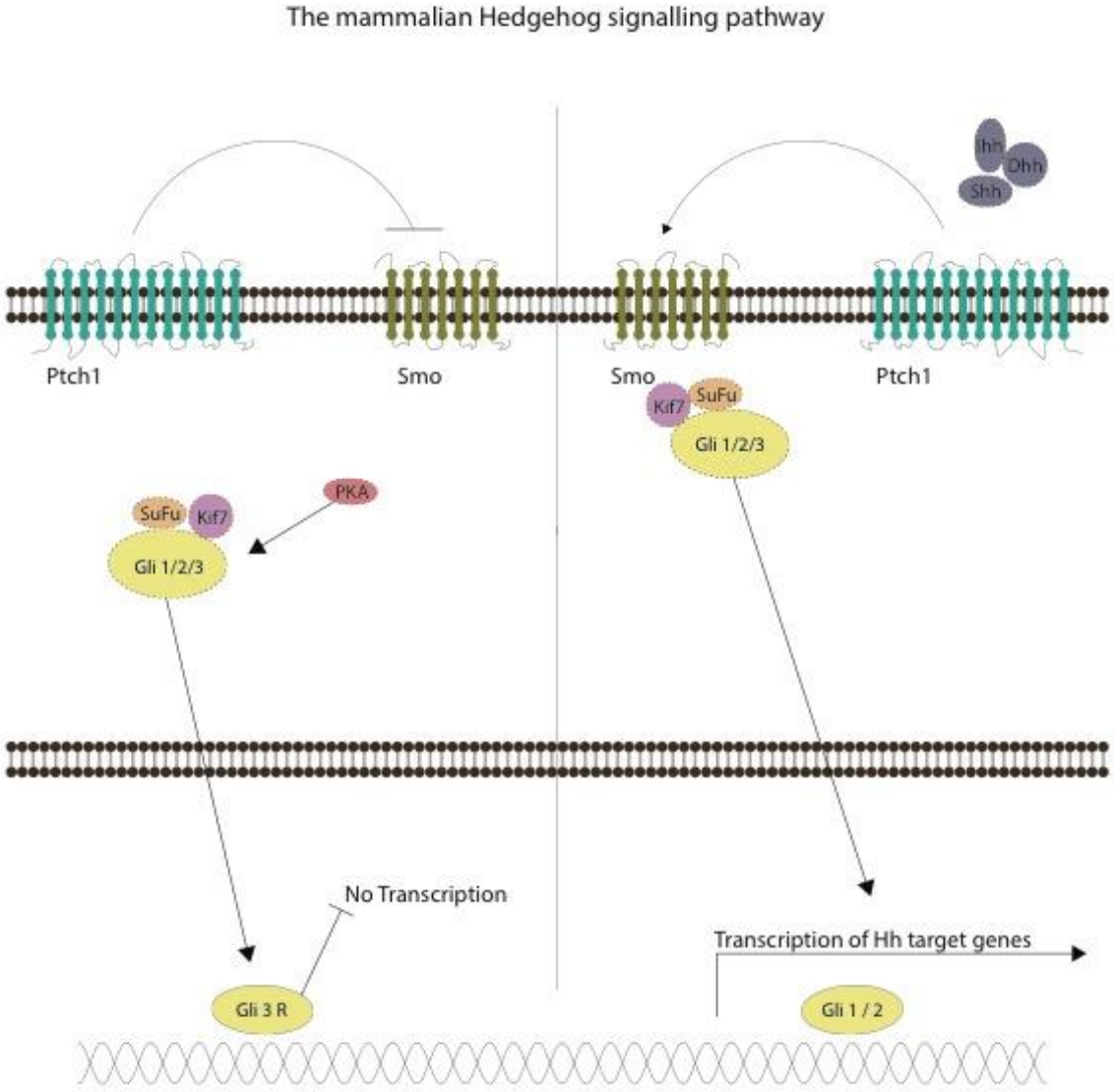
The mammalian Hedgehog signalling pathway
Ihh
Dhh
Shh
Ptch1
Smo
Smo
Ptch1
Kif7
SuFu
Gli 1/2/3
PKA
SuFu
Kif7
Gli 1/2/3
No Transcription
Gli 3 R
Transcription of Hh target genes
Gli 1 / 2

Figure 1.5 The mammalian Hedgehog signaling pathway

In the absence of a member of the Hedgehog family of proteins (Sonic, Indian, Desert), Patched inhibits the constitutive activity of Smoothened, allowing Gli proteins to be recruited to the scaffolding protein Kif7, which also recruits serine/threonine kinases to form the Hedgehog signalling complex. This enables PKA to phosphorylate Gli proteins generating repressor forms of Gli2 and Gli3 that inhibit downstream transcriptional activation. In the presence of a Hedgehog protein, Patched relieves the inhibition on Smo. Smo signals for the phosphorylation of Kif7, allowing the Gli multiprotein complex to dissociate from the microtubule. Activator forms of Gli proteins are released and translocate to the nucleus, leading to transcription of Hedgehog-specific target genes. The middle black dashed line separates the two conditions. The outer membrane represents the cell surface and the inner the nuclear membrane. A blunt ended line indicates inhibition.

Shh - Sonic Hedgehog, Ihh – Indian Hedgehog, Dhh – Desert Hedgehog, Ptc – Patched, Smo – Smoothened, PKA - Protein Kinase A, Fu – Fused, Sufu - Suppressor of Fused, Hhip – Hedgehog inhibiting protein, BMP - bone morphogenetic protein

1.3.4 The role of Shh in T cell development

Shh is the most abundant Hh protein in mammals and plays an important role in many developmental processes, where it controls cellular proliferation and differentiation (Varjosalo and Taipale 2008). Shh signaling is also crucial in organogenesis, most notably in ear, eye and kidney development. It is also essential in embryogenesis, where Shh is expressed in midline tissues, regulating the patterning of embryonic tissue, including the spinal cord, axial skeleton and limbs (Chiang, Litingtung et al. 1996). Not surprisingly, aberrations in Shh signaling cause serious developmental damage in vertebrates and lead to embryonic lethality (Heussler and Suri 2003).

The first evidence showing that the Hh signaling pathway mediates development of immune cells was provided by our lab (Outram, Varas et al. 2000).

In terms of T cell development, Shh is a negative regulator of pre-TCR-induced differentiation from DN to DP cells (Outram, Varas et al. 2000). In this study, mouse fetal thymus organ cultures (FTOCs) treated with recombinant Shh (rShh) showed a developmental arrest in the DN stage, whereas addition of a Hh-neutralising antibody and subsequent neutralization of endogenous Shh resulted in an expansion of DP cells. In 2004, we also showed that Shh signaling regulates differentiation, survival, and proliferation of the earliest double-negative (DN) thymocytes, as thymi from $Shh^{-/-}$ mice contain approximately 10 times fewer thymocytes with a partial arrest at the DN1 to DN2 stage compared to WT littermates (Shah, Hager-Theodorides et al. 2004). The duration and concentration of the Shh-induced signal is believed to account for the dual function of Shh in the DN to DP transition (Crompton, Outram et al. 2007).

More specifically, when Hedgehog signaling was reduced in the $Shh^{-/-}$ and $Gli2^{-/-}$ thymus or by T lineage-specific transgenic expression of a transcriptional-repressor form of Gli2 ($Gli2C_2$), differentiation to DP cell after pre-TCR signal transduction was increased (Rowbotham, Furmanski et al. 2008). In contrast, when Hh signaling was constitutively activated in thymocytes by transgenic expression of a constitutive transcriptional-activator form of Gli2 ($Gli2N_2$), the production of DP cells was decreased (Rowbotham, Furmanski et al. 2008).

Shh is also important in later stages of T-cell development. DP thymocytes are Hh-responsive and thymocyte-intrinsic Shh signaling was recently shown to decrease the CD4:CD8 SP thymocyte ratio (Furmanski, Saldana et al. 2012). In the thymus, Shh is produced by epithelial cells in the medulla, sub-capsular region and in the cortico- medullary region (Outram, Varas et al. 2000), (Virts, Phillips et al. 2006).

1.3.5 The role of Ihh in T cell development

Defects in Ihh signalling have a dramatic effect on bone formation with conditional Ihh KO mice showing reduced proliferation of chondrocytes and osteoblast leading to the truncation of long bones (Razzaque, Soegiarto et al. 2005), (St-Jacques, Hammerschmidt et al. 1999). $Ihh^{-/-}$ embryos die around 1-2 days before birth due to a poorly developed yolk sac (Dyer, Farrington et al. 2001).

Although expression of Ihh is generally more restricted than Shh, DN thymocytes are highly responsive to Ihh, which regulates T cell development and controls thymocytes numbers in both embryos and adult mice.

In fetal $Ihh^{-/-}$ thymi, thymocyte numbers and differentiation to DP were reduced compared to WT littermates. Surprisingly, however, $Ihh^{+/-}$ thymi had increased thymocyte numbers and DP proportions relative to WT, indicating that Ihh both promotes and restricts thymocyte differentiation (Outram, Hager-Theodorides et al. 2009). In adult thymi, Ihh signaling promotes T cell development before pre-TCR signaling but negatively regulates T cell development after pre-TCR signaling has taken place. Of interest, quantitative PCR (qPCR) analysis on expression levels of Ihh and Gli1 showed that Ihh first appears at the DN3 stage and peaks at the DP stage where a six-fold increase in expression is observed. However, Gli1 was not detectable in DP cells with the highest expression seen in the DN3 stage (Outram, Hager-Theodorides et al. 2009). Collectively, these data suggest that DP cells produce and secrete Ihh that then feeds back to DN3 and DN4 cells in order to arrest thymocyte development. Part of this thesis will show data that investigates this ''feedback loop'' hypothesis. DP cells are the major source of Ihh in the human and mouse thymus.

1.3.6 The role of Dhh in T cell development

The role of Dhh signaling in embryonic development is well defined and its function appears to be restricted to testis development (Bitgood, Shen et al. 1996), Schwann cells (Parmantier, Lynn et al. 1999) and erythropoiesis (Lau, Outram et al. 2012). In the thymus, Dhh is produced by epithelial cells in the medulla, sub-capsular region and in the cortico- medullary region (Outram, Varas et al. 2000).

DhhKO mutant mice appear normal and healthy but males are infertile (Clark, Garland et al. 2000).

Material and methods

2.1 Mice

Strain	Origin
C57BL/6	B&K Universal (UK)
$Ihh^{+/-}$	Gift from Andrew McMahon (Harvard University, Cambridge, MA)
$Dhh^{+/-}$	Gift from Andrew McMahon (Harvard University, Cambridge, MA)
$Shh^{+/-}$	Gift from Philip Beachy (The John Hopkins University School of Medicine, Baltimore, MD)
$Gli3^{+/-}$	Purchased from Jackson Laboratories (USA)
$Kif7^{+/-}$	Purchased from Davies, California (USA)
HY-TCR	Purchased from Jackson Laboratories (USA)
CD4-Cre^{+}	Purchased from Jackson Laboratories (USA)
Shh Floxed	Purchased from Jackson Laboratories (USA)
Ihh Floxed	Gift from Beate Lanske (Harvard School of Dental Medicine)
FoxN1-Cre^{+}	Gift from George Holländer (Basel, Switzerland)
GBS-GFP	Gift from James Briscoe (Balaskas, Ribeiro et al. 2012)
Lck-$Gli2N_2$	As described (Rowbotham, 2007)
Lck-$Gli2C_2$	As described (Rowbotham, 2007)

Table 2.1: Strains of mice used

All adult mice used were between 4-8 weeks old. Timed mates were performed by mating a male with two females and monitoring the females for plugs. The day the plug was found was counted as embryonic day 0.5 (E0.5). Mice were bred and maintained at the Institute of Child Health under UK Home Office regulations.

2.2 Antibodies and Flow Cytometry

2.2.1 Cell surface staining

Cell suspensions were prepared by meshing tissue through a 70 μm cell strainer (Falcon, US) using the plunger of a 1ml needleless syringe (Terumo, Philippines). Cells were stained using combinations of the following directly conjugated antibodies (e-Bioscience, US):

1. Murine γδ T cell analysis: anti-CD3$^{PE\text{-}Cy7}$, anti-CD4^{FITC}, anti-CD4^{PE}, anti-CD4$^{PercP\text{-}Cy5.5}$, anti-CD4^{APC}, anti-CD24$^{PercP\text{-}Cy5.5}$, anti-CD25^{Alexa700}, anti-CD27^{FITC}, anti-CD27^{PE}, anti-CD44^{eFluor450}, anti-CD122^{FITC}, anti-γδTCR^{PE}, anti-γδTCR^{APC}, anti-NK1.1$^{PercP\text{-}Cy5.5}$, anti-Vγ1^{PE}, anti-Vγ2^{e710}, anti-CCR6^{e660}.

2. Human γδ T cell analysis: anti-CD3 $^{PercP\text{-}Cy5.5}$, anti-CD27^{eFluor450}, anti-CD45RA$^{PE\text{-}Cy7}$, anti-CD62L$^{APC\text{-}Cy7}$, anti-γδTCR^{FITC}, anti-Vδ1^{APC}, anti-Vδ2^{PE}.

3. Ihh feedback loop hypothesis: anti-CD3^{FITC}, anti-CD3^{PE}, anti-CD3$^{PercP\text{-}Cy5.5}$, anti-CD3^{APC}, anti-CD4^{FITC}, anti-CD4^{PE}, anti-CD4$^{PercP\text{-}Cy5.5}$, anti-CD4^{APC}, anti-CD5^{FITC}, anti-CD8^{FITC}, anti-CD8^{PE}, anti-CD8$^{PercP\text{-}Cy5.5}$, anti-CD8^{APC}, anti-Vb6, anti-Vb8.1/8.2^{FITC}, anti-CD25^{FITC}, anti-CD27^{PE}, anti-CD44^{PE}, anti-CD69^{FITC}, anti-NK1.1$^{PercP\text{-}Cy5.5}$, anti-γδ^{APC}, anti-HSA^{FITC}, anti-B220^{PE}, anti-Qa2^{FITC}, anti-HY (T3.70 clone)^{FITC}.

Suspensions were stained for 20 minutes on ice in 100μL Phosphate buffer saline (Sigma-Aldrich, US) supplemented with 5% Fetal Calf Serum (FCS). Cells were washed in the same medium between incubations and prior to analysis by either C6 (BD Biosciences, US) or LSRII (BD Biosciences, US) flow cytometer. Events (minimum 10^6) were collected using FACSDiva software (BD Biosciences, US) and analysed using Flowjo 7.6 (Tree Star, US).

2.2.2 Annexin-V apoptosis staining assay

Annexin-V staining was carried out using an Annexin-V-FITC apoptosis detection kit (BD Pharmingen, US) according to the manufacturer's protocol. Prior to Annexin-V staining, cells were stained as described in 2.2.1.

2.2.3 Propidium iodide (PI) staining

For PI staining, $2.5x10^5$ cells were permeabilized in 0.1% Triton X-100 (Sigma, UK) and incubated with 50μg/ml PI (Sigma, UK) and 0.1M sodium citrate (Sigma, UK) in PBS for 30 minutes in the dark and at room temperature.

2.2.4 Intracellular stain (ic) for cytokines

2.2.4.1 Activation Assay

Splenocytes and lymphocytes were isolated and cultured in AIM-V medium (Life Technologies, US) supplemented with 50ng/ml PMA (Sigma), 500ng/ml Ionomycin (Sigma) and 2μg/ml Brefeldin A (eBiosciences) at a concentration of 5 x 10^6 cells/ml in 24 well plate at 37°C and 5% CO_2. Cells were harvested at 4h.

2.2.4.2 Intracellular stain

Intracellular cytokine staining for IL-17 and IFN-γ was carried out on cells stained for surface markers as described in 2.2.1, following fixation and permeabilization with the Fix/Perm solutions (BD Biosciences, US) according to the manufacturer's instructions. Anti-IL-17^{FITC}, anti-IFN-γ^{FITC}, anti-IFN-γ^{PE} were supplied by e-Bioscience. Minimum 10^6 cells were stained for 1h in 100ml ice cold PBS supplemented with 5% FCS. Antibodies were used at a 1:25 final ratio.

2.2.5 Cell Sorting

Thymocytes and splenocytes from adult mice (6-8 weeks) were sorted at the ICH/GOSH Flow Cytometry Core facility using a Modular Flow Cytometer (MoFlo XDP; Beckman Coulter, US). Staining with anti-$CD3^{FITC}$ and anti-

CD4^{PE}, anti-CD8$^{PercP\text{-}Cy5.5}$ and anti-CD25^{APC} allowed sorting of the DP, SP and DN thymic populations. Sorting of γδ T cells required anti-CD3^{FITC}, anti-CD4^{PE}, anti-CD8$^{PerCP\text{-}Cy5.5}$ and anti-γδTCR^{APC}. All cells collected fell within the forward scatter/ side scatter (FSC/SSC) live gate.

2.3 Fetal Thymic Organ Cultures (FTOCs)

E14.5 – E19.5 fetal thymi were cultured on 0.8μm membrane filters (Millipore, US) in 1ml AIM-V medium (Invitrogen, US) in 24-well plates for 5 days. Cultures were incubated at 37°C and 5% CO_2. Where appropriate, 1μg of rHhip, rShh or rDhh, all purchased by R&D Systems, US, was added in the medium.

2.4 Skin digestion

Skin samples were collected from anatomically matched locations, minced with scissors and digested with 150μg/ml Liberase (Roche, UK) and 500μg/ml DNAse (Roche, UK) in sterile DMEM (Sigma, UK) for 3 hours at 37^0 C. Every 30 min, the tube was gently swirled to dissociate cells. The sample was filtered through a 70μm filter to obtain a single cell suspension and washed twice.

2.5 RNA extraction and cDNA synthesis

Cell suspensions were pelleted and resuspended in the appropriate amount of lysis buffer and β-mercaptoethanol (Stratagene). RNA was extracted using the Arctutus PicoPure kit (Life Technologies, US) according to the manufacturer's protocol, including the DNAse digestion step. cDNA was synthesized from this RNA using the High Capacity cDNA Reverse Transcription (Life Technologies, US) kit following manufacturer's protocol.

The mix was incubated at 25^0 C for 10 minutes to allow primer binding followed by 37^0 C for 120 minutes to allow elongation and finally 85^0 C for 5 minutes to terminate the reaction. cDNA was stored at -20^0 C.

2.6 Quantitative Reverse Transcribed-Polymerase Chain Reaction (QRT-PCR)

QRT-PCR was carried out in triplicates on the cDNA samples obtained (as described above) on an iCycler (Bio-Rad Laboratories, Hercules, CA) using the iQ SYBR Green Supermix (Bio-Rad, UK) according to the manufacturer's protocol. The housekeeping gene Hypoxanthine Guanine Phosphoribosyl Transferase (HPRT) was used to allow template quantification. For each gene, the amplification was compared to a dilution series of cDNA prepared from embryo head RNA using the Absolutely RNA miniprep (Agilent, US) kit. QuantiTech Primers were purchased by Qiagen (Germany). Each reaction mixture contained: 1µl (~1µg) cDNA, 2µl QuantiTech primers, 10µl iQ SYBR Green Supermix and 7µl DNAse/RNAse-free distilled water (Life Technologies, US). Quantitative Real Time PCR was performed under the conditions of the 2StepMelt Quantitect protocol, according to the manufacturer's instructions.

2.7 DNA extraction and genotyping of mutant mice by PCR

DNA from mice was extracted from 2mm ear biopsies by digesting tissue in 100µL lysis buffer containing 50 mM KCl, 1.5 mM $MgCl_2$, 10 mM Tris-HCl (pH 8.5), 0.01% gelatin, 0.45% Nonidet P-40, 0.45% Tween 20, and 0.5 µg/ml proteinase K (Sigma-Aldrich, US) in ultra-pure water (Invitrogen, US). The samples were incubated at 500rpm at 56^0C overnight for digestion. The

samples were then spun briefly and 1µL supernatant containing the DNA (~1µg) was used as template. Primers used for amplifying the PCR products are listed in Table 2.2. Each PCR reaction consisted of a 20µL mix composed of 10µl GreenTaq DNA Polymerase (Sigma-Aldrich, US) and 1µM of each relevant primer made in ultra pure water (Invitrogen, US). PCR was carried out on a Robocycler (Stratagene, US) or a Prime (Techne, UK) PCR machine as follows: 5 min at 94^0C followed by 30-40 cycles for 90 seconds at 94^0C, a primer-specific step (Table 2.3) and 60 seconds at 72^0C. The products were resolved on 2% agarose (Sigma-Aldrich, US) 1x TBE (Life Technologies, US), stained with 1% GelRed (Biotium, US). A 100bp ladder marker (Bioline, UK) was electrophorised to estimate band size. The gel was visualized under UV light (Herolab, Germany) and a photograph was taken.

Strain	Primer sequence (5’ → 3’)
Ihh WT (St-Jacques, Hammerschmidt et al. 1999)	AGGAGGCAGGGACATGGATAGGGTG
	AGGAACAGACAGAACCGCAGTCGGG
Ihh KO (Outram, Hager-Theodorides et al. 2009)	AGGAGGCAGGGACATGGATAGGGTG
	TACCGGTGGATGTGGAATGTGTGCG
Dhh WT (Lau, Outram et al. 2012)	ATCCACGTATCGGTCAAAGC
	GGTCCAGGAAGAGCAGCAC
Dhh KO (Lau, Outram et al. 2012)	GGCATGCTGGGGATGCGGTG
	CCAGGAAGACGAGCACTGGCGTG
Shh KO (Outram, Hager-Theodorides et al. 2009)	CTGTGCTCGACGTTGTACTG
	AAGCCCGAGACTTGTGTGGA
Gli3 KO (Hager-Theodorides, Dessens et al. 2005)	GGCCCAAACATCTACCAACACAT
	GTTGGCTGCTGCATGAAGACTGAC
KiF7 WT (He, Subramanian et al. 2014)	CTGCCTTTCCCAGCCACCTGACAT
	GGGAGAGGACACTGGGCAAGA
KiF7 KO (He, Subramanian et al. 2014)	CTGCCTTTCCCAGCCACCTGACAT
	GCAGCGCATCGCCTTCTATC
HY-TCR (Kisielow, Teh et al. 1988)	CACATGGAGGCTGGTGCATCAG
	GTTTCTGCACTGTTATCACC
Cre^{+} (Outram, Hager-Theodorides et al. 2009)	CGATGCAACGAGTGATGAGG
	GCATTGCTGTCACTTGGTCGT
Shh Floxed (Zuklys, Gill et al. 2009)	ATGCTGGCTCGCCTGGCTGTGGAA
	GAAGAGATCAAGGCAAGCTCTGGC
Ihh Floxed (St-Jacques, Hammerschmidt et al. 1999)	AGCACCTTTTTTCTCGACTGCCTG
	TGTTAGGCCGAGAGGGATTTCGTG
Lck-Gli2N_2 / Gli2C_2 (Rowbotham, Hager-Theodorides et al. 2007)	CGAACCACTCAGGGTCCTGTG
	GGATTTCTGTTGTGTTTCCTC
Rag WT (Mombaerts, Iacomini et al. 1992)	TAGACACTTCTGCCGCATCTGTGG
	GGAGTCAACATCTGCCTTCACG
Rag KO (Mombaerts, Iacomini et al. 1992)	TAGACACTTCTGCCGCATCTGTGG
	TGACCGCTTCCTCGTGCTTTAC

Table 2.2: The forward (top) and reverse (bottom) primer used for genotyping of different mice strains

Strain	Annealing T	Duration	No of cycles
Ihh WT	66	60	33
Ihh KO	62	60	40
Dhh WT	58	60	35
Dhh KO	58	60	35
Shh KO	58	60	34
Gli3 KO	59	80	34
KiF7 WT	59	45	30
KiF7 KO	59	45	30
HY-TCR	58	60	35
Cre^{+}	61	90	32
Shh floxed	58	60	35
Ihh floxed	62	60	40
Lck-$Gli2N_2$	58	60	30
Lck-$Gli2C_2$	58	60	30
Rag WT	58	60	35
Rag KO	58	60	35

Table 2.3: Specific parameters for genotyping of mutant mice by PCR

2.8 Lipopolysaccharide (LPS) injection

Littermates of 6-8 weeks were injected intraperitoneally (ip) with a single dose of 10-100ng/gram of body weight LPS in 200μl of sterile PBS. The control group was injected ip with 200μl sterile PBS. Injections were performed with a 1ml syringe (Terumo, Philippines) and a 25G needle (BD Microlance, Ireland). Animals were sacrificed 4 days later and blood and tissues were collected for further analysis.

2.9 Hydrocortisone (HC) injection

$Ihh^{+/-}$, Ihhfl/fl-CD4Cre-HY^{-}, Ihhfl/fl-CD4Cre-HY^{+} mice and WT littermates were injected with a single dose of 0.4mg/gram of body weight pure HC (water-soluble HC, Sigma, UK) dissolved in 250µl sterile and filtered PBS using a 0.22µm Millex filter (Millipore, Ireland). For each injection, a 1ml syringe (Terumo, Philippines) and 25G needle (BD Microlance, Ireland) was used. Animals were sacrificed 2, 4 and 6 days later and thymi were collected for further analysis.

2.10 Human γδ analysis

2.10.1 Human γδ selection

Human thymi were collected at Great Ormond Street Hospital from donors undergoing cardiac surgery with informed consent. Thymocyte suspensions were obtained by meshing thymi using a 70µm nylon cell strainer (Corning, US) in RPMI. Peripheral blood mononuclear cells (PBMCs) were isolated from fresh blood donated by healthy donors via the NHS National Blood Service. Lymphocytes were isolated using Lymphoprep (Axis-Shield, Norway) density gradient separation according to manufacturer's instructions. γδ T cells were isolated using the Anti-TCRγδ MicroBead Kit (Miltenyi Biotec, Germany) according to the manufacturer's protocol. On average, starting from a suspension of 10^8 thymocytes, $5x10^5$ – 10^6 cells were obtained with ~95% purity for $CD3^+$ / $γδ^+$ cells, assessed by flow cytometry at C6 (BD Biosciences, US) flow cytometer.

2.10.2 Human γδ expansion culture

γδ T cells were expanded from freshly isolated pure populations of γδ T cells obtained either from thymocytes or PBMCs (see 2.12.1). Cells were cultured at a concentration of $5x10^5$ cells/ml in a 48-well flat bottom plate (Corning, US) in RPMI medium containing 10% FCS, 1% Penicillin/ Streptomycin (PS) (Sigma, UK), 100U/ml IL-2 (PeproTech, US) and 120U/ml IL-21 (PeproTech, US). Irradiated artificial Antigen Presenting Cells (aAPCs), a K562 cell line engineered to express CD86, CD137L and IL-15, were added in the medium every 7 days at a concentration of 1:2 γδTcell:aAPC, to boost expansion. aAPCs were kindly provided by Kenth Gustafsson, Molecular Immunology, ICH, UCL. Cells were transferred to a T-75 flask (Corning, US) after 16-21 days and were harvested 2-3 days later with an average yield of $8x10^7$ cells.

2.10.3 Irradiation

10^7cells/ml aAPCs in RPMI medium were given a single dose of 80 Gy from a ^{60}Co gamma-ray source at a dose rate of 0.28 Gy/min. Irradiated cells were stored at -80°C.

2.10.4 Human γδ recombinant hedgehog (rHh) cultures

Expanded γδ T cells were transferred to 6-well plates (Corning, US) with a concentration of $2x10^6$ cells/well. Each well contained 2ml RPMI 1640 medium (Life technologies, US) supplemented with 10% FCS, 1% PS, 100U/ml IL-2 (PeproTech, US) and 120U/ml IL-21 (PeproTech, US). In addition, 1μg rShh (R&D Systems, US) or 1μg rHhip (R&D Systems, US) was added in each well. An untreated control was included for each time point. Cells were collected and analysed in days 1, 2, 4 and 6 as follows:

- RNA extraction - 10^6 cells
- Flow Cytometry - 5×10^5 cells
- PI stain - 2.5×10^5 cells

- Annexin V stain - 2.5 x 10^5 cells

2.11 Cell Counts

Single cell suspensions were diluted 1:1 in 0.1% w/v Trypan Blue (Sigma-Aldrich, US) in PBS and non-blue cells were counted using a haemocytometer. For spleenocytes counts, erythrocytes were distinguished by their biconcave shape and excluded from the count.

2.12 Experimental Data Analysis

Statistical analysis using at least three independent experiments was performed using GraphPad Prism (GraphPad Inc, US) and Microsoft Excel 2013 (Microsoft Inc, US). An unpaired two-tailed student's t test was used to test the significance of differences observed in WT, Het and KO littermates, unless stated otherwise. Values of $p<0.05$ were considered to be significant.

Results

3. Murine and human γδ cells can transduce Hh signals

3.1. Introduction

The effect of Hedgehog signalling pathway on the ontogeny, differentiation, development, survival, proliferation, localization, function and cytokine production of γδ T cells has not been investigated in depth. One publication has suggested that Hh signalling affects γδ thymocytes in two ways; the first is via Hh's major role in the differentiation and survival of very early T cell progenitors in the thymus, which give rise to both αβ and γδ T cells, and the second involves Hh's interaction with the Wnt signalling pathway, which is known to affect γδ thymocytes (El Andaloussi, Graves et al. 2006), (Melichar and Kang 2007). T-cell factor 1 (Tcf1) deficient mice, a key transcription factor required for Wnt signalling, showed impaired development of intestinal intraepithelial γδ lymphocytes (Ohteki, Wilson et al. 1996).

In addition, our group published data on γδ cells in a paper that investigated the role of Hh signalling in TCR repertoire selection in the thymus, and reported that constitutive transgenic expression of Gli2A in all T-lineage cells resulted in reduced $CD4^{-}CD8^{-}CD3^{+}\gamma\delta^{+}$ cells in the lymph node compared to WT mice (Furmanski, Saldana et al. 2012).

Here, we aim to test the hypothesis that Hh signalling regulates γδ T cell development and homeostasis in peripheral tissues. Investigation of γδ T cells is challenging because of the scarcity of these cells in different tissues. Another difficulty lies in the fact that γδ T cells are still not well characterised both in terms of ontogeny and function. In general, murine γδ T cells have been described in terms of a dichotomy between T-bet, IFNγ, CD27-expressing cells on the one hand and RORγt, IL-17, CCR6-

expressing cells on the other hand, but our understanding of the ontogeny and plasticity of the different γδ T cell populations is incomplete. For example, it is unclear whether TH17 γδ cells are developed postnatally or arise as a result of extrathymic plasticity of adult γδ T cell populations.

In this chapter we test if murine γδ T cells are capable of transducing Hh signals and if they do transduce Hh signals in vivo. We investigate expression of Hh pathway components in murine γδ T cell populations in the thymus and spleen, and use Hh-reporter mice to investigate the extent of Hh pathway activation in γδ T cell populations in different tissues in vivo.

3.2 Results

3.2.1 Hh signalling components are expressed in thymic γδ T cells

In order to investigate whether the Hh pathway plays a role in γδ T cells, we examined the expression of Hh components in γδ T cells from the thymus and spleen of 4 week old mice. In the case of the thymus, mRNA for qPCR was collected from FACS sorted $CD3^{+}\gamma\delta TCR^{+}$ (γδ cells), $CD4^{+}CD8^{+}$ (DP cells), whole thymus and $CD3^{-}CD25^{+}$ cells (DN2/DN3 cells) (Figure 3.1). This last population represents the DN2 and DN3 stages during thymocyte development and thus allows us to compare the expression of Hh components in γδ T cells with expression in thymocyte progenitors (DN2 and DN3 cells).

We found that in the 4 week old murine thymus, several components of the Hh signalling pathway are expressed in γδ cells. We detected *Ihh* at levels higher than in the $CD25^{+}$ DN population, at similar levels to the whole thymus. We failed to detect Shh or Dhh. We also detected expression of *Gli1* and *Gli3*, as well as very low expression of *Gli2*, in all three cases. However, expression was lower than that observed for the DN2/DN3 progenitor population (Figure 3.1). We detected expression of the Hedgehog pathway's key receptors required for Hh signalling, *Smo* and *Ptch*. We also detected expression of *Dispatched*, which is required to secrete Hh proteins, suggesting that γδ T cells can secrete Ihh. *Rab23*, an inhibitor of Hh signalling was also present. *Sox13*, a γδ-specific transcription factor, was used as a positive control, and was detected in the γδ+ thymocytes only (Figure 3.2).

3.2.2 Hh signalling components are expressed in splenic γδ T cells

We then sorted CD4+ T cells, CD8+ T cells and γδTCR+ cells from 4 week old WT spleen and made RNA for qPCR analysis (Figure 3.3). Expression of several Hh components were also present in the T cell populations in the spleen of WT mice. We detected *Ihh* in splenic γδ T cells, as well as in $CD3^{+}\gamma\delta TCR^{-}CD4^{+}$ and $CD3^{+}\gamma\delta TCR^{-}CD8^{+}$ cells. *Ihh* has previously been shown to be expressed in CD4 and CD8 single positive (SP) populations in the thymus, and in CD8+ spleen-derived cytotoxic T lymphocytes (Outram, Hager-Theodorides et al. 2009), (de la Roche, Ritter et al. 2013). Similarly to the thymus, we failed to detect *Shh* and *Dhh*. *Gli1*, a Hh-target gene, was also detected, as was *Gli2*, but we did not detect Gli3. As found in the thymus, *Smo*, *Ptch* and *Dispatched* were expressed in all three populations (Figure 3.3).

3.2.3 Hh-reporter mice show active Hh-mediated transcription in γδ T cell populations in vivo

Our expression analysis showed that γδ T cells from the thymus and spleen express components of the Hh signalling pathway and so are capable of transducing Hh signals. To examine Hh pathway activation status in γδ T cell populations in vivo, we used a transgenic (tg) Hh-reporter mouse. This Gli Binding Site-Green Fluorescent Protein (GBS-GFP) transgene contains multiple Gli Binding Sites with a minimal promoter which drives GFP expression in cells in which Hh-mediated (Gli-mediated) transcription is active. Hh proteins are expressed in the spleen and thymus, and are also involved in regulating tissue homeostasis in non-lymphoid organs such as the lung, skin and gut. The extent of Hh pathway activation in a given γδ T cell will therefore depend on its localization, relative to the source of Hh. We therefore used flow cytometry to measure GFP expression at the single cell level in γδ T cell populations from different tissues (Figure 3.4).

Approximately 6.5% of γδ thymocytes and 8.5% of γδ cells from the spleen were positive for GFP, indicating active Hh-dependent transcription. We gated on GFP(+) γδ cells and examined cell surface CD27 and CD44 expression. In the thymus, all GFP(+) γδ cells were $CD27^{+}$, whereas in the spleen the majority of GFP(+) γδ cells were in the $CD44^{+}CD27^{-}$ population. When we examined CD24 expression, we found that in both thymus and spleen the γδ population that was undergoing active Hh pathway activation expressed cell surface CD24.

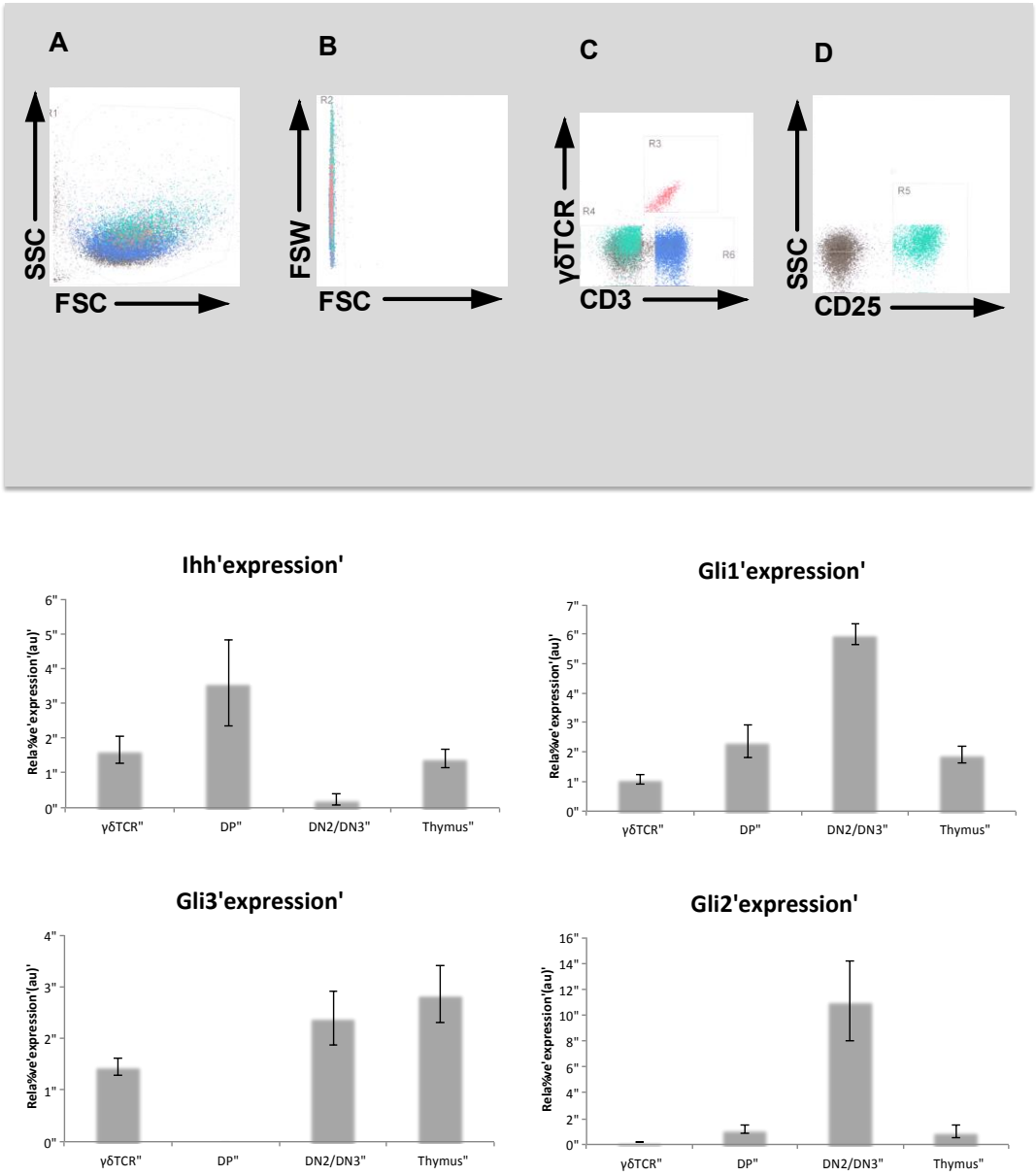

Figure 3.1: Expression of key Hh components in γδ T cells of murine WT thymus

Dot plots show the sorting strategy for γδTCR⁺, DN2 and DN3 thymocytes. A live gate (A) was drawn and (B) doublets were excluded. CD3⁺ γδ T cells were sorted, shown in red. From CD3⁻ cells (DN) cells, those who are CD25⁺ were sorted, named DN2 and DN3, here shown in green. Bar charts show relative transcription of *Ihh, Gli1, Gli2, Gli3* in the FACS sorted thymocyte populations described above. We were unable to detect *Shh* and *Dhh* in any of the populations described above. The scale shows expression normalized to the levels of the housekeeping gene *HPRT*. Error bars represent ±SEM.

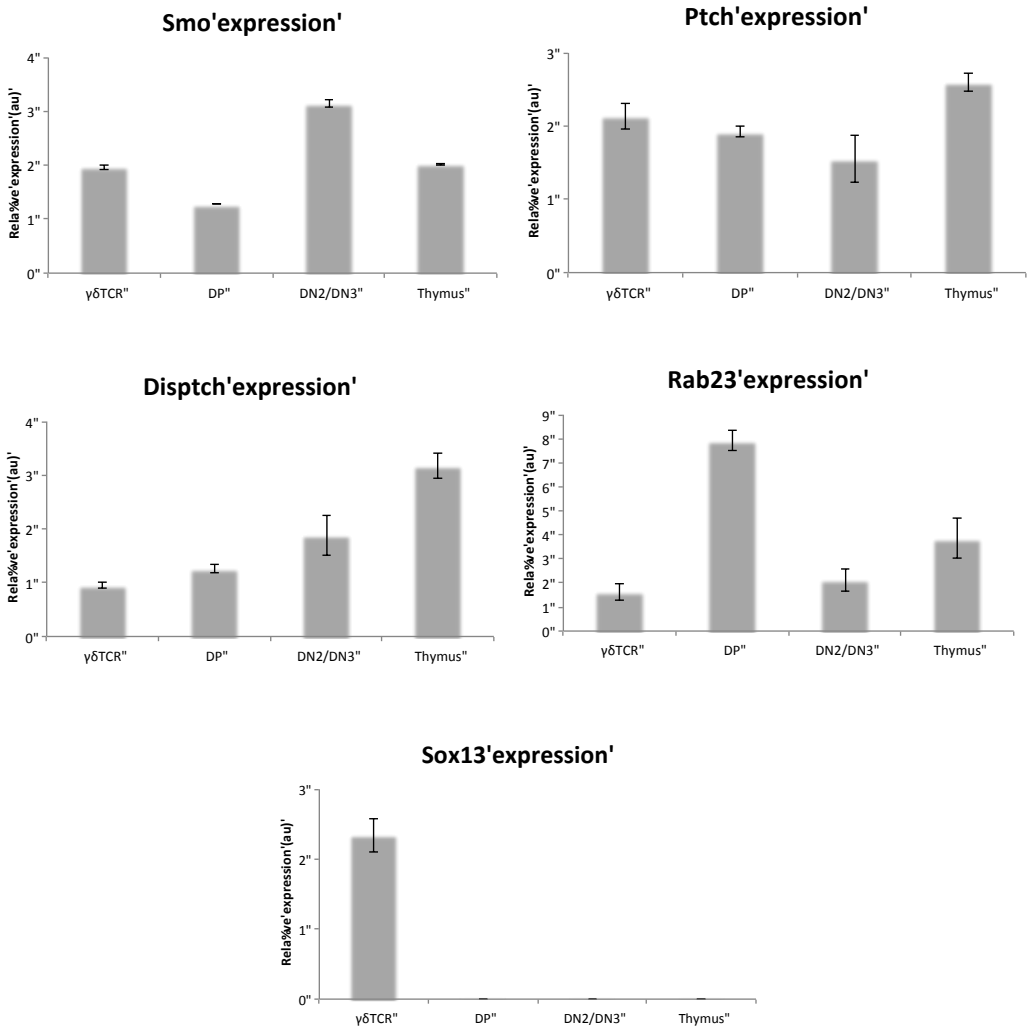

Figure 3.2: Expression of key Hh components and γδ-specific markers in γδ T cells of murine WT thymus

Bar charts show relative transcription of *Smo, Ptch, Disptch, Rab23* and the γδ-specific marker *SOX13*, in the FACS sorted thymocyte populations described above. The scale shows expression normalized to the levels of the housekeeping gene *HPRT*. Error bars represent ±SEM.

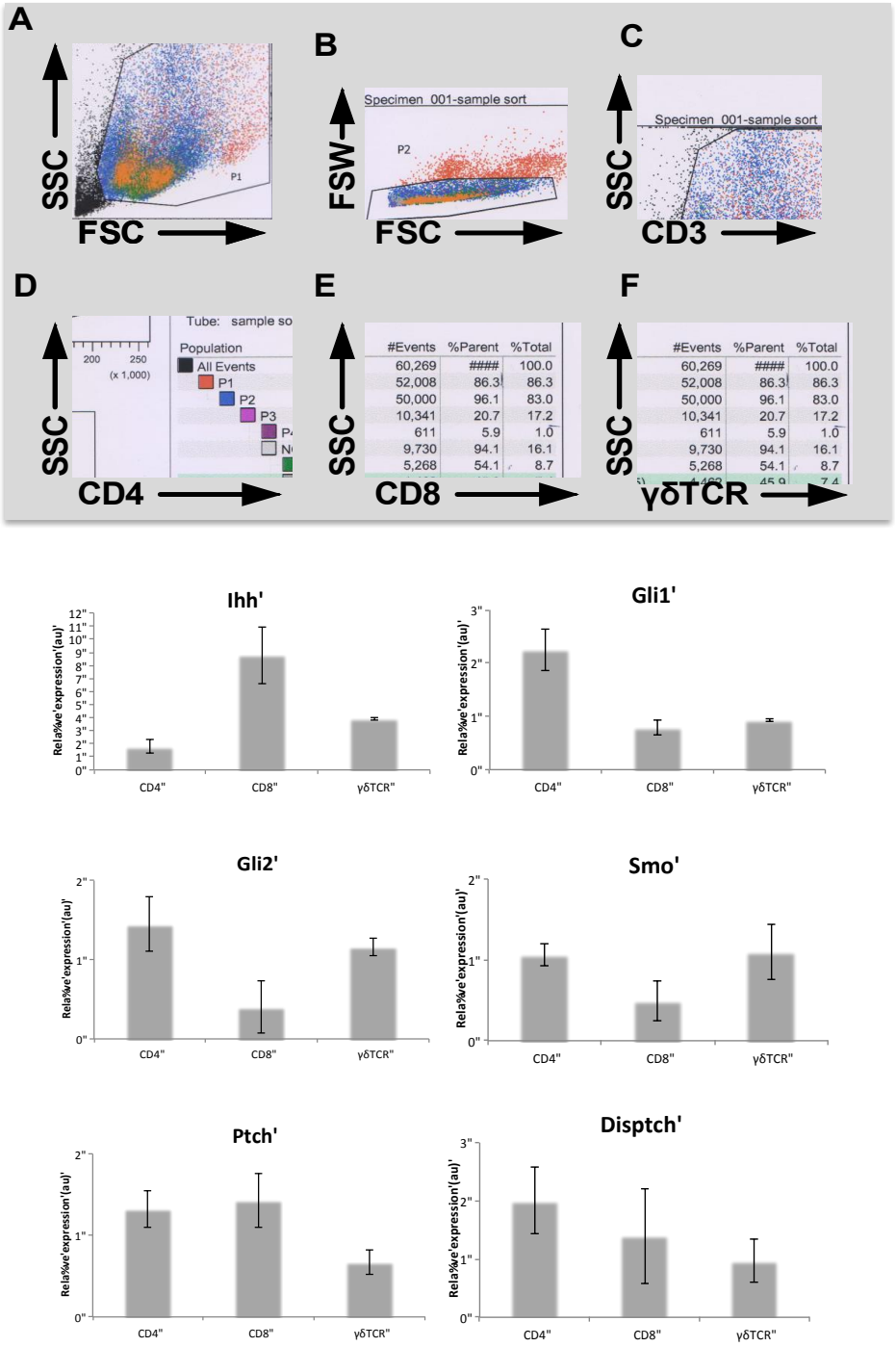

Figure 3.3: Expression analysis of Hh signaling components in the murine spleen

Dot plots show the sorting strategy of CD4, CD8 and γδTCR⁺ splenocytes. (A) A live gate was drawn and (B) doublets were excluded. CD3⁺ cells were sorted in relation to (D) CD4, (E) CD8 and (F) γδTCR⁺ cell surface expression. Bar charts show relative transcription of *Ihh, Gli1, Gli2, Smo, Ptch* and *Disptch*, in the FACS sorted splenocyte populations described above. We were unable to detect expression of *Shh, Dhh* and *Gli3* in any of the above populations. The scale shows expression normalized to the levels of the housekeeping gene *HPRT*. Error bars represent ±SEM.

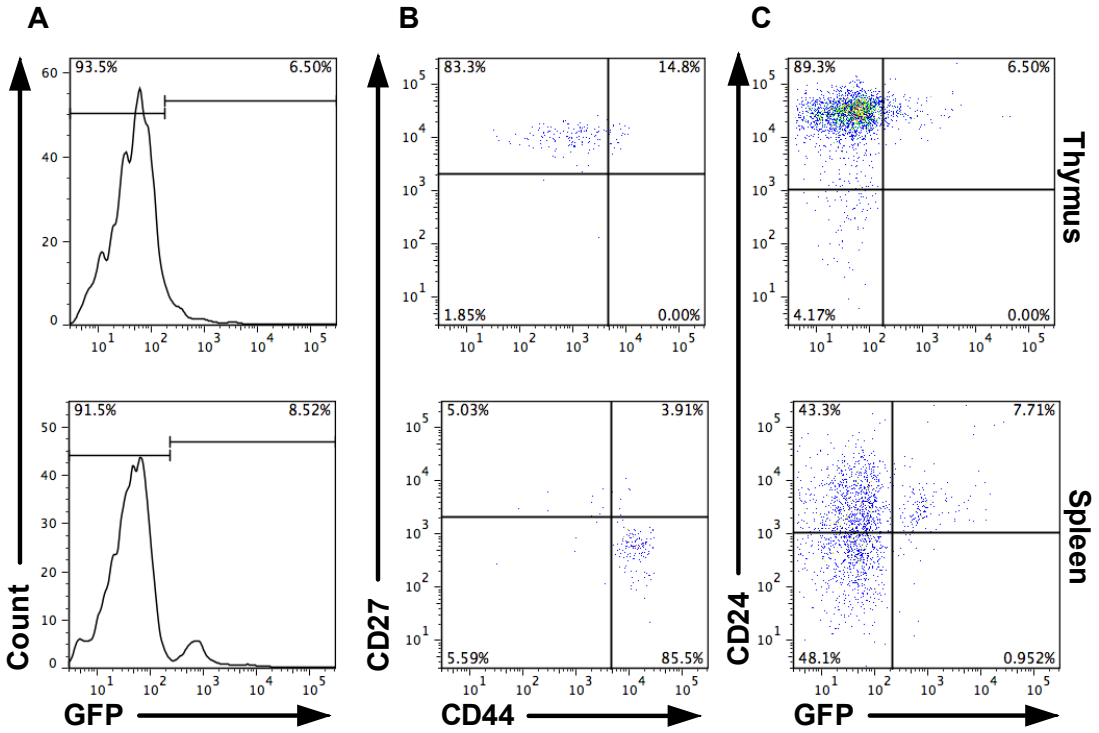

Figure 3.4: Gli Binding Site (GBS) GFP expression in the thymus and the spleen of 3 week old mice

Histogram (A) shows the proportion of thymic and splenic live-gated $CD3^{+}\gamma\delta TCR^{+}$ cells that are positive for GBS-GFP. Dot plots (B) show CD27 and CD44 expression on GFP(+) γδ T cells from thymus and spleen. Dot plots (C) show CD24 staining plotted against GFP.

4. The function of the Hh family proteins in γδ T cell development in the thymus

4.1 Introduction

We showed that thymic γδ T cells express components of the Hh signalling pathway and transduce Hh signals in vivo. In this Chapter we aim to investigate the specific contribution of each of the three Hh family members to γδ T cell development in the thymus. The three family members share a common signalling pathway, but have distinct, although partially overlapping functions. Their distinct functions in development and tissue homeostasis are the result of differences in their temporal and tissue restricted expression patterns, and may also reflect strength of signal induced by each family member. All three Hh family members are expressed in the thymus. Shh is expressed by thymic epithelial cells (TEC), situated mostly at the cortico-medullary junction and subcapsular region (Outram, Varas et al. 2000), (Sacedon, Varas et al. 2003), (El Andaloussi, Graves et al. 2006, Saldana, Solanki et al. 2016). Ihh is expressed by thymocytes and some TEC scattered through out the cortex (Outram, Varas et al. 2000), (Sacedon, Varas et al. 2003), (Outram, Hager-Theodorides et al. 2009)whereas Dhh is expressed by TEC (Sacedon, Varas et al. 2003). Therefore, to investigate the function of each Hh family member in γδ T cell development in the thymus, we first analysed thymic γδ T cell populations in mice mutant in *Shh*, *Ihh*, and *Dhh*.

4.2 Results

4.2.1 The role of Shh in γδ T cell development in the thymus

Shh can function as a morphogen, so that a concentration gradient specifies distinct cell fates according to concentration and duration of the

signal. Our laboratory has previously shown that Shh is an essential regulator of T cell development (Crompton, Outram et al. 2007). Shh is required for the DN1 to DN2 transition (Hager-Theodorides, Dessens et al. 2005), (Shah, Hager-Theodorides et al. 2004) and regulates the DN to DP transition (Outram, Varas et al. 2000), (Rowbotham, Hager-Theodorides et al. 2009) and the DP to SP transition (Rowbotham, Hager-Theodorides et al. 2007), (Saldana, Solanki et al. 2016) whereas the function of Shh in γδ T cells remains unknown.

Here, we used two different mice strains with impaired Shh production to test the hypothesis that Shh regulates γδ T cell development in the thymus. Shh KO is embryonically lethal, so we used $Shh^{+/-}$ mice and Shhfl/fl-FoxN1Cre^{+} tg mice (ShhcoKO) in which Shh is conditionally knocked out in TEC. Comparison between these two systems can provide insight into the source of Shh affecting γδ cells.

4.2.2 Adult γδ T cell populations in the $Shh^{+/-}$ thymus

We did not observe any difference in γδ cell numbers in the $Shh^{+/-}$ thymus compared to WT (Figure 4.1A). However, in the adult $Shh^{+/-}$ thymus, CD27 expression was modestly but significantly downregulated (Figure 4.1B). In addition, the percentage of the $CD44^{+}CD27^{-}$ γδ population was increased (Figure 4.1E), whereas the $CD27^{+}CD44^{+}$ γδ subset was downregulated (Figure 4.1G), and the overall proportion of γδ thymocytes that expressed CD44 was decreased, although these changes were not significant.

4.2.3 $Shh^{+/-}$ γδ thymocytes show reduced Hh-mediated transcription in vivo

Our data show that Shh influences γδ cell development and differentiation in the thymus. Shh may be signalling directly to γδ cells or its effects may be indirect through another cell type. Therefore, to test the impact of Shh-heterozygosity on Hh pathway activation in γδ thymocyte populations in

vivo, we crossed the $Shh^{+/-}$ mice with Hh-reporter mice (GBS-GFP-tg) mice and compared GFP expression by flow cytometry in defined γδ thymocyte populations from $Shh^{+/+}$-GBS-GFP-tg and $Shh^{+/-}$-GBS-GFP-tg thymus (Figure 4.1H). We found that ~1.5% of γδ thymocytes expressed GFP in the $Shh^{+/+}$ thymus, and this was reduced by approximately two-thirds in the $Shh^{+/-}$ mice.

4.2.4 Conditional deletion of Shh from TEC

Thymic epithelial cells are believed to be the main source of Shh in the mouse thymus, so we used Cre-loxP technology to conditionally delete Shh from all TEC using TEC-specific FoxN1-Cre (Saldana, Solanki et al. 2016). In the ShhcoKO adult thymus, the number of γδ thymocytes was reduced, compared to Cre^{-} (WT) littermates (Figure 4.2A and B). This reduction in γδ thymocyte numbers was not observed in the $Shh^{+/-}$ thymus, and suggests that TEC are the major source of Shh in the thymus.

4.2.5 Shh-treatment of WT FTOC

To investigate the impact of recombinant (r) Shh treatment on γδ thymocyte numbers and cell surface phenotype, we cultured E14.5 WT FTOC with rShh for 5 days. Addition of rShh increased the proportion of γδ cells in the E14.5 + 5 day FTOC and significantly increased the proportion of γδ thymocytes that expressed cell surface CD44 (Figure 4.3). This was consistent with the observation that the $CD44^{+}$ γδ thymocytes are undergoing active Hh signalling in the GBS-GFP-tg reporter experiments.

As the increase in the proportion of γδ thymocytes in the rShh-treated cultures may have been the result of the action of rShh to inhibit differentiation from DN to DP thymocyte (Outram et al 2000), we also carried out FTOC with E16.5 WT thymic lobes in the presence of rShh or

rHhip (to neutralize endogenous Hh molecules in the cultures), and analysed them after 5 days. We did not find an influence of rShh treatment on the number of γδ cells in the E16.5 + 5 day FTOC (Figure 4.4A and B). Interestingly, rHhip-treatment of E16.5 WT FTOC led to a significant decrease in the number of γδ thymocytes, indicating that endogenous Hh proteins present in the fetal thymus are required for normal γδ thymocyte production (Figure 4.4C and D). This is consistent with the reduction in γδ cell numbers observed in the ShhcoKO adult thymus. We also observed a significant down-regulation of CD27 in rShh treated E16.5 + 5 day FTOC (Figure 4.4E).

4.2.6 Ihh signalling in γδ T cell development in the thymus

Ihh is expressed by DP and SP thymocyte populations (Outram, Hager-Theodorides et al. 2009) and in sorted γδ thymocytes (Figure 4.7). Ihh-mediated Hh signalling both promotes and restricts T cell development, as Ihh, secreted from DP cells, together with Shh, secreted by TEC, promote differentiation of DN1 cells to DN2. However, Ihh negatively regulates pre-TCR-induced differentiation to DP stage. The role of Ihh on the development γδ T cells had not previously been investigated. We therefore investigated the impact of Ihh-mutation on γδ thymocyte development.

We measured γδ thymocyte population number and cell surface phenotype in $Ihh^{+/-}$ adult thymus, E14.5 and E15.5 Ihh-mutant thymi and $CD4Cre^{+}$-Ihhf/fl (IhhcoKO) adult mice, in which Ihh is conditionally deleted from all cells that have expressed CD4.

Of the three Hh ligands, Ihh affected γδ cells the least. There was no difference in the proportion of γδ thymocytes in adult $Ihh^{+/-}$ thymus compared to WT (Figure 4.5A and B) or in E14.5 or E15.5 Ihh-mutant

thymus or adult IhhcoKO thymus compared to WT littermates (data not shown). We performed a detailed analysis by flow cytometry staining against NK1.1, CD4, CD122, CD27, CD44, CD24, CCR6, CCR7, IFNγ and IL-17, and the only difference we observed was a increase in CD4-expressing γδ cells in the adult $Ihh^{+/-}$ thymus, compared to WT (Figure 4.5C).

4.2.7 The role of Dhh in γδ T cell development

Although not expressed by thymocytes, Dhh is expressed by thymic epithelial cells (Sacedon, Varas et al. 2003). The function of Dhh in γδ T cells is unknown. Unlike mutant Ihh and Shh mice, $Dhh^{-/-}$ mice are born healthy and viable. Therefore, in order to examine the role of Dhh on γδ T cells, we compared WT to $Dhh^{-/-}$ mice.

4.2.8 The adult Dhh-deficient thymus

The $Dhh^{-/-}$ thymus showed a small and non-significant reduction in γδ T cell count and percentage compared to WT (Figure 4.6A,B). The $Dhh^{-/-}$ thymus showed a significant reduction in the proportion of $CD27^{+}CD44^{+}$ γδ cells. Virtually all WT γδ thymocytes are $CCR7^{-}$ and only around 3% stained positive for CCR6. Deletion of Dhh increased CCR6 expression compared to WT (Figure 4.6G). In addition, CD4 expression decreased on Dhh KO γδ thymocytes compared to WT (Figure 4.H).

4.2.9 γδ thymocytes in the fetal Dhh-deficient thymus

We analysed γδ thymocyte populations in E17.5 $Dhh^{-/-}$ thymi. Due to the small size of the fetal tissues and the scarcity of γδ cells, our analysis was restricted to a few γδ markers. As seen in the adult, we found no overall difference in the number of γδ thymocytes (Figure 4.7A) but deletion of Dhh resulted in a higher percentage of $CD44^{+}CD27^{-}$ γδ cells and downregulation of CD24 expression (Figure 4.7B,C). However, as these data were obtained from only one litter, more embryos need to be

examined to confirm our findings. Interestingly, in the fetal spleen Dhh-deficiency also appeared to decrease cell surface expression of CD27 on γδ cells compared to WT, and this observation will also be confirmed when more embryos are available.

4.2.10 Treatment of WT FTOC with rDhh and rHHip

We showed that treatment of WT FTOC with rShh increased the proportion of γδ cells recovered, whereas treatment with rHhip (which binds to Hh proteins and neutralizes them) decreased γδ cells in FTOC. As Dhh and Shh have been suggested to have different binding affinities, we also tested the impact of rDhh treatment on γδ cell numbers in FTOC. We treated E17.5 FTOCs with rDhh or rHhip and analysed them after 6 days in culture. We retrieved more γδ cells from the rDhh-treated culture than control untreated cultures, whereas the rHhip treatment reduced γδ cells, as seen in Figure 4.7D.

4.2.11 The effect of Shh and Dhh double deficiency on γδ T cells

We have investigated the role of the Shh KO and the Dhh KO on γδ T cells in the thymus, but as both Shh and Dhh are expressed by TEC, we tested the impact of double deficiency. We crossed Dhh KO with ShhcoKO ($Shh^{fl/fl}$-$FoxN1Cre^{+}$) mice to generate animals in which both Dhh and Shh are knocked out from TEC in the thymus.

The double KO mice had significantly fewer γδ thymocytes than WT littermates (Figure 4.8A,B). This suggested an additive effect of double deficiency, as neither the DhhKO or the ShhcoKO showed significantly fewer γδ cells in the thymus. Some small and not significant changes were observed on CD27 and CD44 expression (Figure 4.8E). No change was observed in terms of Vγ chain usage (data not shown). In the double KO, we also observed ~30% reduction of $CD122^{+}NK1.1^{+}$ cells, and this change was reversed in the DhhKO $Shh^{+/+}$ littermates (Figure 4.8F).

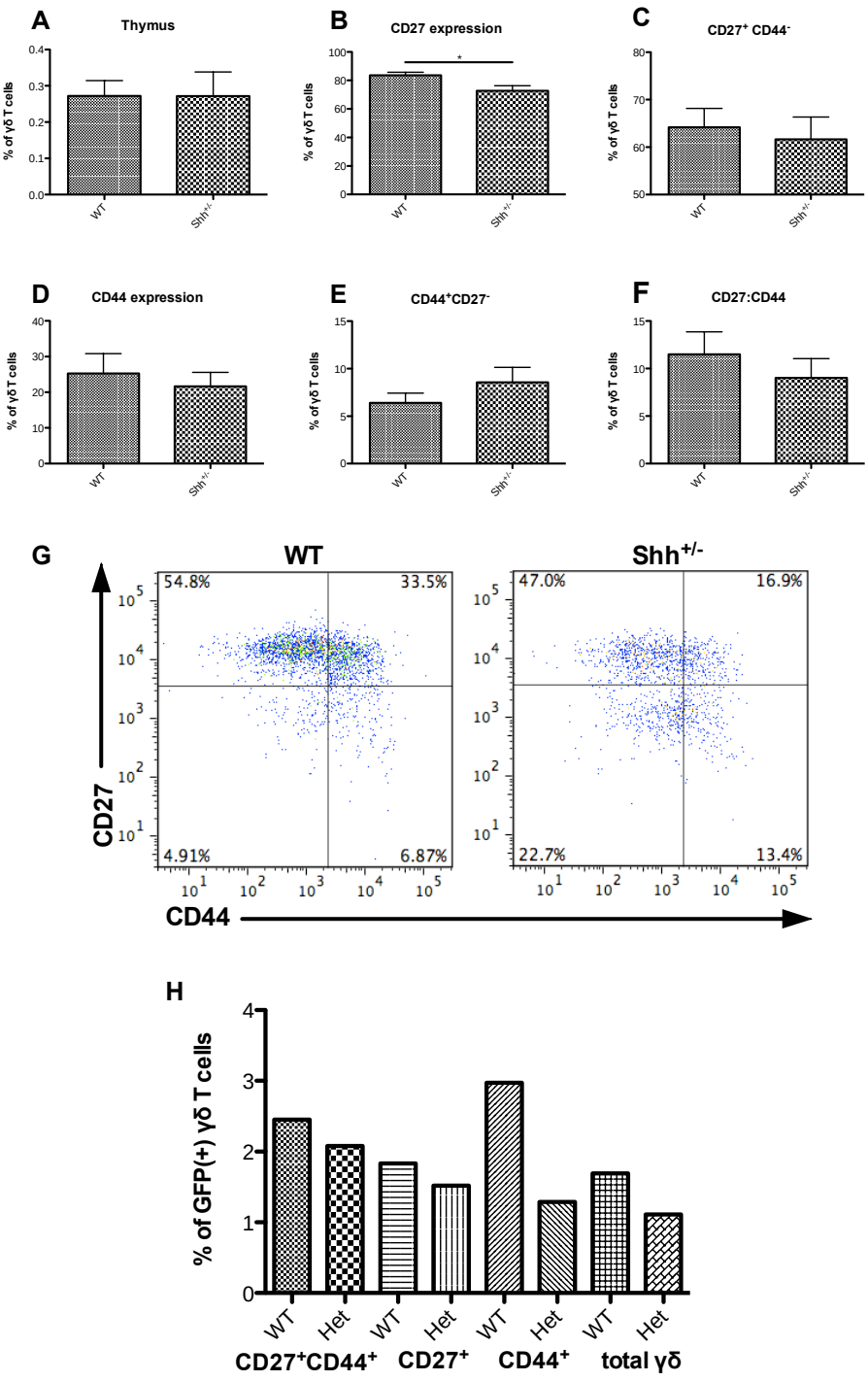

Figure 4.1: Development of γδ T cell subtypes in the adult Shh$^{+/-}$ thymus

Bar chart (A) shows the proportion of live-gated thymocytes that are CD3^{+}γδTCR^{+}. Bar charts show expression of (B) CD27 and (D) CD44 in γδ T cells; (C) shows percentage of γδ cells that are CD27^{+}CD44^{-} and (E) CD44^{+}CD27^{-}. (F) shows the ratio of CD27^{+}CD44^{-} to CD27^{-}CD44^{+} γδ T cells. Error bars represent ±SEM. (G) Representative dot plots show cell surface expression of CD27 and CD44 on γδ T cells from WT and Shh$^{+/-}$ thymus. Bar chart (H) shows expression of GBS-GFP in CD27^{+}CD44^{+}, CD27^{+}CD44^{-} and CD44+CD27- γδ T cell populations in the thymus of young adult Shh$^{+/-}$ and Shh$^{+/-}$-GBS-GFP^{+} mice. *p<0.05, n=11

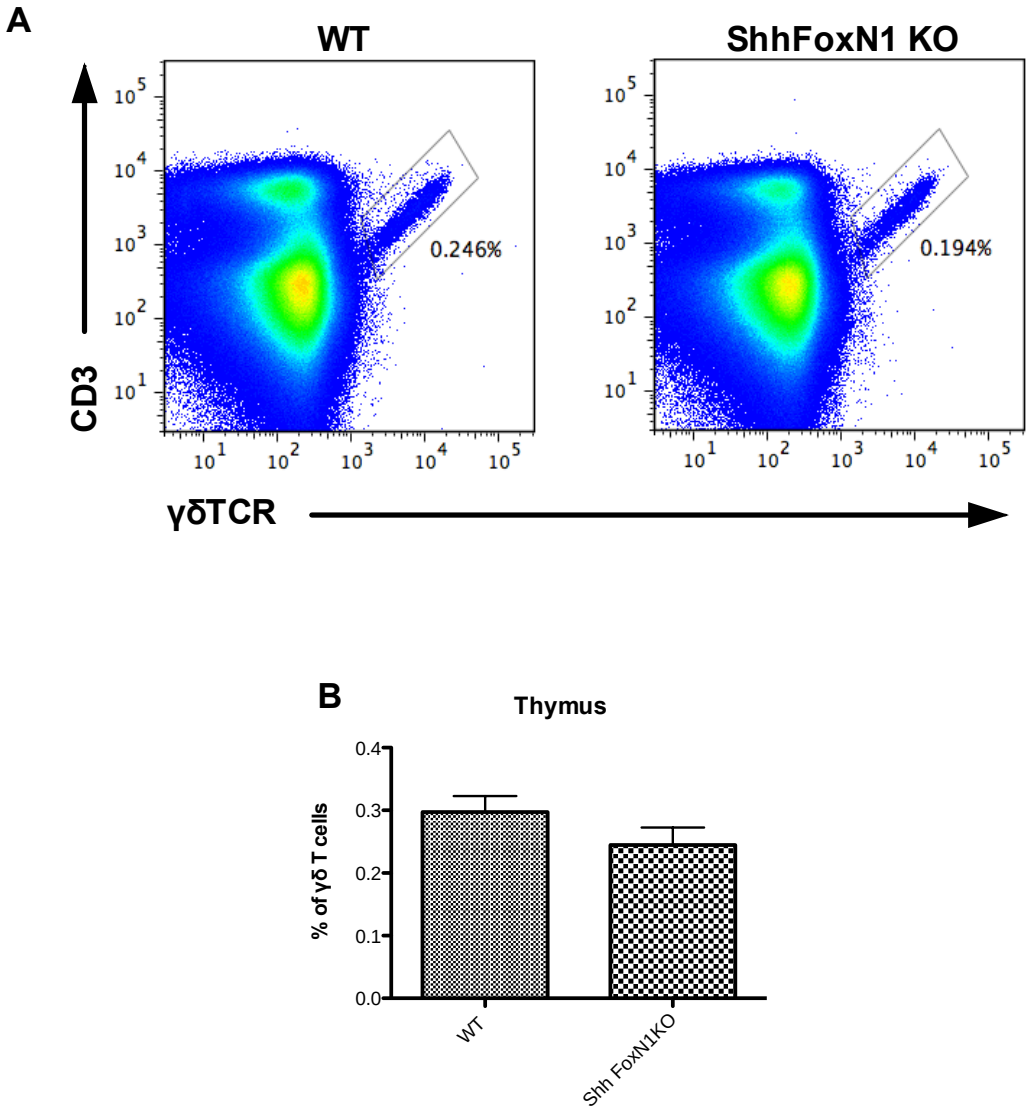

Figure 4.2: Percentages of γδ T cells in Shhfl/fl FoxN1-Cre thymus, spleen and lymph nodes

Representative dot plots (A) show percentage of $CD3^{+}\gamma\delta TCR^{+}$ thymocytes isolated from WT and Shh FoxN1 KO mice. Bar chart (B) show the percentages of $\gamma\delta TCR^{+}$ cells in thymus of WT and Shh FoxN1 KO mice. n=6

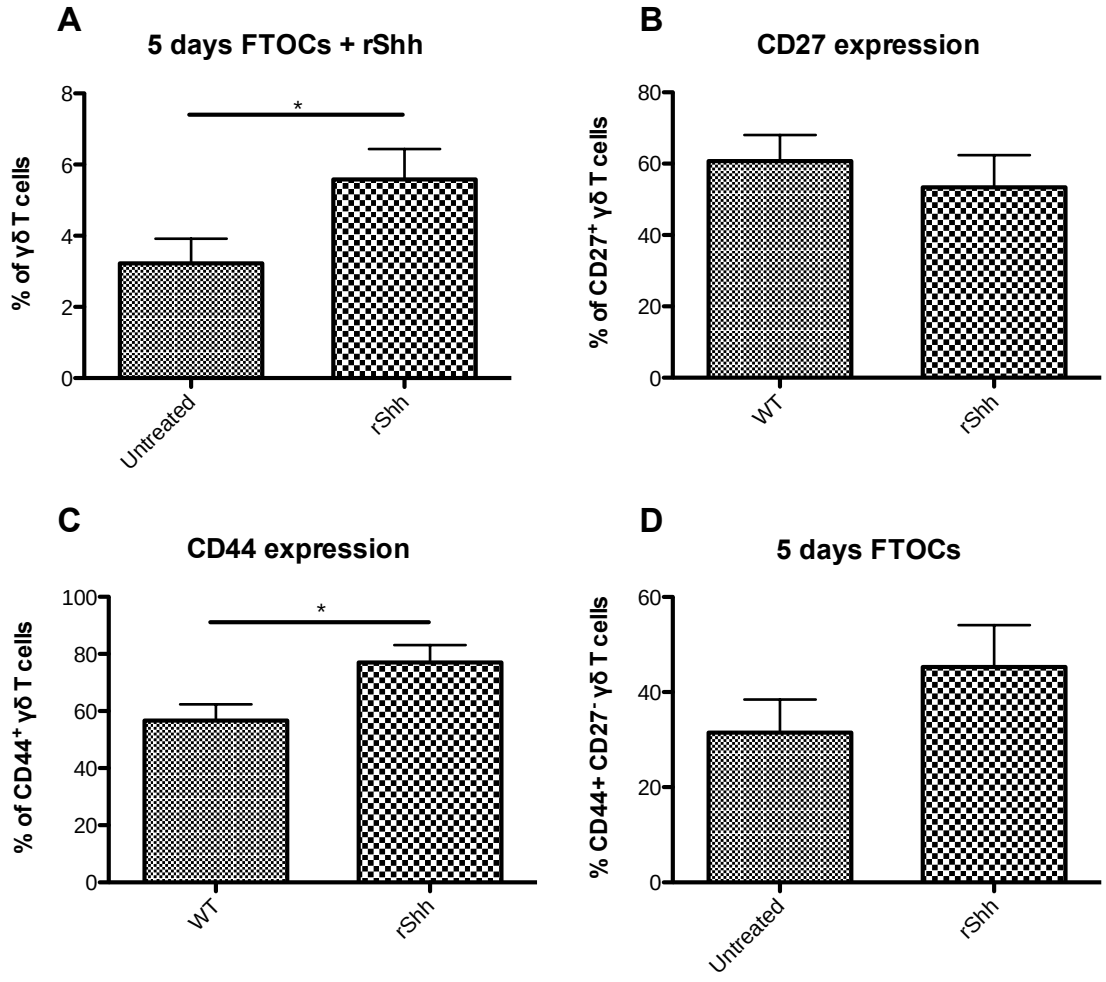

Figure 4.3: Numbers of γδ T cells and surface expression of key markers in E14.5 fetal thymus organ cultures (FTOC)

For each experiment, one E14.5 WT thymic lobe was cultured untreated and the other thymic lobe of the same thymus was cultured in the presence of rShh for 5 days. Histogram (A) shows the percentage of γδ T cells in WT and rShh-treated thymi as analysed by flow cytometry, after 5 days of culture. Histograms show CD27 (B) and CD44 (C) expression of γδ T cells, as well as percentage of $CD44^{+}CD27^{-}$ γδ T cells (D). Error bars represent ±SEM. *$p<0.05$, n=14

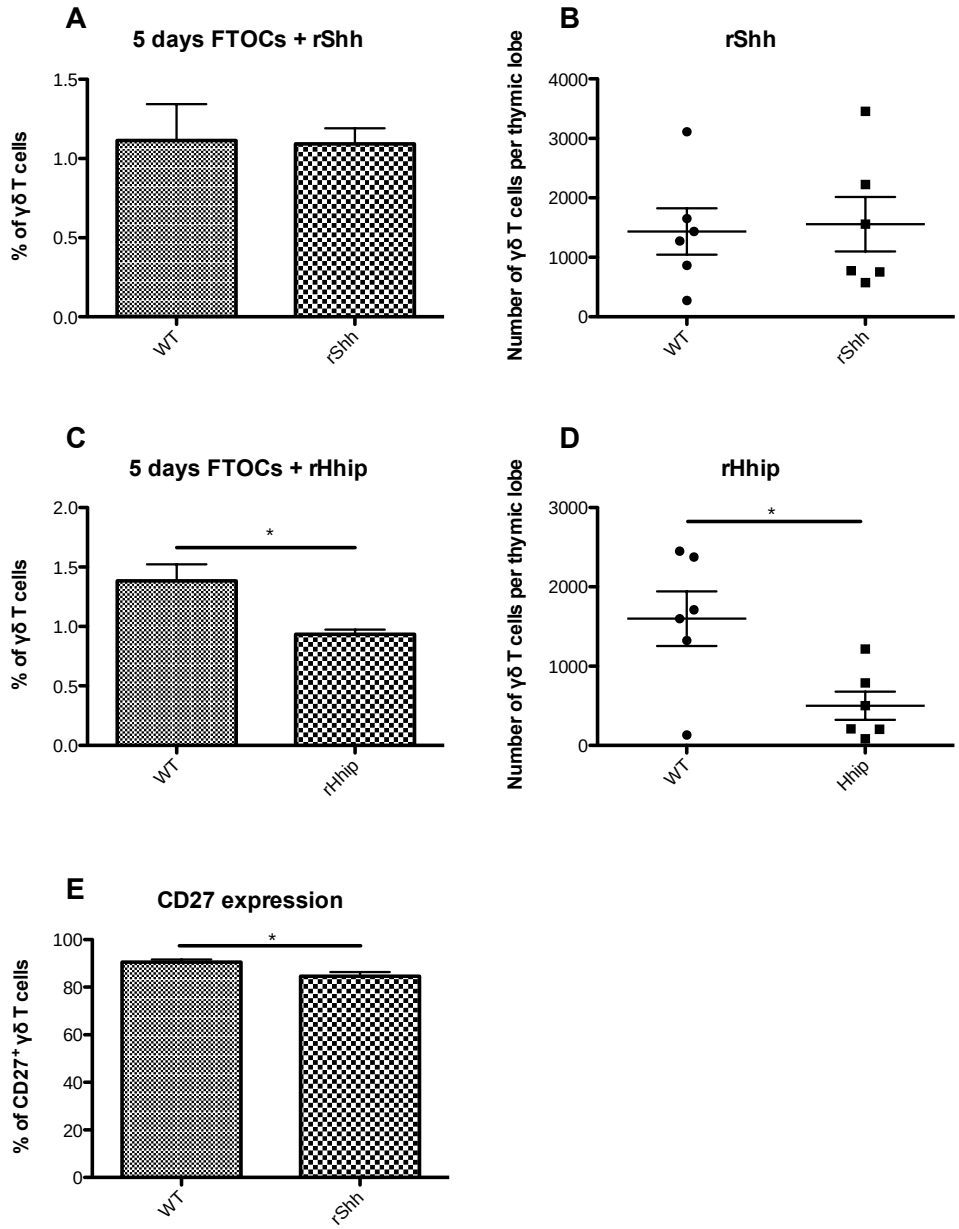

Figure 4.4: Numbers of γδ T cells and surface expression of key markers in E16.5 FTOC

Fetal thymic cells were analysed by flow cytometer to identify the major γδ T cells subtypes based on cell surface expression of CD27 and CD44. For each experiment, one E16.5 WT thymic lobe was cultured for 5 days untreated and the other thymic lobe of the same thymus was cultured for 5 days in the presence of rShh. Scatter graphs show the cell number of each individual WT untreated and (B) rShh-treated or (D) Hhip-treated E16.5 FTOC cultured for 5 days. The mean of each group is indicated by a line. Bar charts show γδ T cell percentages in WT untreated and WT + rShh (A) or WT + rHhip (C) E16.5 thymic lobes, analysed after 5 days in FTOCs. (E) Expression of CD27 in WT and rShh-treated thymic lobes in 5 days FTOCs. Error bars represent ±SEM. *$p<0.05$, n=12

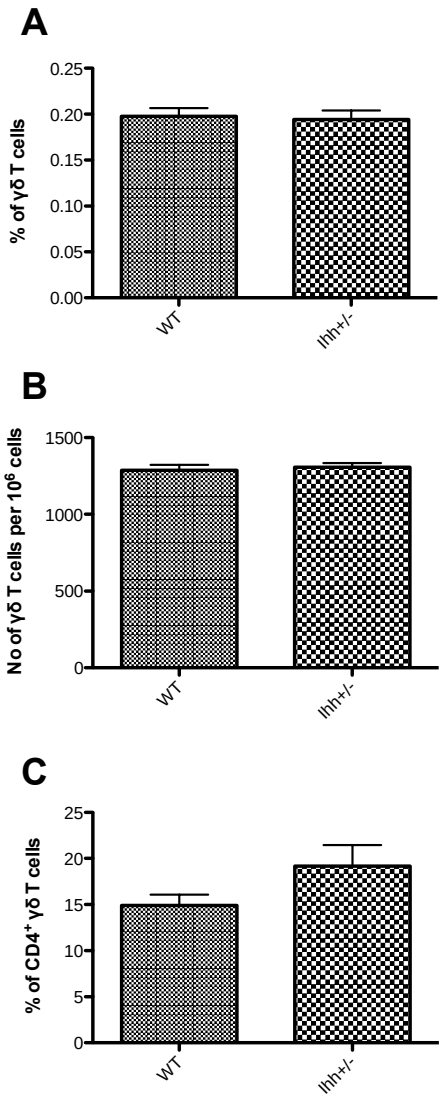

Figure 4.5: The role of Ihh in thymic γδ T cells

Bar charts (A) and (B) show the percentage and cell count of γδ cells in the thymus. (C) shows a small upregulation of CD4 in the thymus of $Ihh^{+/-}$ mice No differences were observed for NK1.1, CD122, CCR6, CCR7, Vγ chains and subtype populations as well as IFNγ and IL-17 production (data not shown). n=10

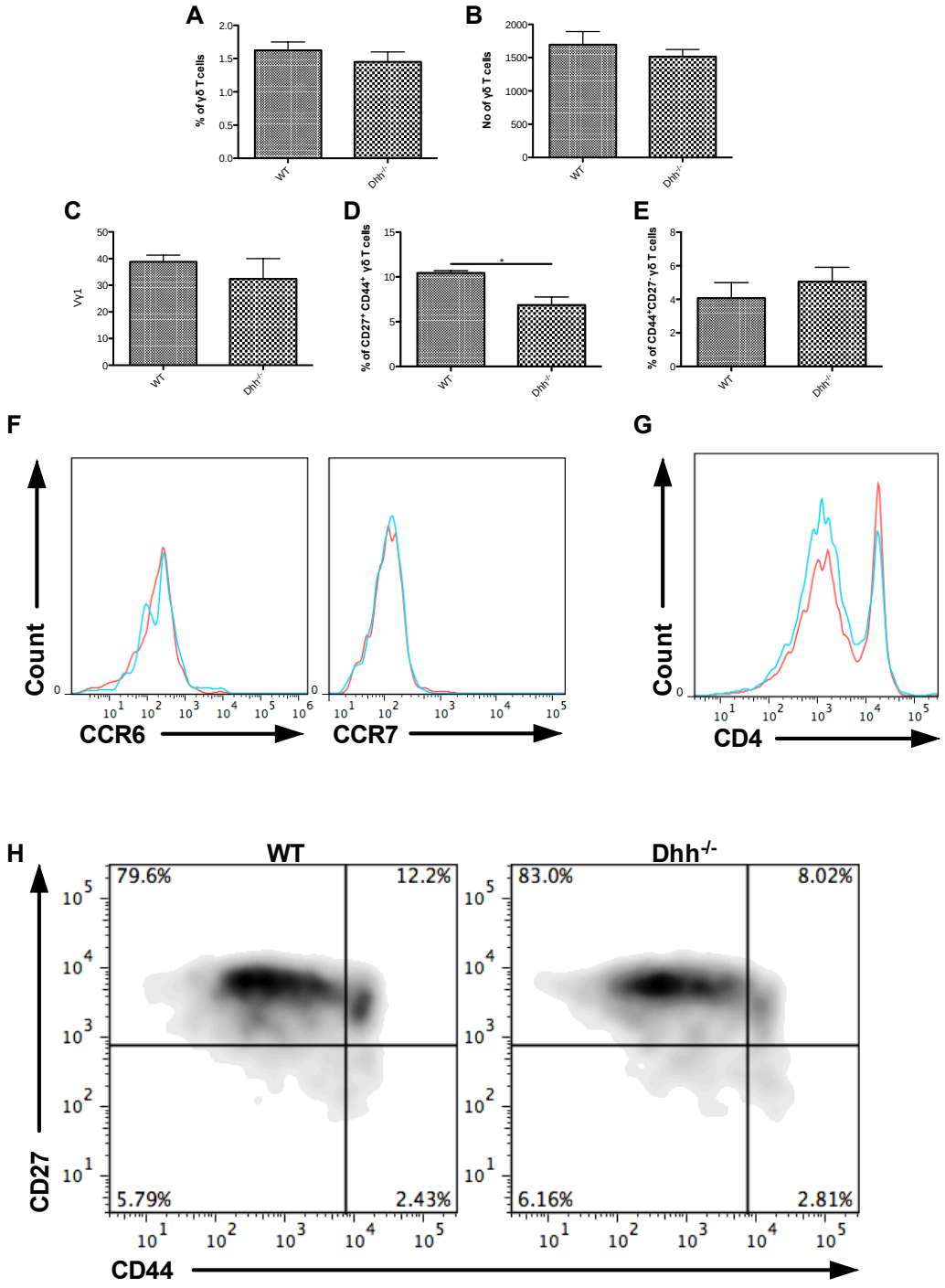

Figure 4.6: The effect of Dhh in γδ T thymocytes

Bar charts (A) and (B) show the percentage and cell count of CD3⁺ γδ T cells in WT and Dhh$^{-/-}$ mice. Bar chartS (C), (D) and (E) show the percentages of the Vγ1, CD27⁺CD44⁺ and CD44⁺CD27⁻ populations, respectively. Representative overlaid histograms (WT / KO) (F) show that deletion of Dhh increases the CCR6 and CCR7 cell surface expression. (G) (WT / KO) shows CD4 expression in WT and Dhh KO mice. Dot plots (H) show CD27 and CD44 expression on WT and Dhh$^{-/-}$ mice. *p<0.05, n=4

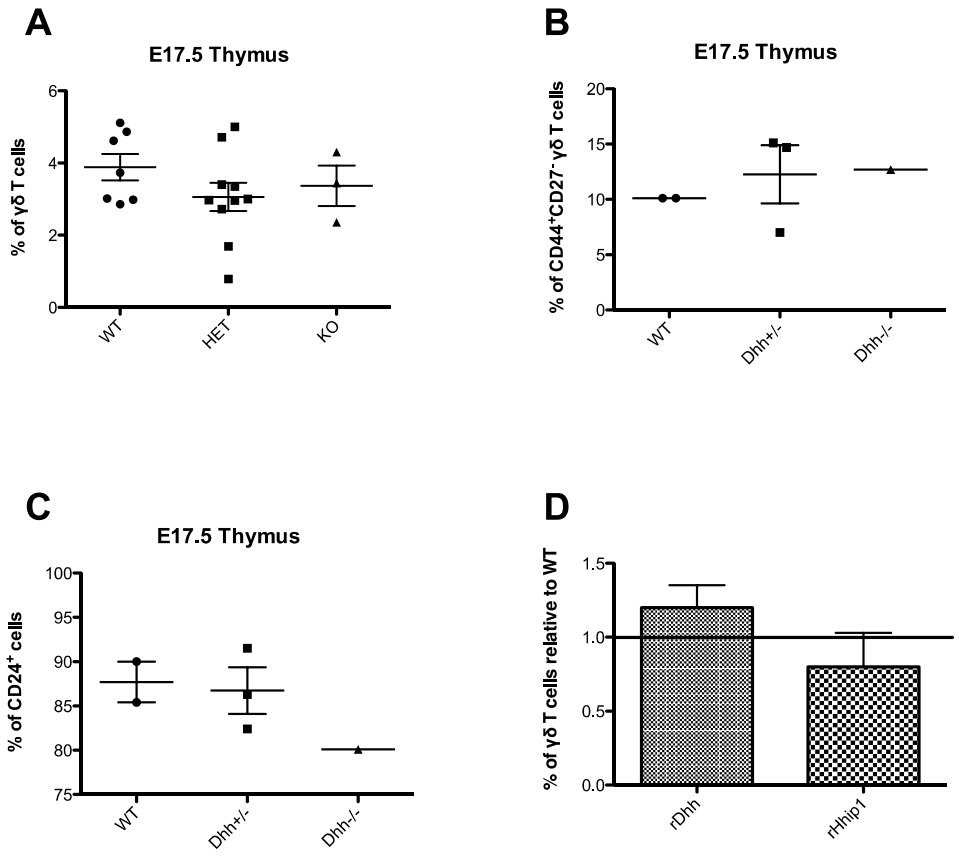

Figure 4.7: The effect of Dhh in E17.5 γδ T cell development in the thymus and the spleen

Scatter plot (A) shows the percentage of γδ T thymocytes on WT, $Dhh^{+/-}$ and $Dhh^{-/-}$E17.5 mice. Scatter plots (B) and (C) show percentage of the $CD44^{+}CD27^{-}$ γδ subset and expression of CD24, respectively; n=19. Bar chart (D) shows percentage of γδ thymocytes in FTOCs after 6 days of culture with rDhh or rHhip1, relative to WT. n=6

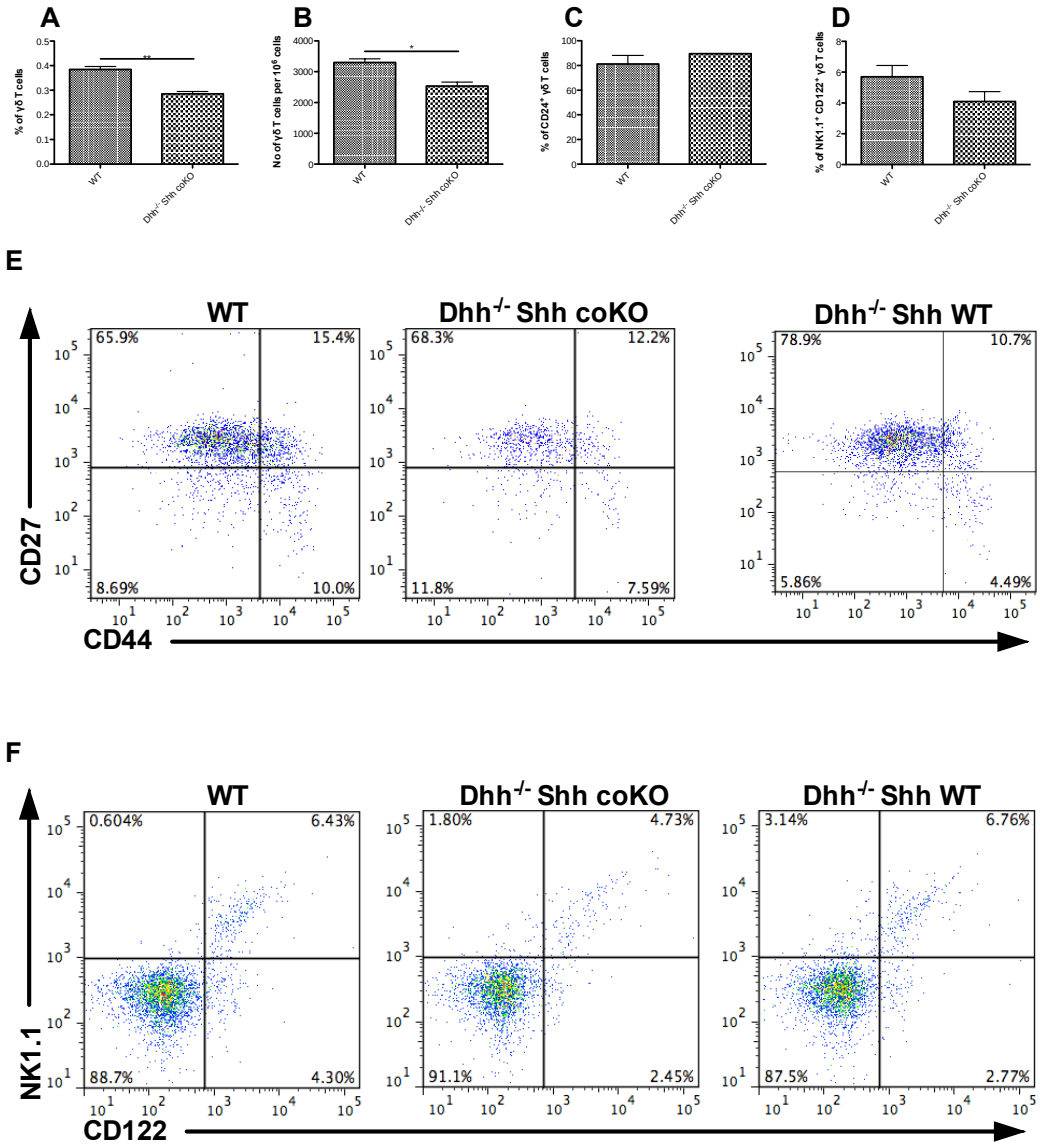

Figure 4.8: The effect of double KO (Dhh$^{-/-}$-Shhfl/fl FoxN1Cre^{+}) on γδ thymocytes

Bar charts show (A) the percentage and (B) cell count of γδ T cells in WT and double KO thymocytes from 3 weeks old mice. (C) shows CD24 expression and (D) shows CD122^{+}NK1.1^{+}. Representative dot plots (E) show CD27 and CD44 expression on γδ T cells from WT, double KO and Dhh$^{-/-}$ ShhWT (Cre^{-}) littermates. Dot plots (F) show CD122 and NK1.1 expression on γδ T cells from WT, double KO and Dhh$^{-/-}$ Shh WT (Cre^{-}) littermates. *p<0.05 **p<0.005, n=5

4.3 Discussion

We analysed γδ thymocyte populations in fetal and adult $Ihh^{+/-}$, IhhcoKO (CD4Cre), $Shh^{+/-}$, ShhcoKO (FoxN1Cre), $Dhh^{-/-}$ and $Dhh^{-/-}$ShhcoKO thymus. We detected no impact of Ihh on γδ cells in the thymus. Both Shh-heterozygosity and Dhh-deficiency resulted in changes in expression of cell surface markers. The $Shh^{+/-}$ thymus showed a significant decrease in CD27 expression. The $CD27^{-}$ γδ T cell population in the thymus is believed to give rise to an IL17-producing population, which express high levels of the transcription factor RORγt in addition to high levels of the γδ-lineage transription factor SOX13. It will therefore be important to investigate this population in peripheral tissues in these mice.

The $Dhh^{-/-}$ thymus showed a significant decrease in the $CD27^{+}CD44^{+}$ population, which are the population of γδ cells that express the transcription factor T-bet, in addition to lower levels of SOX13, and produce IFNγ. In WT FTOC neutralization of endogenous Hh proteins by treatment with recombinant Hhip reduced γδ cell numbers, whereas treatment with recombinant Shh or recombinant Dhh protein increased the proportion of γδ cells. These experiments suggest that Hh signalling promotes the production of γδ thymocytes, but we did not detect statistically significant differences in γδ cell number in the $Shh^{+/-}$ or $Dhh^{-/-}$ thymus, but only in the double knock out $Dhh^{-/-}$ ShhcoKO.

5. Modulation of Hh signalling during γδ T cell development in the thymus

5.1 Introduction

We showed that the development of thymic γδ T cells is influenced by Shh and Dhh signalling in the fetal and adult thymus. In this Chapter, we test the impact of mutation of negative regulators of Hh pathway activation (Gli3 and Kif7) on γδ T cell development in the thymus. In addition, to test the hypothesis that Hh proteins signal directly to thymic γδ cells, we investigate the impact of transgenic expression of activator or repressor forms of Gli2 in γδ cells.

5.2 Results

5.2.1 The role of Gli3 in γδ T cell development in the thymus

Gli3 can be modified to function as a transcriptional repressor or as a transcriptional activator. In the absence of Hh signalling, a truncated form of Gli3 binds Gli binding sites and represses transcription, thereby preventing transcription of Hh target genes. In the presence of Hh signalling, Gli3 functions as a transcriptional activator (Sasaki, Nishizaki et al. 1999). It has been shown that, in some tissues, Gli3 represses transcription of *Shh* and Gli3 deficient mice show an opposing phenotype to Shh deficient mice in many tissues, indicating that Gli3 acts mainly as a transcriptional repressor in vivo (te Welscher, Zuniga et al. 2002). In the fetus, the Gli3-mutant thymus shows the opposing phenotype to the Shh-deficient thymus, and the Gli3-mutant thymus stroma has increased Hh pathway activation, indicating that Gli3 functions to limit Hh signalling in

the thymic stroma (Hager-Theodorides, Dessens et al. 2005), (Saldana, Solanki et al. 2016).

$Gli3^{-/-}$ mice die before birth and exhibit severe developmental defects whereas $Gli3^{+/-}$ mice appear normal, although they form an extra digit in the interior side of the limb, allowing for easy genotyping, and are known as the 'extra toe' mutant (Schimmang, Lemaistre et al. 1992). To test the impact of Gli3 mutation on γδ cell development and differentiation, we analysed the γδ cell population in the adult $Gli3^{+/-}$ thymus. Deletion of one copy of Gli3 resulted in increased numbers of γδ cells in the thymus of young adult mice, but this effect was not statistically significant (Figure 5.1A, B), and we also observed a decrease in CD24 expression on $CD44^{+}CD27^{-}$ γδ cells (Figure 5.1D, E).

5.2.2 The role of Kif7 in γδ thymocyte development

It is believed that the kinesin protein Kif7 is a critical regulator of Hh signalling (Cheung, Zhang et al. 2009). Kif7, a mammalian equivalent of costal2 (Cos2), acts downstream of Smo and physically interacts with Glli transcription factors. It acts as a processing hub that recruits multiple protein kinases which negatively control Gli's stability, hence supressing Hh activity, although in some tissues it has also been described to be required for Hh signal transduction (Zhao, Tong et al. 2007). Of note, mice lacking Kif7 display a Gli3-like skeletal phenotype, but with greater disorganisation, and Kif7 deficiency has been described to both increase or decrease Hh pathway activity, dependent on context (Cheung, Zhang et al. 2009). Here, we analysed γδ cells in the $Kif7^{+/-}$ thymus, in order to investigate the role of Kif7 in γδ T cell development.

5.2.3 The adult Kif7$^{+/-}$ thymus

Kif7$^{-/-}$ mice die before birth and therefore in the adult thymus our experiments were restricted to Kif7$^{+/-}$ young adults, which look normal and are fertile. Deletion of one copy of Kif7 increased the percentage of γδ T cells in the adult thymus (Figure 5.2A, B), but γδ T cell subtypes based on CD27 and CD44 expression were not affected by Kif7 heterozygosity (Figure 5.2C, D, E and F) and no difference was observed in CD4 expression (data not shown).

5.2.4 The fetal Kif7-mutant thymus

In order to investigate the role of Kif7 in early γδ T cell development in the thymus and to test the impact of Kif7 deficiency, we time-mated Kif7$^{+/-}$ and analysed the embryonic thymus on E17.5. No difference was observed between WT and Kif7$^{+/-}$ thymus, although Kif7$^{-/-}$ thymi contained significantly more γδ cells than WT littermates, as the thymus contained more cells (Figure 5.3A and B). We detected a significant reduction in CD44^{+}CD27^{-} γδ thymocyte numbers and an increase in CD27^{+}CD44^{-} γδ cells in the Kif7$^{-/-}$, compared to WT and Kif$^{+/-}$(Figure 5.3A-D).

The increase in γδ cell numbers in the Kif7$^{-/-}$ fetal thymus are consistent with Kif7 functioning as a negative regulator of Hh signalling, as Hh-neutralisation by Hhip-treatment decreased γδ cell numbers in FTOC and the double mutant Dhh$^{-/-}$ShhcoKO thymus contained fewer γδ cells.

5.2.5 Inhibition of Hh-mediated transcription in γδ thymocytes

We found a modest impact of mutation of Shh and Dhh, expressed by TEC on γδ thymocyte development and in addition, that deletion of Kif7 (which is expressed in thymocytes and TEC) significantly increased overall γδ cells in the thymus, and increased the CD27^{+}CD44^{-} population. To ask if Shh and Dhh signal directly to developing γδ thymocytes, or if the impact of Hh signalling on γδ cells is indirect through another cell type, we used

the lck-driven Gli2C2-transgenic (Rowbotham, Furmanski et al. 2008). In this transgenic a truncated form of Gli2, which acts as a repressor of Hh-dependent transcription only, is expressed in all T-lineage cells, including γδ cells.

In the Gli2C2 transgenic thymus of young adult mice the number of γδ T cells was reduced compared to WT (Figure 5.4A, B). The $CD44^{+}CD27^{-}$ γδ population was increased (Figure 5.4C) and CD24, CD122 and CD4 were upregulated (Figure 5.4D-G). Thus, inhibition of physiological Hh-mediated transcription in γδ thymocytes showed that the Hh signalling pathway is active during normal γδ cell development and that it regulates subset distribution and cell surface phenotype.

5.2.6 Constitutive activation of Hh-mediated transcription in γδ thymocytes

We then carried out the reciprocal experiment, and investigated the impact of transgenic expression of the activator form of Gli2 (Gli2N2) to constitutively activate Hh-mediated transcription in γδ thymocytes. (Rowbotham, Hager-Theodorides et al. 2009).

The Gli2N2 transgenic thymus contained significantly more γδ cells than WT (Figure 5.5A, B). Gli2N2-tg mice showed a significant upregulation of CD44 on γδ thymocytes compared to WT, with a significant decrease in the proportion of the $CD27^{+}CD44^{-}$ γδ subset and increase in the $CD27^{+}CD44^{+}$ γδ subset (Figure 5.5D-G). In the Gli2N2-tg thymus we found increased CD122 expression on the expanded $CD27^{+}CD44^{+}$ γδ subset (Figure 5.6F-H). In addition, the Gli2N2-tg $CD27^{+}CD44^{+}$ γδ thymocyte subset expressed lower CD24 than their WT counterparts (Figure 5.6A,).

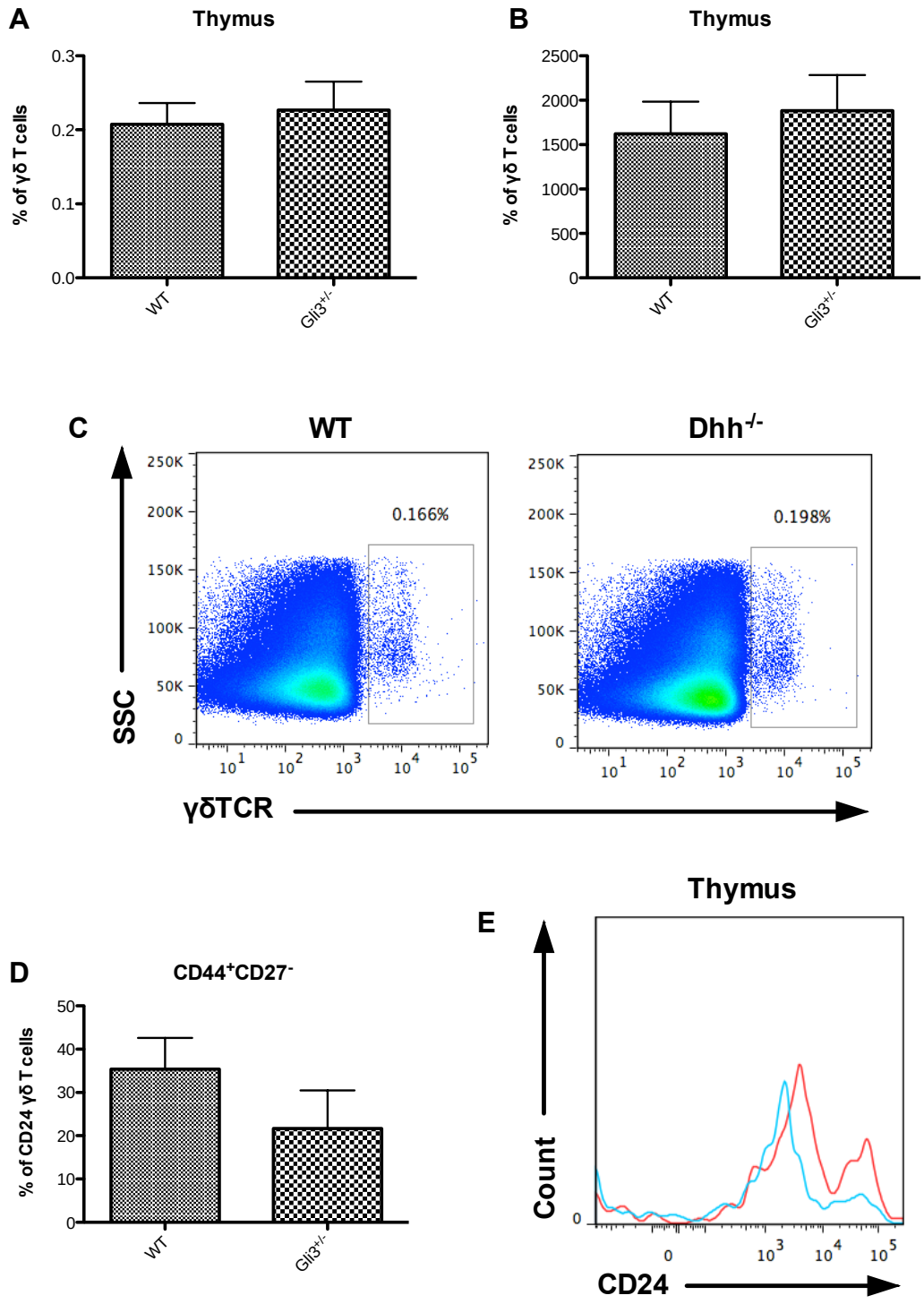

Figure 5.1: The effect of Gli3$^{+/-}$ on the expression of CD24 in γδ T cells

Bar charts show (A) percentages and (B) cell count of thymic γδTCR^{+} cells. Representative dot plots (C) show percentage of γδTCR^{+} thymocytes isolated from WT and Gli3$^{+/-}$ mice. Bar chart (D) shows CD24 expression of the thymic CD44^{+}CD27^{-} γδ population. Representative overlaid histogram (E) (WT / Het) of CD44^{+}CD27^{-} γδ subtypes that express CD24 in the thymus of WT and Gli3$^{+/-}$ young adult mice. n=6

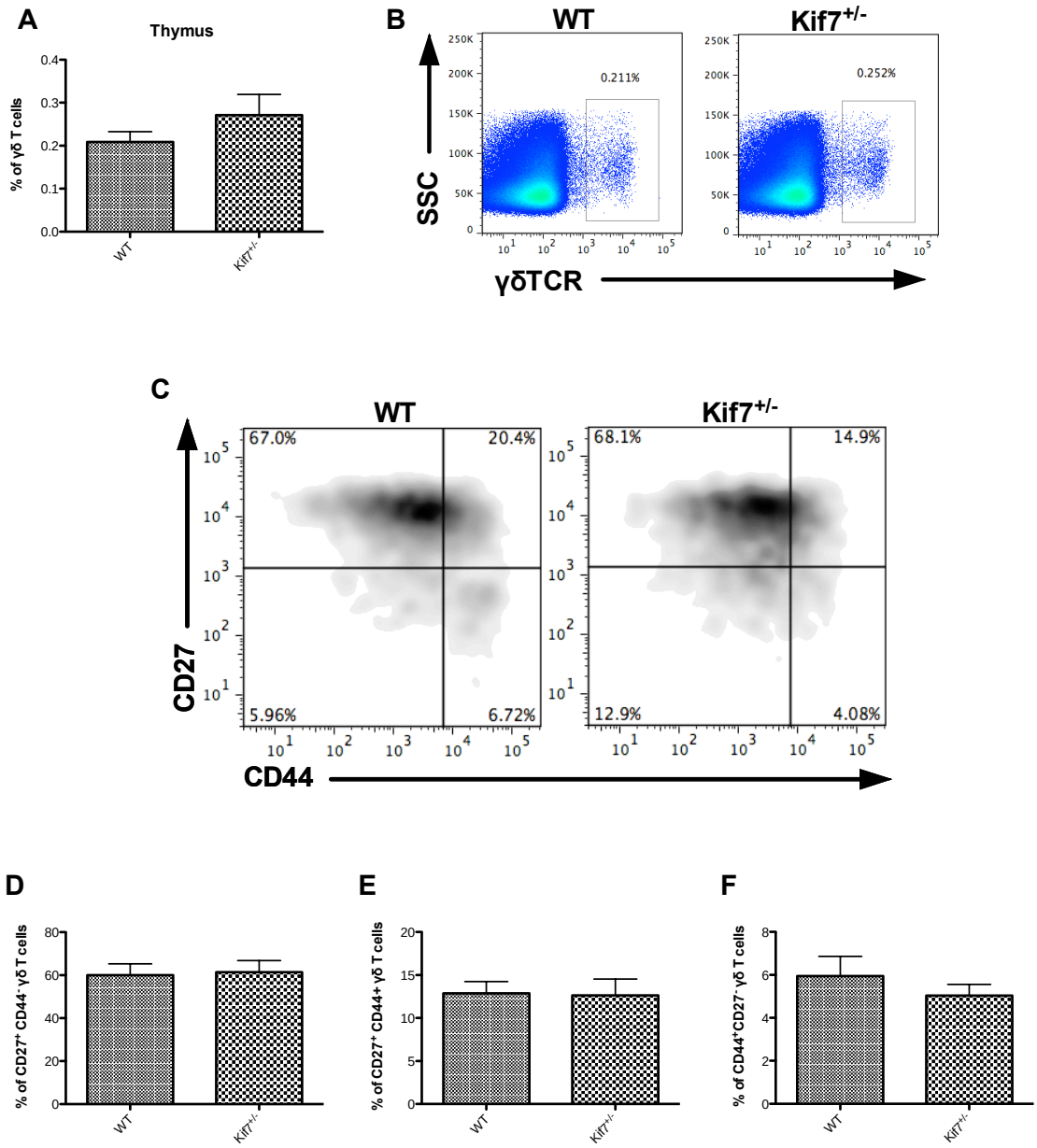

Figure 5.2: The effect of Kif7$^{+/-}$ on γδ T cells from the thymus

Bar chart (A) shows percentages of γδTCR^{+} cells in WT and Kif7$^{+/-}$ in the thymus. Representative dot plots (B) show the proportion of live-gated thymocytes that are γδTCR^{+} in WT and Kif7$^{+/-}$ mice. Representative density plots (C) show expression of CD27 and CD44 in WT and Kif7$^{+/-}$ mouse thymus. Bar charts (D, E, F) show the percentage of three major γδ^{+} populations based on CD27 and CD44 expression. Error bars represent ±SEM. n=6

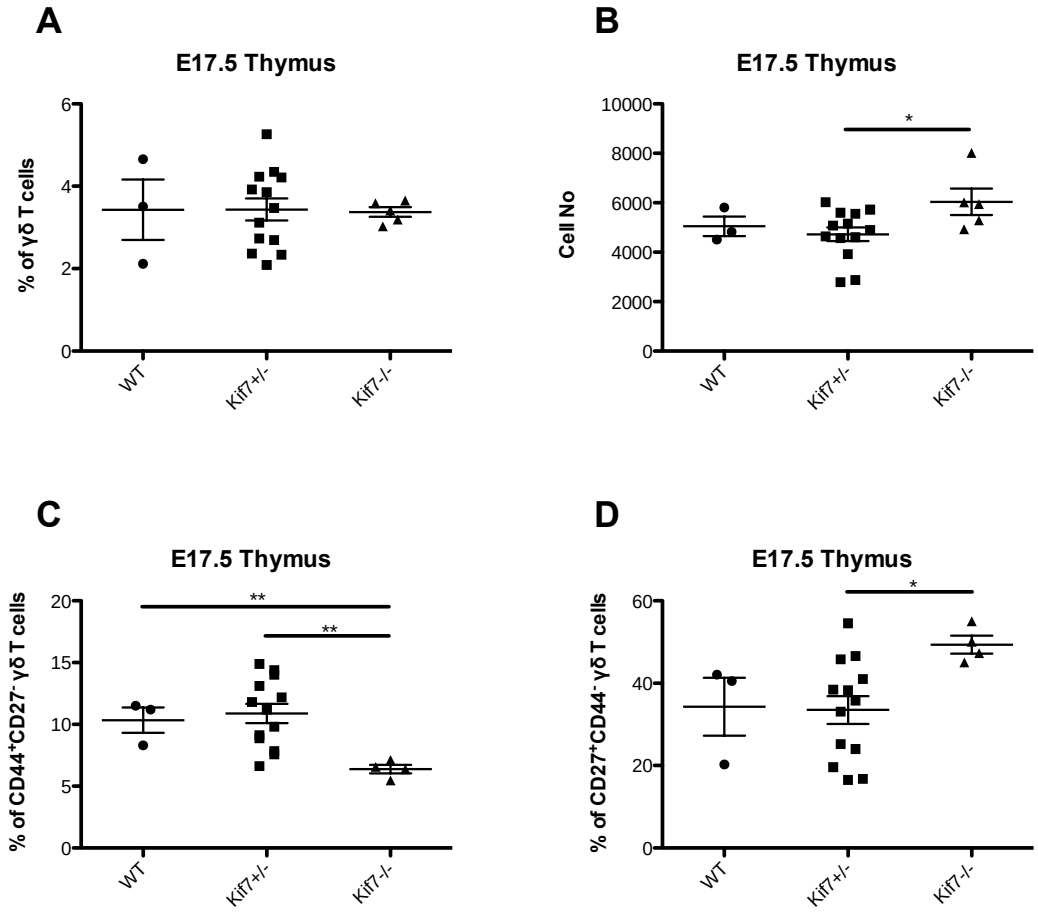

Figure 5.3 The effect of Kif7 on γδ T cells from the thymus of E17.5 littermates

Scatter plots (A) and (B) show the percentage and number of γδ T cells in WT, Kif7$^{+/-}$ and Kif7$^{-/-}$ E17.5 thymi. (C) and (D) show the percentage of γδ T cells that are CD44^{+}CD27^{-} and CD27^{+}CD44^{-} respectively. The mean of each group is represented with a line. *$p<0.05$ **$p<0.005$, n=21

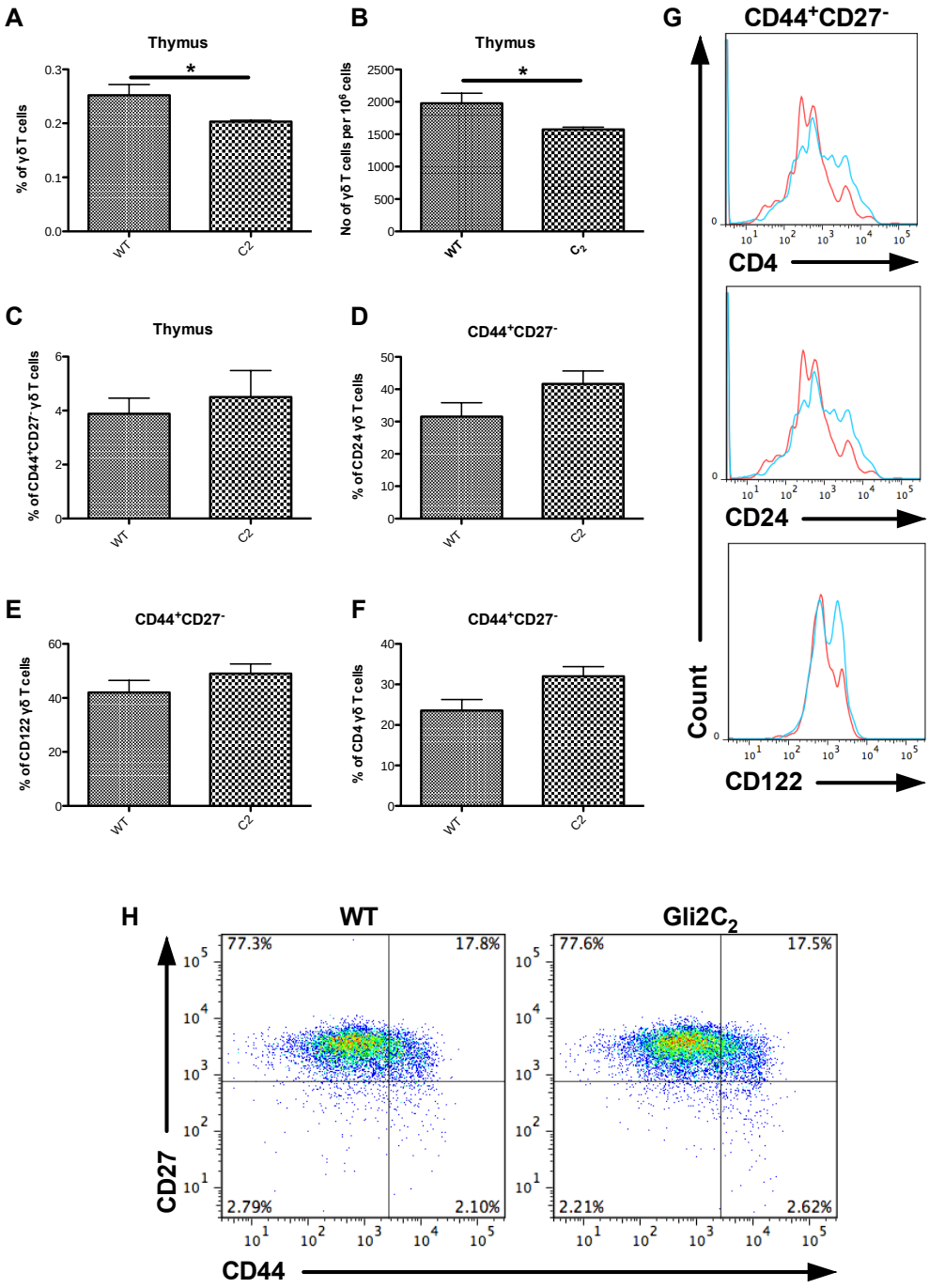

Figure 5.4: The effect of Gli2C$_2$ on the γδ T cell expression of CD4, CD24, CD27, CD44 and CD122

Bar chart (A) and (B) show the percentage and cell count respectively of γδ T cells in the thymus of WT and Gli2C$_2$ mice. (C) shows the thymic CD44$^+$CD27$^-$. Bar charts show the percentage of CD44$^+$CD27$^-$ γδ T cells that express (D) CD24, (E) CD122 and (F) CD4 in the thymus of young adult mice. Representative overlaid histograms (G) (WT / Tg) show expression of CD4, CD24 and CD122 in WT and Gli2C$_2$ thymus of CD44$^+$CD27$^-$ γδ T cells. Representative dot plots (H) show CD27 and CD44 expression of WT and Gli2C$_2$ γδ T cells from the thymus. Error bars represent ±SEM. *p<0.05, n=8

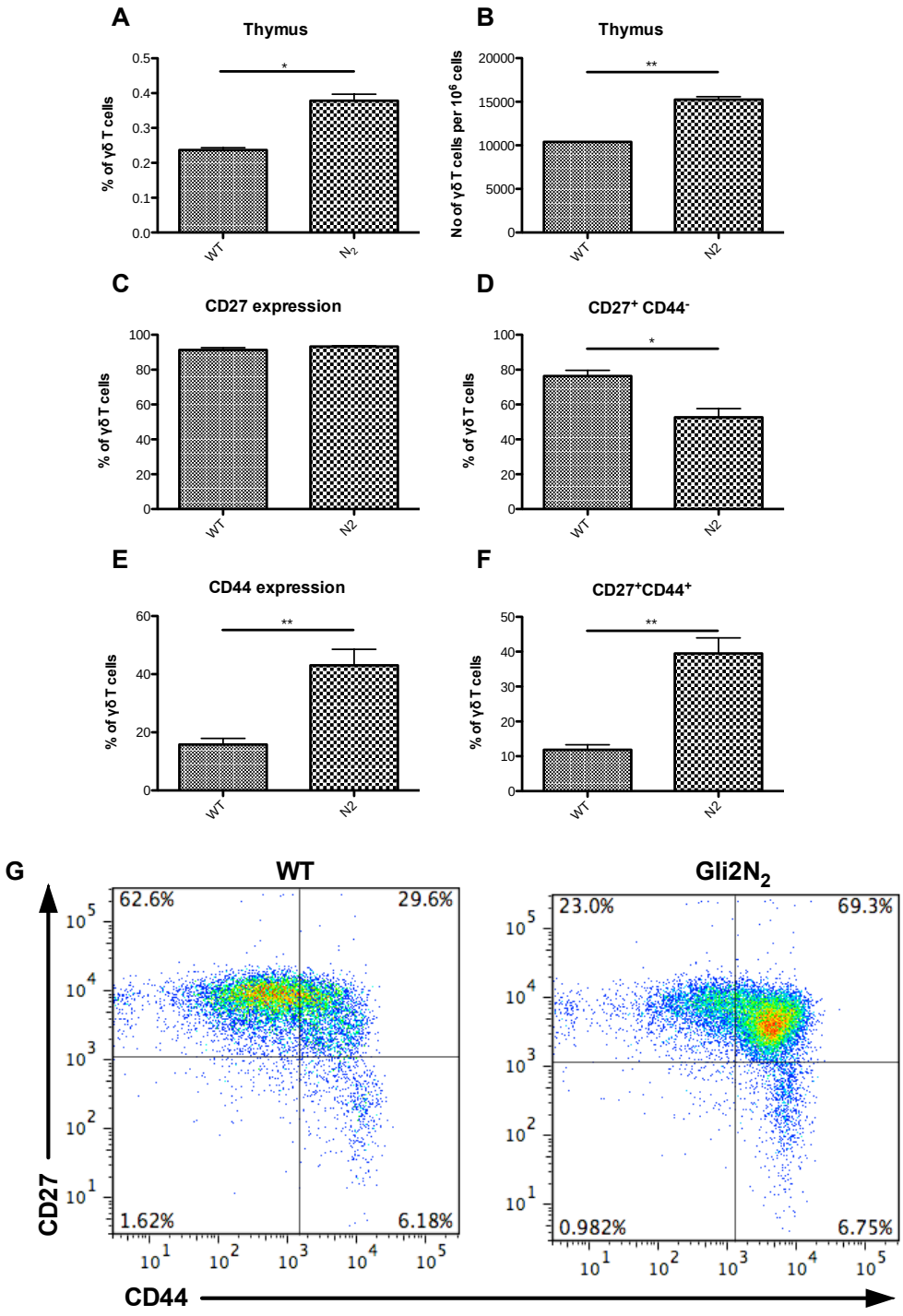

Figure 5.5: The effect of Gli2N$_2$ on CD27 and CD44 expression on γδTCR$^+$ thymocytes

Bar charts (A) and (B) show percentage and cell count, respectively, of WT and Gli2N$_2$ thymocytes. Bar charts (C) and (E) show expression of CD27 and CD44 and the percentage of the CD27$^+$CD44$^-$ (D) and CD27$^+$CD44$^+$ (F) populations in γδ cells from WT and Gli2N$_2$ thymocytes. Error bars represent ±SEM. Representative dot plots (G) show CD27 and CD44 on γδ cells (gated on CD3$^+$γδ$^+$) in WT and Gli2N$_2$ mouse thymus. *p<0.05, **p<0.005, n=4

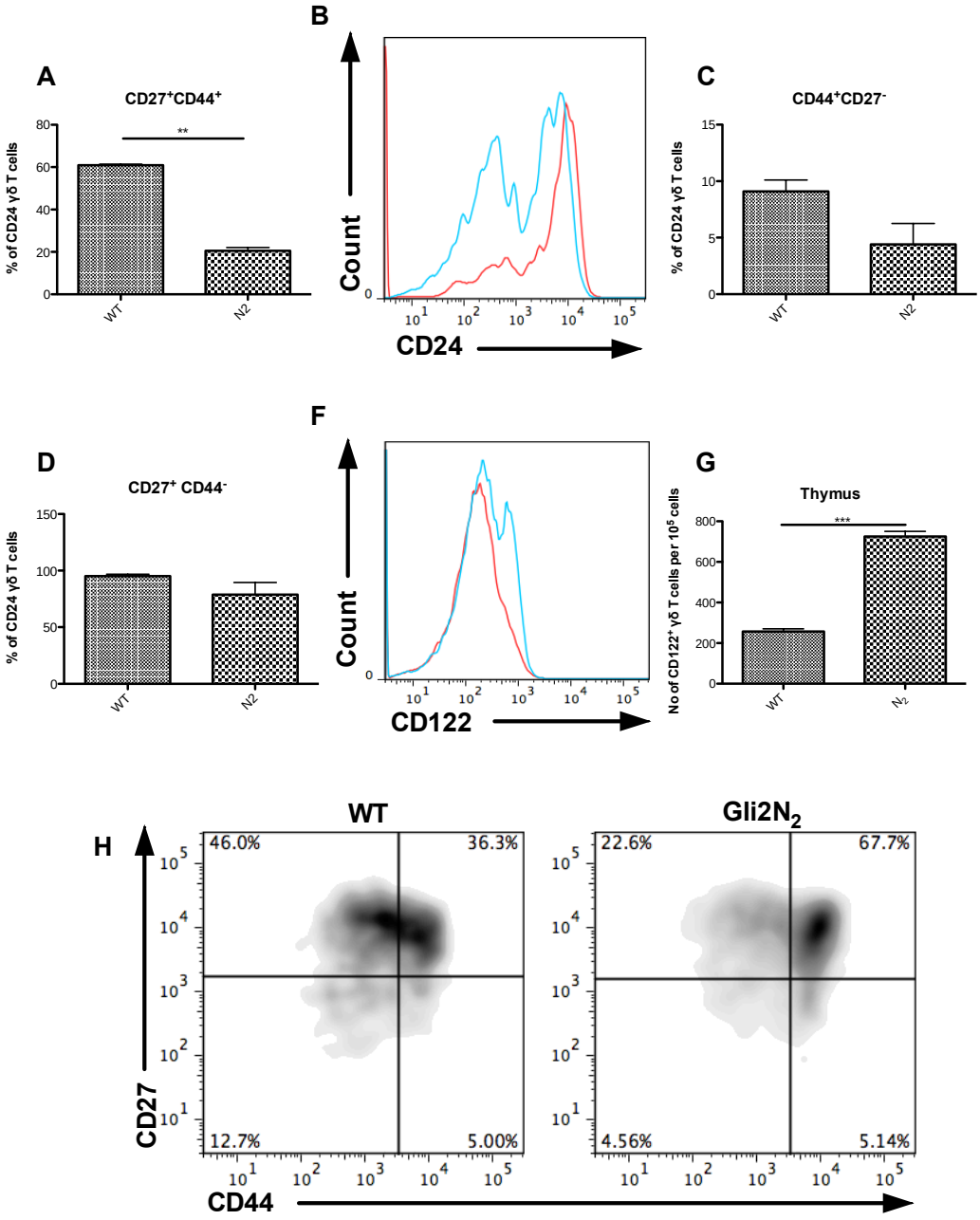

Figure 5.6: The effect of Gli2N$_2$ on CD24 and CD122 expression on thymic γδTCR$^+$ cells.

Bar charts (A), (C) and (D) show the percentage of thymic γδ T cells that express CD24 in each of the three populations: CD27$^+$CD44$^+$, CD44$^+$CD27$^-$ and CD27$^+$CD44$^-$. Representative overlaid histograms (WT / Tg) (B) show the difference between WT and Gli2N$_2$ littermates in CD24 expression on CD27$^+$CD44$^+$ γδ thymocytes. Representative overlaid histograms (E) (WT / Tg) show the difference in CD122 expression on γδ cells in the thymus of young adult WT and Gli2N2 littermate mice, whereas density plots (H) show the CD27 and CD44 phenotype of the same CD122$^+$ γδ T cells. Bar charts (G) show the cell count of the CD122$^+$ γδTCR$^+$ population. Error bars represent ±SEM. **p<0.005 ***p<0.0001

5.3 Discussion

In summary, constitutive Hh-mediated transcription in thymocytes promoted γδ thymocyte numbers and increased CD44 expression and the $CD27^{+}CD44^{+}$ γδ subset, whereas inhibition of physiological Hh-mediated transcription had the opposite effect, and γδ cell numbers and CD44 expression were downregulated. Likewise, cell surface expression of CD24 (HSA), which is highly expressed in immature cells and down-regulated wih maturity, was increased when Hh signalling was inhibited and decreased when the Hh pathway was constitutively active in the Gli2N2-tg thymus.

Taken together, these experiments show that the Hh proteins positively regulate γδ cell development in the thymus, and signal directly to γδ thymocytes to promote differentiation of the $CD44^{+}CD27^{+}$ subset. It will therefore be important to investigate the influence the Hh signalling on the homeostasis and subset distribution of peripheral γδ T cells.

6. Modulation of Hh signalling influences the homeostasis of γδ T cell populations in the periphery

6.1 Introduction

We showed that the development of thymic γδ T cells is influenced by Shh and Dhh signalling in the fetal and adult thymus, and that manipulation of Hh-mediated transcription in γδ thymocytes also affects their development. In this Chapter we test the impact of mutations in components of the Hh signaling pathway on the homeostasis of peripheral γδ T cell populations. The mouse models that we will investigate fall into three groups: in some models the Hh pathway will be affected in the same way in both the thymic and peripheral γδ T cells (Gli2N2 tg and Gli2C2 tg), whereas in the mice in which the Hh ligands, or pathway regulators are constitutively mutated ($Shh^{+/-}$, $Dhh^{-/-}$, $Ihh^{+/-}$, $Gli3^{+/-}$, $Kif7^{+/-}$) the extent of impact of the mutation will depend on the pattern of expression of the molecule in the different tissues. In the ShhcoKO animals, however, the developing γδ thymocytes are exposed to a reduced Hh signal in the thymus, but normal levels of Hh signalling in peripheral tissues.

6.2 Results

6.2.1 The influence of the Gli2N2 transgene on peripheral γδ T cell biology

We first examined the impact of constitutive activation of Hh-mediated transcription on γδ T cell populations in the spleen and lymph nodes. The number of γδ cells was not influenced by the Gli2N2 transgene in the spleen and lymph nodes (Figures 6.1A, B and 6.3). However, in contrast to the thymus, in the spleen CD44 expression was downregulated in the Gli2N2 tg γδ T cells, and the $CD44^{+}CD27^{-}$ γδ population was significantly

decreased by ~10-fold compared to WT, indicating that Hh-mediated transcription negatively regulates the splenic $CD44^{+}CD27^{-}$ γδ population (Figure 6.1C-E). Interestingly, CD4 was significantly upregulated in splenic transgenic γδ cells compared to their WT counterparts (Figure 6.2A, B). We also observed a reduction in intensity of CD44 staining on the $CD44^{+}CD27^{-}$ population in the lymph nodes, and an increase in the $CD27^{+}CD44^{+}$ γδ population compared to WT (Figure 6.3A-D). Gli2N2 tg expression also decreased CD122 expression on γδ cells in the spleen and lymph nodes compared to WT (Figure 6.2C and 6.4E). This was in contrast to our previous observation in the thymus, in which the transgene expression increased cell surface CD122 expression on the $CD27^{+}CD44^{+}$ γδ thymocytes. In the lymph nodes, the Gli2N2 transgene increased cell surface CD24 expression significantly on all γδ subtypes, independently of CD27 and CD44 expression (Figure 6.4A-D), whereas we did not detect an influence of the transgene on CD24 expression in the spleen (data not shown). As CD24 is downregulated during T cell maturation, the increase in CD24 expression suggests that the γδ cells undergoing active Hh-mediated signalling were more immature.

6.2.2 Inhibition of physiological Hh-mediated transcription in peripheral γδ T cells

We then carried out the reciprocal experiment and tested the impact of inhibition of physiological Hh-mediated transcription on peripheral γδ T cell subsets, by analysis of the Gli2C2 transgenic. We did not detect any difference in γδ cell numbers compared to WT litter mates in either the spleen or lymph nodes (Figure 6.5A-D). No major difference was observed in the population distribution in the spleen, but the $CD44^{+}CD27^{-}$ γδ population was affected in the lymph nodes, with an increase in the proportion of $CD122^{+}$ cells (Figure 6.5F), the opposing affect on CD122 expression to that observed in the Gli2N2 tg peripheral γδ T cells.

6.2.3 Dhh signalling in peripheral γδ T cells

Dhh is expressed by epithelial cells distributed throughout the thymus (Sacedon, Varas et al. 2003), and it is also expressed by stromal cells in the spleen, indicating that it could have a role in T cell activation or peripheral maintenance of T cells (Lau, Outram et al. 2012). Dhh expression has not been detected in the lymph nodes (our unpublished data). The role of Dhh in peripheral γδ T cells is unknown.

As Dhh-deficient mice are viable and appear healthy, we investigated the peripheral γδ T cell populations in Dhh KO mice, compared to their WT littermates. In the LN, we did not observe significant differences in the number, subset distribution or phenotype of the γδ T cell population between DhhKO and WT (Figure 6.6A, B), consistent with the fact that we have not detected Dhh expression in the LN.

In the spleen, Dhh KO mice had fewer γδ cells and significantly fewer NK-like γδ cells than their WT littermates (Figure 6.7A, B). We did not observe a significant difference in the distribution of the γδ subsets defined by CD44 and CD27 (Figure 6.7E, G), and cell surface expression of CCR6 was not affected (Figure 6.7F).

In order to investigate if Dhh signals directly to splenic γδ cells, we crossed the Dhh-mutant mice with the Hh-reporter transgenic (GBS-GFP-tg), and compared GFP expression in the γδ subsets in DhhKO and WT littermates. We found that Dhh-deficiency significantly decreased the proportion of GFP+ cells in the $CD44^{+}CD27^{-}$ γδ population, indicating that Hh pathway activation is reduced in these cells, and therefore that Dhh signals directly to this population in the WT spleen (Figure 6.7H, J). Interestingly, however, we found that Dhh-deficiency significantly increased the

proportion of GFP+ cells in the $CD27^{+}CD44^{+}$ γδ subset, indicating increased Hh pathway activation in these cells in the absence of Dhh (Figure 6.7I). This finding is puzzling, and suggests that Dhh functions either to repress another Hh family member that signals directly to these cells, or that Dhh functions to increase expression of a repressor of the pathway in these cells.

We then tested the ability of spleen γδ cells to produce IFNγ and IL17 ex vivo, by intracellular cytokine staining following a short activation. IL17 is made predominantly by the $CD44^{+}CD27^{-}$ population, whereas IFNγ is made predominantly by the $CD27^{+}CD44^{+}$ population that express NK1.1. Dhh did not appear to affect ability of γδ splenocytes to produce IFNγ after 4h of activation with PMA and ionomycin and subsequent intracellular staining, despite the reduction in NK1.1 expression in the DhhKO (Figure 6.8A). However, production of IL17 was reduced by half in the DhhKO compared to WT (Figure 6.8B).

We then investigated the impact of Dhh deficiency on the recovery of the splenic γδ subsets following irradiation. Dhh has previously been shown to accelerate the recovery of the erythroid lineage in the spleen after non-lethal irradiation (Lau et al 2012). We irradiated three 3 week old pairs of Dhh KO and WT mice and analysed them 14 days after irradiation. Overall, the proportion of $CD3^{+}$ cells was lower in the Dhh KO compared to WT (Figure 6.9C), but the proportion of γδ cells was not affected (Figure 6.9D). Interestingly, we observed a significant increase in the proportion of the $CD44^{+}CD27^{-}$ γδ subset in the Dhh KO compared to WT (Figure 6.9E-G) and this was the population that showed increased Hh pathway activation in the absence of Dhh in the steady-state spleen.

6.2.4 Peripheral γδ T cell populations in Shh$^{+/-}$ mice

Shh is expressed in the thymus and spleen (Outram et al 2000, Varas et al 2005) but has not been detected in the lymph node. The Shh$^{+/-}$ spleen had fewer γδ cells than WT, whereas the lymph nodes had more (Figure 6.10A, B). This finding may be the result of Shh affecting either proliferation of tissue-specific γδ cells, or apoptosis or migration of peripheral γδ cells.

In the adult spleen, Shh$^{+/-}$ caused an increase in the CD44^{+}CD27^{-} γδ population (Figure 6.11D, F) and a small decrease in overall CD27 expression compared to WT (Figure 6.11A). Cell surface expression of CD24 was also higher in the Shh$^{+/-}$ γδ cells in all subsets, compared to WT (Figure 6.11 G-I).

In order to test if Shh is signaling directly to γδ cells in the spleen we crossed the Shh$^{+/-}$ mice with the GBS-GFP-tg and compared GFP expression in the different γδ subsets between GBS-GFP-tg-Shh$^{+/-}$ and GBS-GFP-tg-Shh$^{+/+}$. Deletion of one copy of *Shh* decreased GFP expression in all tissues and subsets of γδ cells, consistent with the idea that Shh signals directly to γδ cells (Figure 6.12A). The greatest difference in Hh pathway activity in the spleen was observed in the CD27^{+}CD44^{+} population (Figure 6.12B). However, the CD44^{+}CD27^{-} γδ population is the most responsive to Hh as manifested by the highest proportion of GFP+ cells. When we gated on γδ cells and analysed anti-CD24 staining against GFP-expression, we found that all GFP+ γδ cells were CD24+ in both WT and Shh$^{+/-}$, suggesting that it is the more immature cells that are Hh-responsive (Figure 6.12C).

We then tested the ability of spleen and lymph nodes to produce IFNγ and IL17 ex vivo, by intracellular cytokine staining following a short activation. Shh heterozygosity increased the ability of γδ splenocytes and lymph nodes to produce IFNγ and IL-17 after 4h of activation with PMA and ionomycin and subsequent intracellular staining (Figure 6.13A-C).

6.2.5 Peripheral γδ T cell populations in ShhkoCO mice

To investigate if deletion of Shh from the thymus only, in our ShhkoCO model (Shhfl/fl-FoxN1-Cre-tg), would influence γδ populations in the periphery, we analysed ShhcoKO and WT littermate spleen and lymph nodes. No differences were observed in the spleen whereas in the lymph nodes, more γδ cells are seen (Figure 6.14A), confirming the findings in the $Shh^{+/-}$ mice, and suggesting that the increase is due to reduced Shh signaling during γδ cell development in the thymus. No significant differences were detected in subset distribution in the ShhFoxN1 KO spleen. In lymph nodes, however, both the $CD44^{+}CD27^{-}$ and the $CD27^{+}CD44^{+}$ γδ populations were increased in the ShhcoKO compared to WT (Figure 6.14B).

6.2.6 Peripheral γδ T cell populations in ShhcoKODhhKO double knockout mice

In the spleen we found an increase in γδ cells in the double knockout mice, although this change was not significant (Figures 5.15A, B). This finding was of interest because deletion of neither Shh or Dhh alone influenced the percentage of γδ cells in the spleen, and therefore it will be important to analyse more ShhcoKO-DhhKO spleens in the future. In terms of the γδ subsets, however, the double KO reduced both the $CD27^{+}CD44^{+}$ and the $CD44^{+}CD27^{-}$ population, relative to WT, with an overall reduction in CD44 expression (Figure 6.15C). The effect was similar to that observed in Dhh KO littermates. The $CD122^{+}NK1.1^{-}$ population was increased in the double KO spleen (Figure 6.15D), but variation between samples in the percentages of $CD122^{+}NK1.1^{+}$ and $NK1.1^{+}CD122^{-}$ populations do not allow us to draw concrete conclusions on these two subsets, indicating that analysis of more mice will be important.

In the lymph nodes, the double KO mice had fewer γδ cells both in terms of cell count and as a percentage (Figures 6.16A and B). In Shh WT Dhh KO

littermates, the number of γδ cells was even lower, a finding consistent with our finding that Shh mutant mice have more γδ cells in the lymph nodes. Double KO mice also showed a significant reduction in $CD27^{+}CD44^{+}$ cells with further decrease in Shh WT Dhh KO littermates (Figures 6.16C and D). Finally, consistent with our findings in the thymus and spleen, double KO mice had fewer NK-like γδ cells in the lymph nodes (Figure 6.16E).

6.2.7: Peripheral γδ T cells in $Kif7^{+/-}$ mice

Deletion of one copy of Kif7 increased the percentage of γδ T cells in the spleen and lymph nodes of young mice, with the greatest difference observed in the spleen where the proportion of γδ T cells was doubled (Figure 6.17B). In the spleen we also observed an expansion of the $CD27^{+}CD44^{+}$ γδ population and a decrease in the numbers of the $CD44^{+}CD27^{-}$ population (Figure 6.17A, C, D). Cell surface CD24 expression was decreased in all γδ populations in the $Kif7^{+/-}$ compared to WT, although the only significant difference was on $CD44^{+}CD27^{-}$ γδ splenocytes (Figure 6.17F).

To test the impact of Kif7 heterozygosity on Hh pathway activation in γδ T cell populations, we crossed the $Kif7^{+/-}$ with the GBS-GFP-transgenic mice and measured GFP expression. The proportion of GFP+ cells was increased in all γδ populations, with the greatest difference seen in the $CD44^{+}CD27^{-}$ spleen γδ T cells (Figure 6.17E). The increase in proportion of GFP+ cells indicates that Hh pathway activation is increased in the $Kif7^{+/-}$ heterozygote, and that therefore Kif7 is acting as a negative regulator of the pathway.

Thus, taken together these experiments show that increased Hh signaling to peripheral γδ T cells promotes the splenic γδ population and particularly increases the $CD27^{+}CD44^{+}$ subset.

6.2.8: Impact of Gli3-heterozygosity on peripheral γδ T cells

In the absence of Hh signalling, a truncated form of Gli3 binds GBS preventing transcription of Hh target genes. In the presence of Hh signalling, Gli3 functions as a transcriptional activator (Sasaki, Nishizaki et al. 1999).

Deletion of one copy of Gli3 resulted in increased numbers of γδ cells in the spleen and lymph nodes of young adult mice with the effect being significant only in the lymph nodes (Figures 6.18A, B). However, it will be important to analyse more $Gli3^{+/-}$ spleens to determine if the results in the spleen become significant. In the spleen, we observed a significant decrease in the percentage of $CD44^{+}CD27^{-}$ γδ cells in the $Gli3^{+/-}$ compared to WT (Figures 6.18C and D), similar to that observed in the $Kif7^{+/-}$. Interestingly, the $CD27^{+}$ $CD44^{+}$ γδ cell population was not affected by Gli3 heterozygosity (Figure 6.18D). Furthermore, similarly to $Kif7^{+/-}$ deletion of one copy of Gli3 reduced CD4 expression on γδ splenocytes (Figures 6.18E, G). Finally, we observed that CD24 expression decreased in the $CD44^{+}CD27^{-}$ γδ population (Figures 6.18F, I).

The percentage of NK cells remained constant in the spleens of WT and $Gli3^{+/-}$ mice, but the number and percentage of NK-like γδ cells, which are positive for both γδTCR and NK1.1 markers, increased significantly, and the increase was greater than that of the γδ cells that are negative for NK1.1 (Figures 6.20A, B).

We then investigated Hh pathway activation by crossing the $Gli3^{+/-}$ mice with the GBS-GFP-transgenic Hh-reporter mice. Surprisingly, the proportion of cells that expressed GFP decreased in $Gli3^{+/-}$ γδ splenocytes compared to WT, although the decrease was significant only in the NK-like γδ population (Figures 6.21B). The mean fluorescence intensity of GFP fluorescence, which is a measure of the extent of Gli activity in individual cells, was also decreased in the $Gli3^{+/-}$ γδ splenocytes compared to WT, and this difference was greatest in the NK-like γδ cells (Figure 6.21C). Our data thus show that NK-like γδ cells are more sensitive to Hh activity than $NK1.1^{-}$ γδ cells. Although, the $Kif7^{+/-}$ and $Gli3^{+/-}$ γδ populations show similar phenotypes in terms of cell number and cell surface markers, the Hh-reporter experiments show that in the $Kif7^{+/-}$ γδ splenocytes Hh signaling is increased, whereas in the $Gli3^{+/-}$ γδ splenocytes Hh signaling is decreased. It is possible that in Gli3 acts as a transcriptional activator in peripheral γδ cells, so that Hh pathway activation is decreased when it is decreased. However, this would presumably give rise to a different phenotype from $Kif7^{+/-}$ in which Hh pathway activation is increased, as expected. It would also be interesting in the future to have data on NK-like γδ cells from $Kif7^{+/-}$ in order to confirm the resemblance between Gli3 and Kif7 mutant's phenotype. However, when we analysed $Kif7^{+/-}$ mice, NK1.1 was not included in our analysis.

We activated splenocytes with PMA and Ionomycin ex vivo and investigated the effect of Gli3-heterozygosity on key γδ cytokines after 4h of activation. We found that partial deletion of Gli3 decreased intracellular IFNγ and IL-17, and the change was significant in the case of IL-17-producing $CD44^{+}CD27^{-}$ γδ cells (Figures 6.21C, E).

In the peritoneal cavity, the percentage of peritoneal $CD44^{+}CD27^{-}$ γδ cells was decreased more than three-fold (Figures 6.19A, B) in the $Gli3^{+/-}$

compared to WT, whereas the number of $CD27^{+}CD44^{+}$ γδ cells almost doubled (Figures 6.19A, B). The number of $CD44^{+}CD27^{+}$ γδ cells was also increased in the lungs of the same littermates (Figures 6.19A, C).

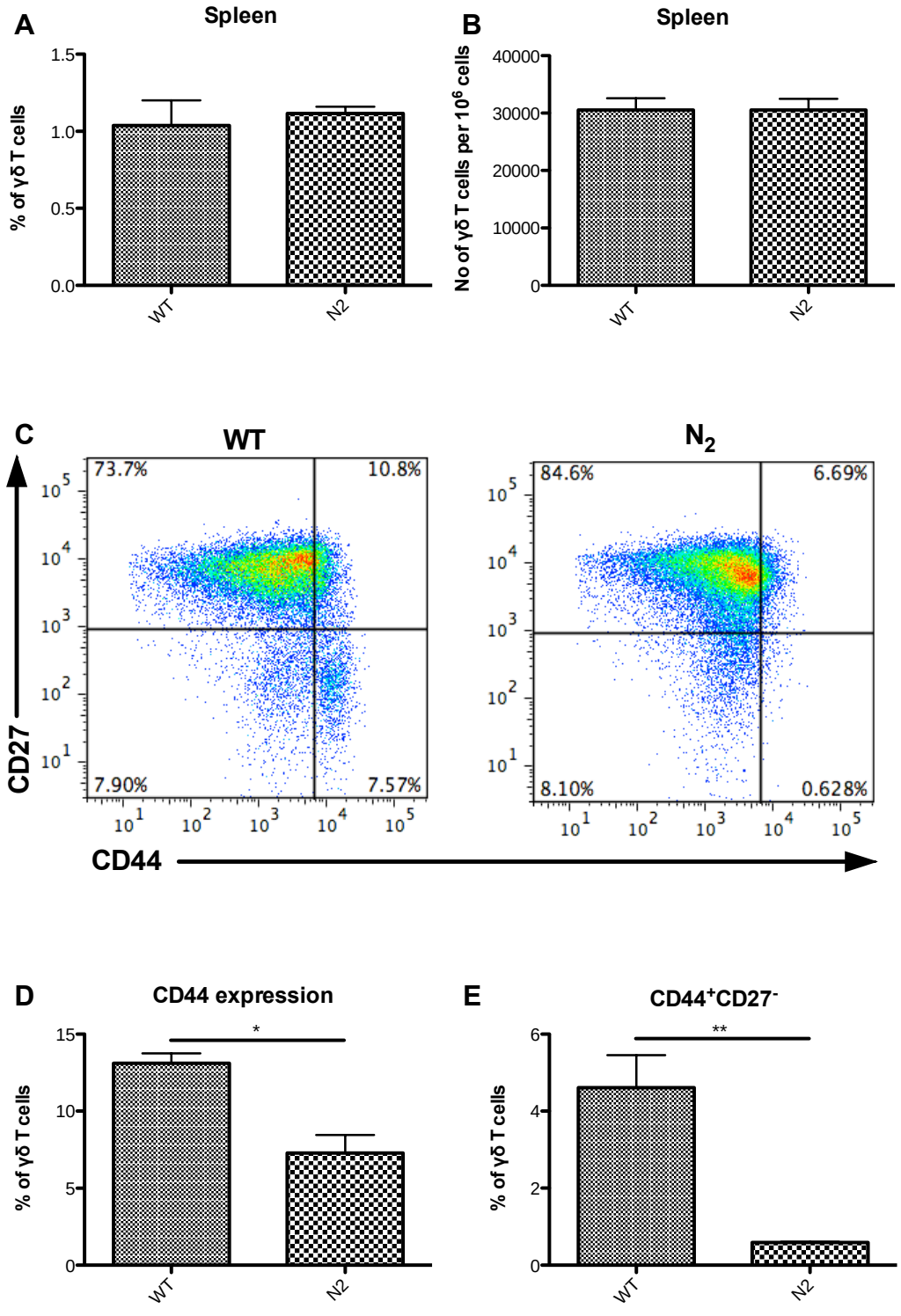

Figure 6.1: The effect of Gli2N2 on γδ T cell splenocytes

Bar charts show (A) the proportion and (B) cell count of γδ T cells in the spleen of Gli2N2 young mice. Representative dot plots (C) show CD27 and CD44 on $CD3^{+}\gamma\delta^{+}$ cells. Bar chart (D) shows CD44 expression and (E) the proportion of $CD44^{+}CD27^{-}$ γδ cells in WT and $Gli2N_2$ mouse spleens. *p<0.05, ***p<0.0001, n=4

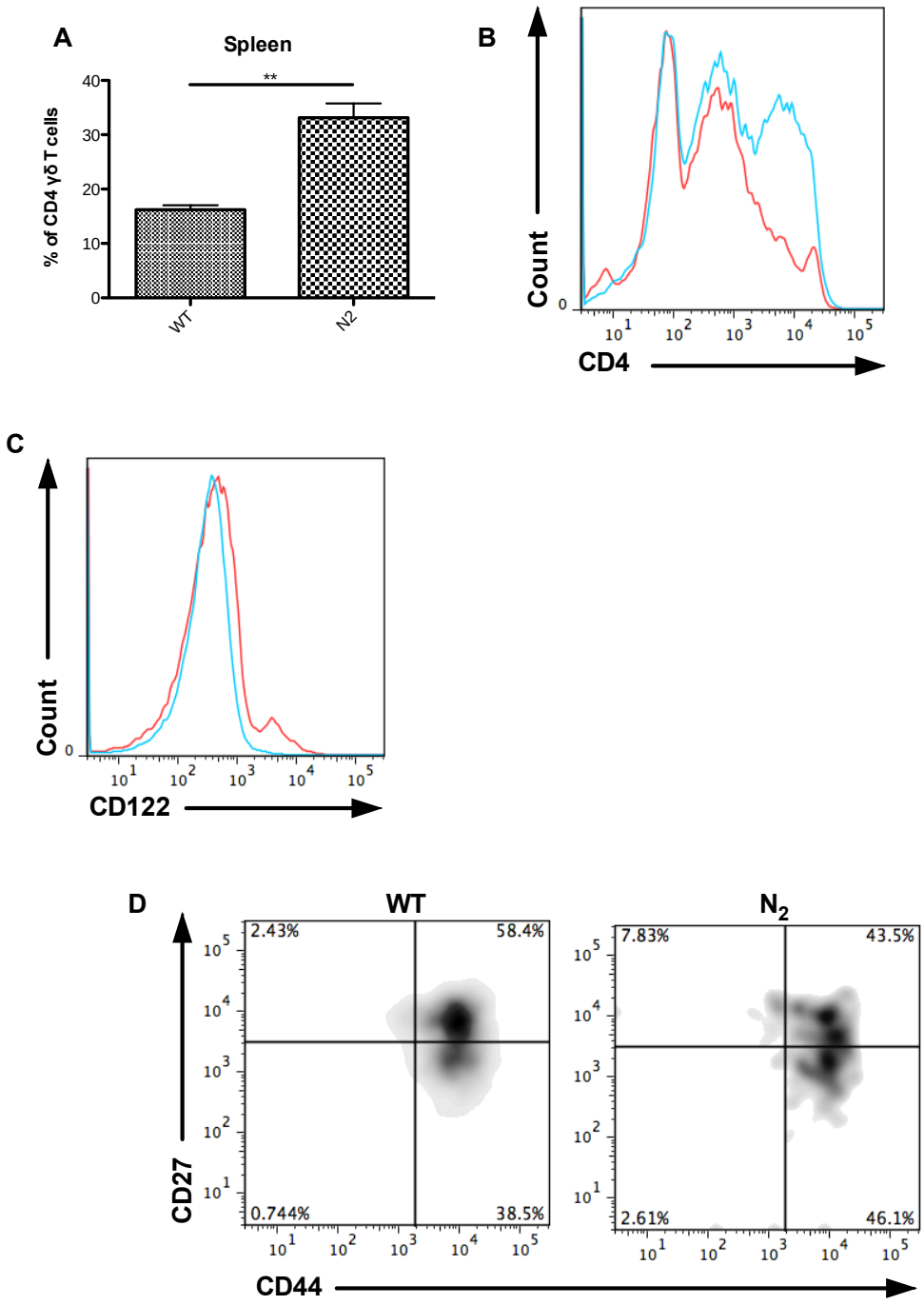

Figure 6.2: The effect of Gli2N2 on CD4 and CD122 expression of γδ T cell splenocytes

Bar chart (A) and representative overlaid histogram (B) (WT / Gli2N2) show the proportion of γδ splenocytes that are positive for CD4 in WT and Gli2N2 mice. Representative overlaid histogram (C) (WT / Gli2N2) shows CD122 expression on γδ splenocytes and density plots (D) show CD27 and CD44 expression of the $CD122^{+}$ γδ splenocytes. **p<0.001, n=4

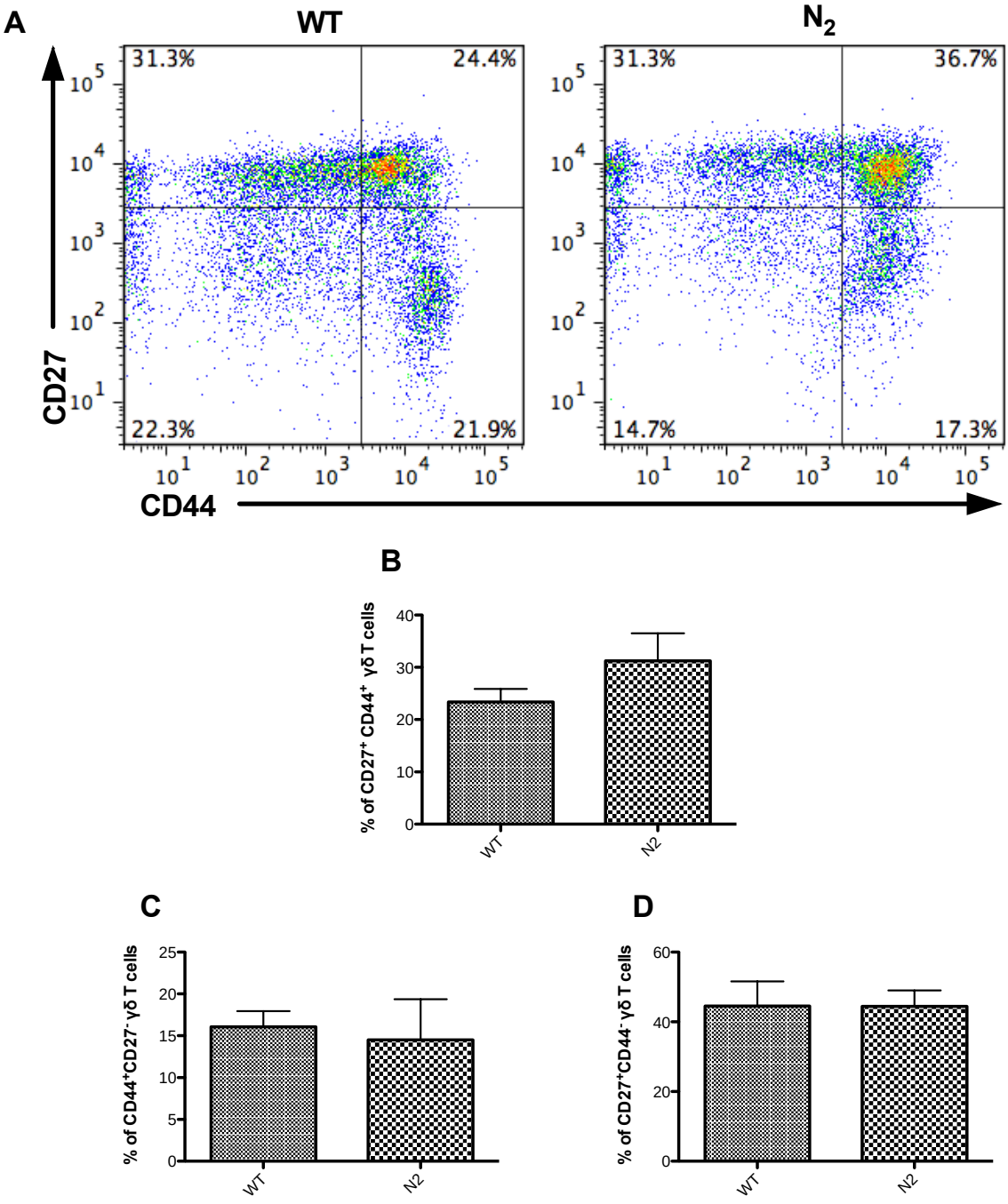

Figure 6.3: The effect of Gli2N2 on γδ T lymphocytes

Representative dot plots (A) show CD27 and CD44 on $CD3^{+}\gamma\delta^{+}$ cells from WT and Gli2N2 LN cells. Bar chart (B, C and D) show proportion of γδ cells that are $CD27^{+}CD44^{+}$, $CD44^{+}CD27^{-}$, $CD27^{+}CD44^{-}$, respectively, in WT and $Gli2N_2$ mice. n=6

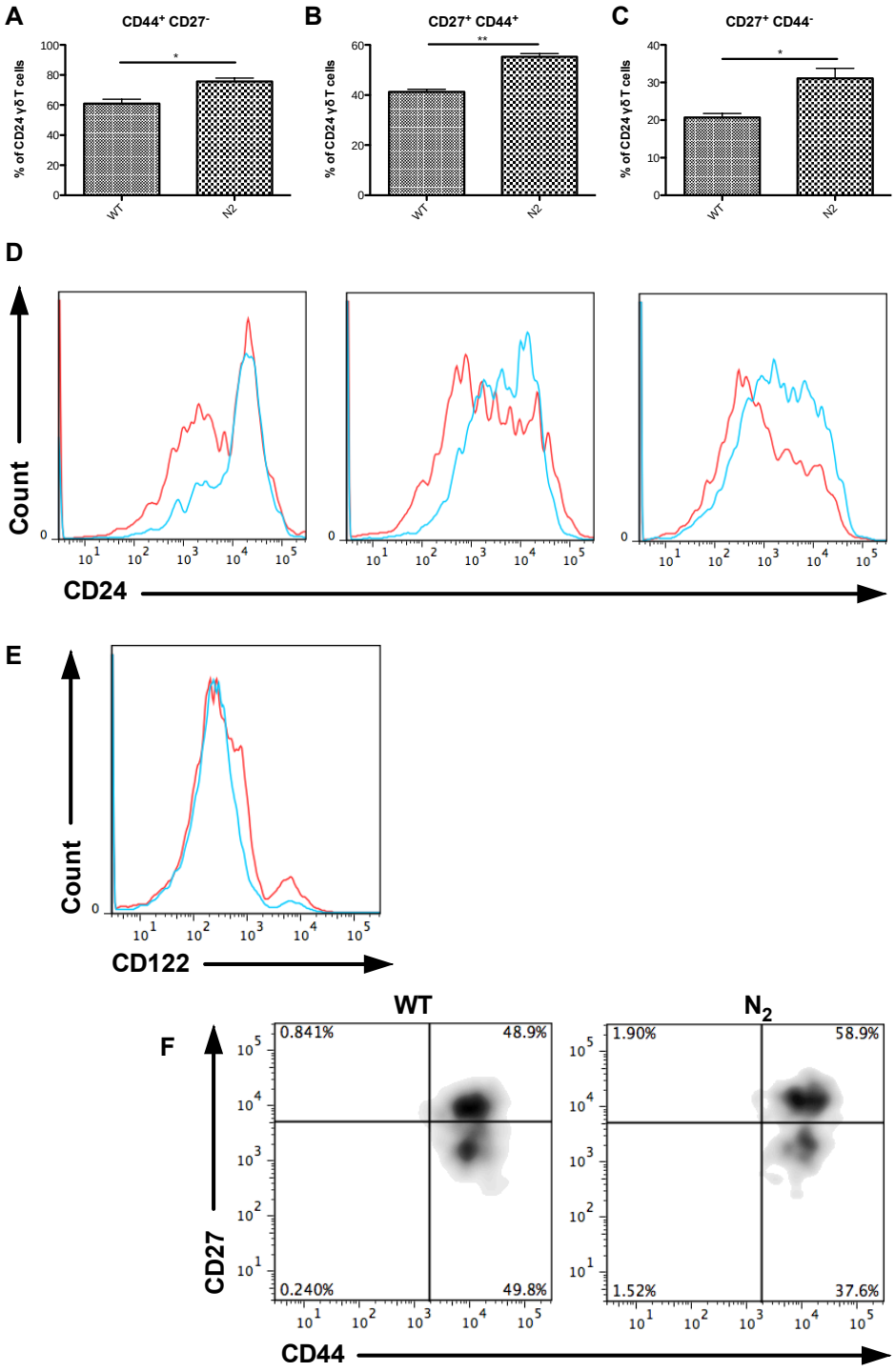

Figure 6.4: The effect of Gli2N2 on CD24 and CD122 expression of γδ T cell lymphocytes

Bar chart (A-C) and representative overlaid histogram (D) (WT / Gli2N2) show the proportion of $CD44^{+}CD27^{-}$, $CD27^{+}CD44^{+}$ and $CD27^{+}CD44^{-}$ γδ splenocytes, respectively, that are positive for CD24 in WT and Gli2N2 mice. Representative overlaid histogram (E) (WT / Gli2N2) shows CD122 expression on LN γδ cells and density plots (D) show CD27 and CD44 expression of the $CD122^{+}$ γδ LN cells. *p<0.005, **p<0.001, n=6

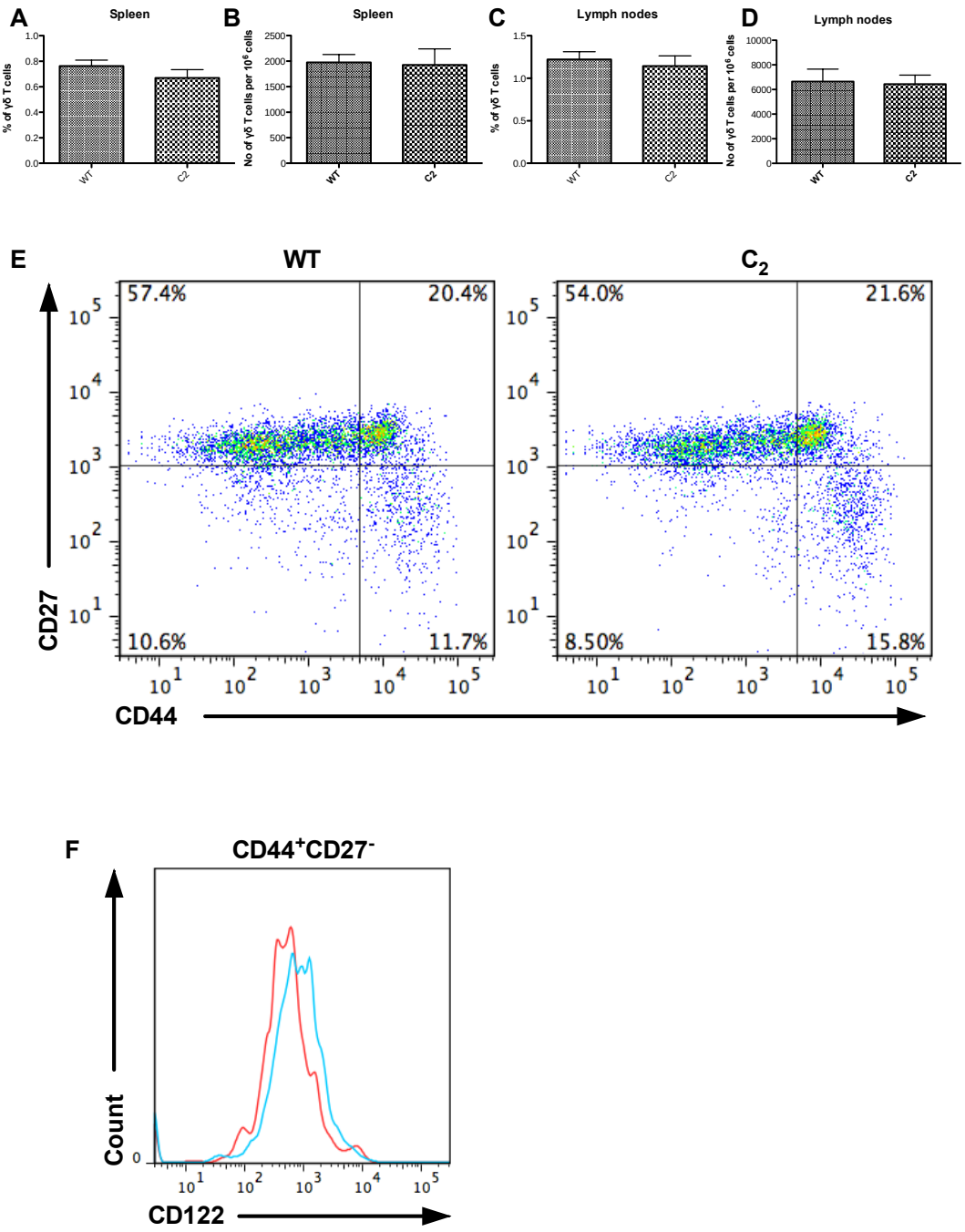

Figure 6.5: The effect of Gli2C2 on γδ T lymphocytes

Bar charts (A-D) show the proportion and cell number of γδ T cells in the spleen and lymph nodes of WT and Gli2C2 young mice. Representative dot plots (C) show the CD27 and CD44 expression on γδ T cells from the lymph nodes of WT and Gli2C2 young mice. Representative overlaid histogram (F) (WT / Gli2C2) shows the proportion of γδ lymphocytes that are positive for CD122. n=8

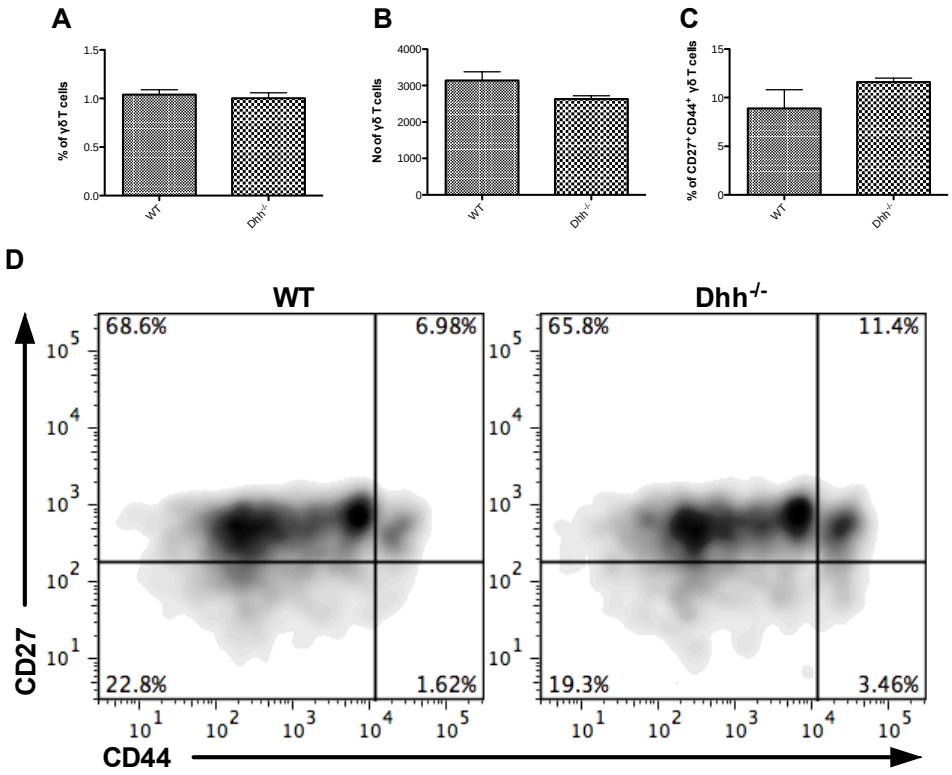

Figure 6.6: The role of Dhh in γδ T cells from the LN

Bar charts (A) and (B) show the percentage and cell count of $CD3^+$ γδ T cells n WT and $Dhh^{-/-}$ mice. Bar chart (C) shows the percentage of $CD27^+CD44^+$ γδ T cells. Dot plots (D) show CD27 and CD44 expression on γδ cells from LN WT and $Dhh^{-/-}$ mice. n=4

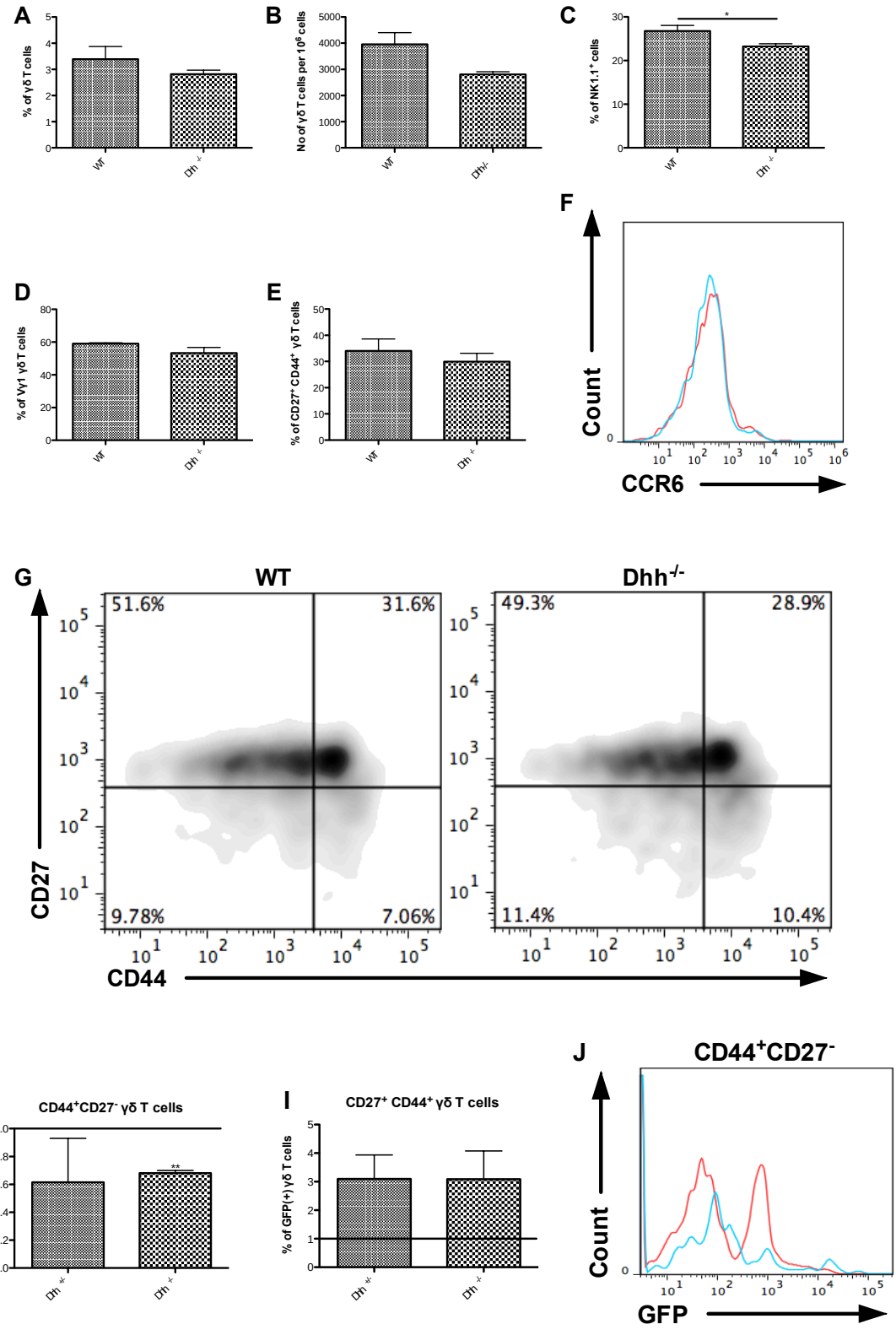
A
% of γδ T cells
WT
Dhh-/-
B
No of γδ T cells per 10^6 cells
C
% of NK1.1+ cells
*
D
% of Vγ1 γδ T cells
E
% of CD27+ CD44+ γδ T cells
F
Count
CCR6
G
WT
Dhh-/-
51.6%
31.6%
9.78%
7.06%
49.3%
28.9%
11.4%
10.4%
CD27
CD44
H
CD44+CD27- γδ T cells
% of GFP(+) γδ T cells
**
I
CD27+ CD44+ γδ T cells
J
CD44+CD27-
Count
GFP

Figure 6.7: The role of Dhh in γδ T splenocytes

Bar charts (A) and (B) show the percentage and cell count of $CD3^+$ γδ T cells in WT and $Dhh^{-/-}$ spleen. Bar chart (C) shows the percentage of γδ NKT cells and (D), (E) and show the percentages of the Vγ1 and $CD44^+CD27^+$ populations, respectively. Representative overlaid histogram (WT / KO) (F) show that deletion of Dhh decreases CCR6 cell surface expression. Dot plots (G) show CD27 and CD44 expression on γδ cells from WT and $Dhh^{-/-}$ spleen. Bar charts (H) and (I) show GBS-GFP expression of the $CD44^+CD27^-$ and $CD27^+CD44^+$ populations, relative to the WT. Representative overlaid histogram (WT / KO) (J) shows GFP expression of $CD44^+CD27^-$ γδ T splenocytes *$p<0.05$, **$p<0.001$, n=8

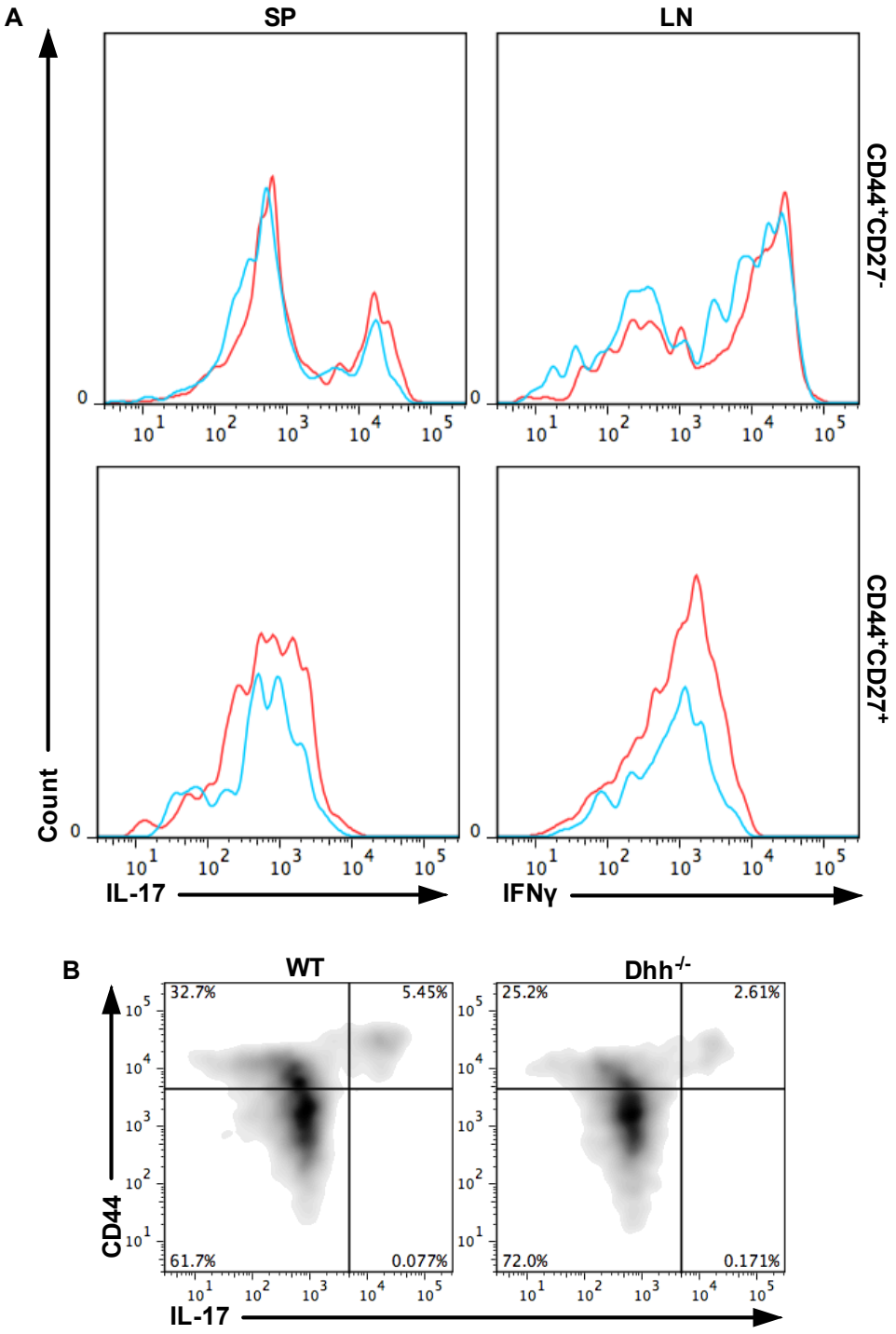

Figure 6.8: The effect of Dhh on γδ T cell production of IFNγ and IL-17 in the lymph nodes and the spleen of 4 week old mice.

Representative overlaid histograms (A) show IL-17 and IFNγ expression from $CD44^{+}CD27^{-}$ and $CD27^{+}CD44^{+}$ γδ T cells from the spleen (SP) and the lymph nodes (LN) of young mice. Representative density plots (B) show extracellular expression of CD44 versus intracellular IL-17 on WT and $Dhh^{-/-}$ γδ splenocytes. n=2

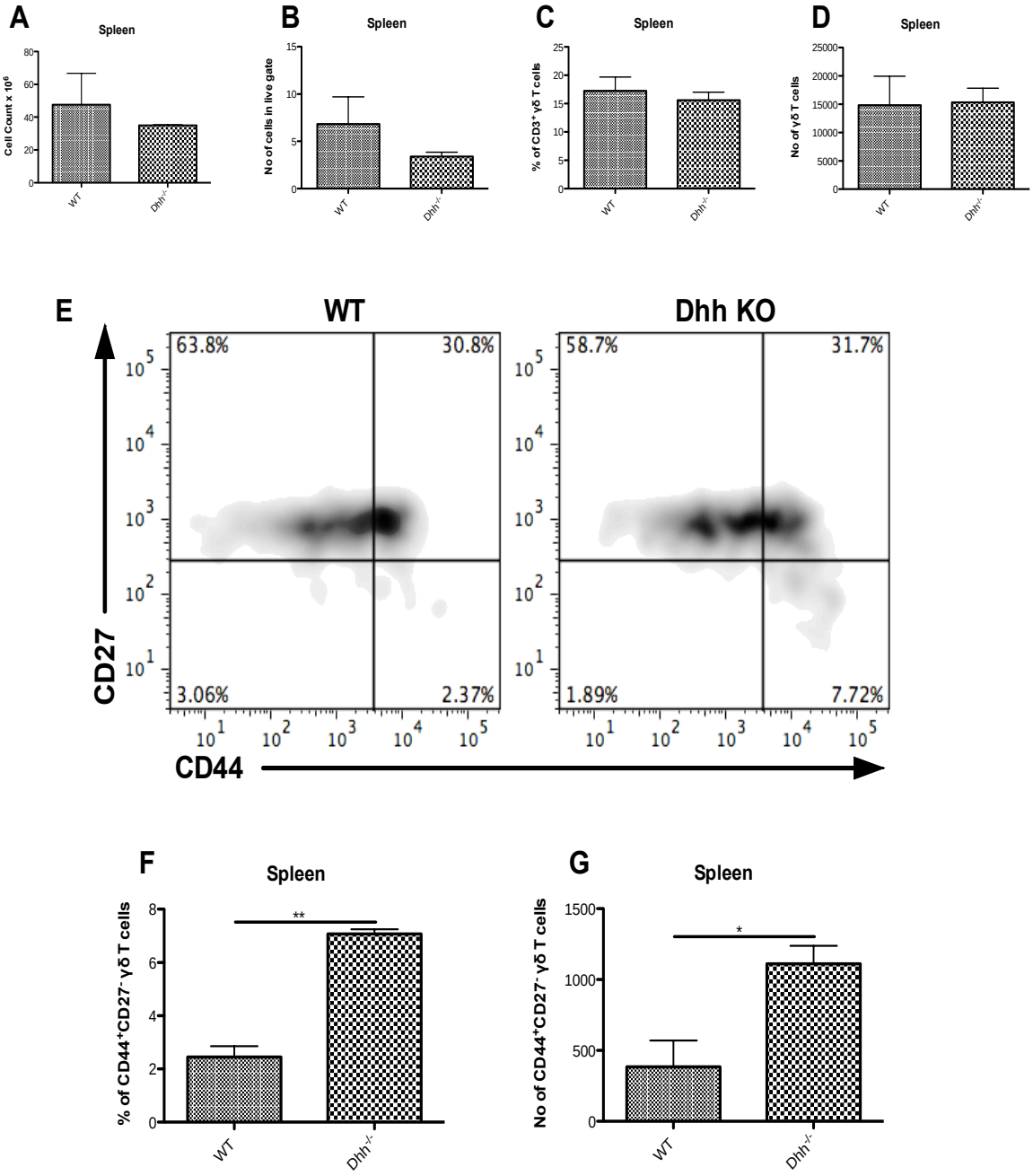

Figure 6.9: Reconstitution of γδ T cell populations in the spleen of 3 week old mice, 14 days after irradiation in WT and Dhh$^{-/-}$ littermates.

Bar chart (A) shows the total cell count of WT and Dhh$^{-/-}$ spleens, 14 days after irradiation. (B) shows the percentage of CD3+ T cells and (C) and (D) show the percentage and cell count of γδ T cells. Density plots (E) show CD27 and CD44 expression of WT and Dhh$^{-/-}$ spleens, 14 days after irradiation. Bar charts (F) and (G) show the percentage and cell count of CD44^{+}CD27^{-} γδ T cells. *p<0.05, **p<0.0005, n=8

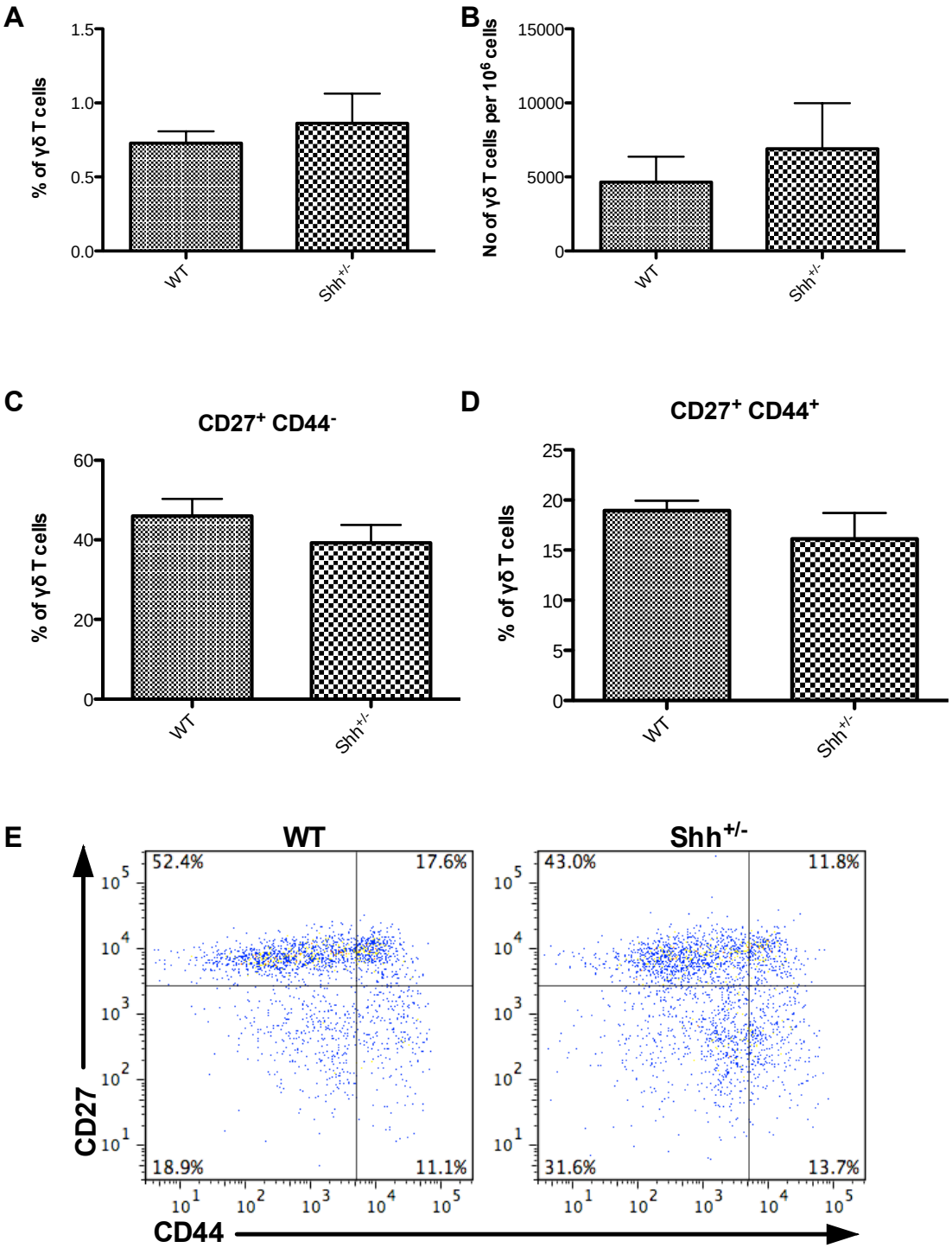

Figure 6.10: γδ T cell subtypes in adult lymph nodes of Shh$^{+/-}$ and WT mice

Bar charts (A and B) show the percentage and cell count of LN γδ T cells in WT and Shh$^{+/-}$ mice. Bar charts (B and C) show percentage of CD27^{+}CD44^{-} and CD27^{+}CD44^{+} γδ T cells, respectively. Overall, CD27 expression is reduced in the Shh$^{+/-}$, whereas overall expression of CD44 is unchanged. Representative dot plots (E) show T cell populations in relation to cell surface expression of CD27 and CD44 from WT and Shh$^{+/-}$ mice. n=6

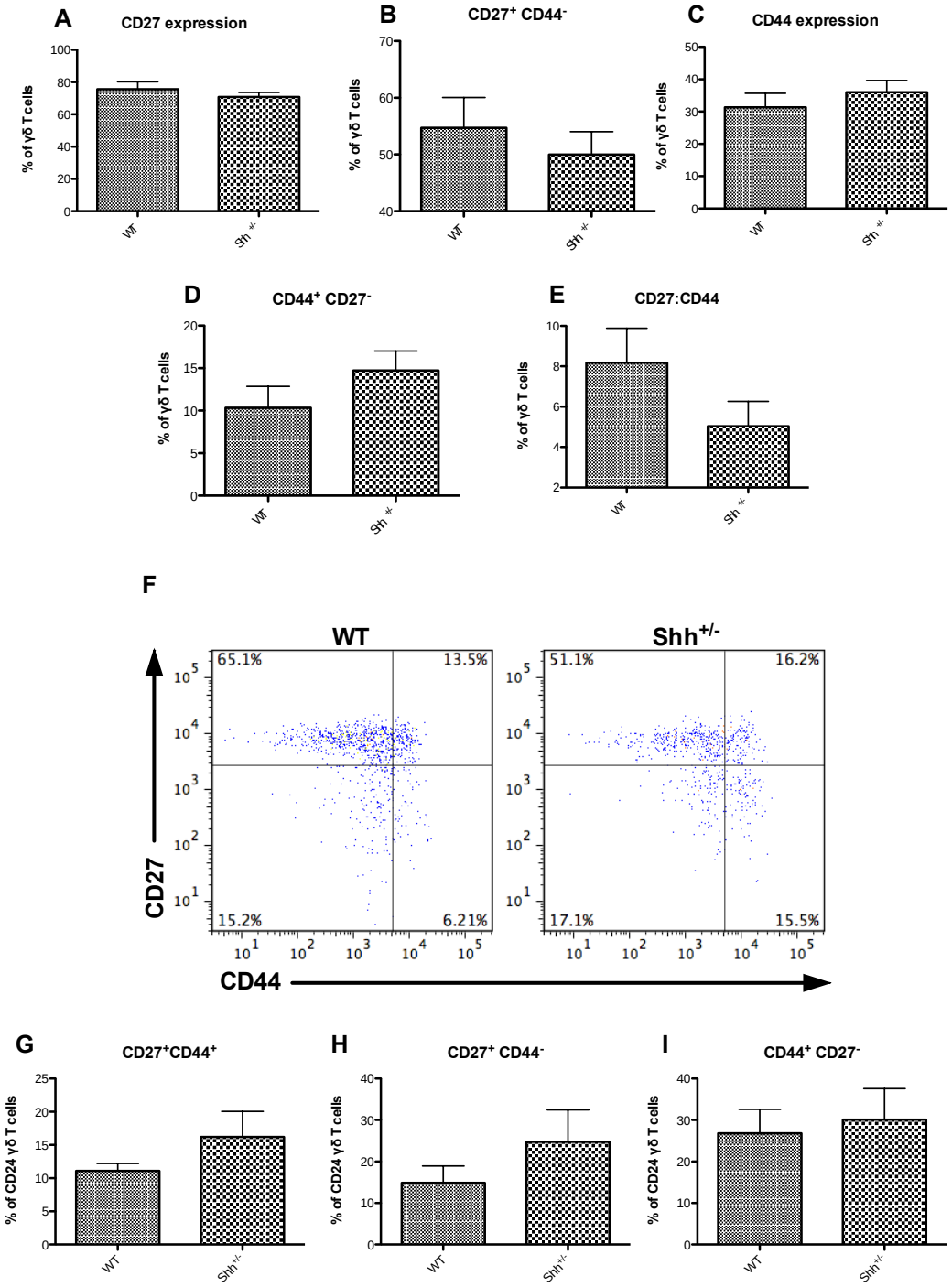

Figure 6.11: Development of γδ T cell subtypes in the adult spleen Shh$^{+/-}$ and WT mice

Bar charts show (A) expression of CD27 and (C) CD44 in γδ T cells, (B) shows percentage of the CD27^{+}CD44^{+} γδ population and (D) the percentage of CD44^{+}CD27^{-} γδ population. (E) shows the ratio of CD27^{+}CD44^{-} to CD44^{+}CD27^{-} γδ T cells. Representative dot plots (F) show cell surface expression of CD27 and CD44 on γδ T cells from WT and Shh$^{+/-}$ mice. Bar charts (G-I) show the proportion of three γδ populations that are CD24^{+}. Error bars represent ±SEM.

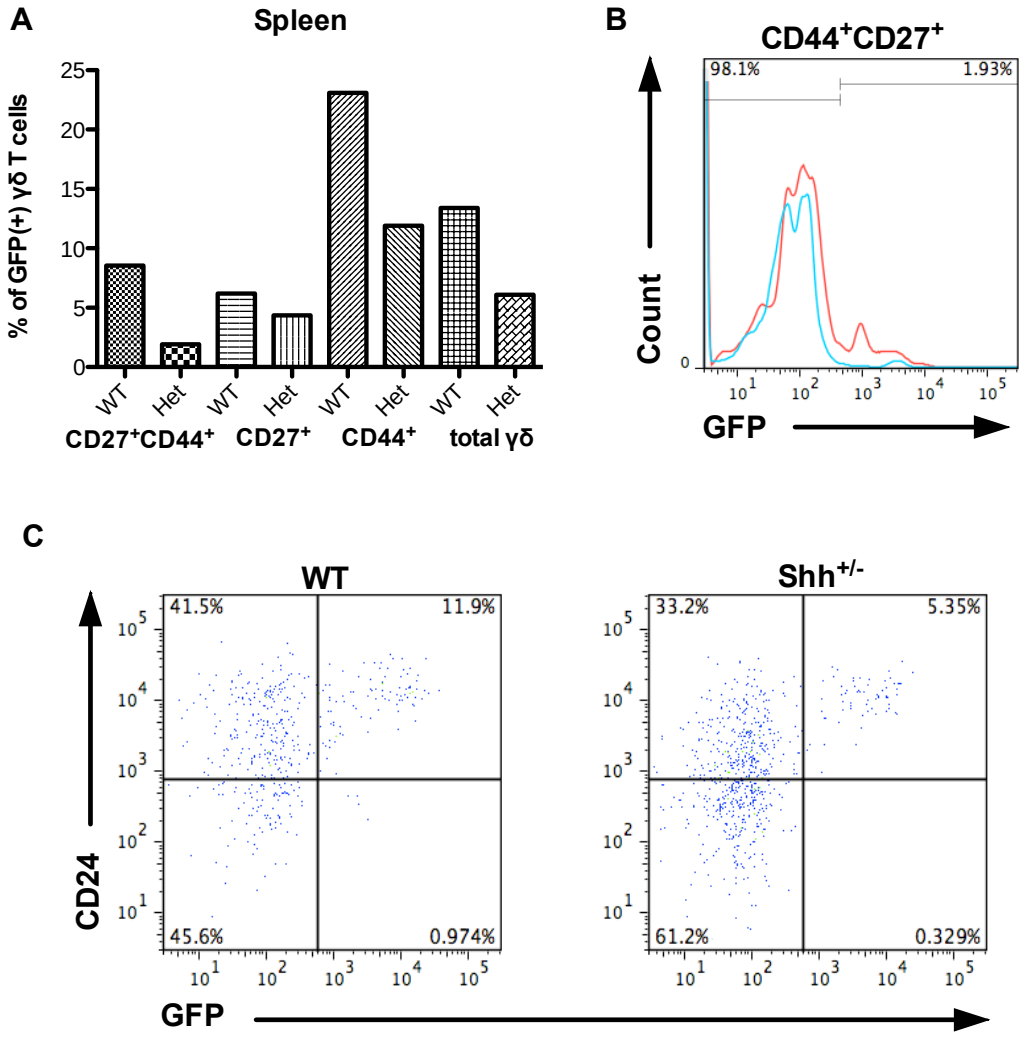

Figure 6.12: Expression of GBS-GFP in Shh$^{+/-}$ and WT spleen on major γδ T cell populations according to CD27 and CD44 cell surface expression

Bar chart (A) shows expression of GBS-GFP in CD27^{+}CD44^{+}, CD27^{+}CD44^{-} and CD44+CD27- γδ T cell populations in the spleen of young adult Shh$^{+/-}$ and Shh$^{+/-}$-GBS-GFP^{+} mice. Overlaid histogram (B) (WT / Het) shows GFP expression in CD27^{+}CD44^{+} γδ populations. Dot plots (C) show CD24 and GFP expression in γδ T cells of WT and Shh$^{+/-}$ splenocytes. n=2

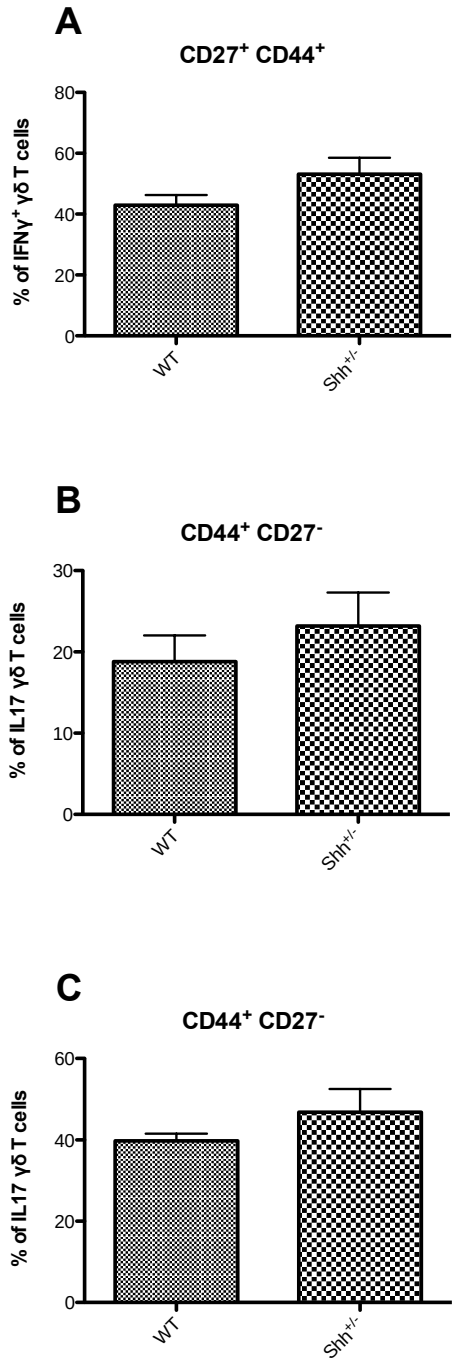

Figure 6.13: The effect of Shh in the production of key cytokines IFNγ and IL-17 in γδ T cells

Bar charts show the percentage of $CD27^{+}CD44^{+}$ cells that produce IFNγ in the spleen (A), the percentage of $CD44^{+}CD27^{-}$ γδ T cells that produce IL-17 in the spleen (B) and lymph nodes (C). Error bars represent ±SEM. n=11

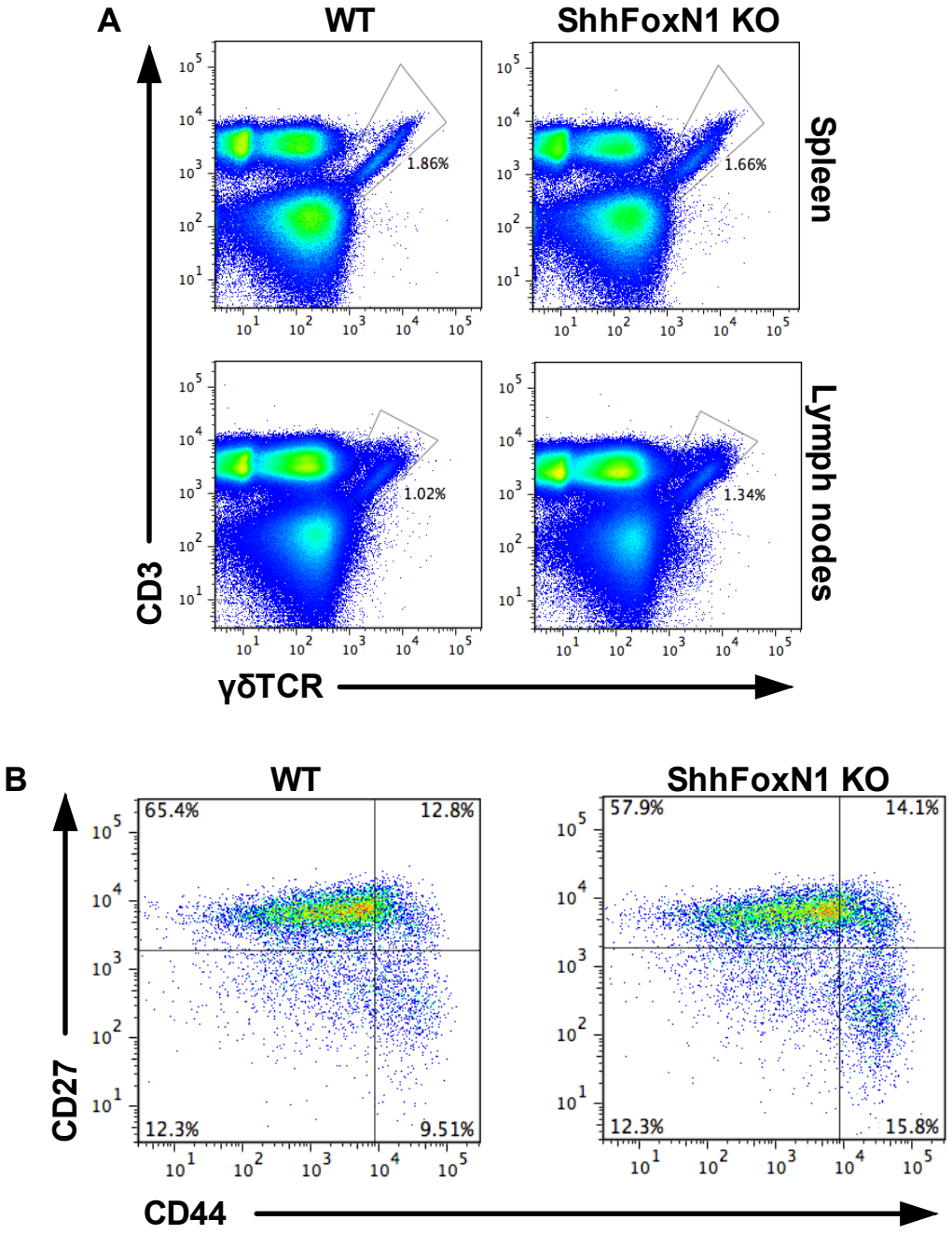

Figure 6.14: The effect of conditional deletion of Shh on peripheral γδ T cells

Dot plots (A) show CD3 and γδTCR expression of live-gated splenocytes and lymphocytes of young mice from WT and ShhFoxN1-Cre^{+} young mice. Representative dot plots (B) show CD27 and CD44 expression on LN CD3^{+} γδ cells from the same mice. n=2

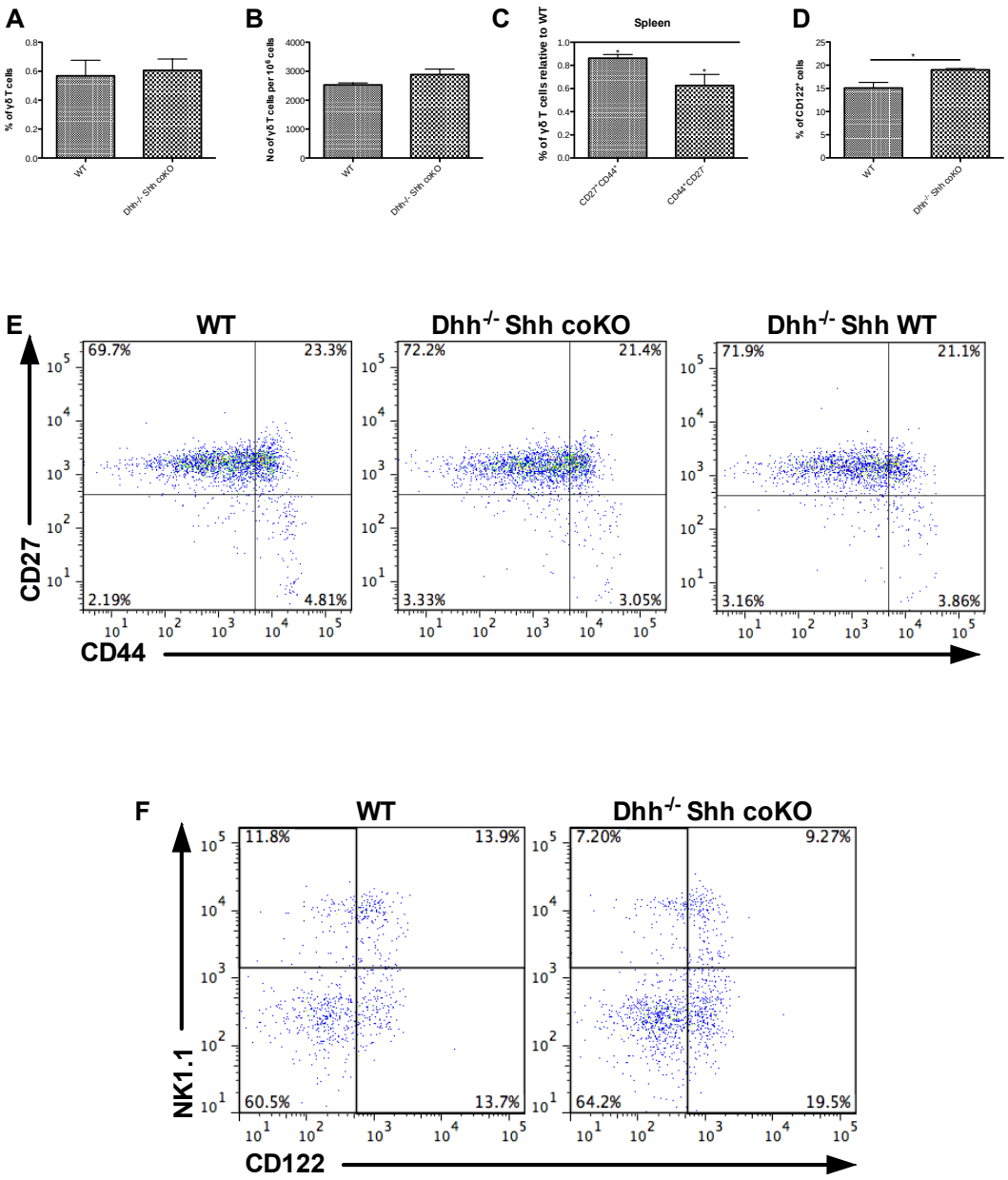

Figure 6.15: The effect of double Shh and Dhh KO on γδ splenocytes

Bar charts show (A) the percentage and (B) cell count of γδ T cells in WT and double KO splenocytes from 3 weeks old mice. (C) shows the percentage of $CD27^{+}CD44^{+}$ and $CD44^{+}CD27^{-}$ γδ subsets relative to the WT and (D) shows CD122 expression. Representative dot plots (E) show CD27 and CD44 expression on γδ T cells from WT, double KO and $Dhh^{-/-}$ ShhWT (Cre^{-}) littermates. Dot plots (F) show CD122 and NK1.1 expression on splenic γδ T cells from WT and double KO young littermates. n=6

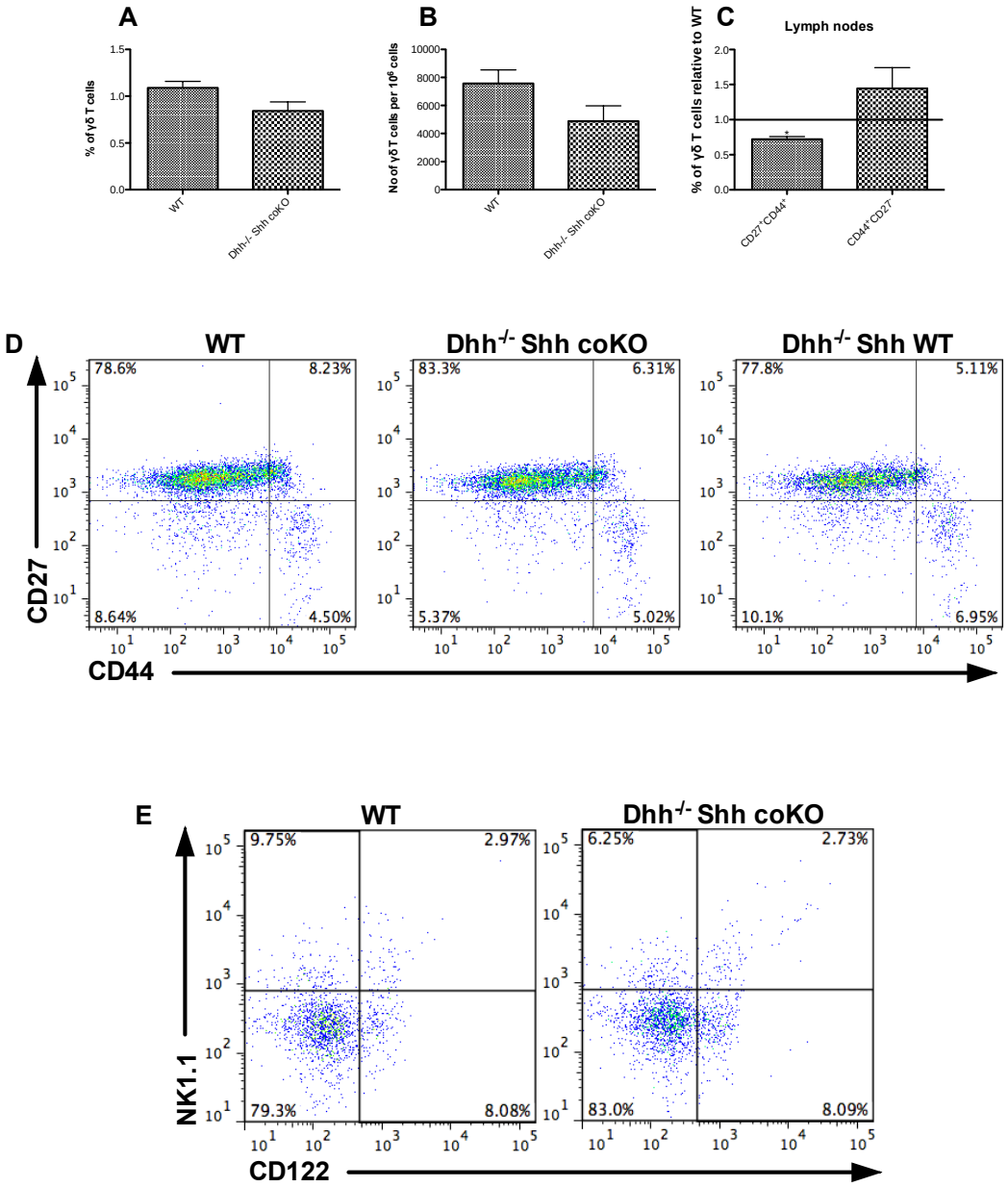

Figure 6.16: The effect of double Shh and Dhh KO on LN γδ

Bar charts show (A) the percentage and (B) cell count of γδ T cells in WT and double KO splenocytes from 3 weeks old mice. (C) shows the percentage of $CD27^{+}CD44^{+}$ and $CD44^{+}CD27^{-}$ γδ subsets relative to the WT. Representative dot plots (E) show CD27 and CD44 expression on γδ T cells from WT, double KO and $Dhh^{-/-}$ ShhWT (Cre^{-}) littermates. Dot plots (F) show CD122 and NK1.1 expression on γδ T cells from WT and double KO young littermates. n=4

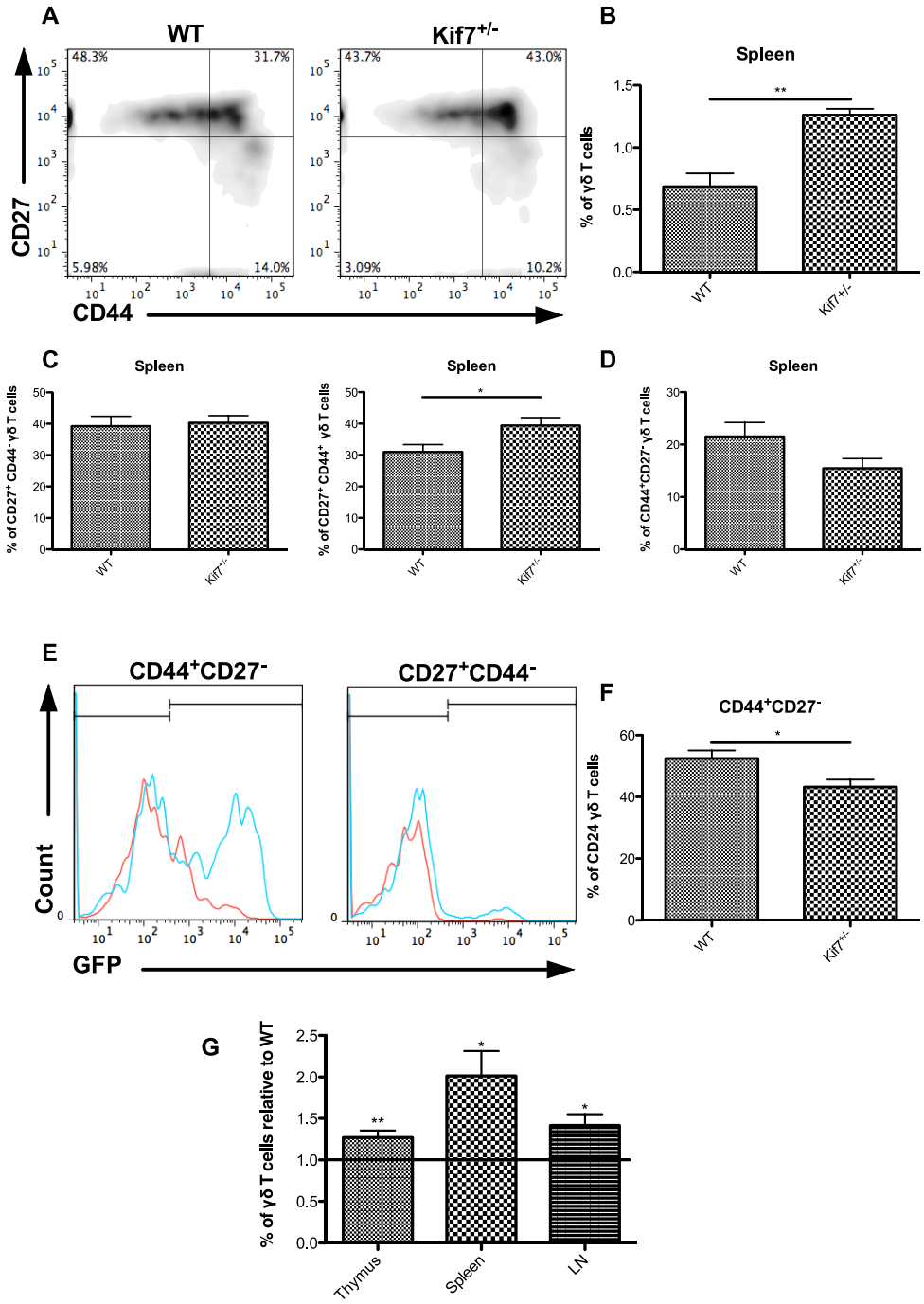

Figure 6.17: Development of γδ T cell subtypes in the adult Kif7$^{+/-}$ spleen

Representative dot plots (A) show expression of CD27 and CD44 in WT and Kif7$^{+/-}$ mouse spleen. Bar charts (B) show percentages of splenic γδTCR^{+} cells in WT and Kif7$^{+/-}$. Bar charts (C) shows the percentage of CD27^{+}CD44^{-}, CD27^{+}CD44^{+} and (D) CD44^{+}CD27^{-} populations in WT and Kif7$^{+/-}$ spleens. Representative overlaid histograms (E) show GBS-GFP expression (WT / Het) in CD44^{+}CD27^{-} and CD27^{+}CD44^{-} γδ populations in the spleen of 4 weeks mice. Bar charts (F) show the percentage of CD44^{+}CD27^{-} splenic γδ T cells that express CD24 and (G) shows the percentage of γδTCR^{+} cells relative to WT in three tissues of Kif7$^{+/-}$ mice. Error bars represent ±SEM. *p<0.05 **p<0.01, n=11

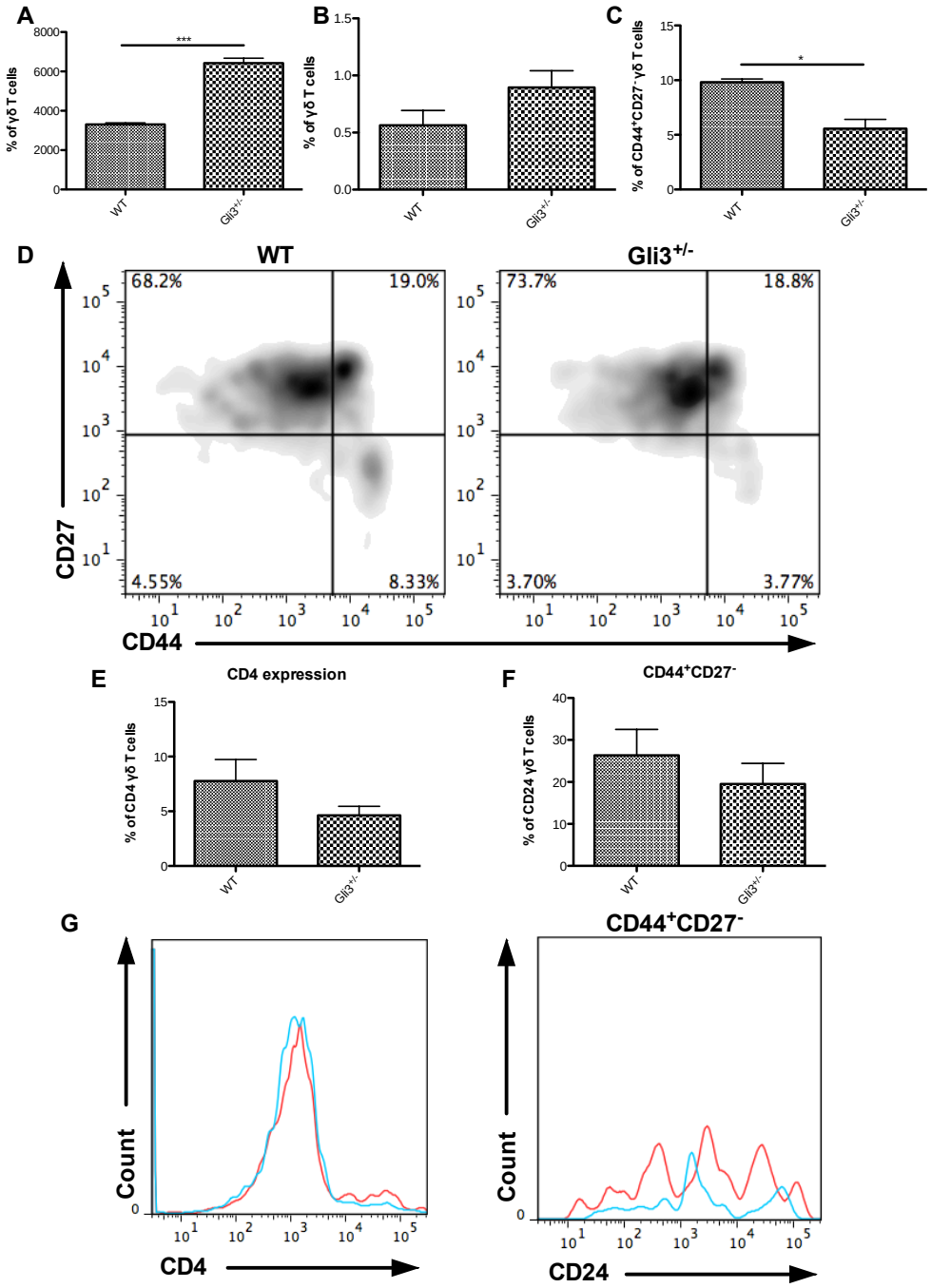

Figure 6.18: The influence of Gli3 on peripheral γδ populations of young adult mice

Bar charts (A and B) show the number and proportion of γδ cells from the spleen of WT and Gli3$^{+/-}$ mice. Representative density plots (D) show CD27 and CD44 cell surface expression in WT and Gli3$^{+/-}$ γδ splenocytes. Bar chart (C) shows percentage of CD44^{+}CD27 γδ cells. Bar charts (E and F) show percentage of γδ T cells that express CD4 and CD24 in the spleen of WT and Gli3$^{+/-}$ mice, respectively. Representative overlaid histograms (G and I) (WT / Het) show CD4 and CD24 expression in γδ T cells, respectively. Error bars represent ±SEM. *p<0.05, ***p<0.0001, n=6

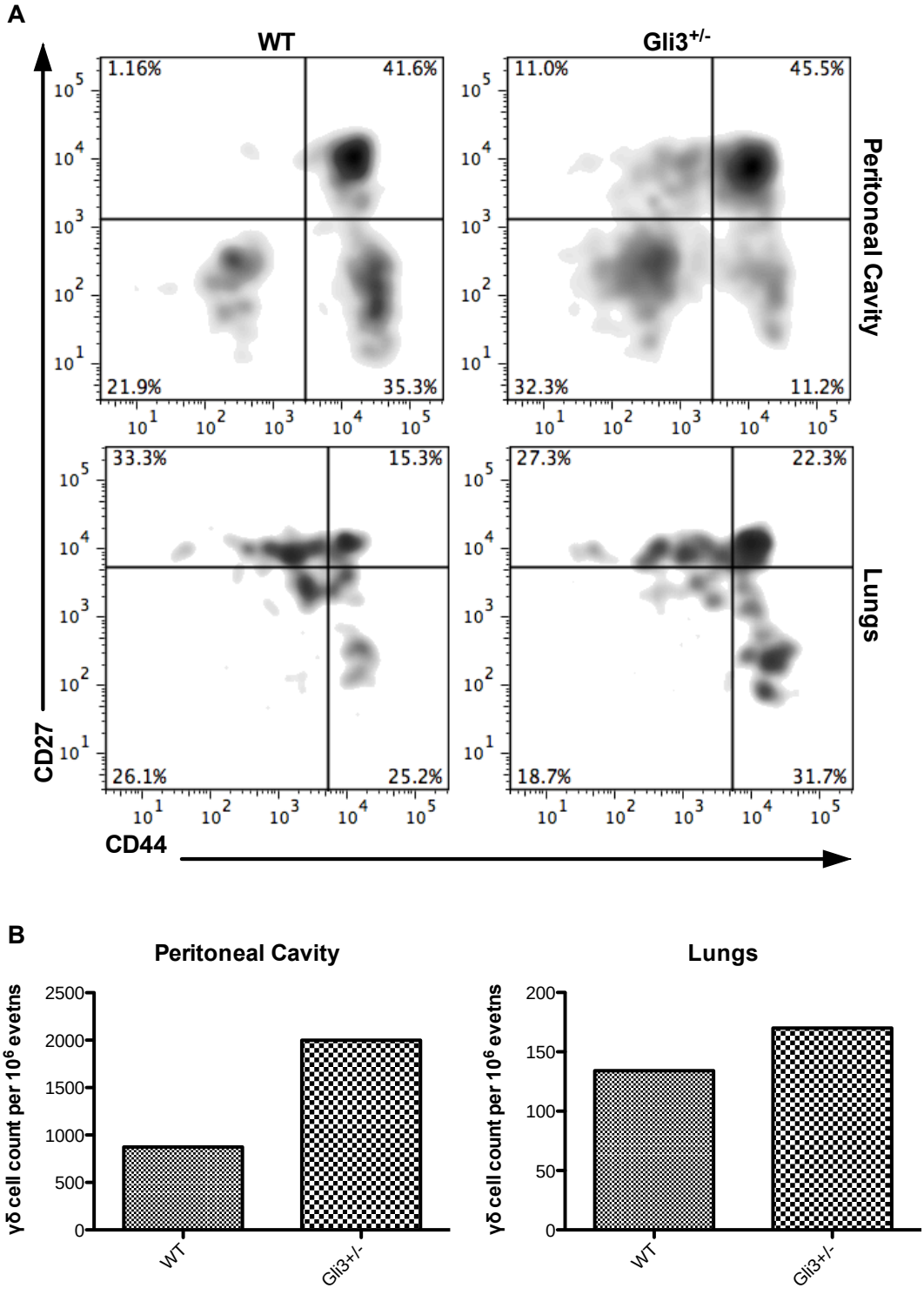

Figure 6.19: The effect of Gli3 on γδ populations in the peritoneal cavity and the lungs of young adult mice

Density plots (A) show CD27 and CD44 expression on WT and Gli3$^{+/-}$ γδ T cells from the peritoneal cavity and lungs of young littermates. Bar charts (B) show the γδ cell count per million events collected by flow cytometry. n=2

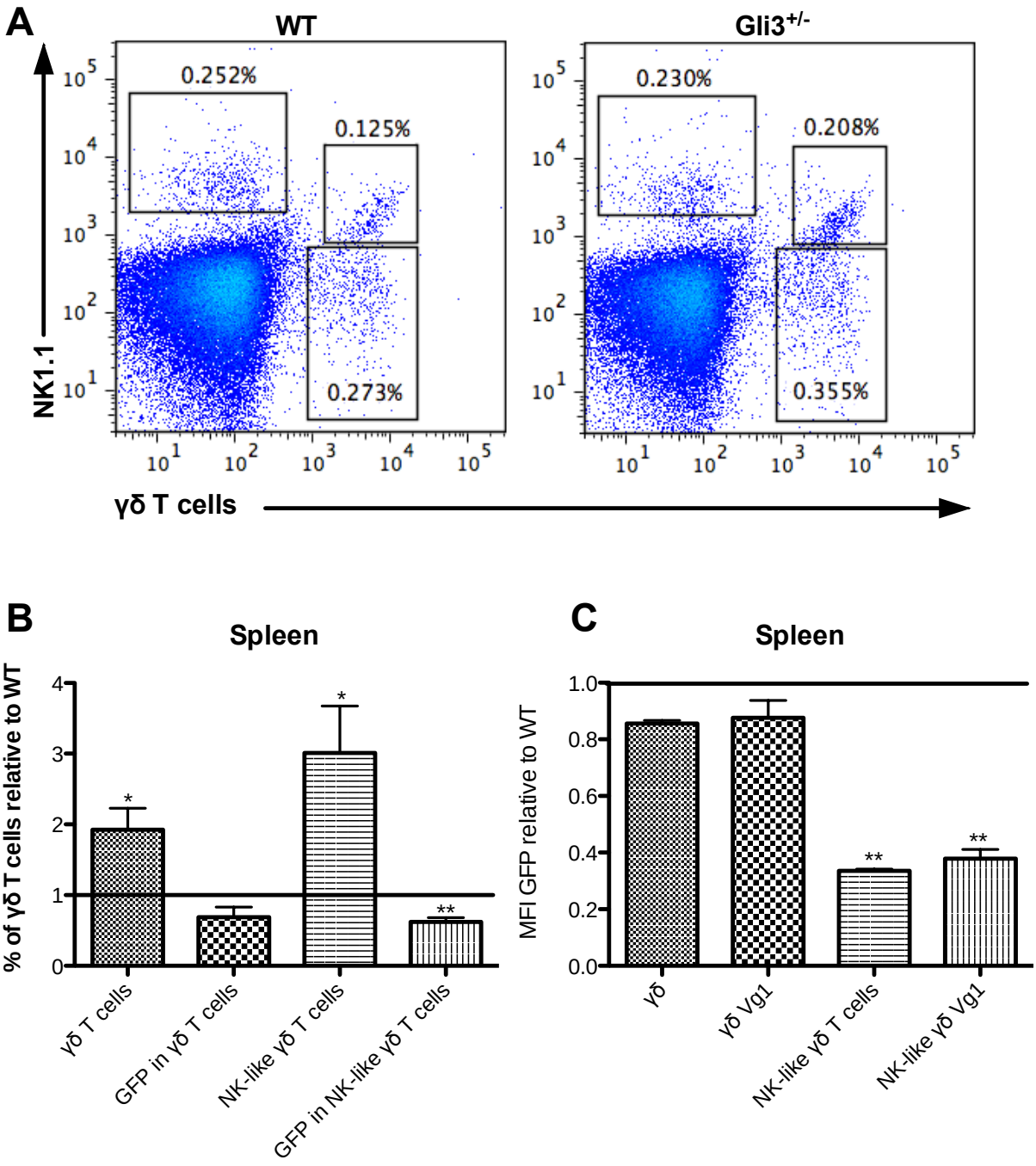

Figure 6.20: Hedgehog reporter transgenic (GBS-GFP-Tg) show reduced Hh pathway activation in γδ cells from Gli3$^{+/-}$ mice.

Dot plots (A) show the gating strategy from CD3^{+} thymocytes in order to identify three T cell populations: NK cells, NK-like γδ T cells and γδ T cells. Bar chart (B) shows percentage and GBS-GFP activity of γδ and NK-like γδ T cells, relative to WT and (C) shows mean fluorescent intensity (MFI) of γδ, NK-like γδ T cells and the Vγ1 chain, relative to WT. Error bars represent ±SEM. *p<0.005, **p<0.0005, n=4

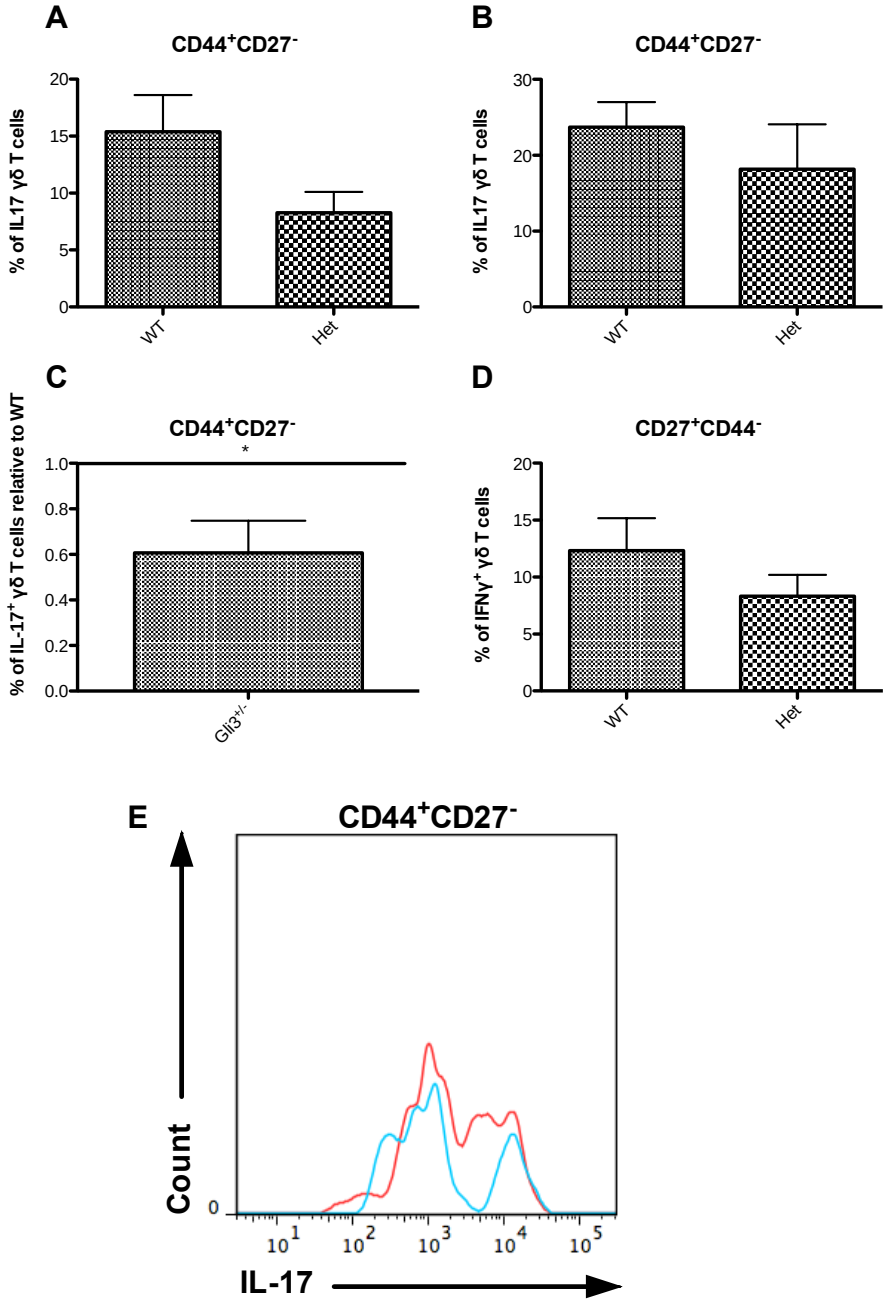

Figure 6.21: The role of Gli3 in the production of key γδ T cell cytokines

Bar charts show the percentage of IL-17-producing CD44$^+$CD27$^-$ γδ T cells in the (A) spleen and (B) lymph nodes of 4 weeks old mice, upon 4h T cell activation with PMA and Ionomycin. (C) shows the difference in splenic γδ IL-17 production, relative to WT. Bar charts (D) show production of IFNγ in CD27$^+$CD44$^-$ γδ T cells. Representative overlaid histogram (E) (WT / Tg) shows reduction in IL-17 production in splenic Gli3$^{+/-}$ CD44$^+$CD27$^-$ γδ T cells compared to WT. *$p<0.05$, n=6

7. The effect of Hedgehog signalling on γδ T cells in an LPS mouse model

7.1 Introduction

We have investigated the role of Hh signalling in the development and differentiation of murine γδ T cells in the thymus and the periphery. However, the impact of Hh signalling in the activation and cytokine secretion of γδ T cells has been explored only through short PMA / Ionomycin activation assays. Therefore, we used a mouse disease model of experimental sepsis by injecting Lipopolysaccharide (LPS) intraperitoneally (ic) in order to investigate γδ-mediated immune responses upon infection and inflammation in more detail.

Toll-like receptors (TLR) are pattern recognition receptors (PRR) that recognize various structurally conserved molecules derived from microbes and they often lead to indirect activation of the adaptive immune responses (Wesch, Peters et al. 2011). LPS consists of a hydrophobic lipid A component, a hydrophilic core oligosaccharide and an O-antigen. It is believed that murine γδ cells recognize LPS via TLR2 whose ligand is the lipid A component of LPS. Murine Vγ6 CCR6^{+} IL-17-producing γδ T cells respond directly to TLR2 resulting in enhanced proliferation and cytokine secretion in a TCR-independent manner (Martin, Hirota et al. 2009). In humans, γδ T cells respond indirectly to TLR4 (via monocyte-derived dendritic cells) in a CD1c/CD1d-restricted manner.

We decided to focus our analysis on the two strains that gave the strongest phenotype in previous experiments; the Gli2N2 tg and the Shh deficient strains (either Shh$^{+/-}$ or conditional FoxN1 Shh deletion). Since the set of

experiments in this chapter followed the ones shown on previous chapters, our flow cytometry analysis is expanded further to include more makers and can therefore offer better insight into murine γδ T cell biology.

7.2 Results

7.2.1 The effect of Gli2N2 on γδ cells from LPS-injected young adult mice

For our experiment, we used three sex-matched pairs (WT and Gli2N2) of 6 week old littermate mice. We injected intraperitoneally with a single dose of 100ng/gram of body weight LPS in 200μl of sterile PBS. The control group was injected ip with 200μl sterile PBS. Mice were sacrificed four days later and analysed by flow cytometry.

In the Gli2N2 thymus, we observed a significant increase in the numbers of $CD27^{+}CD44^{+}$ cells (Figure 7.1A,B,D) compared to WT. We also observed a significant increase in the number of γδ cells bearing a Vγ1 chain (Figure 7.1F). This $CD27^{+}CD44^{+}$ population is negative for CCR6 (Figure 7.1H). A more detailed analysis of the phenotype of various Vγ chains revealed that the expanding $CD27^{+}CD44^{+}$ population includes Vγ1 cells (Figure 7.2A), most of which were positive for NK1.1 (Figure 7.2B). It also very interesting that a shift takes place between Vγ2 and other Vγ chains in relation to $CD44^{+}CD27^{-}$ cells. In the Gli2N2 mice, Vγ2-bearing $CD44^{+}CD27^{-}$ cells disappear completely, whereas the same subset bearing other Vγ chains, shows a 10fold expansion (Figure 7.2A).

In the spleen, we also observed a significant increase in $CD27^{+}CD44^{+}$ Vγ1 cells, $CCR6^{-}$ γδ cells (Figures 7.3A, B, D, E) in the Gli2N2 compared to WT. Similarly to the thymus, the Vγ2 $CD44^{+}CD27^{-}$ γδ subset virtually disappears (Figure 7.3D). A similar effect was observed in γδ cells of the

lymph nodes (Figures 7.3), although the γδ cells in the lymph nodes did not increase in numbers significantly in the Gli2N2 compared to WT.

Interestingly, when we performed the same analysis in the peripheral blood of our samples, we found a massive reduction in CD27-expressing γδ cells as well as a great increase in CD44-expressing cells (Figure 7.4C, D) in the transgenic compared to WT. Collectively, our data suggest that it is likely that in the Gli2N2 mice, $CD27^{+}CD44^{+}$ Vγ1 cells fail to exit the thymus and therefore accumulate in the thymus. Analysis of skin showed a reduction in γδ cells (Figure 7.4E, F). Upon activation with PMA and ionomycin for 4h, γδ splenocytes from LPS-treated Gli2N2 mice, showed a large reduction in both IL-17 and IFNγ expression (Figure 7.5A). IFNγ reduction is attributed mostly to Vγ2-bearing cells (Figure 7.5B).

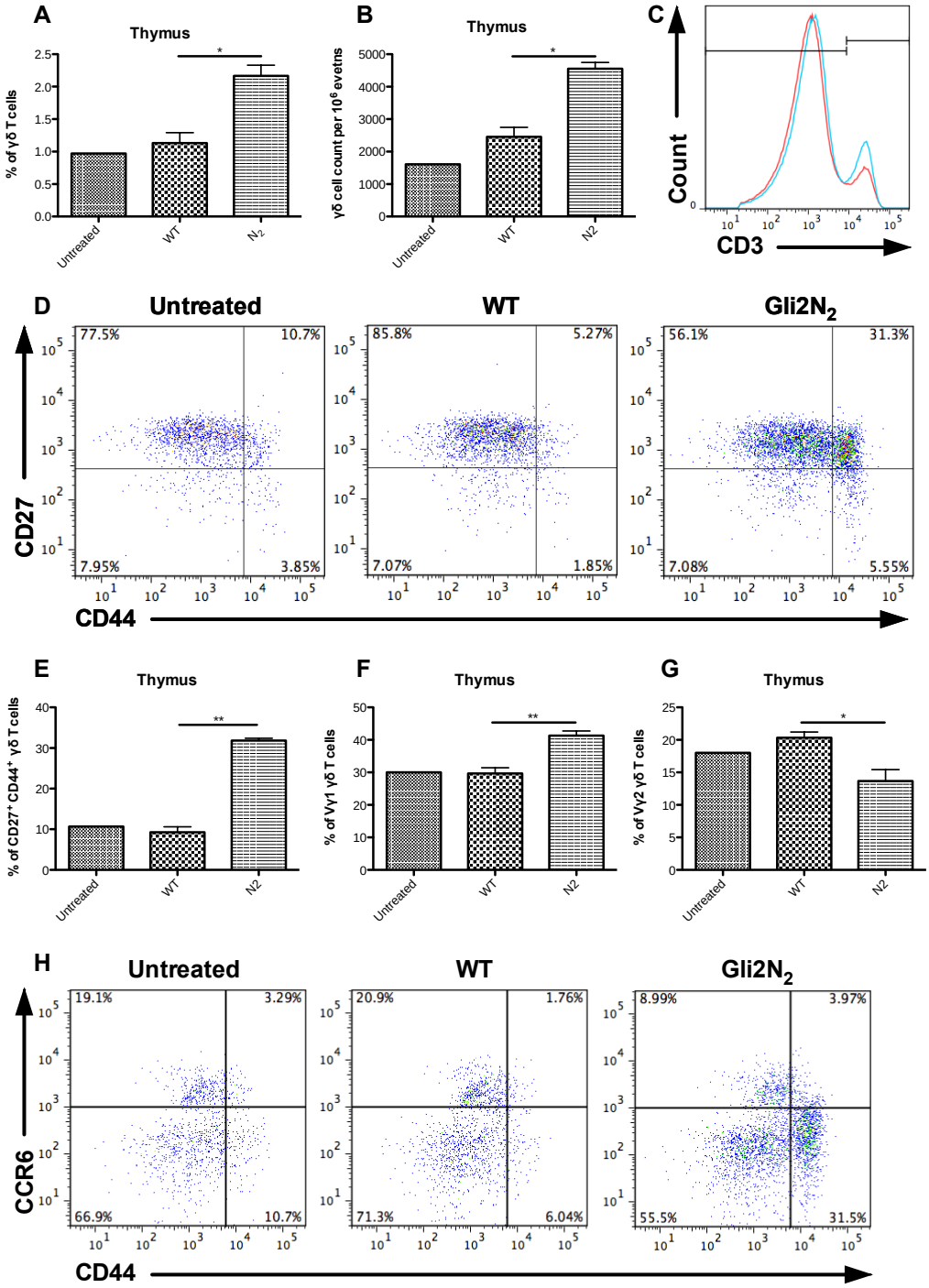

Figure 7.1: The effect of transgenic expression of Gli2N2 in LPS-treated γδ thymocytes

Bar chart (A) show the percentage of γδ T cells in the thymus of WT and Gli2N2 littermates, 4 days after LPS treatment and (B) shows the thymic γδ cell count. Overlaid histogram (C) shows CD3 expression in the live gate of WT (untreated / LPS-treated WT) littermates. Dot plots (D) show CD27 and CD44 expression on untreated and LPS-treated γδ T cells from WT and Gli2N2 littermates. Bar charts show (E) the percentage of $CD27^{+}CD44^{+}$, (F) Vγ1 and (G) Vγ2 γδ thymocytes. Dot plots (H) show expression of CD44 and CCR6 in γδ thymocytes. n=5

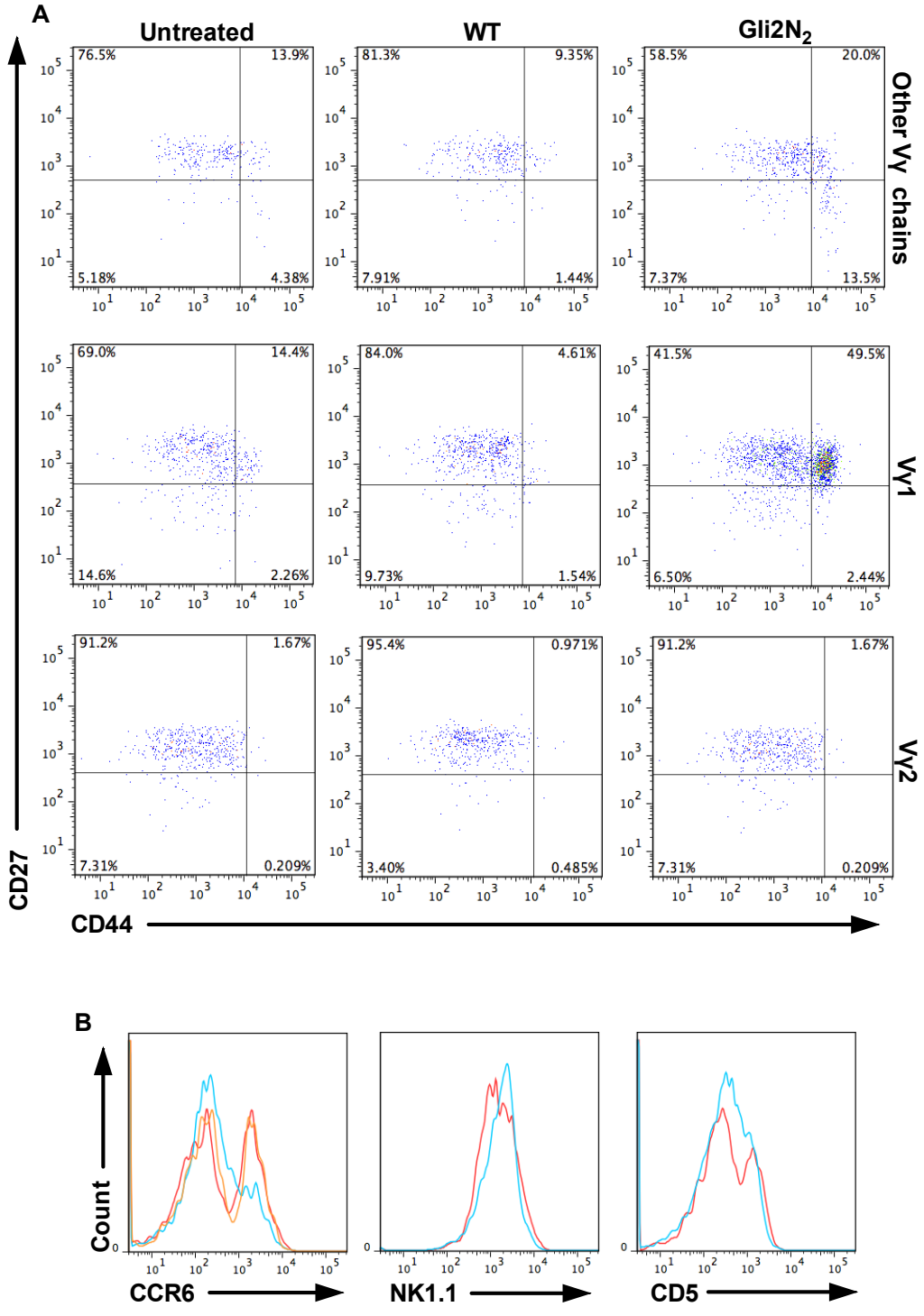

Figure 7.2: The effect of transgenic expression of Gli2N2 on LPS-injected γδ subsets

Dot plots (A) show CD27 and CD44 expression on γδ cells gated on Vγ1, Vγ2 and other Vγ chains from untreated and LPS-treated γδ T cells from WT and Gli2N2 littermates. Overlaid histograms (B) (untreated / WT / Gli2N2) show CCR6, NK1.1 and CD5 expression on γδ T cells. n=5

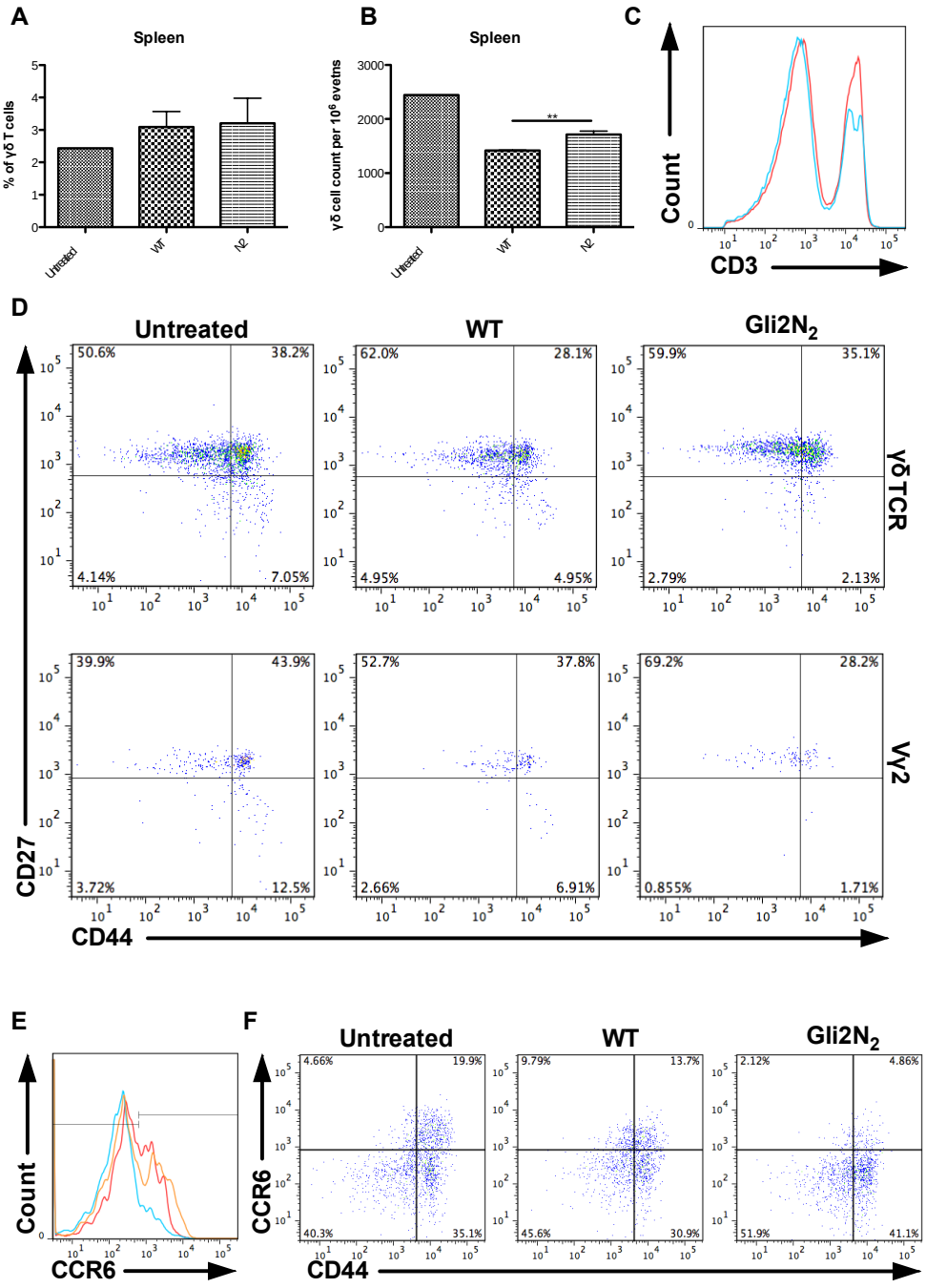

Figure 7.3: The effect of transgenic expression of Gli2 on LPS-treated γδ splenocytes

Bar chart (A) show the percentage (from the CD3⁺ gate) of γδ T cells in the spleen of WT and Gli2N2 littermates and (B) shows the γδ cell count per million splenocytes, 4 days after LPS treatment. Overlaid histogram (C) (untreated / LPS-treated WT) shows live-gated CD3 expression. Dot plots (D) show CD27 and CD44 expression on untreated and LPS-treated γδ T cells and Vγ2 bearing γδ T cells from WT and Gli2N2 littermates. Overlaid histogram (E) (untreated / WT / Gli2N2) shows the expression of CCR6 on γδ T cells and dot plots (F) show expression of CCR6 and CD44 on γδ T cells. n=5

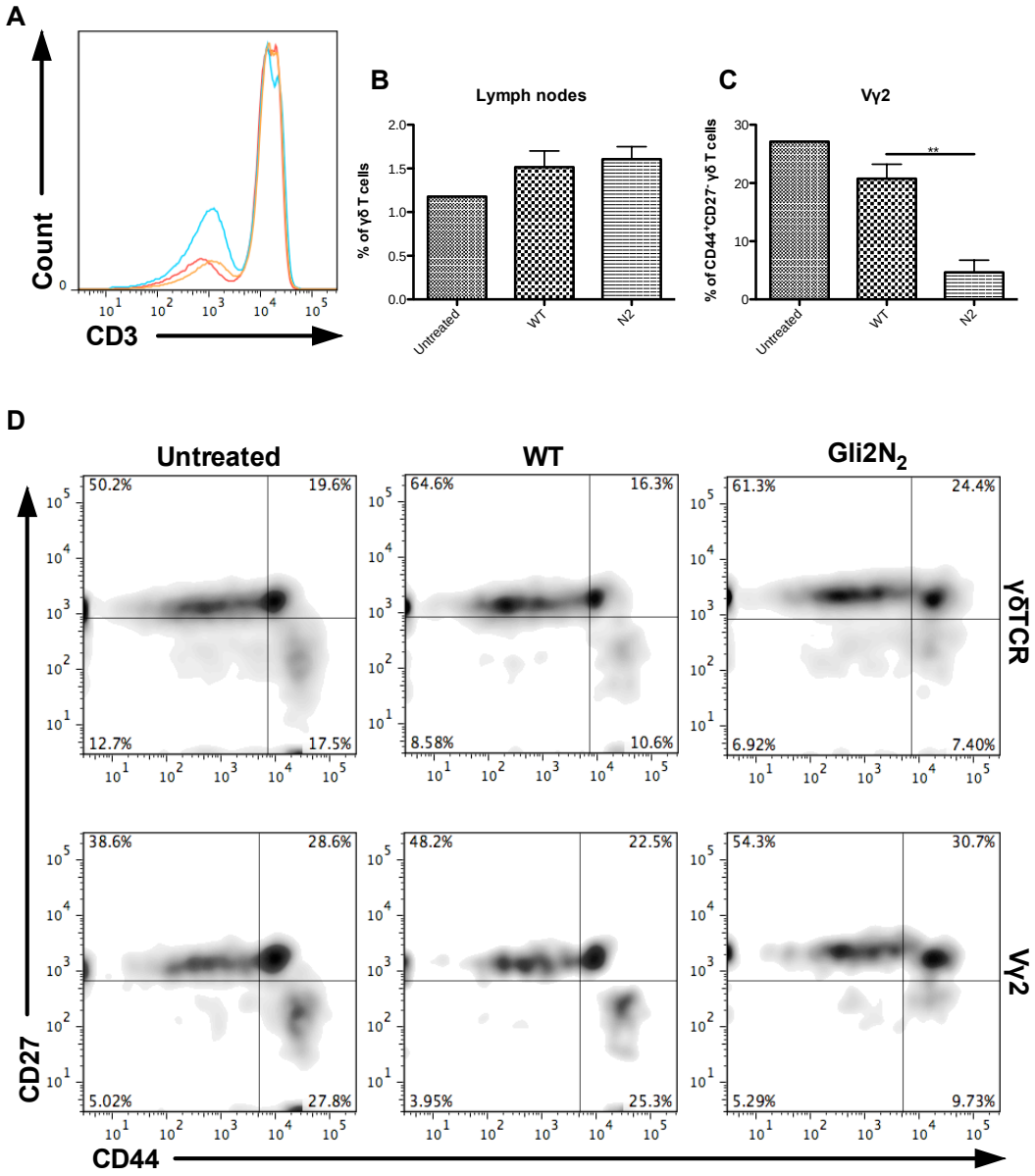

Figure 7.4: The effect of transgenic expression of Gli2 on LPS-treated γδ cells in lymph nodes

Overlaid histogram (A) (untreated / WT / Gli2N2) shows CD3 expression in the live gate of 6 weeks old littermates. Bar chart (B) show the percentage (from the $CD3^+$ gate) of γδ T cells in the lymph nodes of WT and Gli2N2 littermates and (C) shows the percentage of $V\gamma2^+$ γδ cells. Density plots (D) show CD27 and CD44 expression on untreated and LPS-treated γδ T cells and Vγ2 bearing γδ T cells from WT and Gli2N2 littermates. **p<0.005, n=5

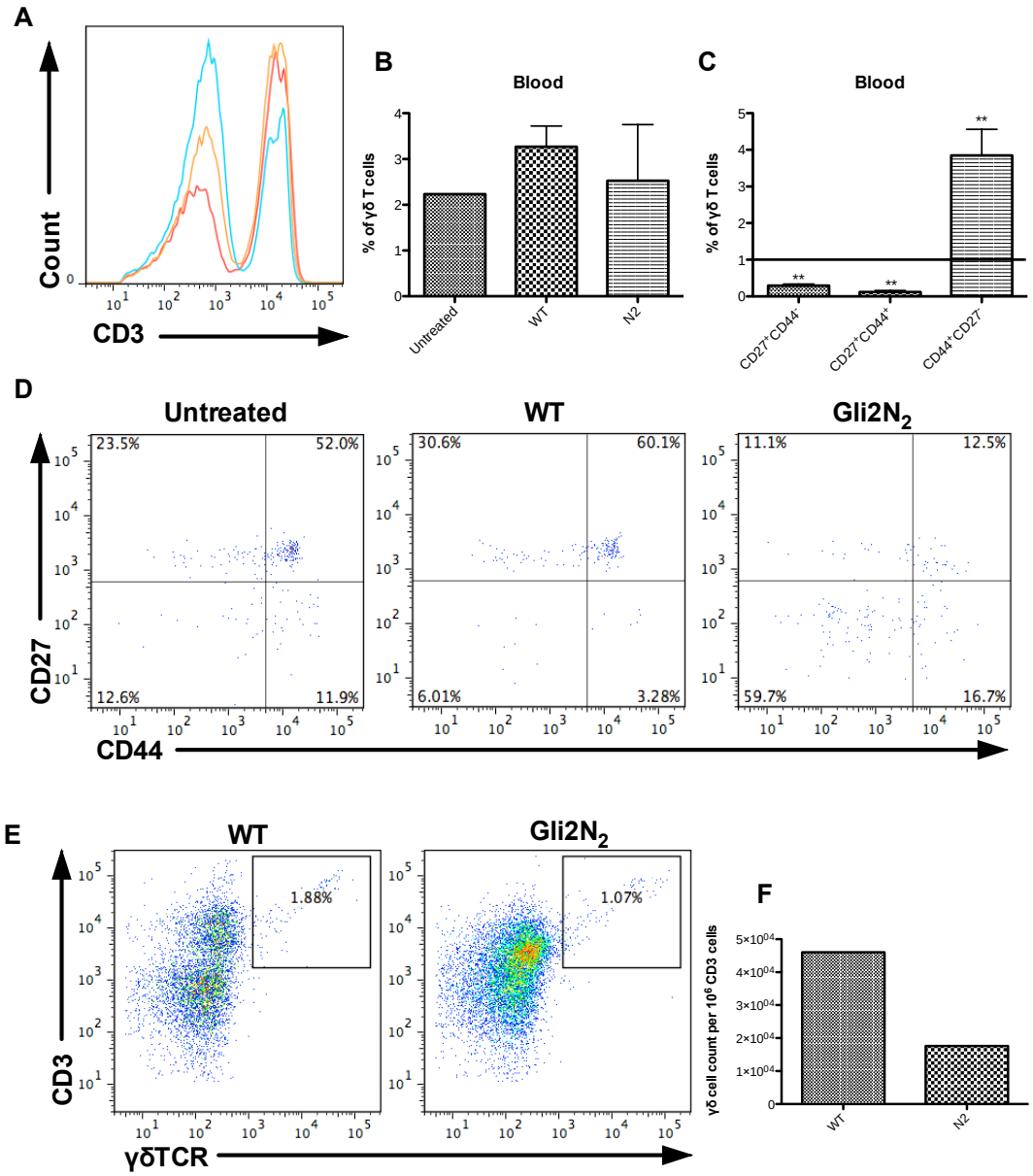

Figure 7.5: The effect of transgenic expression of Gli2 on LPS-treated γδ T cells from the blood and the skin of young mice.

Overlaid histogram (A) (untreated / WT /Gli2N2) shows CD3 expression in the live gate of young littermates. Bar chart (B) shows the percentage of γδ T cells in the blood of WT and Gli2N2 littermates, 4 days after LPS treatment. Bar chart (C) shows the percentage of γδ subtype populations, based on CD27 and CD44 cell surface expression, in relation to the WT. Dot plots (D) show CD27 and CD44 expression on untreated and LPS-treated γδ T cells from the blood of WT and Gli2N2 littermates. Dot plots (E) show the percentage of $CD3^+$ γδ T cells in the skin of WT and Gli2N2 littermates, 4 days after LPS treatment. Bar chart (F) shows the cell count of γδ T cells per 10^6 $CD3^+$ skin cells. **p<0.005, n=5

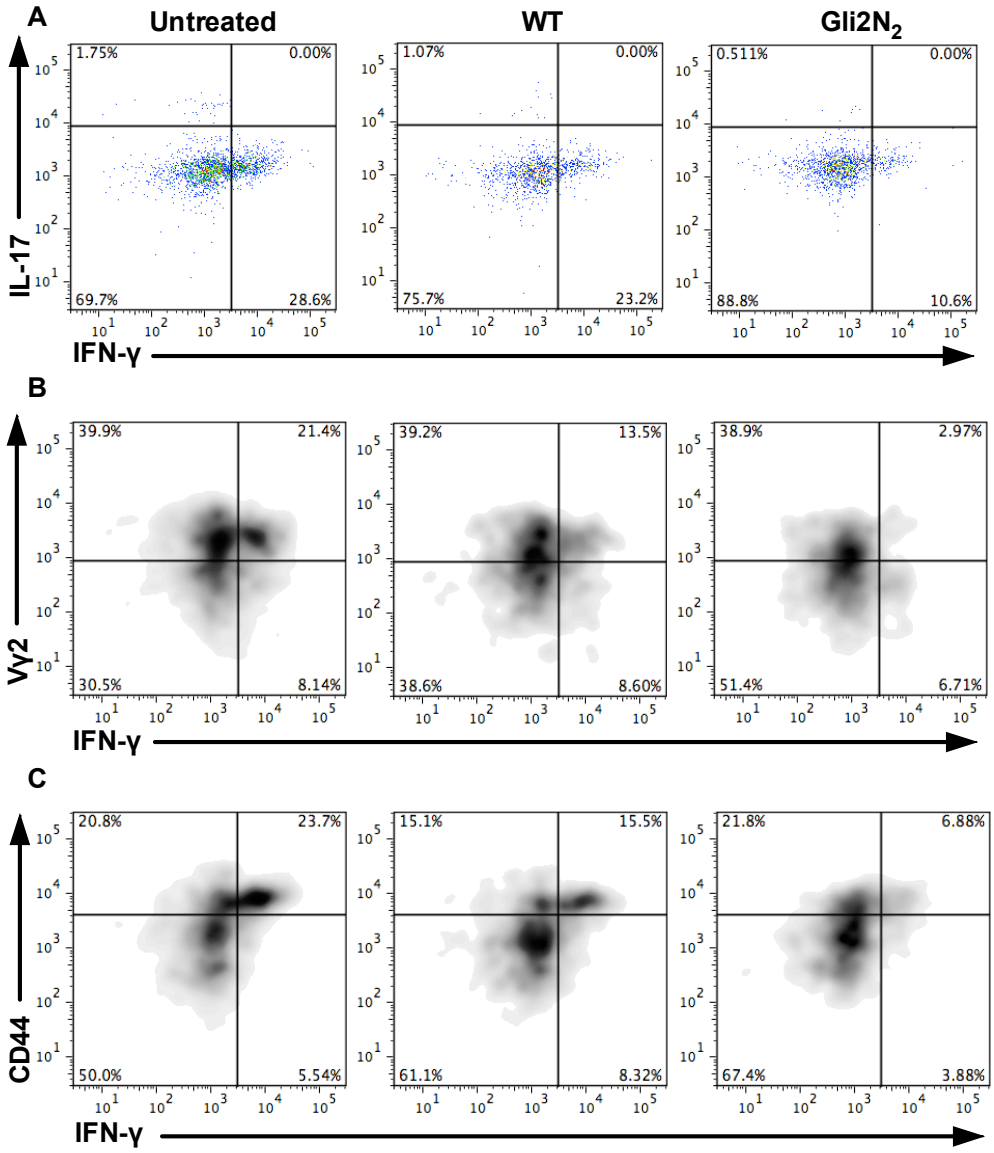

Figure 7.6: The effect of transgenic expression of Gli2 on LPS-treated γδ thymocytes

Density plots show (A) intracellular IL-17 and IFN-γ, (B) Vγ2 and IFN-γ and (C) CD44 and Vγ2 expression on untreated and LPS-treated γδ T cells from WT and Gli2N2 splenocytes. n=5

7.2.2 The effect of Shh on γδ cells from LPS-infected young adult mice

For this experiment, we used three sex-matched pairs (WT and Shhfl/fl FoxN1-Cre^{+}) of 6 week old littermate mice. We injected intraperitoneally with a single dose of 100ng/gram of body weight LPS in 200μl of sterile PBS. The control group was injected ip with 200μl sterile PBS. Mice were sacrificed four days later and analysed by flow cytometry.

In LPS-injected Shh-FoxN1 coKO mice, we observed a reduction in the percentage and number of γδ cells compared to WT in all tissues examined and most notably in the thymus (Figure 7.7A, B). We also observed a reduction in the percentage and number of CD27^{+}CD44^{+} as well as CD44^{+}CD27^{-} γδ cells (Figure 7.7D). A more detailed analysis of γδ cells bearing various Vγ chains revealed that the decrease in both subsets is irrelevant to Vγ chain (Figure 7.8A, B, C). CD24 expression was not affected (Figure 7.8D).

In the spleen and lymph nodes, we observed only minor changes. Of note, the dissapearing thymic Vγ2 CD44^{+}CD27^{-} γδ subset is only slightly decreaed in the spleen (Figure 7.9E) and, surprisngly, it is upregulated in the Shh coKO lymph nodes (Figure 7.9D), suggesting that the subset is indeed developed in the thymus but perhaps leaves the thymus quicker, thus decreasing its thymic presence.

In the spleen of LPS-injected mice with conditional deletion of Shh, Vγ2 γδ cells showed a reduction in IL-17-producing capacity, upon 4h activation with PMA and ionomycin compared to WT (Figure 7.10A) although MFI for IL-17 for the Vγ2 subset did not change Figure 7.10B).

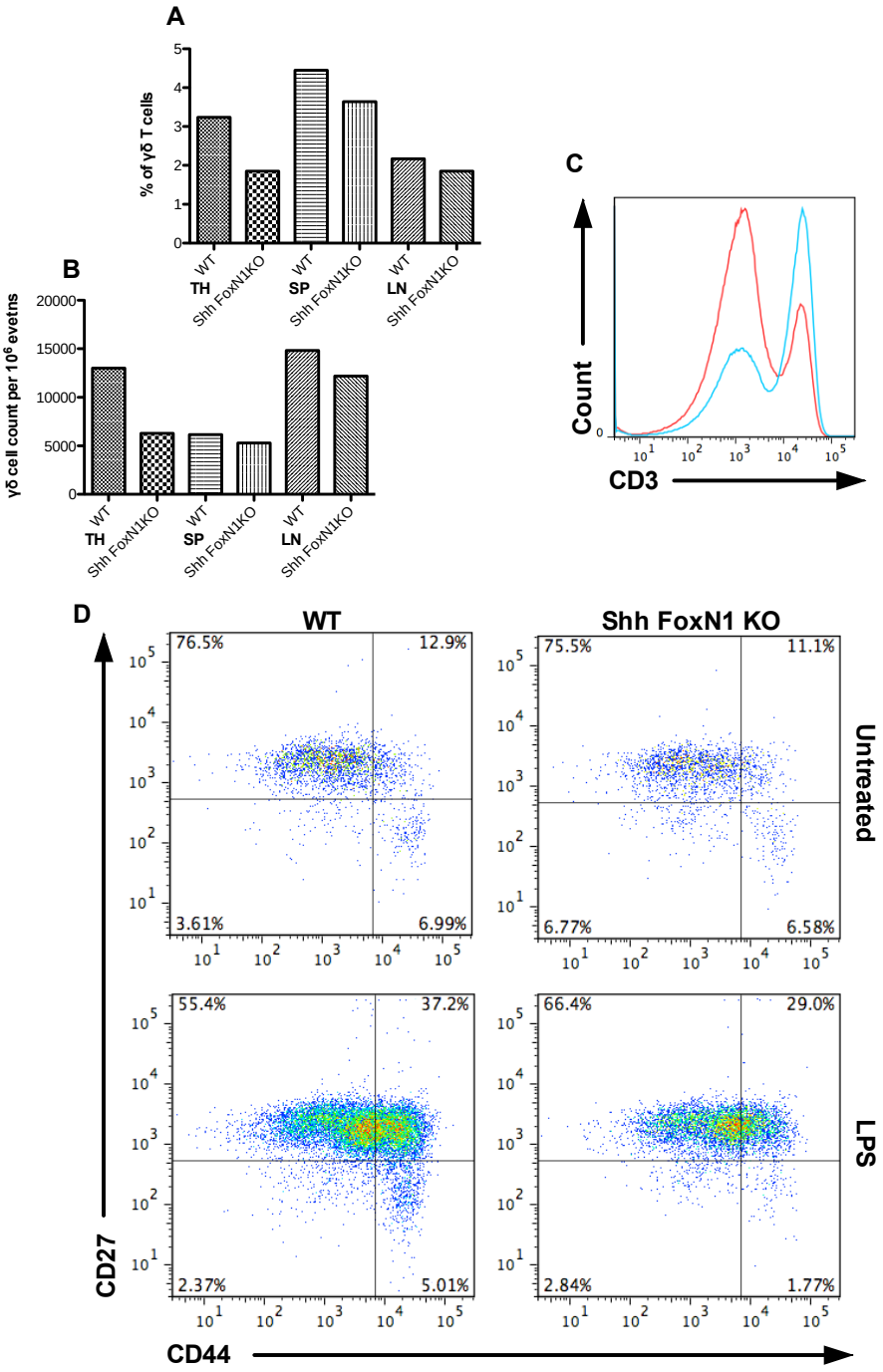

Figure 7.7: Activation of murine γδ T cells with LPS causes important changes in the percentage, cell count and surface expression of key γδ markers in the thymus of Shh FoxN1 KO mice after 4 days of LPS treatment.

Bar charts (A) show the percentage of γδ T cells in the thymus, spleen and lymph nodes of WT and Shh FoxN1 Cre^{+} littermates, as measured by flow cytometry from the CD3^{+} gate. Bar chart (B) shows the γδ cell count from the same organs. Overlaid histogram (C) shows CD3 expression in WT (untreated / LPS-treated WT) littermates Dot plots (D) show CD27 and CD44 expression on untreated and LPS-treated γδ T cells from WT and conditional Shh KO littermates. n=4

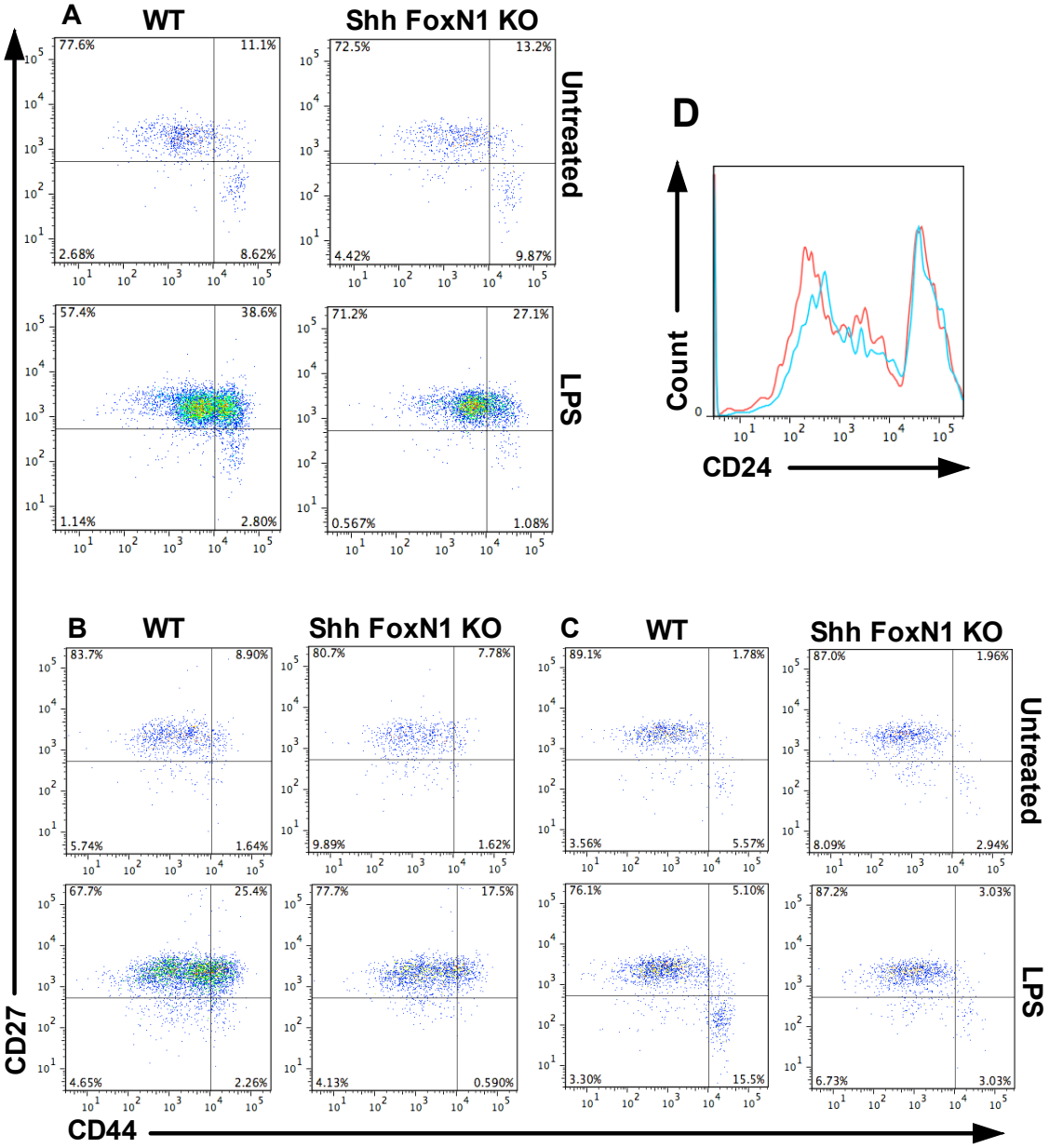

Figure 7.8: The effect of Shh FoxN1 coKO on subtype populations of γδ thymocytes after 4 days of LPS treatment.

Dot plots show the effect of conditional Shh KO on untreated and LPS-treated γδ thymocytes bearing different Vγ chains; (A) Vγ chains other than Vγ1 and Vγ2 (named ''Other Vγs"), (B) Vγ1 chain and (C) Vγ2 chain. Overlaid histogram (D) (WT/Gli2N2) shows that conditional Shh KO does not have an impact on CD24 surface expression. n=4

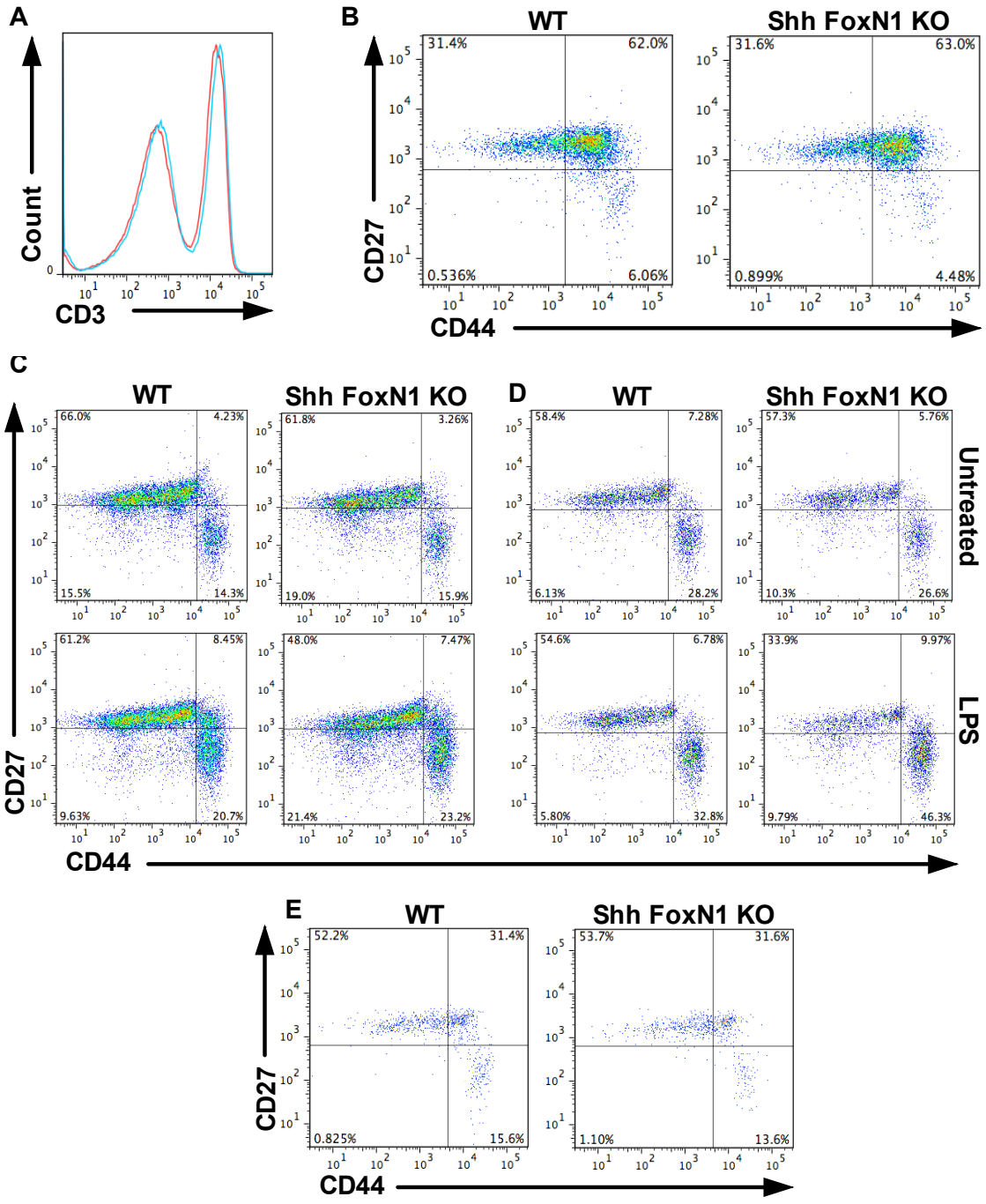

Figure 7.9: The effect of Shh FoxN1 KO on several subsets of γδ T cells in the spleen and lymph nodes after 4 days of LPS treatment.

Overlaid histogram (A) shows CD3 expression from the live gate of spleen of WT (untreated / LPS-treated WT) littermates. Dot plots (B) show CD27 and CD44 expression on LPS-treated splenic γδ T cells from WT and conditional Shh KO littermates. Dot plots show the effect on CD27 and CD44 of conditional Shh KO on untreated and LPS-treated γδ cells in the lymph nodes (C) and Vγ2 γδ cells in the lymph nodes (D) and spleen (E). n=4

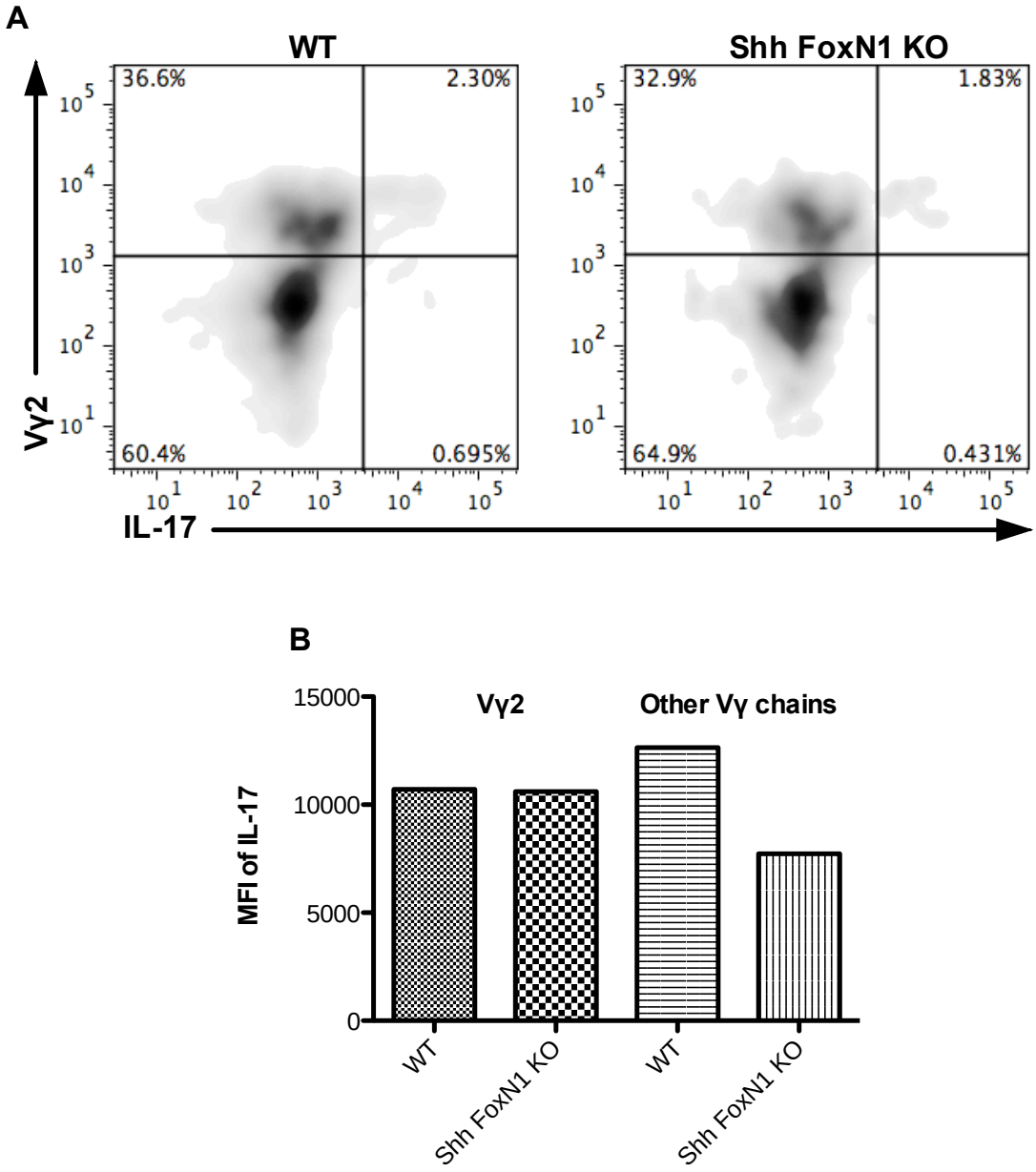

Figure 7.10: The effect of conditional Shh KO on IL-17 secretion on LPS-treated spleens.

Density plots (A) show that conditional deletion of Shh reduces IL-17 secretion. Bar chart (B) shows the MFI of IL-17$^+$ γδ cells. n=4

8. The role of Hh signalling in human γδ T cells

8.1 Introduction

There are three reasons why we decided to study the effect of Hh signalling on human γδ T cells. Firstly, the role of Hh signalling in human γδ T cell biology has not been investigated yet. Secondly, our detailed analysis of murine γδ cells made us question what parallels could be drawn between murine and human γδ T cells in relation to Hh signalling. Last, our team collaborates with clinicians at Great Ormond Street Hospital who provide us with whole fresh human thymi obtained from young children who undergo corrective heart surgery. Therefore, we are given the unique opportunity to study human γδ T cell thymopoiesis using fresh human tissues.

Due to this collaboration, I decided to try to expand fresh human γδ thymocytes using artificial antigen presenting cells (aAPCs) loaded with anti-γδTCR antibodies, a method that allows the expansion of the complete γδ T cell repertoire from human blood, without bias towards specific TCRs (Fisher, Yan et al. 2014). All samples were processed immediately upon arrival and approximately three weeks after setting up the expansion cultures, 10^7 γδ cells were washed in RPMI and transferred to new culture plates. The cultures were supplemented with either rHhip or rShh. We followed their development for 6 days by Annexin V-including immunophenotyping, PI stain and qPCR for crucial components of the Hh pathway. Here, we report the results of one experiment, although three additional expansion cultures using different samples had been previously set up while optimizing the expansion protocol for fresh γδ thymocytes. Of note, expansion of thymic samples seem to be more efficient than PBMC-derived γδ cells as addition of aAPCs at the beginning of the expansion

cultures suffices to expand them to the desired level whereas addition of aAPC every approximately two weeks is required in the case of peripheral γδ cells.

8.2 Results

8.2.1 γδ expansion cultures from human thymocytes

In order to set up the expansion cultures, we meshed the human thymus and stained 10^7 thymocytes for CD3, γδTCR, Vδ1 and Vδ2 chains (Figure 1A, B). Flow cytometry analysis showed that approximately half of all γδTCR$^+$ cells were stained bright for CD3 (Figure 8.1C). All CD3$^-$ γδTCR$^+$ cells were also negative for Vδ1 and Vδ2 chains (Figure 8.1D), suggesting that some of these cells are not ''real'' γδ cells. Around 85% of the CD3$^+$ γδTCR$^+$ cells were also bearing a delta chain other than Vδ1 and Vδ2. (Figure 1D).

We then collected 10^9 thymocytes for positive selection using the Milltenyi kit. Selection resulted in the acquisition of around $2x10^5$ cells. A small fraction was taken to analyse by flow cytometry using the same panel and parameter as we did in the whole thymus. After selection, 98% of the live gate consisted of γδTCR$^+$ cells (Figure 8.1F) that were all positive for CD3 (Figure 8.1I). Only a quarter now expressed a delta chain other than Vδ1 or Vδ2, while the majority of γδ cells expressed a Vδ1 chain (Figure 8.1G).

8.2.2 The effect of Hh signalling on cell surface markers

In Figure 8.2, we see the immunophenotypic analysis of the untreated sample on day 2. Our culture contained approximately 72% live cells, all of which were expanded CD3$^+$ γδ cells (Figure 8.1A, B). In further analysis, we separated γδ cells according to Vδ-bearing chain and then plotted CD62L versus CD45RA in order to identify the activation state of those

cells (Figure 8.2C). Figure 8.3 shows the complete immuophenotypic profile of our samples over the course of a week. Left column (Figures 8.3A, C and E) shows the proportion of naive γδ cells in relation to their Vδ chain, whereas the right column (Figures 8.3B, D and F) shows the proportion of terminally differentiated γδ cells Overall, we observed that γδ cells treated with rHhip differentiated slightly quicker to the Td state, independently of Vδ chain expressed.

8.2.3 The effect of Hh signalling on proliferation of human γδ T cells

In order to assess the effect of Hh signalling on human thymic γδ T cell proliferation and apoptosis, we performed cell count (Figure 4A), Annevin V stain (Figure 4B) as well as PI stain which revealed the cell cycle status of the expanded human γδ cells (Figure 4C, D) over the course of a week. Although results on the cell count are inconclusive, inhibition of the Hh pathway using rHhip resulted in reduced programmed cell death. A representative example of the PI and Annexin V analysis is also given (Figures 4E, F, G, I).

8.2.4 Expression analysis of key Hh components

For each condition and time point, we continued our analysis by extracting mRNA from 2,5 $x10^5$ cultured cells in order to perfrom qPCR and expression analysis for basic components of the Hh pathway. Cells treated with rHhip immediately decreased Gli1 expression, indicating γδ cells responded to the Hh inhibitor (Figure 8.5A, B). In rShh-treated γδ cells, Gli1, Gli2 as well as Shh expression were higher than the untreated or the Hhip-treated γδ cells for the first 2 days of culture, a trend that reverses on later time points, when rHhip-treated γδ cells show higher expression for the same genes.

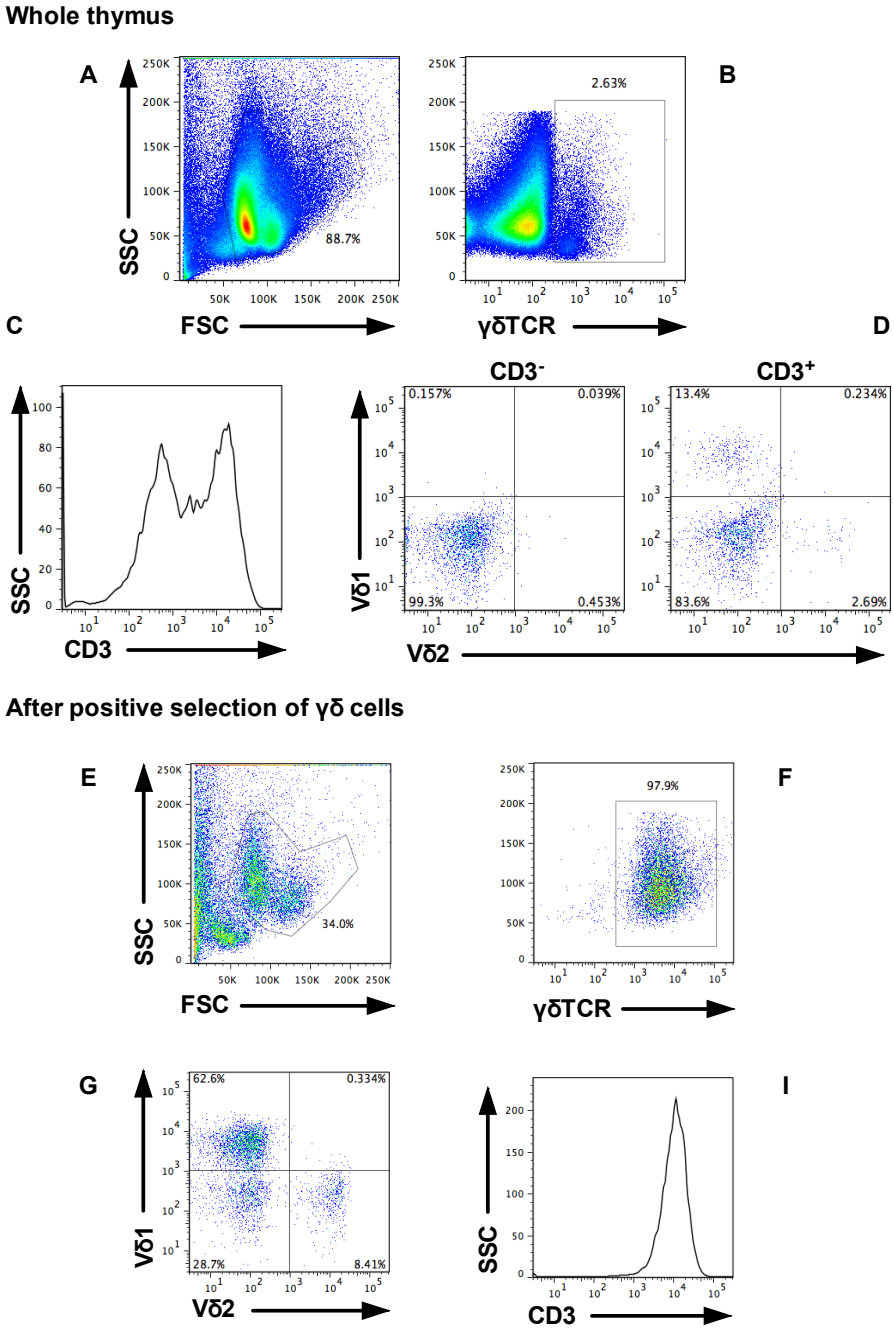

Figure 8.1: Positive selection of γδTCR⁺ cells prior to expansion culture

Dot plot (A) shows the live gate and (B) the γδTCR⁺ cells from the live gate of a fresh human thymus. (C) shows that approximately half of all γδ cells are $CD3^{low}$ and (D) shows the Vδ1 and Vδ2 phenotype of the $CD3^{low}$ and $CD3^{+}$ γδ populations. The rest of the figures shows the γδ cells collected after one round of positive selection. (E) and (F) show the live gate and the γδTCR cells, respectively that are (I) all $CD3^{+}$. Dot plot (G) displays the Vδ1 and Vδ2 phenotype.

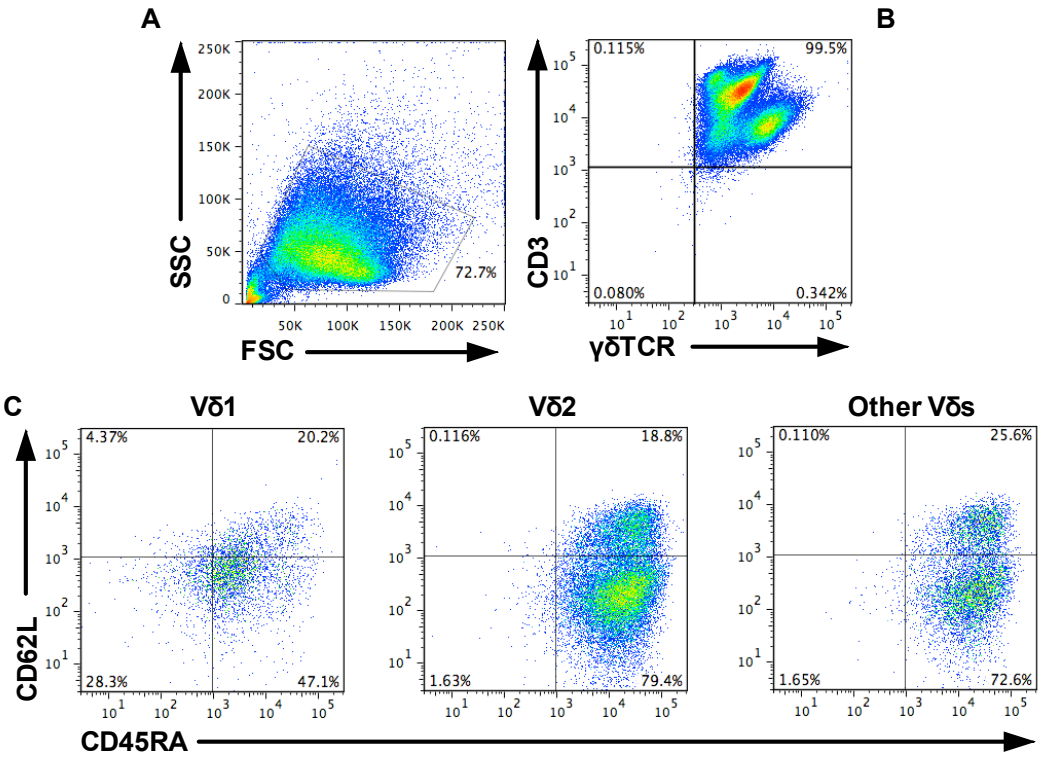

Figure 8.2: Hh signalling and the effector fate of expanded human γδ thymocytes

Dot plot (A) shows a representative example of the live gate of the expanded cells and (B) the proportion of $CD3^+$ $\gamma\delta TCR^+$ cells, exhibiting the characteristic two populations, commonly observed in expanded γδ cells. Representative dot plots (C) show CD62L and CD45RA expression of $CD3^+$ $\gamma\delta TCR^+$ cells.

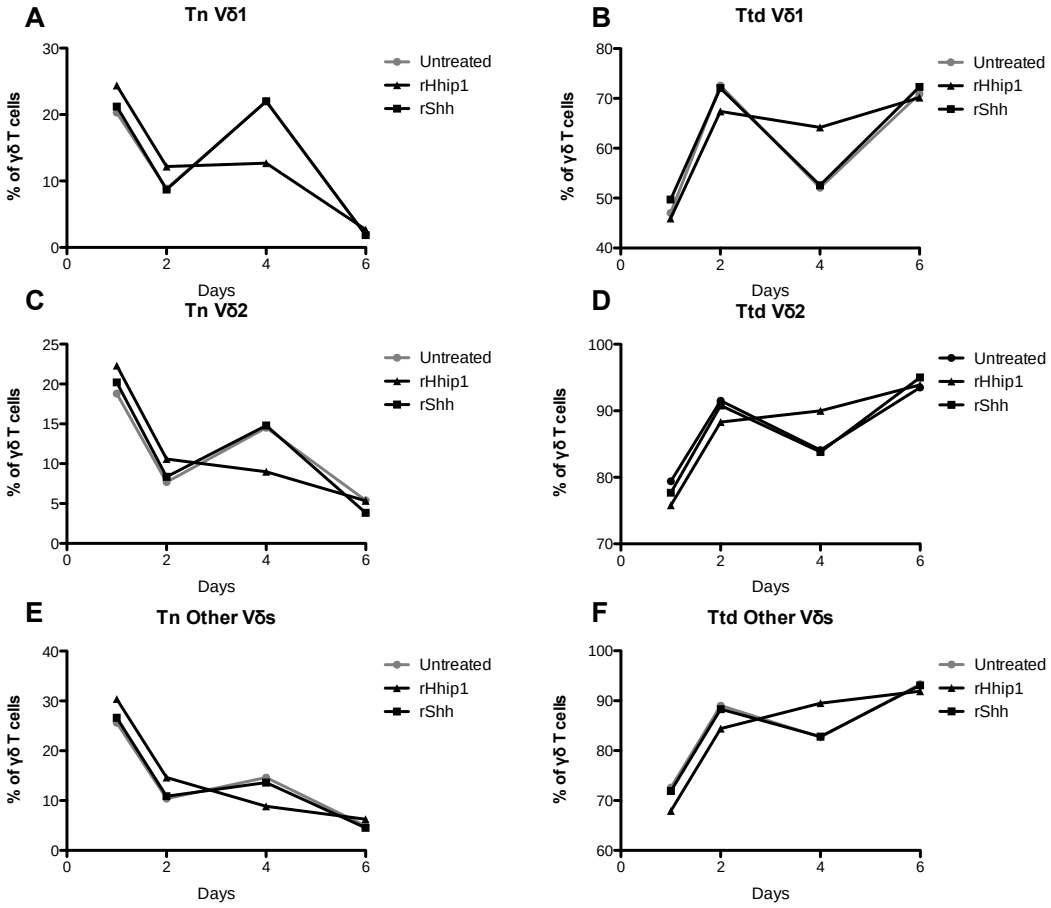

Figure 8.3: Hh signalling and the effector fate of expanded human γδ thymocytes

Plots (A, C, E) and (B, D, F) show the proportion of naïve and terminally differentiated γδ cells, respectively, gated on Vδ1, Vδ2 and other Vδ chains over the course of a week of treatment with rShh or rHhip1 compared with control untreated culture.

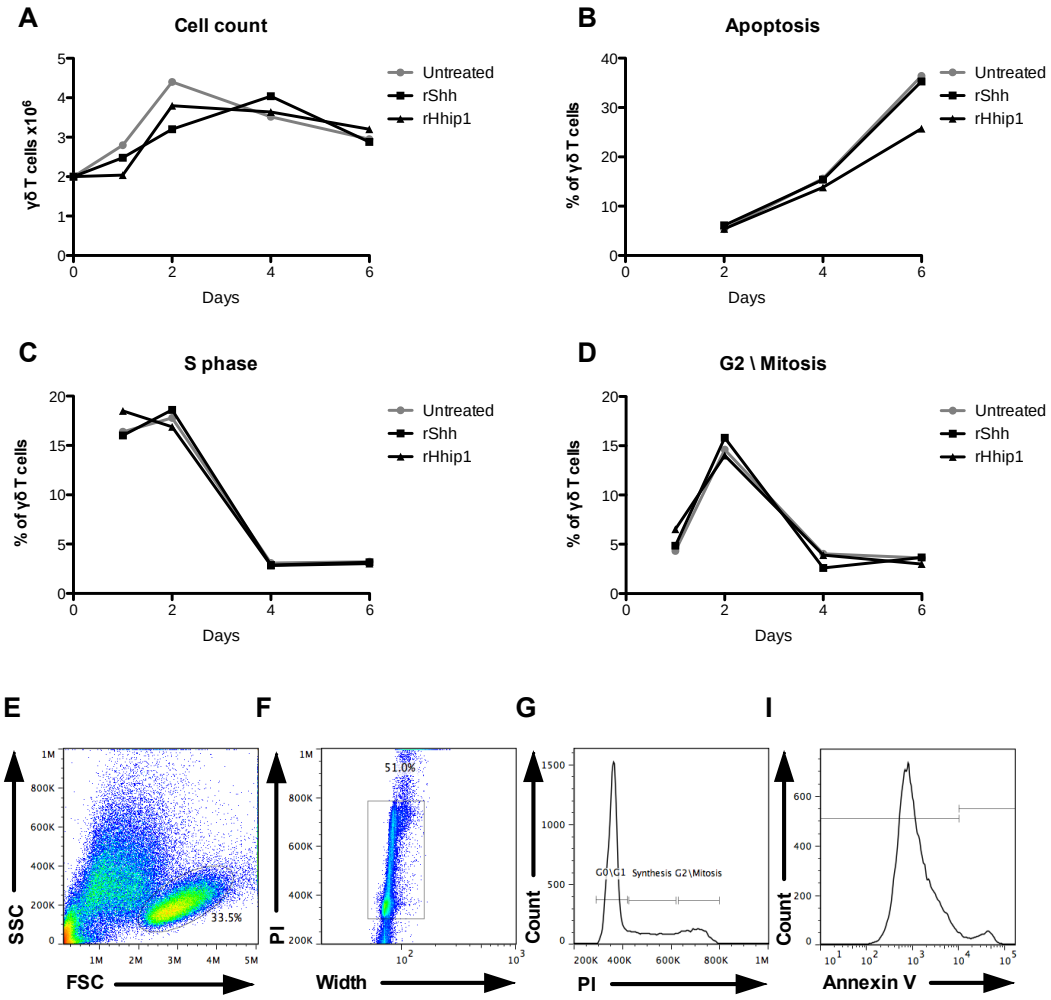

Figure 8.4: The effect of Hh signalling on the cell cycle and apoptosis of human expanded γδ thymocytes

Plots (A) and (B) show the cell count and apoptosis of expanded human γδ cells over the course of 6 days after treatment with either rHhip or rShh. (C) and (D) show synthesis and G2/Mitosis in the same cells and under the same conditions. Representative dot plot (E) shows the untreated live gate on day 2 and the subsequent strategy for (F) aggregate exclusion, (G) PI stain and (I) Annexin V stain in order to assess apoptosis.

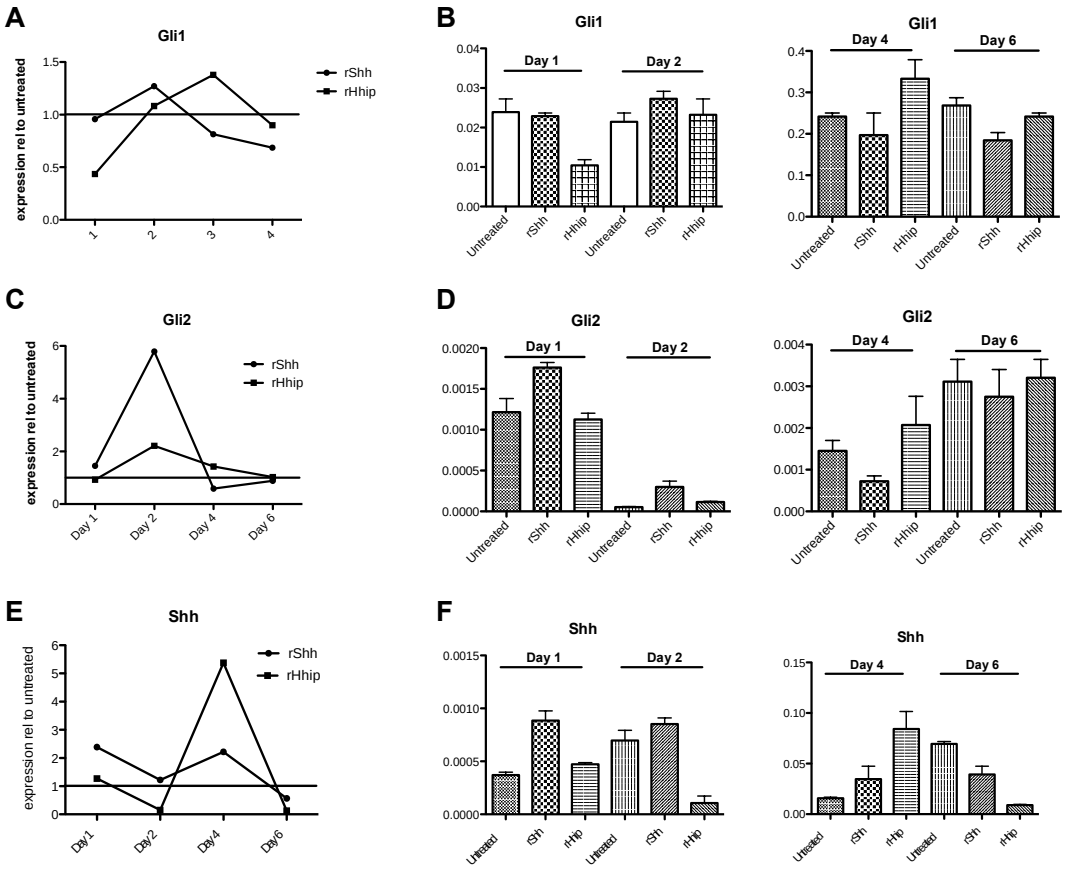

Figure 8.5: The effect of Hh signalling on the transcription of several components of the Hh pathway as assessed by mRNA expression analysis from expanded human γδ cells, treated with rHhip or rShh over the course of 6 days.

Plots (A, C and E) show the relative expression of Gli1, Gli2 and Shh, respectively, for rHhip and rShh-treated expanded γδ thymocytes, relative to the untreated sample, over the course of 6 days. Bar charts (B, D and F) show the expression of the same genes in arbitrary units at four different time points.

8.3. Discussion

The purpose of this chapter is two-fold. First, to demonstrate the successful expansion of fresh human γδ thymocytes using aAPCs. Secondly, it displays a template for future work. We anticipate that our strategy to identify any potential impact of Hh signalling in these cells, based on deep immunophenotyping (Vδ chains and memory phenotype according to CD62L and CD45RA expression), together with cell cycle and apoptosis assessment and mRNA expression analysis for several Hh components, is a strategy that we aim to apply in future experiments.

Using this experimental methodology, we intend to continue analyzing human thymi using aAPCs as well as other expansion protocols with skewed Vδ outcomes, such as IL-2 plus Zoledronate-based expansion (Kondo, Izumi et al. 2011), which, as a nonpeptide phosphoantigen, shows a preference for $V\delta2^{+}$ γδ cells.

We observed that by day 2, the last naïve cells had become Ttd cells, minimizing the chance of being responsive to Hh signalling. This is a problem that cannot be overcome using our current technologies for sorting or positively selecting γδ cells. There are, therefore, two ways to overcome this problem. The first involves using kits that enrich γδ cell populations by negative selection, keeping the γδTCR intact and hence inactivated. The second option relies on culture of small fresh thymic chunks on filters and then identifying γδ cells by flow cytometry, therefore avoiding any selection. The first option is expensive and unreliable, as commercially available kits use for their exclusion, markers that are present in some γδ cells (such as CD56 in the case of Milltenyi's γδTCR negative selection kit), and γδ cells would anyway be activated during consequent expansion culture in the presence of aAPCs. The second option

would only allow us to carry out immunophenotyping as the number of γδ cells extracted from our filter cultures would not suffice to sort γδ cells for expression analysis or even carry out PI and Annexin V stains.

This particular experiment that we present here puzzled us as we would expect to find many γδ cells showing an effector memory or central memory phenotype, similar to γδ cells derived from PBMCs after positive selection using the same kit and same protocol (Fisher, Yan et al. 2014). Nevertheless, I found virtually no CD45RA^{-} γδ cells, manifesting that γδ thymocytes could either potentially ''jump'' from a naïve phenotype to a terminally differentiated one, without upregulation of CD45RA or naïve cells simply died and Td cells acquired their terminal phenotype during the 3 weeks of expansion. Future replications of this experiment will shed light on the mechanism.

In terms of cell cycle, we found that untreated and rShh-treated cultures results were always remarkably identical whereas γδ cells treated with rHhip were slightly different. The major change was observed in Vδ1 cells, followed by Vδ2, suggesting that Vδ1 are potentially more highly responsive to Hh signalling. rHhip-treated γδ cells also showed reduced apoptosis but no definite conclusion could be drawn about Hh's impact on cell cycle progression or cell count until the experiment is repeated at least twice. Overall, the final rHhip and rShh treatment cultures seemed to have worked well, as manifested by the sharp downregulation in Gli1 expression in Hhip-treated γδ cells.

Overall, there has been increasing interest in human γδ T cells over the last 5 – 10 years, primarily due to their potent antitumor cytotoxic properties. γδ T cells can exhibit IFNγ-mediated antitumor responses whereas IL17-producing γδ cells have shown unanticipated tumor-

promoting functions (Silva-Santos, Serre et al. 2015). We believe that further elucidation of the role of the Hh signalling pathway in γδ cells will provide a better insight into this developmentally and functionally complex subtype of T cells and could also be translationally useful as it could potentially improve *in vitro* methods for the production of γδ T cells for therapeutic applications.

9. The Investigation of an Ihh-mediated feedback loop that controls thymus size

9.1 Introduction

Hh signalling plays an important role in regulating several stages of survival, proliferation and differentiation during T cell development. Here, based on published findings from our laboratory, we aim to further investigate the role of Ihh ın T cell development.

In 2009, our lab showed that Ihh both promotes and restricts T cell development (Outram, Hager-Theodorides et al. 2009). Hh signalling is known to affect DN1 to DN2 transition and Shh, Gli3 and Smo have been shown to play a role in this transition. Analysis of $Ihh^{-/-}$ (and $Shh^{+/-}$) thymi on days E13.5 and E14.5, when the transition from DN1 to DN2 first happens, did not reveal a significantly smaller thymus, whereas in $Shh^{-/-}$ and $Shh^{+/-}Ihh^{-/-}$ mutants mice, the proportion of DN2 cells was significantly reduced, indicating that Ihh plays a positive regulatory role at the DN1 to DN2 transition that, in the absence of Ihh, can be compensated by Shh.

In later stages of T cell development, Ihh seems to both negatively and positively regulate the transition from DN to DP cells. Analysis of E16.5 $Ihh^{-/-}$ thymi, when the transition first occurs, revealed a reduction in thymus size by half, however, the $Ihh^{+/-}$ thymus was 1.4 times larger, containing 2.4 times more DP cells.

Moreover, treatment with exogenous rHh protein promoted thymocyte development in $Ihh^{-/-}$ FTOCs but inhibited thymocyte development in $Ihh^{+/-}$ FTOCs. The data suggest that Ihh promotes DN thymocyte

development before pre-TCR signal transduction but becomes a negative regulator after pre-TCR signalling. This finding was also confirmed with anti-CD3 treatment of of $Rag^{-/-}Ihh^{+/-}$ FTOCs.

As Ihh is produced at low levels in DN populations, we believe that Ihh is secreted from DP cells, which are known to produce more Ihh, and feeds back to DN progenitors in order to regulate differentiation and control cell number. This hypothesis is important because very little is known about the intrinsic thymic processes that control thymus size. The control of the thymus has been assumed to rely on competition between thymocyte precursors for limiting concentrations of mitogenic or survival factors. Our lab has suggested that Ihh restricts thymus size by providing a negative regulatory feedback from the Ihh-producing DP cells to their DN progenitors.

This project aims to investigate the proposed negative feedback loop in greater detail as well as to test if Ihh also regulates differentiation from DP to SP cell. For this purpose, in addition to the Ihh mutant mice, we also used Ihhfl/fl-$CD4Cre^{+}$ tg mice to specifically delete Ihh from all thymocytes that have expressed CD4 (hence CD4SP, CD8SP and DP cells), thereby losing the potential negative regulatory feedback. This will test the hypothesis directly that Ihh secreted by DP and SP cells regulates the rate of differentiation of their DN progenitors.

9.2 Results

9.2.1 Conditional deletion of Ihh from thymocytes

In order to investigate in more detail the proposed negative regulatory effect of Ihh on the DN to DP transition, we analysed 3 week old mice with conditional deletion of Ihh from all $CD4^+$ thymocytes ($Ihh^{fl/fl}$-$CD4Cre^+$, Ihh coKO) and compared them to WT littermates. The Ihh coKO thymus was marginally smaller (Figure 9.1C) but no other difference was observed in the CD4SP, CD8SP, DP or DN populations (Figure 9.1B, D, E, F). DP cells expressed less CD3 but this was not significant (Figure 9.1G) and there was no difference in CD5 expression. Finally, we did not detect differences in HSA and B220 expression (Figure 9.1H). Analysis of the DN population revealed that the coKO thymus showed more DN3 and less DN4 cells than WT (Figure 9.2A).

We also investigated the effect of conditional deletion of Ihh in T cells from the spleen and lymph nodes of young mice. In both tissues, we observed a small increase in the proportion of CD4SP and CD8SP cells (Figures 9.3A, 4A). which were positive for CD3 (Figures 9.3C, D, 4B, C).Ihh coKO spleens and lymph nodes showed higher MFI for CD5 on both CD4 and CD8 T cells (Figure 9.3F, 4D). Surprisingly, the coHet spleen contained significantly less and the coKO significantly more T cells than the WT (Figure 9.3B).

To assess the role of Ihh in TCR-β rearrangement and expression, we analysed DN3 and DN4 thymocytes for intracellular (ic) expression of the TCRβ chain. We found that conditional deletion of Ihh led to an increase in the proportion of TCRβ cells in both DN3 and DN4 thymocytes. This increase in ic TCRβ expression could be a result of increased TCRβ rearrangement or because cells that have rearranged their TCRβ chain are arrested at the DN stage. This is consistent with the published observation

that the proportion of TCRβ^{+} cells was increased in the DN3 population of Ihh$^{-/-}$ fetal thymus compared to WT (Outram et al 2009).

9.2.2 Introduction of a transgenic TCR

We then crossed the Ihhfl/fl-CD4-Cre^{+} tg to the male specific antigen HY in order to test if the transgenic TCR influenced differentiation from DN to DP and to assess the effect of Ihh on negative selection. As HY is a male specific antigen, analysis by flow cytometry was performed in a gender specific manner. Contrary to the HY^{-} mice, analysis of Ihh coKO HY^{+} male mice revealed a larger thymus and the Ihhfl/WT-Cre^{+} thymus (coHet) was larger than the WT and the coKO (Figure 9.6A). We also observed a small decrease in the proportion of CD8SP and CD4SP cells (Figure 9.6D, E, F, G) as well as the DN population (Figure 9.6B), which also contained more CD3 and Vβ8.1/8.2 (Figure 9.6H). The coKO also exhibited higher T3.70 expression on DP, CD4SP and CD8SP cells (Figure 9.7A, B).

Peripheral T cell analysis revealed significantly higher CD3 expression in splenic CD4SP cells (Figure 9.8A) but no other difference was detected in the spleen or the lymph nodes (Figure 9.8).

We have only had the opportunity to analyse a single female pair of Ihhfl/fl-CD4-Cre^{+}-HY^{+} and WT-HY mice due to problems with re-derivation and more analysis will be carried out as soon as we have more pairs available. Further investigation of these mice is crucial as it can elucidate Ihh's effect on positive selection.

The IhhcoKO-HY thymus was smaller than the WT (Figure 9.9A) and it also showed more DN and fewer DP cells (Figures 9.9C, D), whereas no change was observed in the DN populations or CD3 expression (Figures 9.9D, E).

The Ihh coKO-HY spleen was smaller with a smaller live gate (Figure 9.10A) and there was no difference in CD3 or CD5 expression (Figure 9.10B, C). We observed less $CD3^+$ CD4SP and more $CD3^+$ CD8SP cells but more pairs need to be analysed to draw firm conclusion.

9.2.3 The impact of Ihh deficiency on thymocyte differentiation in the fetal thymus

We analysed E16.5 Ihh mutant thymi after 6 days in FTOCs. As DP cells first appear in E16.5, we expect our analysis to reveal the rate of progression from DN to DP and DP to SP cells. We found that IhhHet mice showed a significant increase in thymus size (Figure 9.11A). Interestingly, WT thymi were on average slightly smaller than the KO. Previous analysis from our lab has shown that E16.5 $Ihh^{+/-}$ thymi contained on average 1.4 more thymocytes than WT thymi, a difference that is increased further after 6 days in culture. We also discovered that IhhKO thymi contained more CD4SP and DN cells than WT thymi (Figure 9.11C, D) whereas the proportion of CD8SP cells was not affected (Figure 9.11E). The difference in CD4SP cells increased dramatically in $CD3^+$-only thymocytes, indicating that deletion of Ihh results in a much faster rate of differentiation from the DP to SP stage of development (Figure 9.11I). Conditional KO DP cells showed reduced CD3 expression (Figure 9.11H).

We then time-mated Ihh coKO HY^+ mice and analysed E18.5 male littermates. The $Ihh^{fl/fl}$-CD4-Cre^+ HY^+ thymus was 50% smaller than the WT (Figure 9.12B), a result attributed to the remarkable decrease in the live gate (Figure 9.12A). We also observed a reduction in the proportion of DN cells coupled with an increase in the DP in the conditional null thymus (Figure 9.12B). Conditional deletion of Ihh resulted in a higher expression of T3.70 (Figures 9.13B, 14A) and HSA (Figure 9.14C) on DN cells and CD8SP cells (Figure 9.14C). However, HSA expression on CD4SP cells was

not affected. We also detected lower Vβ6 expression on CD4SP cells in the coKO compared to WT (Figure 9.14B).

9.2.4 Recovery of DP and SP populations following Hydrocortisone (HC) treatment in Ihh deficient thymus

In order to assess the developmental progression of $Ihh^{+/-}$ thymocytes in a synchronized wave in adults, we injected intraperitoneal HC and observed the recovery of the thymocyte populations during the week after the injection. Four days after the injection, we observed that the $Ihh^{+/-}$ thymus was larger (Figure 9.15A). CD4SP and CD8SP proportions were increased with a decreased proportion of DP cells (Figure 9.15F). We also detected increased thymic CD5 expression (Figure 9.15D). There was an increase in Qa2 and CD3 expression for the CD4SP population (Figure 9.17B, C), whereas expression of CD24 was decreased for the same population (Figure 9.15F). Thus, the CD4SP population seemed more mature in the $Ihh^{+/-}$ compared to WT. Analysis of the DN population revealed that the $Ihh^{+/-}$ thymi contained overall more DN cells than WT but the distribution of subsets was quite similar between $Ihh^{+/-}$ and WT (Figure 9.16A). Moreover, we observed higher Qa-2 expression in $Ihh^{+/-}$ DN cells compared to WT (Figure 9.16B, C).

Six days after ip HC treatment, the $Ihh^{+/-}$ thymus was still larger than the WT (Figure 9.17A) and showed higher CD5 expression (Figure 9.17B). Furthermore, the $Ihh^{+/-}$ thymus contains fewer DN and more DP cells, whereas CD4SP and CD8SP cells do not show any difference in proportion between mutants and WT littermates and the DN subset distribution was similar in both genotypes (Figure 9.17D).

Overall, we observed a faster thymic recovery in the $Ihh^{+/-}$ thymus (Figure 9.18A). CD8SP cells showed reduced CD3 expression four days after injection and the effect disappeared two days later (Figure 9.18C). We also

analysed a triplet (WT, coHet, coKO) of HY^+ 4 week old female mice, four days after ip HC injection. Remarkably, the coKO thymus displayed a thymus size that was about ten times larger than the WT and coHet littermates (Figure 9.18B) but it was nevertheless smaller than its HY^- counterparts. The DP population showed decreased CD3 and the DN decreased CD25 expression (Figure 9.18D).

9.2.5 Reconstitution of DP and SP populations following anti-CD3 treatment in Ihh deficient $Rag^{-/-}$ thymus

To determine the regulatory effect of Ihh after pre-TCR signalling, we generated a Ihhfl/fl-CD4-Cre^+ $Rag^{-/-}$ mouse strain and set up anti-CD3-treated FTOCs that mimic pre-TCR signalling. We analysed the FTOCs seven days after treatment. The coKO thymus showed a 5fold increase in size compared to WT (Figure 9.19A). It also contained a higher proportion of DN cells (Figure 9.19B), which displayed higher HSA expression (Figure 9.19D). We also observed an increased in the proportion of CD8SP cells (Figure 9.19F).

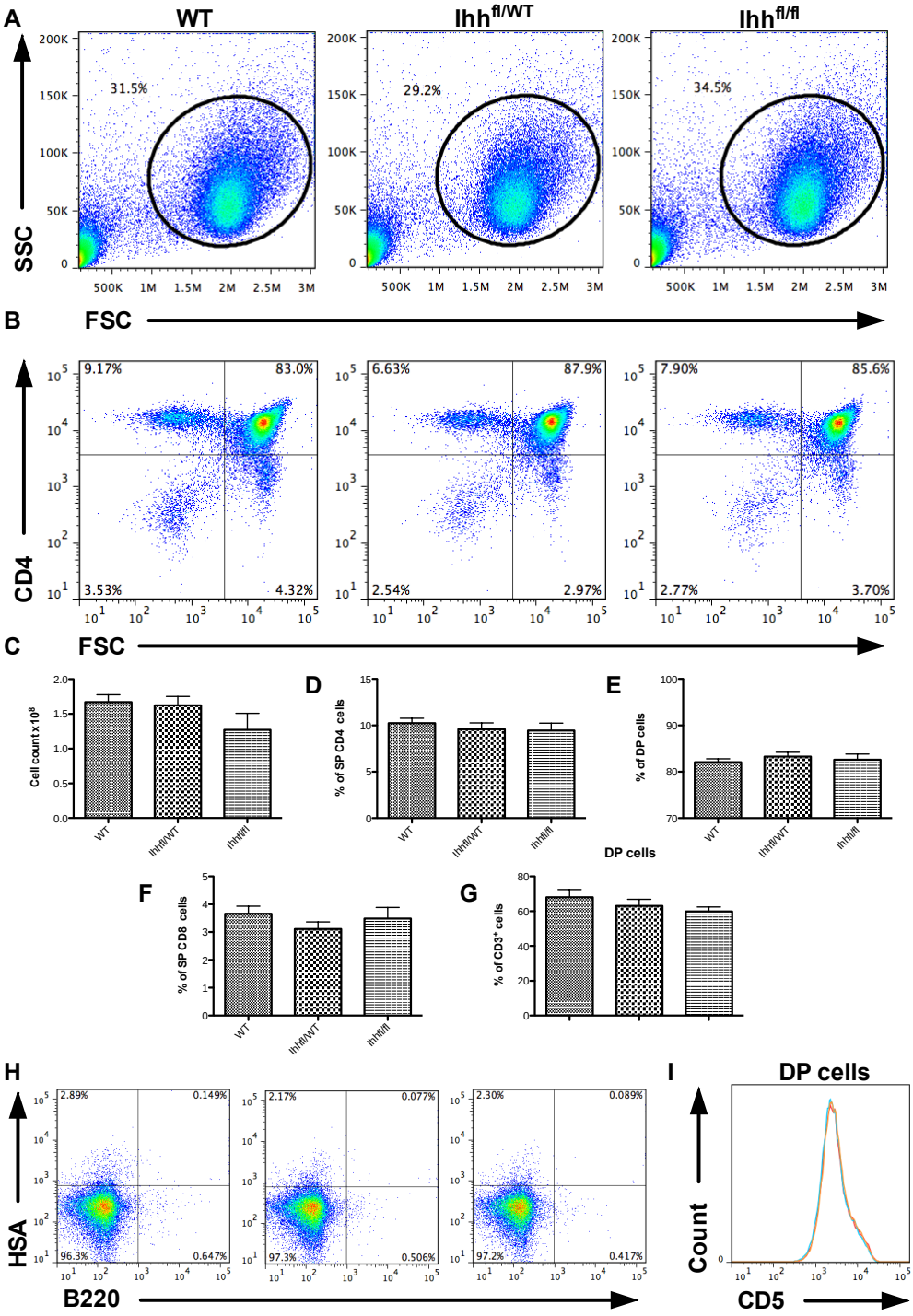

Figure 9.1: The effect of conditional Ihh deletion (CD4Cre$^+$) on thymocytes of young adult mice

Dot plots (A) show the live gate and (B) the CD4 and CD8 expression of WT, Ihh$^{fl/WT}$ and Ihh$^{fl/fl}$ Cre$^+$ thymocytes. Bar charts (C) shows the cell count and (D), (E) and (F) show the percentage of CD4SP, DP and CD8SP thymocyte populations, respectively. Bar charts (G) shows the CD3 expression of DP cells. Dot plots (H) shows HSA and B220 expression of live-gated WT, Ihhfl/WT and Ihhfl/fl thymocytes and overlaid histograms (I) (WT / coHet / coKO) shows CD5 expression on DP cells. n=12

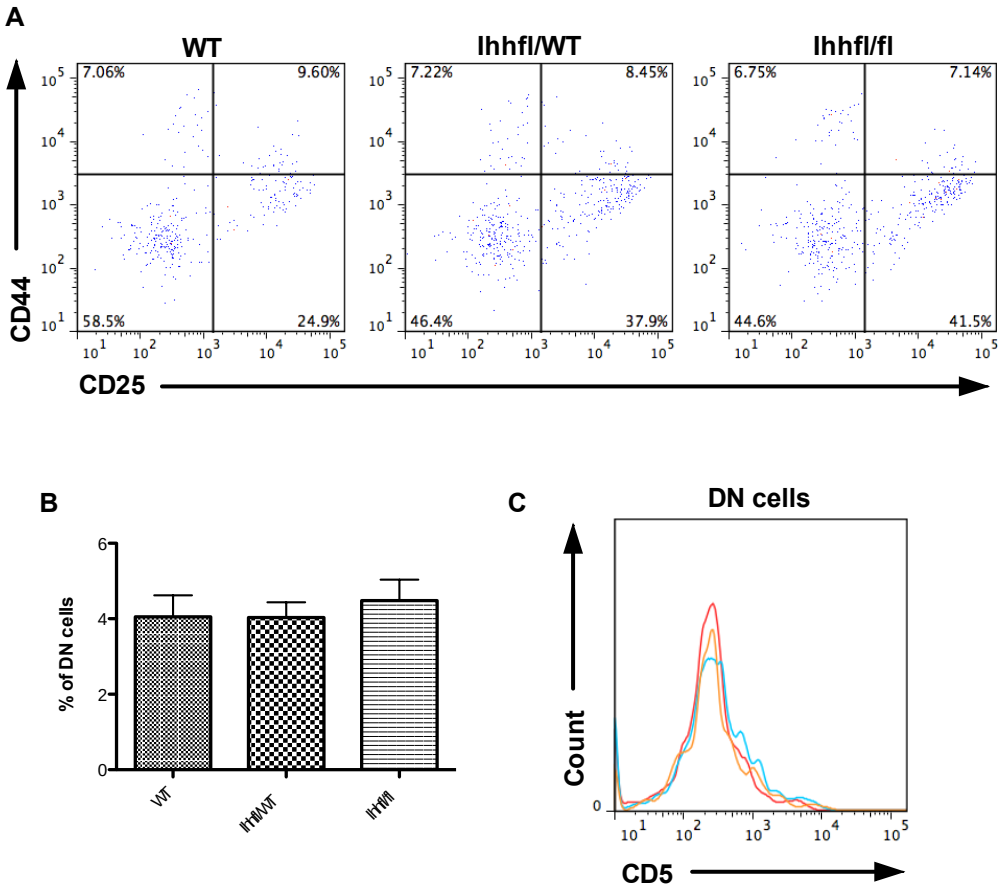

Figure 9.2: The effect of conditional Ihh deletion (CD4-Cre+) on DN thymocytes of young adult mice

Dot plots (A) show CD44 and CD25 expression of WT, $Ihh^{fl/WT}$ and $Ihh^{fl/fl}$ DN thymocytes. Bar charts (B) show the proportion of DN cells and overlaid histogram (C) (WT / coHet / coKO) shows CD5 expression in DN cells. n=11

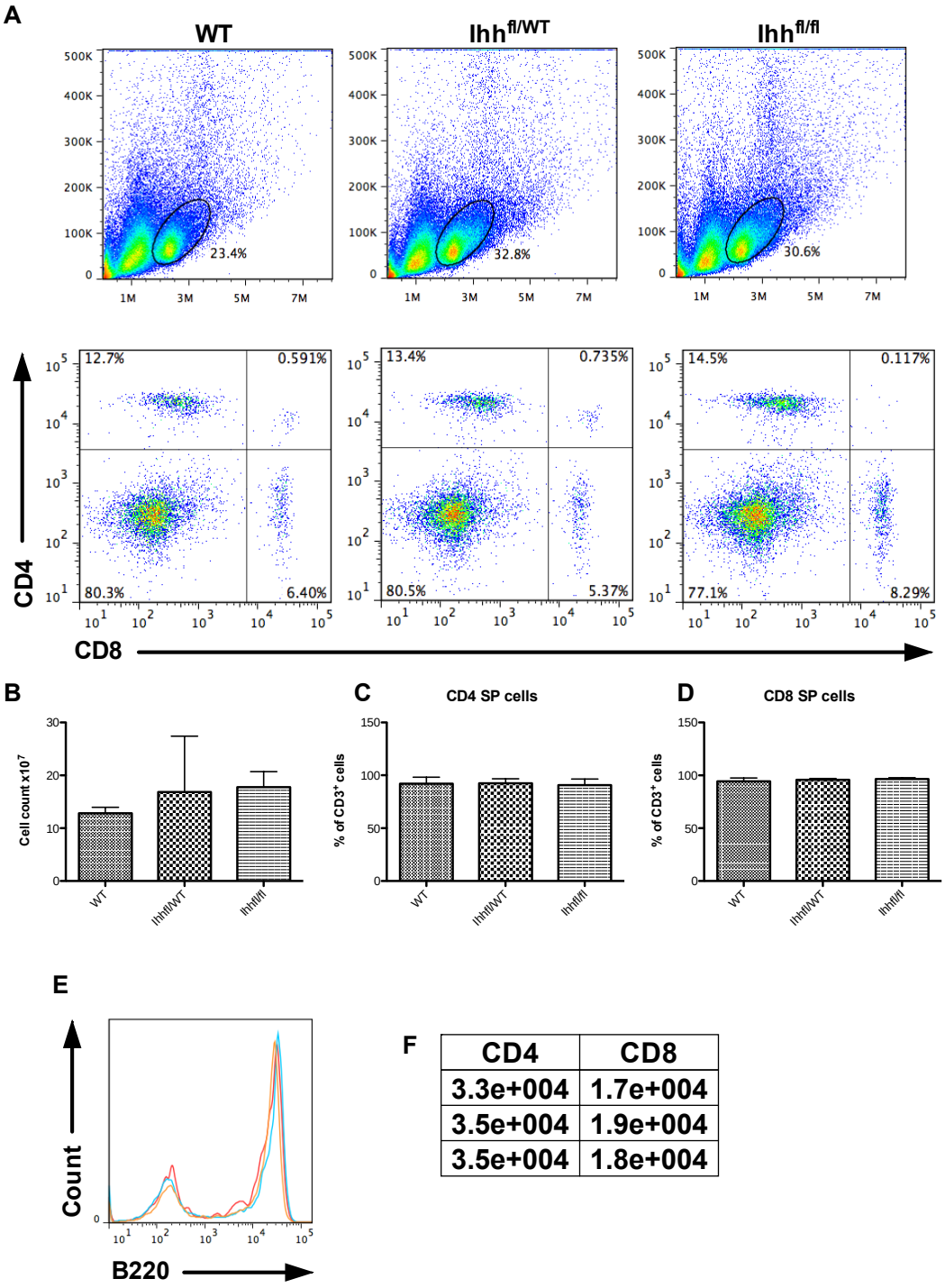

Figure 9.3: The effect of conditional Ihh deletion (CD4-Cre+) on T splenocytes of young adult mice

Dot plots (A) show the live gate and CD4 and CD8 expression of WT, $Ihh^{fl/WT}$ and $Ihh^{fl/fl}$ Cre^{+} T splenocytes. Bar charts (B) shows the T cell count, (C) and (F) show the proportion of CD4SP and CD8SP populations that express CD3, respectively. Overlaid histogram (E) (WT / coHet / coKO) shows B220 expression of live gate and (F) shows MFI of CD5 of WT, $Ihh^{fl/WT}$ and $Ihh^{fl/fl}$ CD4SP and CD8SP splenocytes. n=6

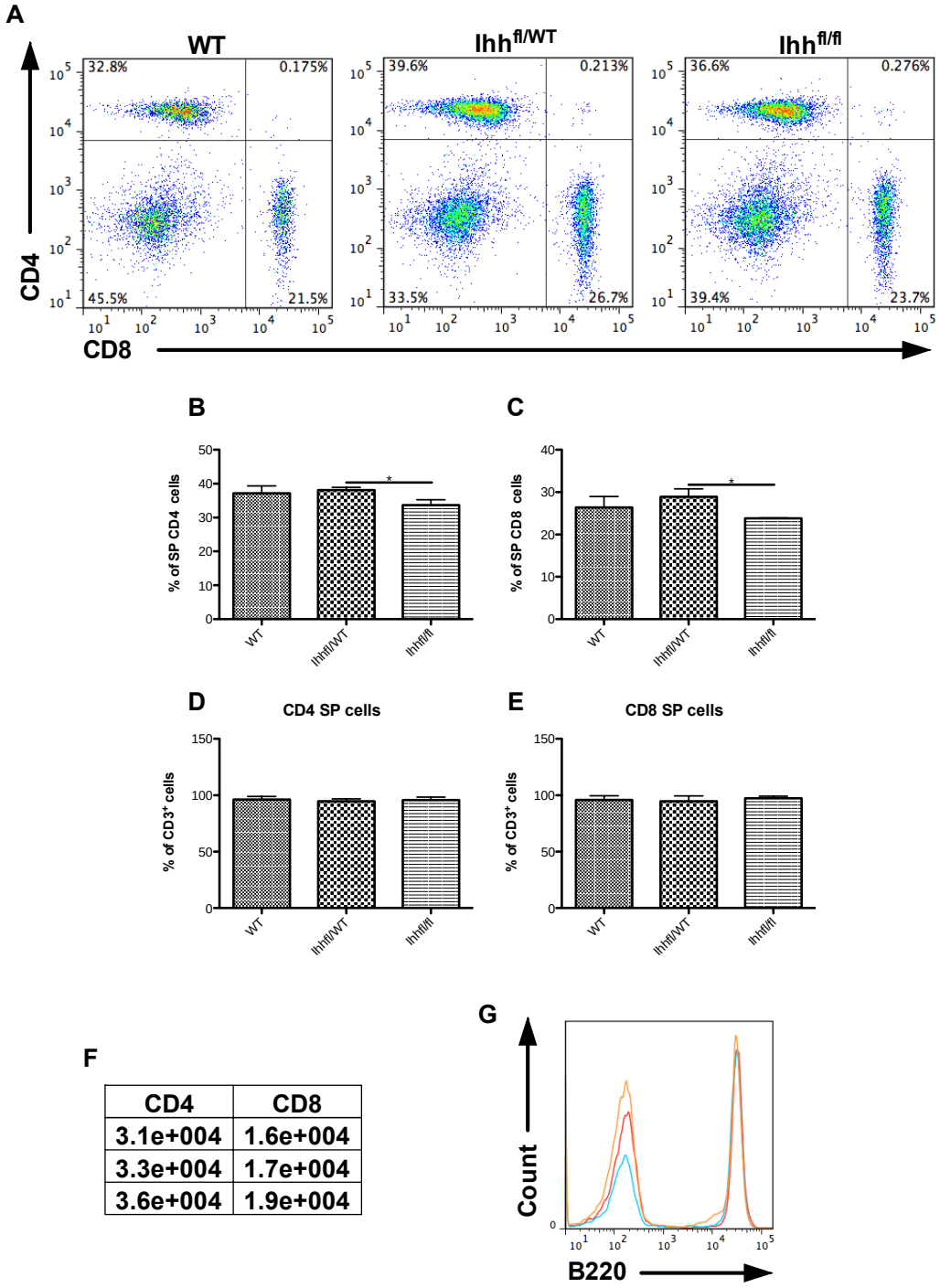

CD4	CD8
3.1e+004	1.6e+004
3.3e+004	1.7e+004
3.6e+004	1.9e+004

Figure 9.4: The effect of conditional Ihh deletion (CD4-Cre+) on T cells from the lymph nodes of young adult mice

Dot plots (A) show the CD4 and CD8 expression of WT, $Ihh^{fl/WT}$ and $Ihh^{fl/fl}$ T lymphocytes. Bar charts (B) and (C) show the proportion of CD4SP and CD8SP cells. Bar charts (D) and (E) show that conditional deletion of Ihh does not affect CD3 expression of CD4SP and CD8SP populations, respectively. Table (F) shows MFI of CD5 of WT, Ihhfl/WT and Ihhfl/fl CD4SP and CD8SP lymphocytes. Overlaid histogram (G) (WT / coHet / coKO) shows B220 expression of the live gate. n=6

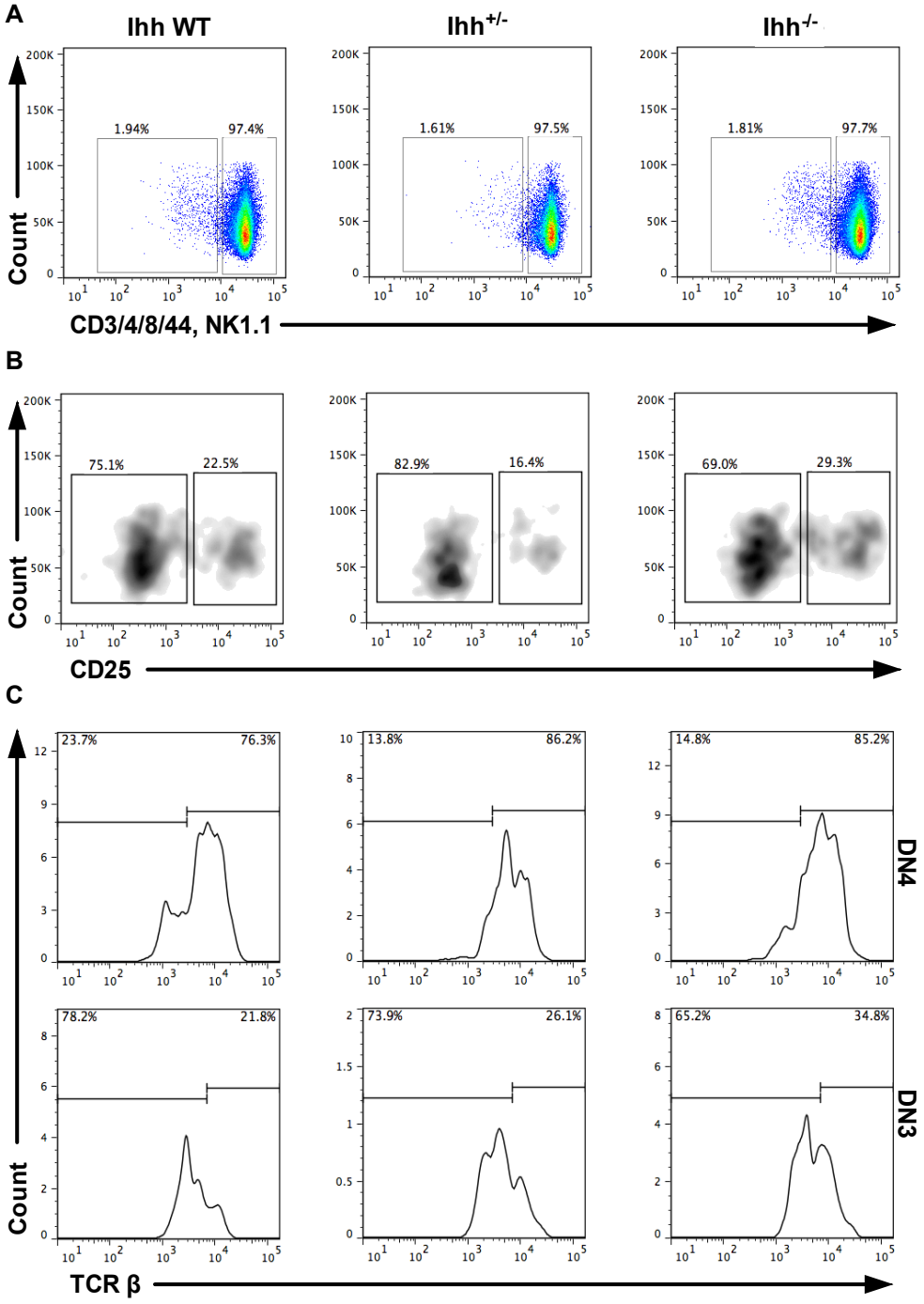

Figure 9.5: The effect of conditional Ihh deletion on intracellular TCRβ expression in DN cells

Dot plots show the gating strategy for intracellular detection of TCRβ on WT, $Ihh^{fl/WT}$ and $Ihh^{fl/fl}$ Cre^{+} mice. (A) shows selection of thymocytes negative for CD3, CD4, CD8, CD44 and NK1.1 cells, so that DN3 and DN4 cells are represented in the negative gate. (B) shows density plots for CD25, thus allowing the distinction between DN3 and DN4 cells and histograms (C) show the percentage of DN4 and DN3 thymocytes that are positive for TCRβ. n=3

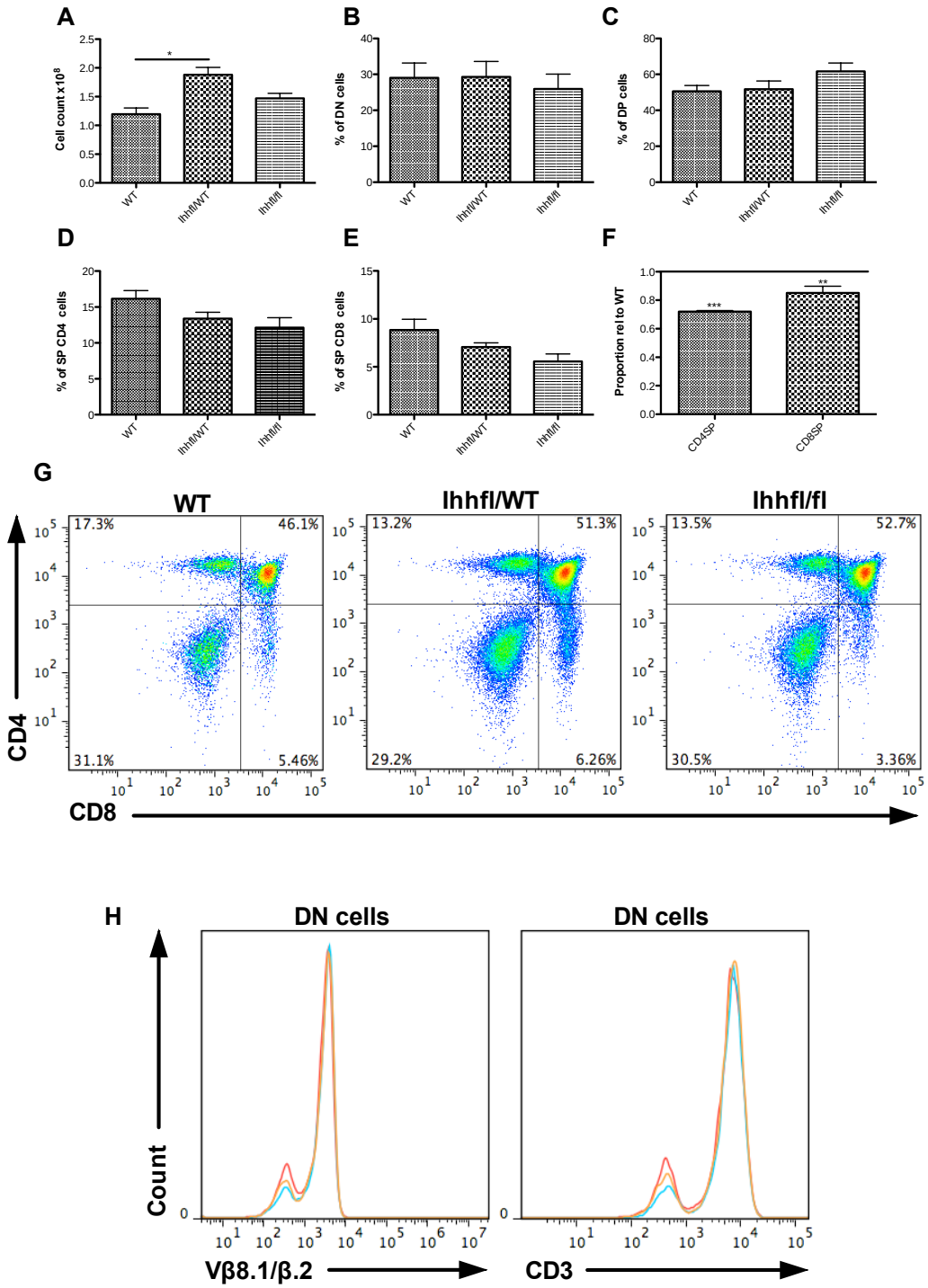

Figure 9.6: The effect of conditional Ihh deletion on thymocytes of young adult male mice crossed with the male-specific HY TCR.

Bar chart (A) shows the cell count of WT-HY, CD4-Cre^{+} Ihh$^{fl/WT}$-HY and CD4-Cre^{+} Ihh$^{fl/fl}$-HY thymocytes. Bar charts (B), (C), (D) and (E) show the percentage of DN, DP, CD4SP and CD8SP, thymocytes, respectively. Bar chart (F) shows coKO-HY CD4SP and CD8SP proportions relative to WT. Representative dot plots (H) show Vβ8.1/8.2 and CD3 expression of DN CD4-Cre^{+} Ihh$^{fl/fl}$-HY cells compared to WT-HY. *p<0.05, **p<0.005, ***p<0.0001, n=10

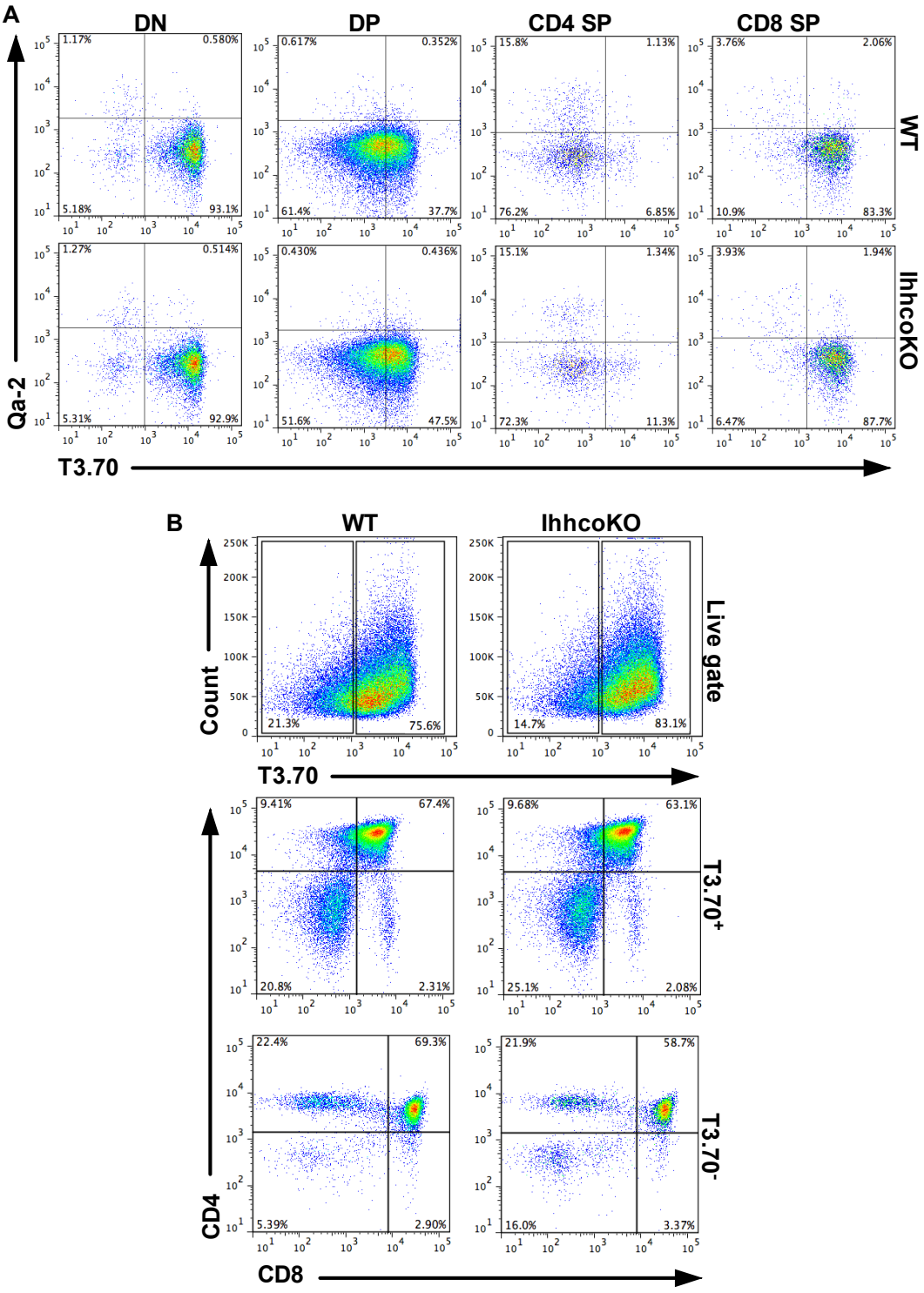

Figure 9.7: The effect of conditional Ihh deletion on thymic T3.70 expression in young adult male mice crossed with the male-specific HY TCR.

Dot plots (A) show Qa-2 and T3.70 expression of WT-HY and coKO-HY DN, DP, CD4SP and CD8SP populations. Dot plots (B) show the proportion of WT-HY and coKO-HY thymocytes in the live gate that express T3.70. Expresion of CD4 and CD8 from $T3.70^{+}$ and $T3.70^{-}$ thymocytes is also shown.

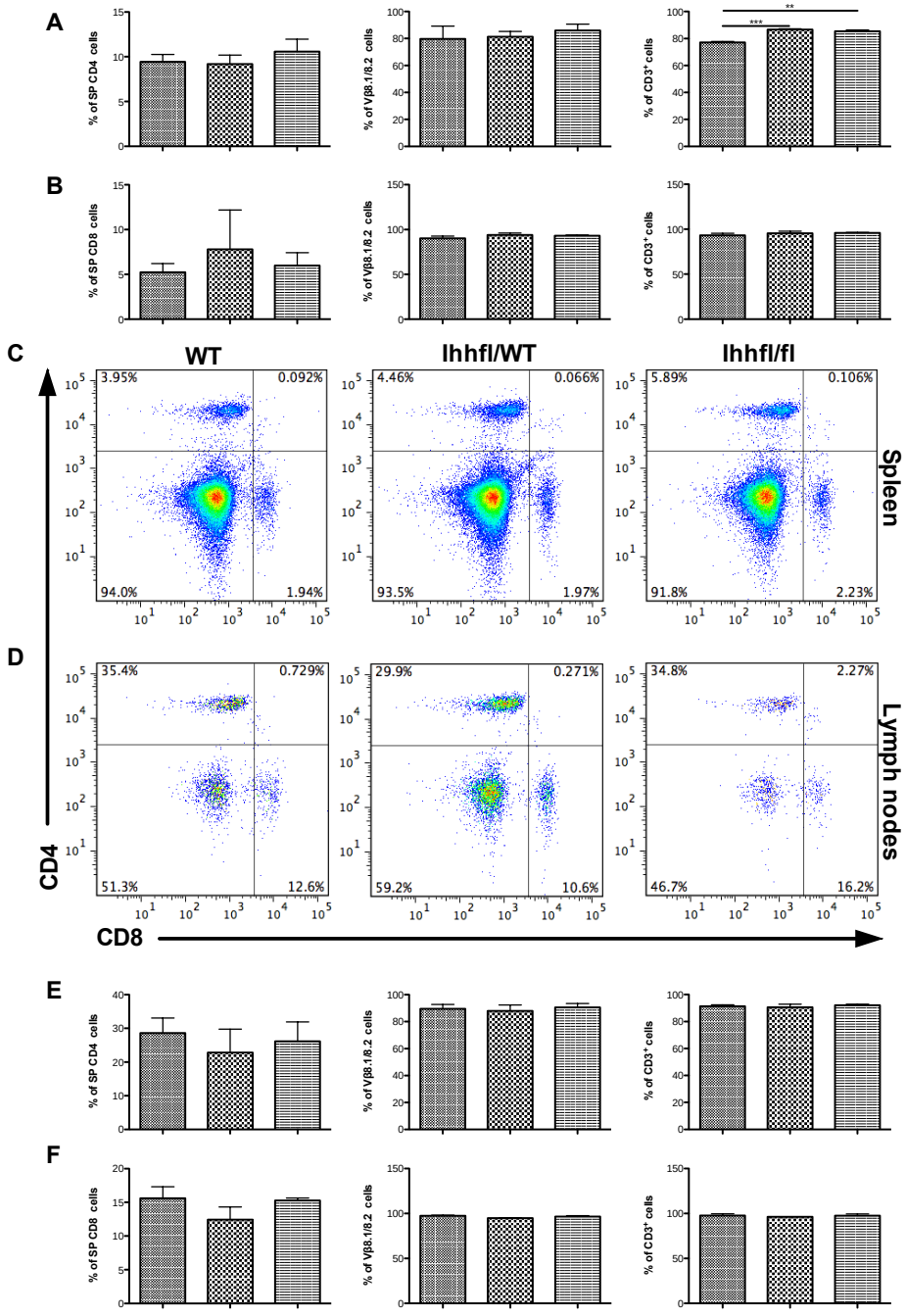

Figure 9.8: The effect of conditional Ihh deletion on T cells from the spleen and lymph nodes of young adult male mice crossed with the male-specific HY TCR.

Bar charts (A) and (B) show the proportion of CD4SP and CD8SP splenocytes, respectively and expression of Vβ8.1/8.2 and CD3 for the same populations. Dot plots (C) and (D) show CD4 and CD8 expression from the spleen and lymph nodes of WT-HY, coHet-HY and coKO-HY live gates, respectively. Bar charts (E) and (F) show the proportion of CD4SP and CD8SP lymphocytes, respectively and expression of Vβ8.1/8.2 and CD3 for the same populations. **p<0.005, ***p<0.0001

A

WT	coKO
1.30e+007	6.10e+006
1.50e+007	2.90e+006
1.60e+006	9.00e+005

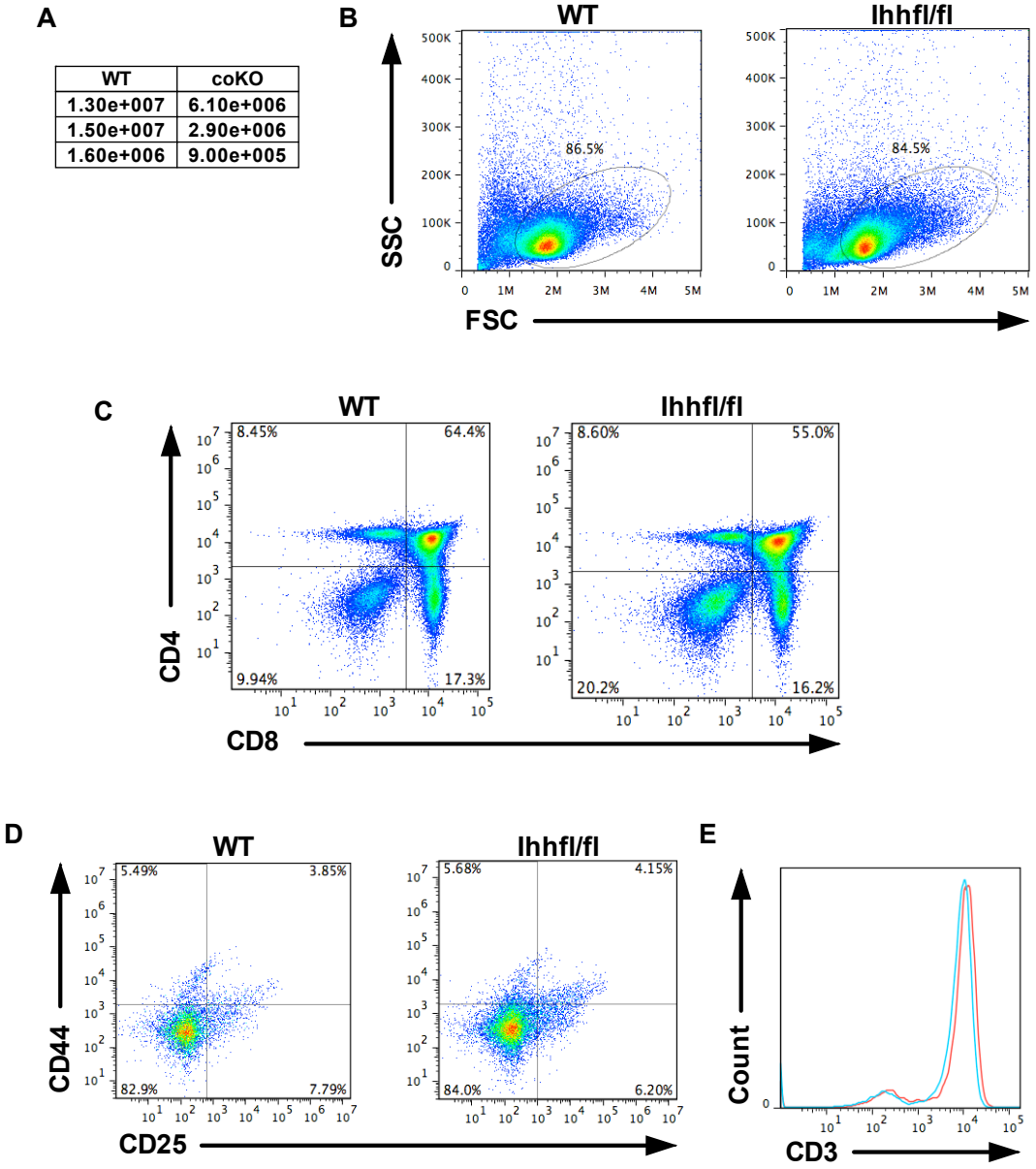

Figure 9.9: The effect of conditional Ihh deletion on thymocytes of young adult female mice crossed with the male-specific HY TCR.

Table (A) shows the cell count of WT-HY and CD4-Cre^{+} Ihh$^{fl/fl}$-HY thymocytes in the thymus, spleen and lymph node. Dot plots (B) show the live gate and (C) shows CD4 and CD8 expression of WT-HY and Ihh coKO-HY littermates. (D) shows CD44 and CD25 expresison of DN cells. Overlaid histogram (E) shows live-gated CD3 expression. n=2

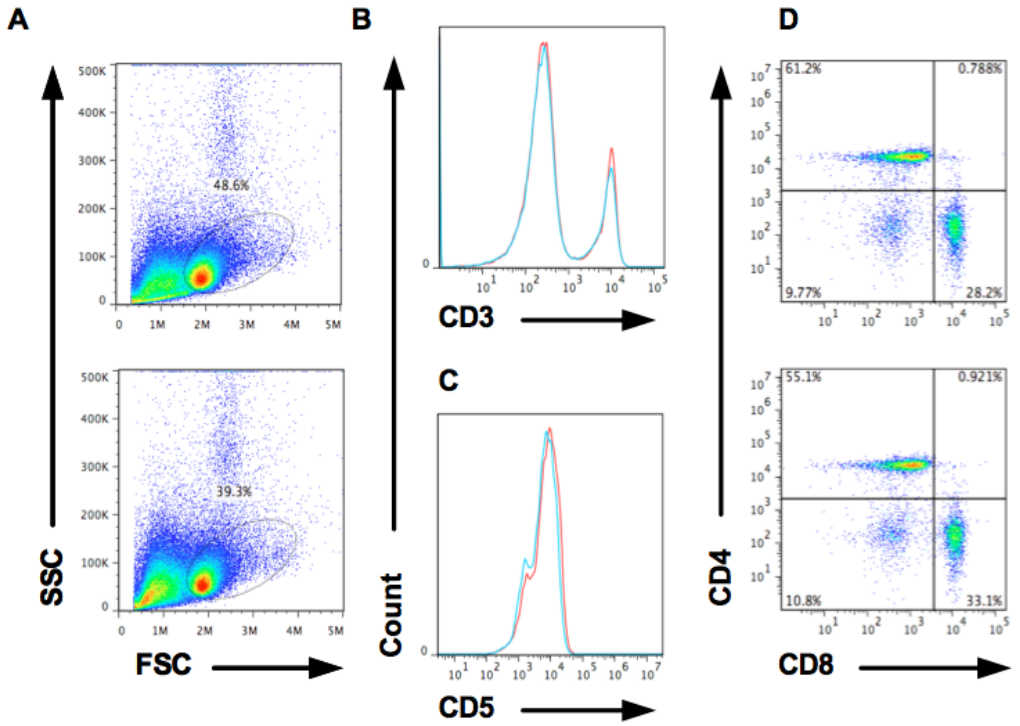

Figure 9.10: The effect of conditional Ihh deletion on T cells from the spleen of young adult female mice crossed with the male-specific antigen HY.

Dot plots (A) show live gate of WT-HY and CD4-Cre^{+} Ihh$^{fl/fl}$-HY thymocytes in the spleen of 6 week old female littermates. Overlaid histograms (B and C) show CD3 and CD3-gated CD5 expression, respectively. n=2

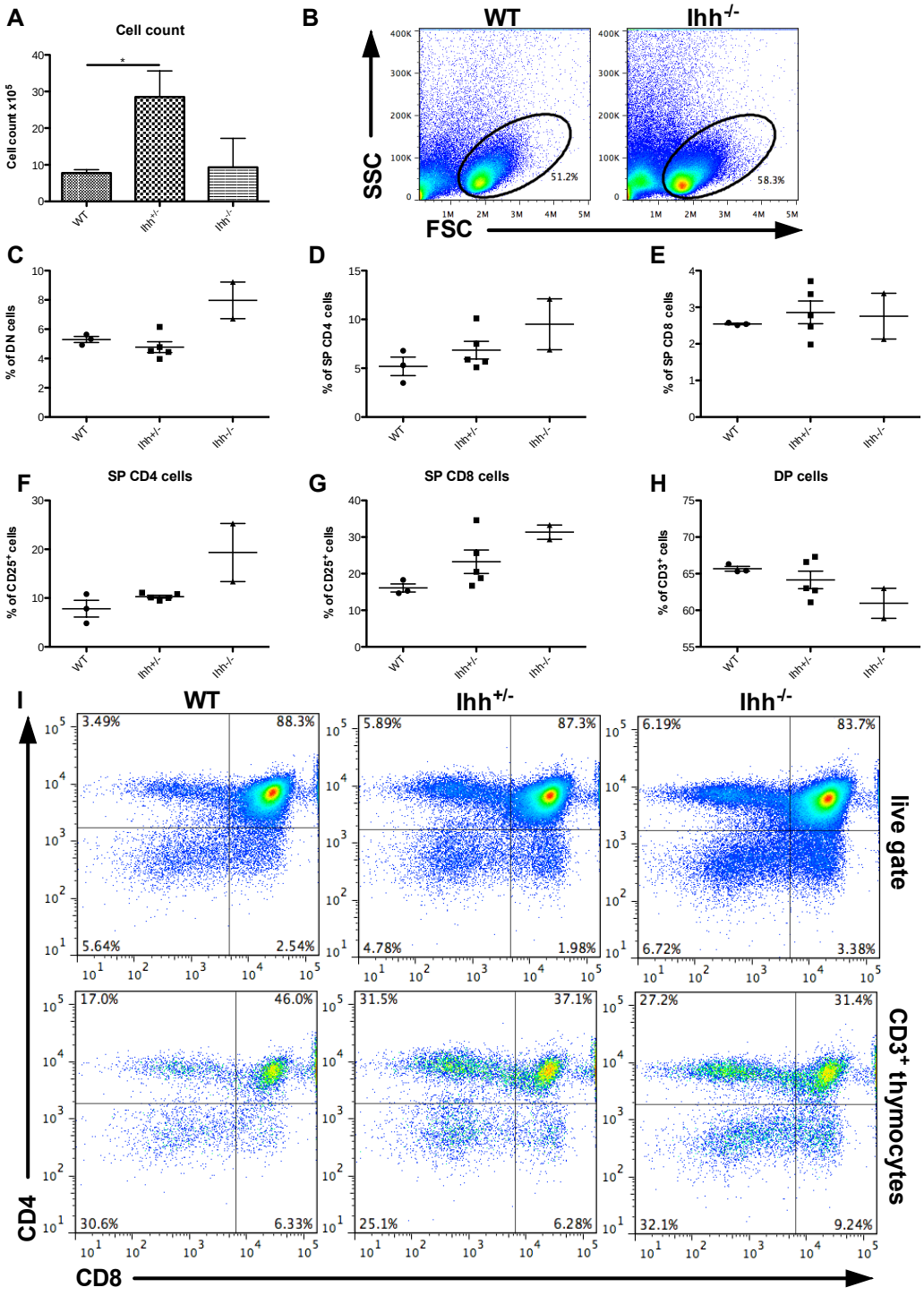

Figure 9.11: The effect of Ihh on E16.5 FTOC + 6 days in culture

Bar chart (A) shows the cell count of WT, Ihh$^{+/-}$ and Ihh$^{-/-}$ E16.5 thymus after 6 days in culture. Dot plots (B) show the live gate. Scatter graphs show the percentage of (C) DN, (D) CD4SP and (E) CD8SP cells. The percentage of CD25^{+} SP CD4 and SP CD8 cells is shown in scatter plots (F) and (G) respectively and plot H shows the proportion of DP cells that are positive for CD3. Dot plots (I) show CD4 and CD8 expression of thymocytes from the live gate and the CD3^{hi} compartment. n=10

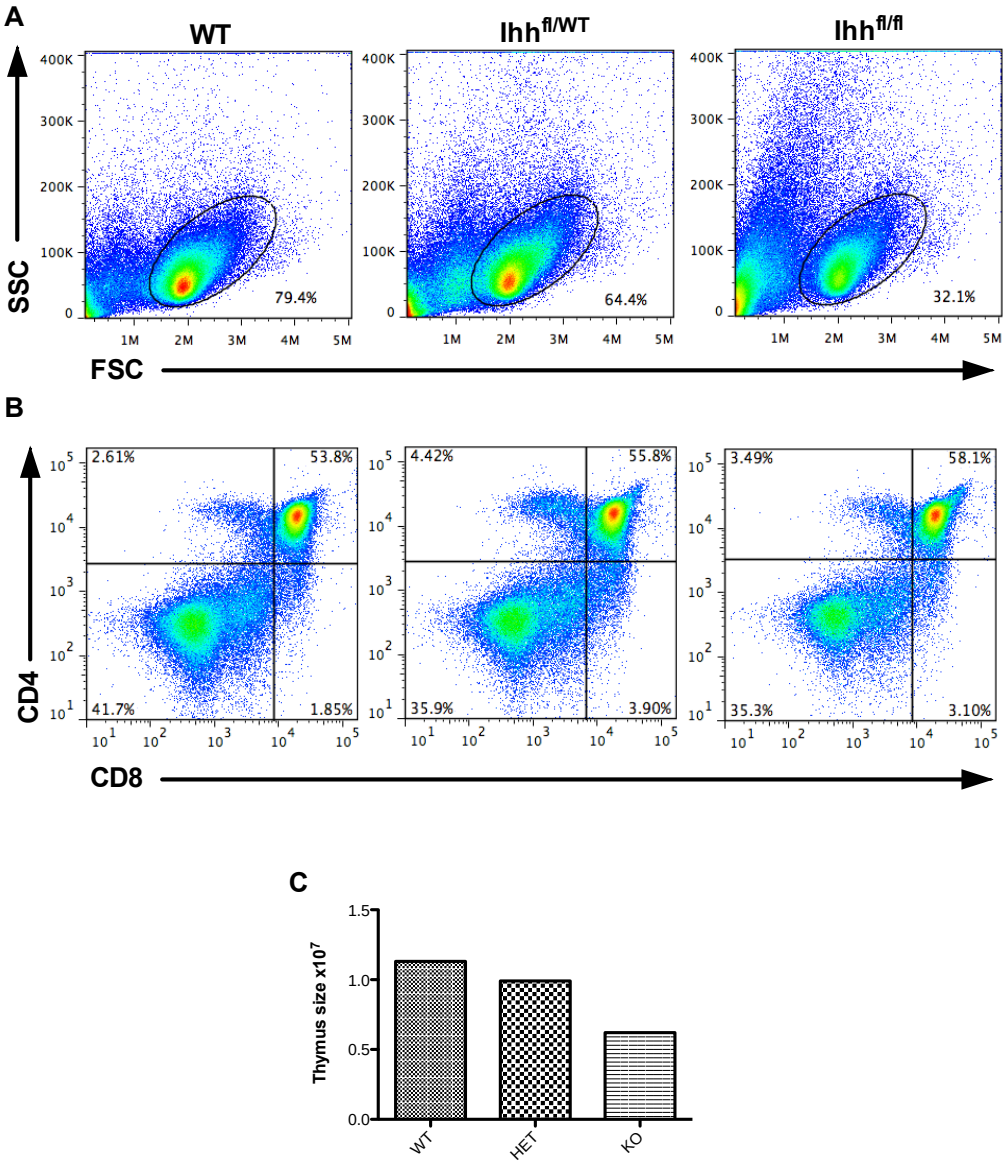

Figure 9.12: The effect of conditional Ihh deletion on HY⁺ E18.5 thymocytes in male mice

Dot plots show (A) the live gate and (B) CD4 and CD8 expression. Bar chart (C) shows the cell count of WT, $Ihh^{fl/WT}$ and $Ihh^{fl/fl}$ E18.5 thymus. n=3

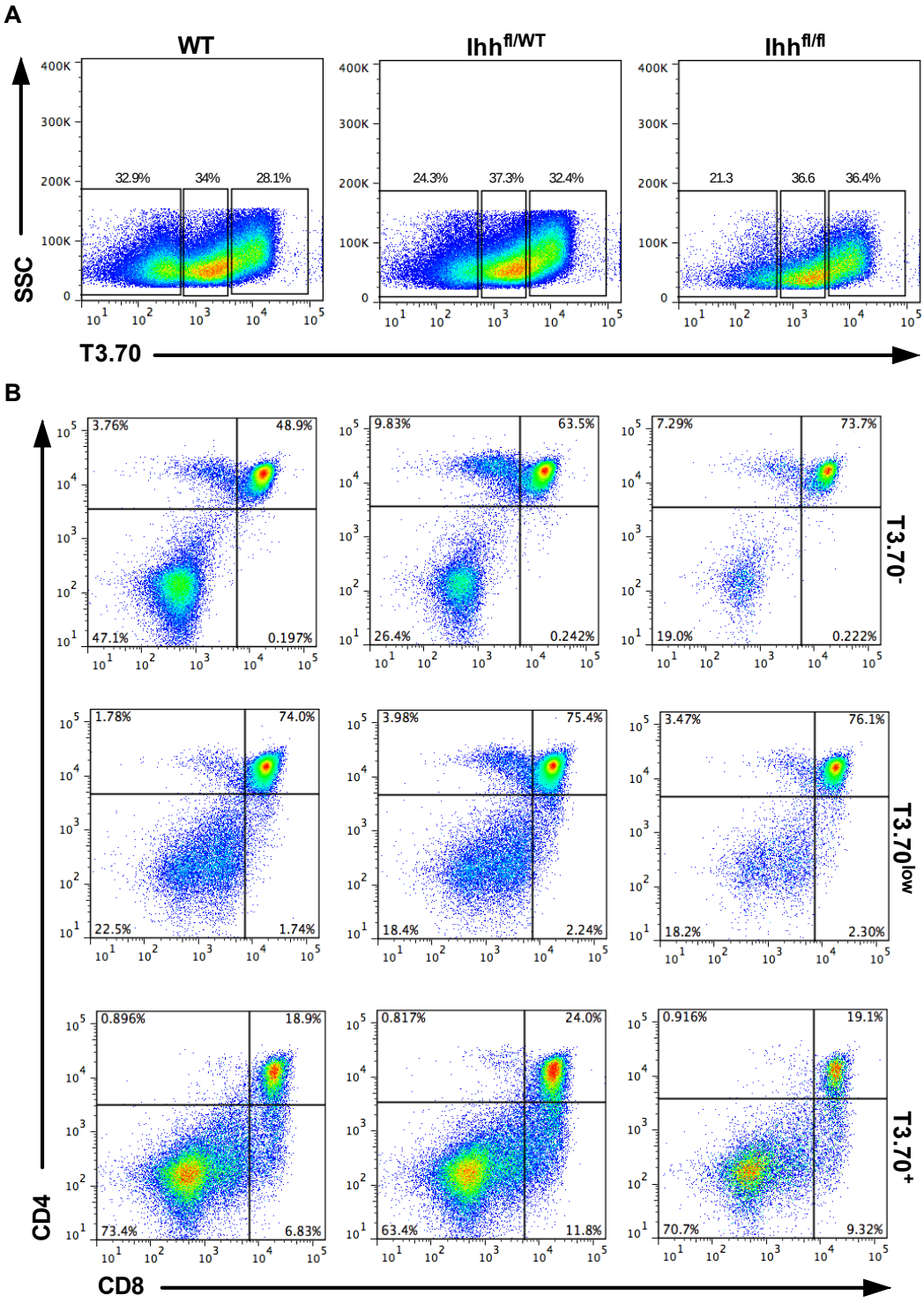

Figure 9.13: The effect of conditional Ihh deletion on HY⁺ E18.5 thymocytes in male mice

Dot plots (A) show T3.70 expression from the live gate of WT, $Ihh^{fl/WT}$ and $Ihh^{fl/fl}$ E18.5 thymus and (B) shows CD4 and CD8 expression of the $T3.70^{-}$, $T3.70^{low}$ and $T3.70^{high}$ gates. n=3

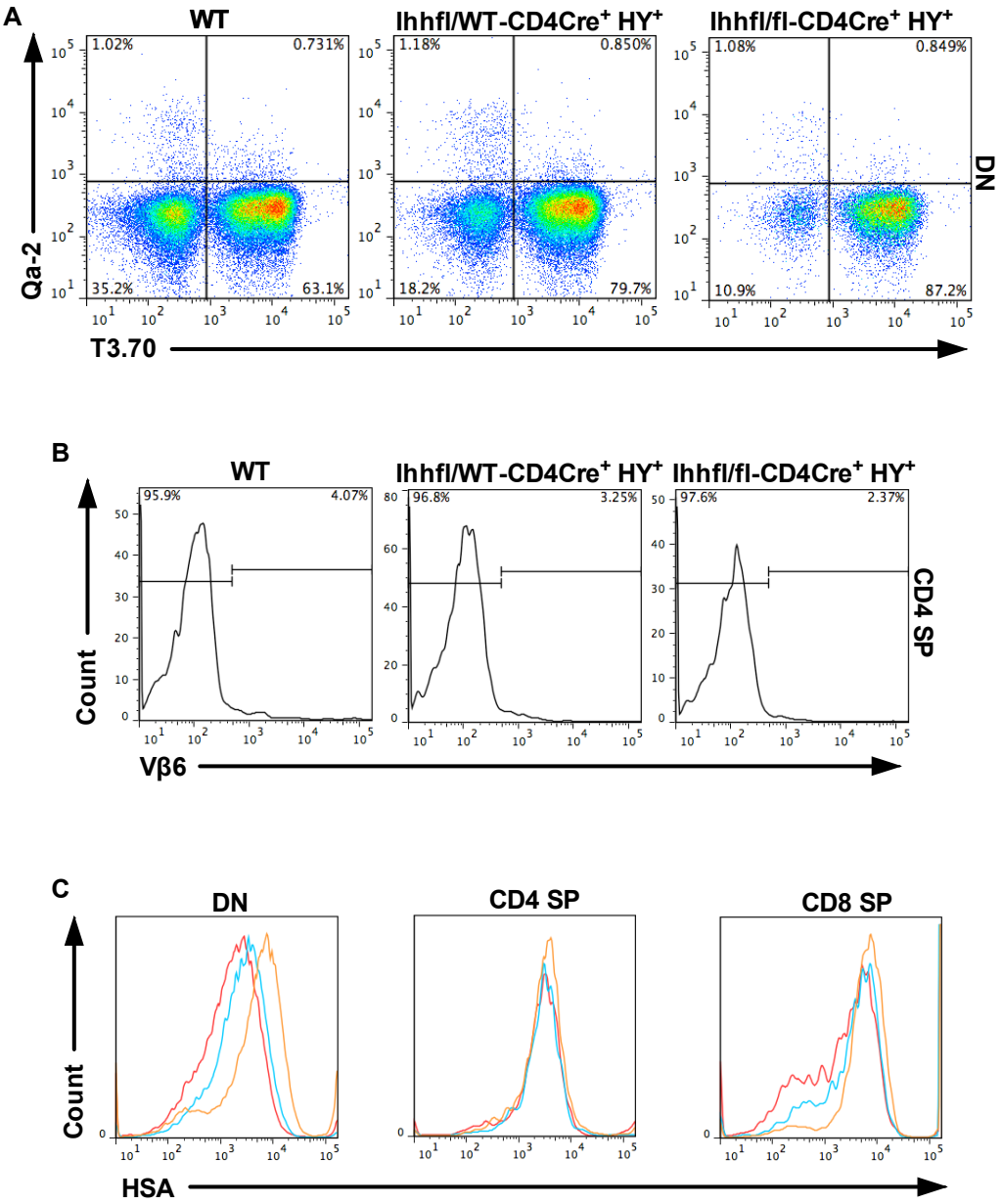

Figure 9.14: The effect of conditional Ihh HY+ on E18.5 thymocytes in male mice

Dot plots (A) show Qa-2 and HY expression on DN cells. Histograms (B) show Vβ6 expression on CD4 SP cells. Overlaid histogram (C) shows HSA expression on (WT / het / KO) DN, CD4SP and CD8SP cells.

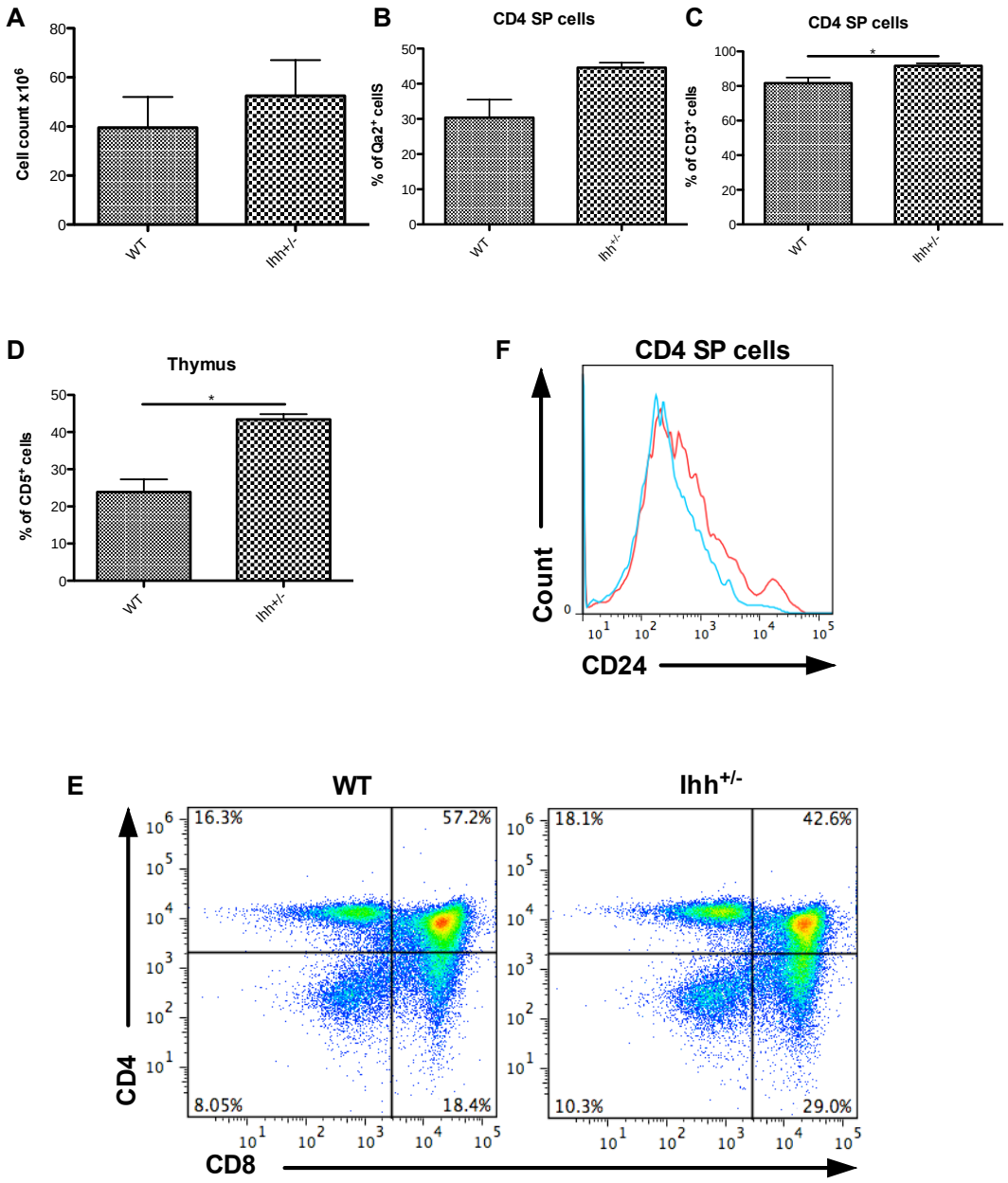

Figure 9.15: Thymocyte recovery of DP and SP populations 4 days after HC injection on Ihh$^{+/-}$ 4 weeks old mice

Bar chart (A) shows the cell count on live-gated thymocytes, 4 days after HC injection. Bar charts (B) and (C) show Qa-2 and CD3 expression on CD4SP cells. (D) shows CD5 expression in the thymus. Representative dot plots (E) show CD4 and CD8 expression and histogram (F) (WT / het) shows CD24 expression on CD4 SP cells. *p<0.05, n=6

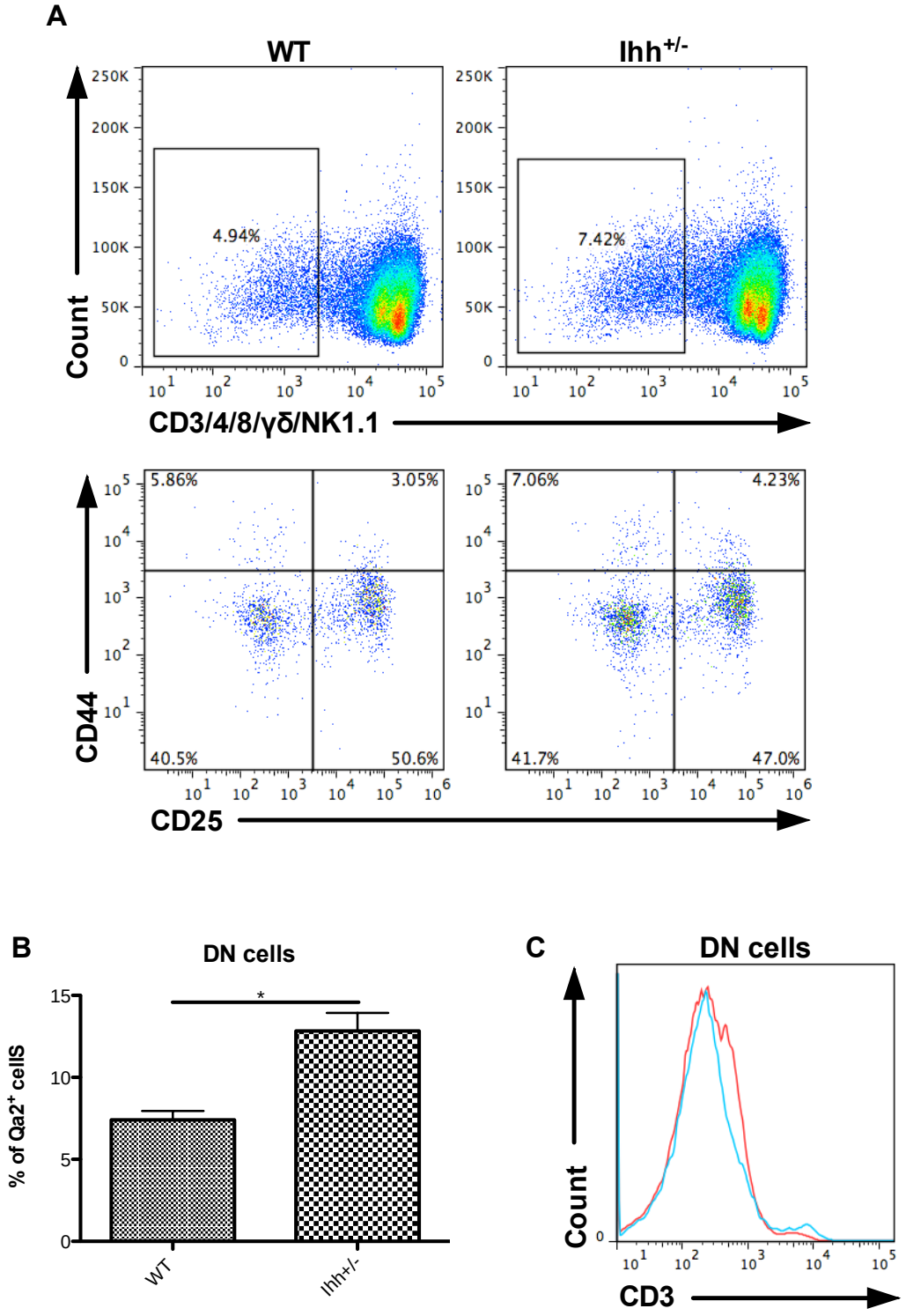

Figure 9.16: Thymocyte recovery of DN populations 4 days after HC injection on Ihh+/- 4 weeks old mice

Representative dot plots (A) show the gating strategy for the DN thymic populations. Bar chart (B) shows Qa2 expression on DN cells and histogram (C) (WT / het) shows CD3 expression on the same population. *p<0.05, n=6

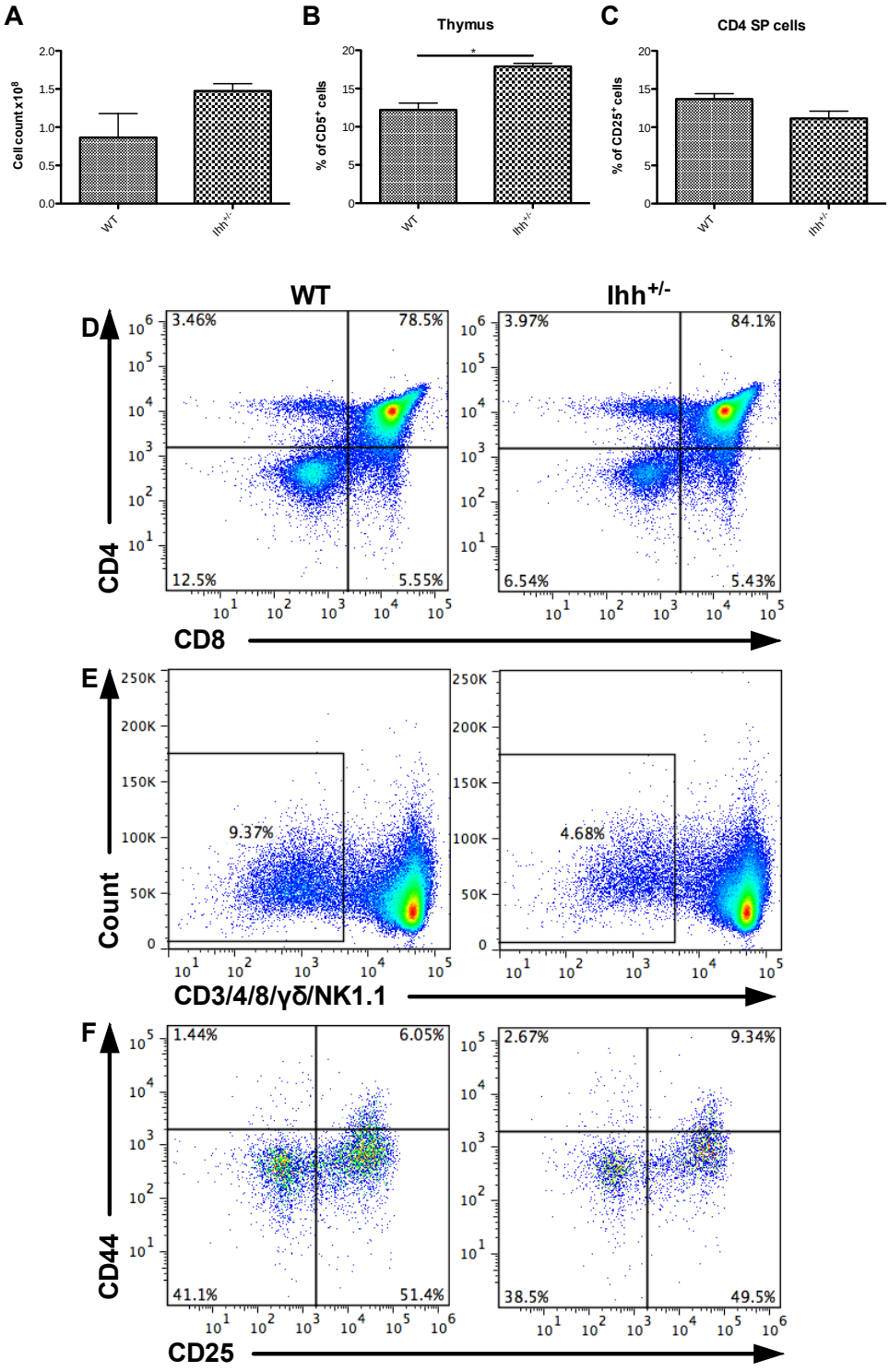

Figure 9.17: Thymocyte recovery 6 days after HC injection on Ihh$^{+/-}$ 4 weeks old mice

Bar chart (A) shows the cell count of thymocytes, 6 days after HC injection. (B) shows CD5 expression on live-gated thymocytes and (C) shows CD25 expression on CD4SP. Representative dot plots (D) show CD4 and CD8 expression and (E) shows the gating strategy for the (F) DN thymic populations. *p<0.05, n=4

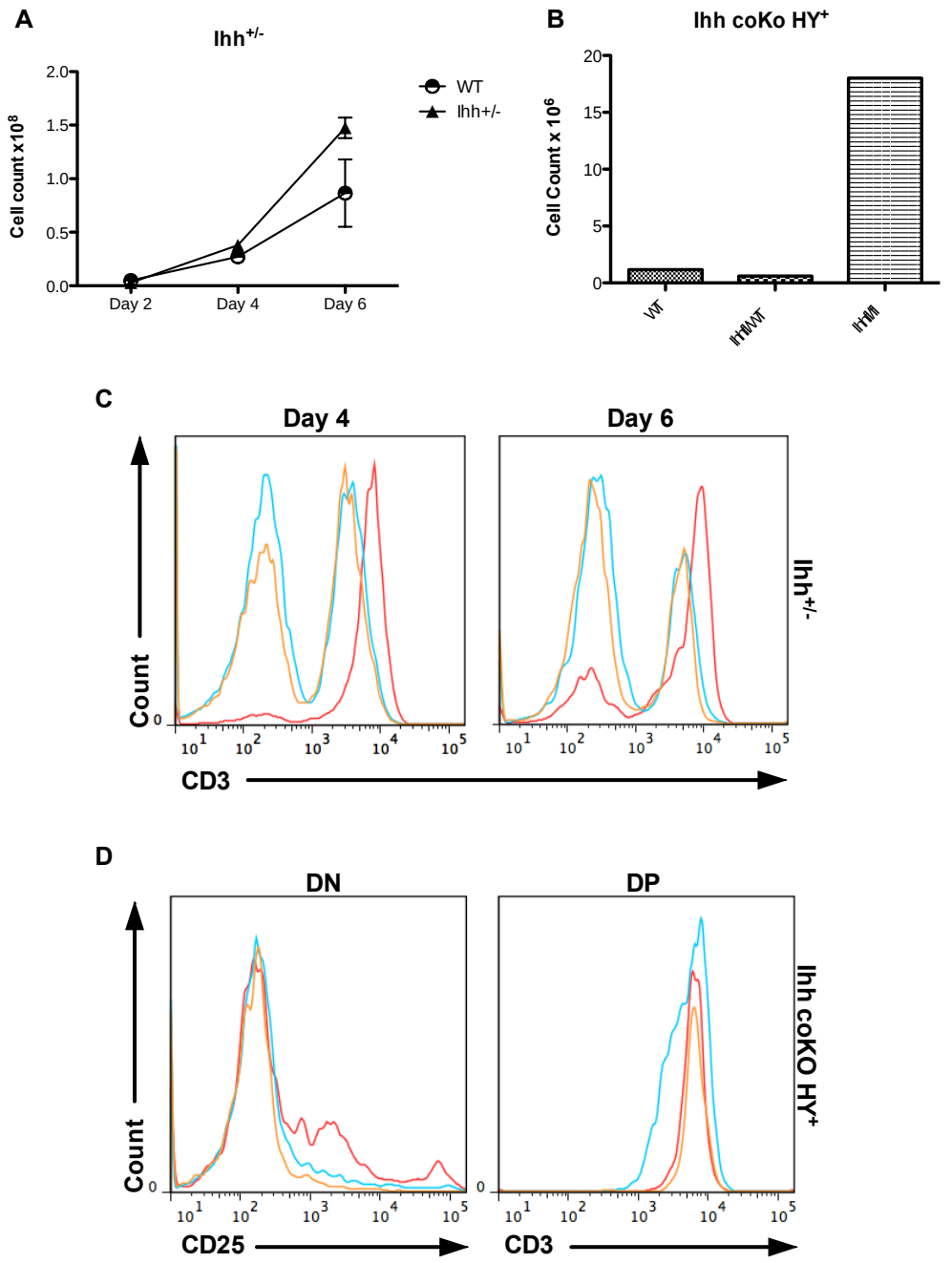

Figure 9.18: Thymocyte recovery in HC-injected Ihh$^{+/-}$ and conditional Ihh KO mice.

Graph (A) shows thymus size post HC injection in WT and Ihh$^{+/-}$ mice. Chart (B) shows cell count of HY-crossed WT, Ihhfl/WT CD4Cre^{+} and Ihhfl/fl CD4Cre^{+} 3 weeks old mice, 4 days after HC injection. Overlaid histogram (C) shows CD3 expression on WT CD4SP, WT CD8SP and Ihh$^{+/-}$ CD8SP cells, 4 and 6 days after HC injection. (D) shows CD25 expression on DN and CD3 expression on DP cells on HY-crossed WT, coHet and coKO young mice 4 days after HC injection.

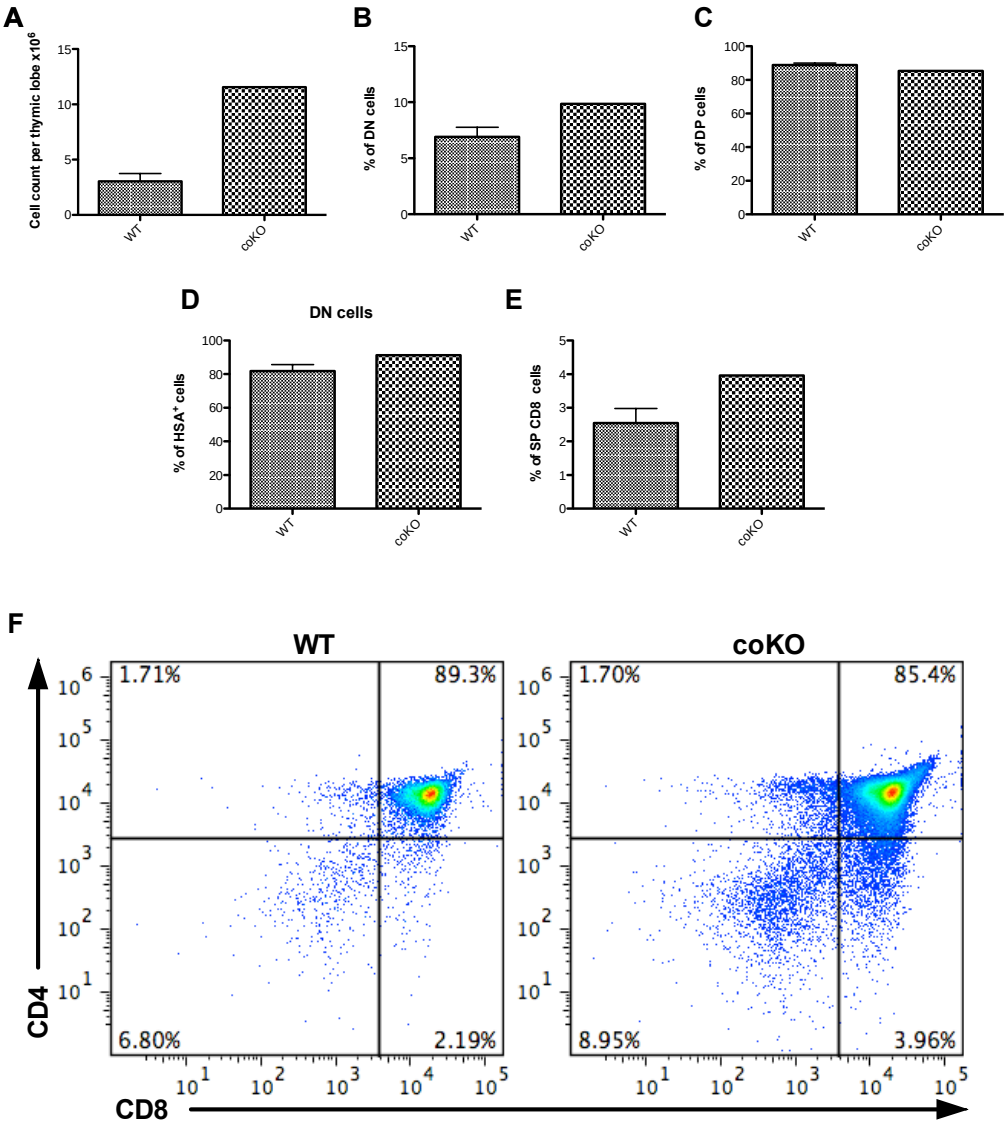

Figure 9.19: Thymocyte populations 7 days after α-CD3 stimulation on Rag$^{-/-}$ conditional Ihh KO FTOCs.

Bar chart (A) shows the cell count of thymocytes per thymic lobe, 7 days after α-CD3 treatment on FTOCs. Bar charts (B), (C), (E) show the percentage of DN, DP, CD8SP cells. Bar chart (D) shows the percentage of DN cells positive for HSA. Representative dot plots (F) show CD4 and CD8 expression of live-gated thymocytes. n=4

9.3 Discussion

9.3.1 Transition from DN to DP stage of development

Our hypothesis predicted that Ihh, secreted by DP cells, feeds back to DN progenitors and restricts their development, providing a negative feedback loop that controls the size of the thymus. According to this hypothesis, we expected that conditional deletion of Ihh from DP cells would result in loss of negative feedback and a significant expansion in thymus growth and size, accompanied with an expansion of the DP population. Nevertheless, our data revealed that the adult conditional null mice display a smaller thymus and unchanged proportions of DP cells compared to the WT. However, male conditional mice that were HY^{+}, displayed an enlarged thymus that contained a higher proportion of DP cells. We also observed larger thymi in HC experiments as well as Ihhfl/fl-$CD4Cre^{+}Rag^{-/-}$ FTOCs treated with anti-CD3. It seemed, however, that although we could clearly observe the negative impact that Ihh has on thymus size, we could not understand why this was not manifested on the conditional null HY^{-} mice due to what seems to be an arrest on the DN3 stage. As ic TCRβ expression is higher in the Ihh coKO, this arrest is not caused by decreased rearrangement. Nevertheless, the reason for this increased TCRβ expression is not clear as it could be a result of thymocytes being arrested on the DN stage or it can be a manifestation of genuine higher capacity for rearrangement.

Analysis of male IhhcoKO-HY^{+} mice revealed that male coKO mice showed less deletion and higher T3.70 DN cells in the thymus, suggesting that deletion of Ihh results in partial reduction in negative selection. We plan to carry out TCR sequencing on these mice, which will test if Ihh is influencing extent of endogenous TCR rearrangement.

We report several signs that collectively suggest that conditional deletion of Ihh results in a quicker transition from DN to DP stage. In a number of experiments, we observed higher CD5 expression on DN populations as well as the whole thymus. Another piece of evidence arises from HSA expression, which is downregulated as thymocytes mature. HSA levels are high on DN cells and gradually decrease in DP cells until they become undetectable in SP cells. High HSA expression of thymocytes results in pronounced reduction in DP and SP cell numbers, suggesting that downregulation of HSA is a critical event in thymocyte development that can act as an indicator of progression to the DP stage (Hough, Takei et al. 1994). In the absence of Ihh, DN cells seem to downregulate HSA quicker, as seen on the E18.5 Ihh coKO HY^+ experiment, consistent with accelerated maturation.

Furthermore, we detected much higher HY-TCR expression on DN cells in E18.5 IhhcoKO male mice as well as weaker CD3 expression on DP cells on E16.5 thymocytes after 6 days in FTOCs as well as during reconstitution of the DP population in HC-treated Ihh coKO HY^+ male mice. The narrowed time period that DN cells have to express CD3 during an accelerated progression from the DN to DP stage could explain the above finding. Our hypothesis is also backed by our observation that commonly in our Ihh KO or Ihh coKO experiments, where the thymus size is reduced, the live gate is also significantly smaller, suggesting increased apoptosis.

Overall, we believe that deletion of Ihh causes a significant acceleration of thymocyte development after the pre-TCR signal transduction. It is possible that this quick transition from DN to DP cells does not give thymocytes the necessary time to undergo normal TCR rearrangement, resulting in elimination of these faulty thymocytes during selection processes in later steps of T cell development and overall reduction in

thymus size. Despite the quicker transition, having an already rearranged TCR, the HY^+ thymocytes can pass selection successfully, which allows us to observe a larger thymus.

In order to test the expected higher apoptotic rate of DP cells in the absence of Ihh and a rearranged TCR, we are planning to use Annexin V stain on DP populations from WT and Ihhfl/fl-CD4Cre$^+$HY$^-$ mice. We are also planning to carry out TCR sequencing on sorted DP, CD4SP and CD8SP from WT and Ihhfl/fl-CD4Cre$^+$HY$^-$ mice. As T cells progress faster in the absence of Ihh, we expect to find a limited diversity of TCRs on the conditional null mice. Finally, we will carry out RNA sequencing on DN3, DN4, as well as DP cells on the same strain, in order to identify sets of genes which could provide an explanation for the accelerated transition from DN to DP cells and the increased thymic growth triggered by Ihh's deletion.

9.3.2 Transition from DP to SP stage of development

Our lab has previously shown that Shh and Gli2 affect later stages of T cell development, affecting TCR signal strength, positive and negative selection as well as CD4 versus CD8 lineage commitment (Crompton, Outram et al. 2007). However, the role of Ihh on later stages of T cell development has not been investigated yet. Here, we showed that Ihh is a negative regulator of the latest stages of thymic T cell development. In our experiments (eg. E16.5 and mutant Ihh 6 days FTOCs, anti-CD3-treated Ihh coKO $Rag^{-/-}$), we observed an increase in the proportions of CD4SP and CD8SP cell populations. The phenotype was even stronger in analysis of $CD3^+$ thymocytes.

Interestingly, this increase in the CD4SP and CD8SP populations was not clear in adult IhhcoKO and IhhcoKOHY$^+$ experiments. We believe that development of thymocytes in the adult thymus has reached a steady state

which limits the observation of events that need a synchronized progression to be manifested. We are planning to investigate the way Ihh regulates DP to SP progression further and we also intend to perform RNA sequencing on DP, CD4SP and CD8SP cells from WT and Ihhfl/fl-CD4Cre^{+} mice to elucidate those genes downstream Ihh which influence the DP to SP transition.

Overall, our research has revealed some interesting findings and even more interesting ideas that we can test in the near future. However, mice with conditional deletion of Ihh are very bad breeders and the subsequent lack of a constant supply of litters hindered our project. We will need to analyse more animals from these strains to confirm our results.

9.3.3 Effect of Ihh in periphery

Delaroche et al recently proposed that peripheral CD8 cells produce and secrete Ihh. Therefore, changes in peripheral T cells can be a result of either intrathymic processes that take place before T cell migration and persist in the periphery or a direct consequence of Ihh's absence in the periphery.

Interestingly, the conditional KO spleen contained more T cells than the WT, which is the opposite of what we saw in the thymus but no other difference was observed. Introduction of the HY antigen caused a significant upregulation of CD3 in the male spleen, consistent with the thymus. Finally, conditional deletion of Ihh did not affect B cell numbers, as shown by B220 analysis.

Discussion

10.1 Murine γδ T cells

10.1.1 Effect of Hh signalling on γδ cell numbers

We believe that Hh signalling positively regulates γδ T cells in the thymus during early developmental stages. Our lab has previously shown that Gli3 deletion blocks DN1 to DN2 transition, therefore we hypothesize that this finding is γδ-exclusive. In mutant strains in which inhibition of Hh activity is lifted and so overall Hh signalling is increased, such as Gli3 and Kif7, we detected a significant increase in the numbers of γδ T cells. We showed a similar effect in Gli2N2-tg mice in which Hh-mediated transcription is increased in T lineage cells. Our results were confirmed by double Dhh and Shh mutants as well as E16.5 FTOCs + 5 days in the presence of Hhip.

Interestingly, E17.5 Kif7 KO spleens have more γδ cells, although this is not the case in the E17.5 KO thymus. Furthermore, Kif7 mice show their highest increase in γδ count in the spleen and Gli3 in the lymph nodes. Overall, our data indicate that the rise in γδ cell numbers must be attributed to either an increased intrathymic turnover or to increased peripheral proliferation. In addition, the fact that in Kif7 and Gli3 mutant mice all γδ populations increase, suggests that the effect mediated by these mutant mice occurs early in γδ T cell development and affects γδ cells independently of subtype and effector fate.

Both Dhh KO and $Shh^{+/-}$ thymi show a small reduction in the numbers of γδ cells, which are not comparable to the phenotype observed in Kif7 or Gli3 heterozygotes. However, in the double Shh and Dhh KO, the reduction in total thymic γδ cell numbers becomes significant, indicating that, at least in terms of cell numbers, loss of Shh is largely compensated by Dhh and vice versa.

10.1.2 The effect of Hh signalling on the CD27^{+}CD44^{+} γδ subset

In the thymus, constitutive Gli2 activity causes an increase in the number of CD27^{+}CD44^{+} γδ cells, although we have not yet concluded whether this effect is the result of expansion of the existing CD27^{+}CD44^{+} population or a biased differentiation towards this lineage, neither have we investigated yet the exact nature of this subtype and its cytokine secretion capacity. We found that Kif7 and Gli3 do not influence this phenotype, as differences between WT and mutant littermates were not significant. Nevertheless, mutant Shh and Dhh mice show a significant downregulation of this population, indicating that these two ligands directly control the size of the thymic CD27^{+}CD44^{+} γδ population. We have little doubt that Hh signalling is a key positive regulator of this γδ subtype, which is known to be skewed for the Vγ1 chain, overall indicating that increased Hh activity supports the development of CD27^{+}CD44^{+} cells. There are three possible explanations for the increase in CD27^{+}CD44^{+} γδ subset.

Firstly, this population may appear by upregulating CD44 on Vγ1-biased CD27^{+}CD44^{-} γδ cells. This naïve CD27^{+}CD44^{-} (and CD122^{-}) γδ population is associated with an absence of TCR ligation during development (Ribot, Chaves-Ferreira et al. 2010). CD44 plays a role in adhesion and is known as an indicator for Ag-experienced cells and acquisition of a effector memory phenotype (Baaten, Tinoco et al. 2012). Details about the role of CD44 on γδ T cells remain unclear but it is possible that increased Hh activity leads to increased CD44 expression on the otherwise CD27^{+}CD44^{-} γδ population.

Secondly, this population may represent an expansion in the NK-like γδ population. We observed a strong upregulation on LPS-infected GliN2 mice. Our data point towards the idea that increased Hh activity promotes the development of NK-like γδ thymocytes. Several experiments support this hypothesis. For example, Gli3$^{+/-}$ mice showed a small increase in the

thymic numbers of NK-like γδ cells. Similarly, in double conditional Shh and Dhh, the percentage of NK-like γδ cells decreased, overall signifying that Hh signalling is likely to be a positive regulator of NK1.1-expressing γδ cells in the thymus. It will be important to add this marker when we carry out further analysis of the Gli2N2 tg strain, although in LPS-injected Gli2N2 tg mice, NK1.1 was sharply upregulated and in non-LPS-injected Gli2N2 tg mice, CD122, a marker strongly associated with NK-like γδ cells, increased significantly. Upregulation of CD122 expression suggests dependence on IL-15 (Sumaria, Roediger et al. 2011). The fact that NK-like γδ cells are Vγ1(Vδ6.3/6.4)-biased supports our hypothesis as we have shown that Hh signalling is a positive regulator of Vγ1 cells. However, most NK-like T cells residue in the murine liver and bone marrow (Lees, Ferrero et al. 2001), tissues which are beyond the scope of this project but which will investigate in the future. It is possible that differentiation of γδTCR-expressing cells towards an NK-like cell fate requires a specific extent, in terms of duration and strength, of TCR signalling. It is therefore possible that upregulation of the Hh pathway as exhibited by constitutive Gli2 activity or deletion of one copy of Gli3 promotes stronger or longer TCR signals which result in an upregulation of Vγ1-skewed, $CD27^{+}CD44^{+}$ NK-like γδ cells, which would have become naïve $CD44^{-}$ γδ cells in the absence of the increased TCR signals. In addition, $Vγ1^{+}CD27^{+}CD44^{+}$ NK-like γδ cells are one of the few γδ subtypes that require a γδTCR-ligand binding during their generation from thymic progenitors (Azuara, Levraud et al. 1997), and it is, alternatively possible, that Hh signalling increases the proliferation of this small pre-existing NK-like γδ population. Based on the above indirect evidence and published data from our lab that showed that Hh signalling affects TCR signal strength in αβ T cells, our next step will test this hypothesis and the implication of TCR signal strength in γδ T cells and more specifically in the upregulation of $NK1.1^{+}$ γδ cells in Gli2N2 and Shh mutant mice.

A third hypothesis implicates δ/αβ T cells, a newly identified and very enigmatic γδ T subset in humans, expressing TCRs comprised of a TCR-δ variable gene (Vδ1) fused to Joining α and Constant α domains, paired with an array of TCRβ chains (Pellicci, Uldrich et al. 2014). Within the Vδ1$^+$ population, the ratio of δ/αβ to γδ T cells varied widely with a mean of about 45%. Since this population is abundant in human PBMCs, we would not be surprised if we identify a murine population with similar characteristics. Currently, the focus on human δ/αβ cells lies on revealing the function of its TCR and recognising its antigens and therefore little is known about its ontogeny. A stronger TCR signal during β-selection can induce the production of δ chains which can then join the rearranging αβTCR, creating a surrogate δ/αβ TCR.

In LPS experiments that we performed on Gli2N2 tg mice and included NK1.1, the expanding population was NK1.1 positive, strongly suggesting that the expansion involves NK-like γδ cells. In the near future, we will explore the exact phenotype of this subtype using various readily available experimental ways. We have already shown that this population is unable to produce IL-17 and has a limited capacity for IFNγ production but we suspect that more key γδ cytokines are implicated which will help us identify the nature of this subset. Hence, we will test its cytokine production capacity for IL-4, IL-10 and IL-15 upon short PMA/Ionomycin activation. Furthermore, we will dissect and analyse the thymus and the periphery, including the liver and bone marrow, for NK-like γδ T cells. Additionally, co-staining with γδTCR and αβTCR antibodies will elucidate whether δ/αβ surrogate TCR T cells are present in the murine thymus. If we find this to be the case, we will sort this population from the adult thymus and sequence its TCR in order to identify its exact TCR configuration and its clonal diversity. We will perform RNAseq on sorted

$CD27^+CD44^+$ γδ cells from Gli2N2 tg and Shhfl/fl-$FoxN1Cre^+$ tg mice in order to reveal the Hh target genes and molecular pathways implicated in this phenotype.

10.1.3 The effect of Hh signalling on the $CD44^+$ $CD27^-$ γδ subset

IL-17-producing γδ cells derive directly from DN2 cells (DN3 cells give rise to IFNγ-producing γδ cells exclusively) (Shibata, Yamada et al. 2014), relying on ligand-independent TCR signals in the thymus (Jensen, Su et al. 2008) and their ontogeny is restricted in embryonic development (Haas, Ravens et al. 2012, Michel, Pang et al. 2012) so that adult mice rely on lifelong peripheral maintenance for this γδ subtype.

In the fetal thymus, E14.5 FTOCs + rShh for 5 days showed an increase in the $CD44^+CD27^-$ γδ subset. This contradicts all other relevant experiments that showed that Hh activity negatively regulates this population in the thymus. Adult Shh mutant mice show an increase in the percentage of this population and Kif7 and Gli3 mutant mice, which are expected to enhance Hh-mediated signals, show a strong downregulation of this population. The same applies in Kif7 fetal thymus, indicating that Hh signalling regulates γδ development already from the DN2 stage in around E15-E16, when IL-17-producing γδ cells first appear.

Shh-mediated Hh activity causes a downregulation of CD27 expression, together with an upregulation of CD44 expression as shown in adult and fetal thymi, spleens and lymph nodes. The upregulation of CD44 should be attributed to an expansion of the $CD27^+CD44^+$ γδ subset. The $CD44^+CD27^-$ population is actually reduced significantly, despite the overall upregulation of CD44.

In the Gli2N2 mice, CD44 expression increased dramatically but this is attributed exclusively to a remarkable upregulation of the $CD27^{+}CD44^{+}$ population and the $CD44^{+}CD27^{-}$ is not affected, indicating that Gli2 is not directly implicated to this thymic subset.

10.1.4 The effect of Hh signalling on splenic γδ T cells

In the spleen, Hh signalling causes a dramatic decrease in the $CD44^{+}CD27^{-}$ γδ cell population, as exhibited by Gli3, Kif7, Shh, Dhh and Gli2N2 experiments, indicating that Hh strongly suppresses this population, most likely directly via Gli2 signalling.

Concerning the $CD27^{+}CD44^{+}$ subtype, Ihh, Shh, Gli3 and Gli2 have no impact whereas $Kif7^{+/-}$ mice show a significant increase on the same population, suggesting that Kif7 acts independently of Gli2 and Gli3.

10.1.5 The effect of Hh signalling on cytokine production of splenic γδ cells

Hh activity also shows to weaken IL-17-secreting capacity as displayed on Gli3 and Shh mutant mice, upon 4h of PMA and Ionomycin activation. Interestingly, Dhh shows the opposite effect as we showed Dhh to be a positive regulator of IL-17 production on γδ splenic cells. Again, this constitutes another indication that Dhh may influence γδ T cells by acting as a suppressor of overall Hh activity in the spleen.

10.1.6 The effect of Hh signalling on CD24 expression of γδ cells

CD24 is considered to be a maturity marker for γδ thymocytes, with mature cells downregulating CD24 before entering the periphery. We discovered that Hh activity reduces significantly the percentage of $CD24^{+}$ γδ thymocytes, as exhibited by our Gli2N2 and Gli3 mice strains. Of note, according to our GBS-GFP data, $CD24^{-}$ γδ thymocytes are not responsive to

Hh signalling. Around 90% of CD27-expressing and 50% of CD44-expressing γδ thymocytes are positive for CD24 (Li, Zheng et al. 2004). We hypothesize that Hh activity promotes γδ cell maturation and a faster turnout rate, downregulating thymic CD24. Similarly, data on Shh, consistently with Gli3, Kif7 and Gli2N2 experiments in the spleen, suggest that increased Hh activity reduces percentage of peripheral γδ T cells that are positive for CD24.

CD24 has been implicated in homeostatic proliferation in αβ T cells. We noticed that there is a correlation between CD24 expression and cytokine-secreting capacity in the spleen as increased Hh signalling downregulates both CD24 and IL-17 production. However, we need further investigation to understand if and how the two observations affect each other. It is possible that strong Hh activity results in a stronger TCR signal which downregulates CD24 and favors an IFNγ-secreting capacity. In fact, a recent publication that elegantly tested the effect of TCR signal strength on the DN lineage commitment in a $Rag2^{-/-}$ mouse model in which both TCR-β and γδ-TCR are simultaneously expressed via retroviral transduction, showed that a strong TCR signal favored differentiation towards a γδ T cell lineage with a significant decrease in CD24 expression (Zarin, Wong et al. 2014).

Alternatively, we also hypothesize that Hh's negative effect on IL-17-producing cells can be CD24-mediated in a direct manner. The connection between CD24 and IL-17 production could be explain If Hh signalling causes a reduction in CD24 expression on $CD44^{+}CD27^{-}$ γδ cells which rely on CD24 for their peripheral proliferation and postnatal maintenance.

10.1.7 The effect of Hh signalling on γδ cells residing in the murine lymph nodes

The lymph nodes do not show GBS-GFP activity, however, Hh signalling influences γδ cell numbers in the lymph nodes. More specifically, Gli3 and Kif7 positively regulate γδ cells as mutant mice of both strains show increased γδ cell numbers. Interestingly, Gli3 displays a very strong phenotype, doubling the number of γδ cells.

Dhh seems to slightly promote γδ cells in the lymph nodes and Shh clearly suppresses it as $Shh^{+/-}$ and ShhcoKO show an increase in the numbers of γδ cells. The mechanism is not elucidated although we believe that the observed phenotype relies on events that occur prior to γδ cells homing to the lymph nodes. In any case, the opposing effects of Dhh and Shh on the LN γδ cells can be seen at the double Shh and Dhh KO experiments where rescue of Shh partly reverses the phenotype seen on the double KO (data not shown).

10.2 The effect of Hh signalling on γδ cells upon LPS infection

In the GliN2 mice, we saw an expansion of the $CD27^{+}CD44^{+}$ thymic population, which becomes $NK1.1^{+}$, $CCR6^{-}$ and Vγ1-biased, thus displaying all the typical characteristics of the NK-like γδ cells. We could not determine the peripheral destination of this subtype, as the thymic cell count increase was not reflected in the spleen, lymph nodes, blood or skin. It is believed that tissue localization of NK-like γδ cells relies on properties intrinsic to NKT cells, independently of the nature of TCR, hence we may find the expanding population occupying mainly the liver and bone marrow, in a way similar to NKT cells (Lees, Ferrero et al. 2001). In ShhcoKO LPS-injected mice, this population is downregulated, strongly suggesting that observed expansion of this population upon T cell activation is controlled by Shh upstream of Gli2. Interestingly, half of

splenic WT $CD27^{+}CD44^{+}$ γδ cells produce IFNγ upon PMA and ionomycin activation, whereas in the tg mice, the ratio drops to 3:1, indicating that the expanded cell population is not capable of IFNγ production. It has been shown that NK-like γδ cells can also secrete IL-4 or IL-15 upon activation (Vicari, Mocci et al. 1996), so we aim to investigate this in the near future.

In the Gli2 tg mice, the Vγ2-bearing $CD44^{+}CD27^{-}$ population disappears whereas $CD44^{+}CD27^{-}$ γδ cells bearing a Vγ chain other than Vγ1 and Vγ2 expand massively, overall increasing the number of $CD44^{+}CD27^{-}$ γδ cells. We are unable to explain this Gli2-induced substitution from Vγ2 to other Vγ-bearing $CD44^{+}CD27^{-}$ γδ cells, a finding which is also reflected in the spleen and lymph nodes, where the number of $V\gamma2^{+}$ $CD44^{+}CD27^{-}$ γδ cells decreases dramatically. We found that Gli2 triggers the $CD44^{+}CD27^{-}$ γδ subtype to remain in the peripheral blood, suggesting that LPS treatment changes cell migration. It has been shown that splenic murine γδ T cells recognize a B cell antigen called phycoerythrin, which triggers expansion of the IL17-producing $CD44^{+}CD27^{-}$ γδ subtype, together with reduction in CCR7 and upregulation of CCR2 expression (Zeng, Wei et al. 2012). This pattern is commonly associated with the acquisition of a new cell migration pattern in antigen-activated naïve αβ T cells (Meneghin and Hogaboam 2007). We are therefore interested to investigate whether a similar mechanism exists in γδ cells and how Gli2 activity can affect expression of the chemokine receptors, allowing $CD44^{+}CD27^{-}$ γδ cells to remain in blood circulation. Finally, Shh promotes IL-17 production, overall indicating that in LPS infection, despite the outstanding $CD27^{+}CD44^{+}$ NK-like γδ expansion, Hh signalling is likely to favor a TH17 response. This hypothesis, if proven correct, is translationally important as γδ T cells are the major IL-17 producers for a large number of infectious disease models, including *E.coli* infection.

Summary

This thesis focused on the role of Hh signalling and its mediators in the development and function of two distinct T cell subtype populations, γδ and αβ T cells. Here, we provided evidence that underline the importance of Hh signalling in these populations.

In terms of γδ T cells, we showed that Hh signalling both positively and negatively regulates distinct populations in the fetal and adult thymus, depending on numerous factors including functional capacity and tissue localization (Figure 10.1). Using an array of mutant mouse strains ($Gli3^{+/-}$, $Kif7^{+/-}$, Gli2N2, $Shh^{+/-}$ and $Dhh^{-/-}$) we showed that increased Hh signalling increased the proportion of γδ T cells in all tissues examined, both fetal and adult. In the adult thymus, Hh signalling, mediated directly via Shh and Gli2, promoted the intrathymic proliferation of Vγ1-biased NK-like γδ T lineage, possibly by providing a strong TCR signal that is required for the development of this subtype. Interestingly, loss of Shh significantly increased the numbers of γδ cells in the lymph nodes. Depending on tissue and γδ subtype population, Shh and Dhh showed overlapping or opposing effects, highlighting the diverse plasticity and fluidity of Hh-mediated signals and Hh ligands. In LPS treatment experiments, increased Hh activity as mediated by Gli2N2-tg, caused $Vγ2^{+}$ IL-17-producing cells to remain in peripheral blood.

We are the first to expand human γδ T thymocytes in a Vδ-unbiased way using an expansion protocol based on co-culturing with irradiated artificial antigen presenting cells (aAPCs). However, expanded γδ cells were activated *en masse* during expansion, becoming unresponsive to Hh signalling. Therefore, our subsequent preliminary analysis failed to

provide insight into the function of Hh signalling in human γδ T cell development.

DP αβ thymocytes produce Ihh that feeds back to DN progenitors to restrict their development, overall controlling thymus size. Despite published evidence on the existence of this negative feedback loop, little is known about its exact mode of action. Our investigation revealed that, contrary to our hypothesis, conditional deletion of Ihh from all CD4-expressing cells did not result in a larger thymus. Further investigation using the male specific HY TCR revealed that deletion of Ihh negatively affects negative selection whereas HC and Rag KO experiments showed that the feedback loop is manifested when requirement for TCR rearrangement is overcome in developing thymocytes and when developing thymocytes progress in a synchronized way. Overall, we hypothesize that deletion of Ihh accelerates differentiation so that thymocytes progress without a correct TCR rearrangement, followed by apoptosis of these cells, resulting in a small thymus.

Mice with conditional deletion of Ihh are bad breeders and the lack of samples delays the progress of this research and many details remained to be elucidated.

We also discovered that Ihh plays a role in DP to SP transition. Experiments where progression from DP to SP stage of development has not reached a steady state (analysis of fetal thymi as well as HC and RagKO experiments) showed that deletion of Ihh increased the proportion of mature CD4SP and CD8SP populations.

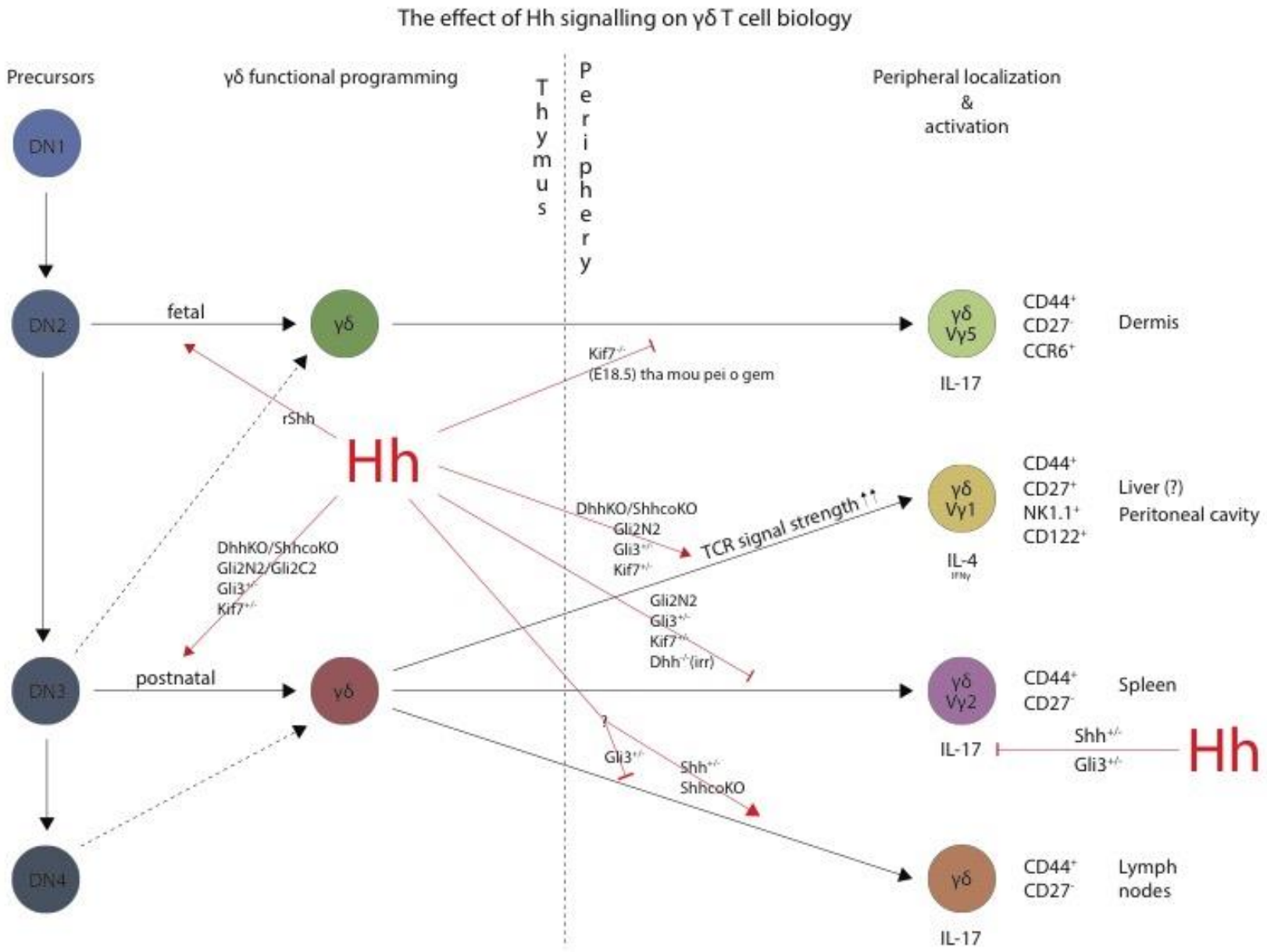
The effect of Hh signalling on γδ T cell biology
Precursors
γδ functional programming
Thymus
Periphery
Peripheral localization & activation
DN1
DN2
DN3
DN4
fetal
postnatal
γδ
rShh
Hh
DhhKO/ShhcoKO
Gli2N2/Gli2C2
Gli3+/-
Kif7+/-
Kif7-/-
(E18.5) tha mou pei o gem
DhhKO/ShhcoKO
Gli2N2
Gli3+/-
Kif7+/-
TCR signal strength↑↑
Gli2N2
Gli3+/-
Kif7+/-
Dhh-/- (irr)
?
Gli3+/-
Shh+/-
ShhcoKO
γδ Vγ5
IL-17
CD44+
CD27-
CCR6+
Dermis
γδ Vγ1
IL-4
IFNγ
CD44+
CD27+
NK1.1+
CD122+
Liver (?)
Peritoneal cavity
γδ Vγ2
IL-17
CD44+
CD27-
Spleen
Shh+/-
Gli3+/-
Hh
γδ
IL-17
CD44+
CD27-
Lymph nodes

Figure 10.1: The effect of Hh signalling on murine γδ T cell biology

The figure summarizes the effect or Hh signalling on murine γδ subtypes in the fetal and adult thymus and periphery. Red arrows symbolize promotion and dashed arrows symbolize inhibition. Mouse strains on top of red arrows indicate experiments where the effect was observed.

DN – Double negative, DP – double positive, γδ – γδTCR, Hh – Hedgehog signalling, IL – Interleukin, IFNγ – Interferon gamma.

Future directions

In the near future, we will analyse the liver and bone marrow of untreated and LPS-injected Gli2N2 and Shhfl/fl-FoxN1Cre adult mice for proportions of γδ cells and capacity for IL-10 and IL-4 production, in order to investigate the role of Hh signalling on NK-like γδ cells directly in the tissue where this subtype resides. Furthermore, we will investigate the strength of TCR signalling on developing γδ cells from the same mouse strains in order to understand whether Hh signalling promotes the NK-like γδ phenotype by directly influencing TCR signal strength. In order to identify the Hh target genes and molecular pathways which promote the NK-like γδ phenotype, we will carry out RNA sequencing on sorted NK-like γδ cells.

We will also investigate further the inability of Vγ2-biased IL-17-producing $CD44^{+}CD27^{-}$ γδ cells to harbor in secondary lymphoid organs as observed in LPS experiments. Using a flow cytometry-based technique, we aim to perform an extensive analysis of chemokine receptors, hoping to identify what triggers this γδ subtype to remain in blood circulation in Gli2N2 mice.

Finally, we showed that IL-17-producing $CD44^{+}CD24^{+}CD27^{-}$ γδ cells are particularly responsive to Hh signalling but their response varies according to tissue localization and other parameters which are not clear. As this population is abundant and important in the protection of skin and peritoneal cavity, we aim to explore the effect of Gli2C2 and Gli2N2-mediated altered Hh signalling by immunofluorescent staining on skin γδ cells and flow cytometry on peritoneal γδ cells.

We hope that our research will provide the evidence for new insights on Hh signalling and murine γδ T cell biology and identify novel factors which affect γδ lineage determination, tissue localization and functional capacity.

In terms of the role of Ihh on the development of αβ T cells, there is much to be done in order to test our hypothesis and confirm that deletion of Ihh causes increased apoptosis due to inability of developing thymocytes to successfully rearrange a functional TCR.

First of all, we need to continue analyzing E16.5/E18.5 and E16.5/E18.5 + 6 days FTOCs conditional Ihh embryos for markers that can indicate faster TCR rearrangement and DN to DP transition as well as apoptosis. Similar analysis must be performed on HC and additional anti-CD3-treated RagKO experiments. In order to confirm the dramatic increase in thymus size in HC-treated Ihh coKo HY^+ mice, we aim to inject HC to more pairs of Ihh coKo HY^+ and WT littermates.

Finally, we predict to detect oligoclonal diversity of TCRs in the conditional Ihh thymi because we expect that death of developing thymocytes in these transgenics correlates with time taken to successfully rearrange their TCR, controlling the size of TCR of surviving cells. Therefore, we aim to carry out TCR sequencing expecting to identify a restricted TCR repertoire consisting of long TCR chains.

Publications arising from this work

Hh signalling regulates differentiation and homeostasis of γδ T cells.
Mengrelis K, Saldaña J, Lau C, Furmanski A, Gustafsson K, Crompton T. In preparation

Hh signalling in the embryonic thymus
Mengrelis K, Ross S, Solanski A, Lau C, Al Shammary A, Crompton T. In preparation

Thymus transplantation for complete Di George syndrome: European experience
E Graham Davies, Melissa Cheung, Kimberly Gilmour, Jesmeen Marmaris , Joe Curry, Anna Furmanski, Neil Sebire, Stuart Adams, Jolanta Bernatoniene, Ronald Bremner, Michael Browning, Blythe Devlin, Hans-Christian Erichsen, Bobby Gaspar, Winnie Ip, Marianne Iversen, Ronan Leahy, Elizabeth McCarthy, Konstantinos Mengrelis, Despina Moshous, Kim Neuling, Malgorzata Pac, Kate Parsley, Luigi Poliani ,Waseem Qasim, Tiia Voor, Austen Worth, Tessa Crompton, M Louise Markert, Adrian J Thrasher. In preparation

REFERENCES

Alcedo, J., M. Ayzenzon, T. Von Ohlen, M. Noll and J. E. Hooper (1996). "The Drosophila smoothened gene encodes a seven-pass membrane protein, a putative receptor for the hedgehog signal." Cell **86**(2): 221-232.

Allison, J. P. and W. L. Havran (1991). "The immunobiology of T cells with invariant gamma delta antigen receptors." Annual review of immunology **9**: 679-705.

Anderson, M. S., E. S. Venanzi, L. Klein, Z. Chen, S. P. Berzins, S. J. Turley, H. von Boehmer, R. Bronson, A. Dierich, C. Benoist and D. Mathis (2002). "Projection of an immunological self shadow within the thymus by the aire protein." Science **298**(5597): 1395-1401.

Angelini, D. F., G. Borsellino, M. Poupot, A. Diamantini, R. Poupot, G. Bernardi, F. Poccia, J. J. Fournie and L. Battistini (2004). "FcgammaRIII discriminates between 2 subsets of Vgamma9Vdelta2 effector cells with different responses and activation pathways." Blood **104**(6): 1801-1807.

Aza-Blanc, P., H. Y. Lin, A. Ruiz i Altaba and T. B. Kornberg (2000). "Expression of the vertebrate Gli proteins in Drosophila reveals a distribution of activator and repressor activities." Development **127**(19): 4293-4301.

Azuara, V., J. P. Levraud, M. P. Lembezat and P. Pereira (1997). "A novel subset of adult gamma delta thymocytes that secretes a distinct pattern of cytokines and expresses a very restricted T cell receptor repertoire." European journal of immunology **27**(2): 544-553.

Azuara, V., J. P. Levraud, M. P. Lembezat and P. Pereira (1997). "A novel subset of adult gamma delta thymocytes that secretes a distinct pattern of cytokines and expresses a very restricted T cell receptor repertoire." Eur J Immunol **27**(2): 544-553.

Azuma, M., D. Ito, H. Yagita, K. Okumura, J. H. Phillips, L. L. Lanier and C. Somoza (1993). "B70 antigen is a second ligand for CTLA-4 and CD28." Nature **366**(6450): 76-79.

Baaten, B. J., R. Tinoco, A. T. Chen and L. M. Bradley (2012). "Regulation of Antigen-Experienced T Cells: Lessons from the Quintessential Memory Marker CD44." Front Immunol **3**: 23.

Bai, C. B., W. Auerbach, J. S. Lee, D. Stephen and A. L. Joyner (2002). "Gli2, but not Gli1, is required for initial Shh signaling and ectopic activation of the Shh pathway." Development **129**(20): 4753-4761.

Bai, C. B. and A. L. Joyner (2001). "Gli1 can rescue the in vivo function of Gli2." Development **128**(24): 5161-5172.

Balaskas, N., A. Ribeiro, J. Panovska, E. Dessaud, N. Sasai, K. M. Page, J. Briscoe and V. Ribes (2012). "Gene regulatory logic for reading the Sonic Hedgehog signaling gradient in the vertebrate neural tube." Cell **148**(1-2): 273-284.

Beachy, P. A., S. G. Hymowitz, R. A. Lazarus, D. J. Leahy and C. Siebold (2010). "Interactions between Hedgehog proteins and their binding partners come into view." Genes Dev **24**(18): 2001-2012.

Bitgood, M. J., L. Shen and A. P. McMahon (1996). "Sertoli cell signaling by Desert hedgehog regulates the male germline." Current biology : CB **6**(3): 298-304.

Borst, J. and J. J. van Dongen (1990). "Repertoire selection of human gamma delta T cells." Research in immunology **141**(7): 663-668.

Brandes, M., K. Willimann and B. Moser (2005). "Professional antigen-presentation function by human gammadelta T Cells." Science **309**(5732): 264-268.

Brenner, M. B., J. McLean, D. P. Dialynas, J. L. Strominger, J. A. Smith, F. L. Owen, J. G. Seidman, S. Ip, F. Rosen and M. S. Krangel (1986). "Identification of a putative second T-cell receptor." Nature **322**(6075): 145-149.

Briscoe, J. and J. Ericson (1999). "The specification of neuronal identity by graded Sonic Hedgehog signalling." Seminars in cell & developmental biology **10**(3): 353-362.

Caccamo, N., S. Meraviglia, V. Ferlazzo, D. Angelini, G. Borsellino, F. Poccia, L. Battistini, F. Dieli and A. Salerno (2005). "Differential requirements for antigen or homeostatic cytokines for proliferation and differentiation of human Vgamma9Vdelta2 naive, memory and effector T cell subsets." Eur J Immunol **35**(6): 1764-1772.

Carpenter, A. C. and R. Bosselut (2010). "Decision checkpoints in the thymus." Nat Immunol **11**(8): 666-673.

Casetti, R., C. Agrati, M. Wallace, A. Sacchi, F. Martini, A. Martino, A. Rinaldi and M. Malkovsky (2009). "Cutting edge: TGF-beta1 and IL-15 Induce FOXP3+

gammadelta regulatory T cells in the presence of antigen stimulation." J Immunol **183**(6): 3574-3577.

Chan, S. H., D. Cosgrove, C. Waltzinger, C. Benoist and D. Mathis (1993). "Another view of the selective model of thymocyte selection." Cell **73**(2): 225-236.

Chen, L. and D. B. Flies (2013). "Molecular mechanisms of T cell co-stimulation and co-inhibition." Nat Rev Immunol **13**(4): 227-242.

Cheung, H. O., X. Zhang, A. Ribeiro, R. Mo, S. Makino, V. Puviindran, K. K. Law, J. Briscoe and C. C. Hui (2009). "The kinesin protein Kif7 is a critical regulator of Gli transcription factors in mammalian hedgehog signaling." Sci Signal **2**(76): ra29.

Chi, S., S. Huang, C. Li, X. Zhang, N. He, M. S. Bhutani, D. Jones, C. Y. Castro, R. Logrono, A. Haque, J. Zwischenberger, S. K. Tyring, H. Zhang and J. Xie (2006). "Activation of the hedgehog pathway in a subset of lung cancers." Cancer Lett **244**(1): 53-60.

Chiang, C., Y. Litingtung, E. Lee, K. E. Young, J. L. Corden, H. Westphal and P. A. Beachy (1996). "Cyclopia and defective axial patterning in mice lacking Sonic hedgehog gene function." Nature **383**(6599): 407-413.

Ciofani, M., G. C. Knowles, D. L. Wiest, H. von Boehmer and J. C. Zuniga-Pflucker (2006). "Stage-specific and differential notch dependency at the alphabeta and gammadelta T lineage bifurcation." Immunity **25**(1): 105-116.

Ciofani, M. and J. C. Zuniga-Pflucker (2010). "Determining gammadelta versus alphass T cell development." Nature reviews. Immunology **10**(9): 657-663.

Clark, A. M., K. K. Garland and L. D. Russell (2000). "Desert hedgehog (Dhh) gene is required in the mouse testis for formation of adult-type Leydig cells and normal development of peritubular cells and seminiferous tubules." Biol Reprod **63**(6): 1825-1838.

Constant, S. L. and K. Bottomly (1997). "Induction of Th1 and Th2 CD4+ T cell responses: the alternative approaches." Annu Rev Immunol **15**: 297-322.

Crompton, T., S. V. Outram and A. L. Hager-Theodorides (2007). "Sonic hedgehog signalling in T-cell development and activation." Nature reviews. Immunology **7**(9): 726-735.

Crompton, T., S. V. Outram and A. L. Hager-Theodorides (2007). "Sonic hedgehog signalling in T-cell development and activation." Nat Rev Immunol **7**(9): 726-735.

Curotto de Lafaille, M. A. and J. J. Lafaille (2009). "Natural and adaptive foxp3+ regulatory T cells: more of the same or a division of labor?" Immunity **30**(5): 626-635.

Dahmane, N., J. Lee, P. Robins, P. Heller and A. Ruiz i Altaba (1997). "Activation of the transcription factor Gli1 and the Sonic hedgehog signalling pathway in skin tumours." Nature **389**(6653): 876-881.

Davis, C. B., N. Killeen, M. E. Crooks, D. Raulet and D. R. Littman (1993). "Evidence for a stochastic mechanism in the differentiation of mature subsets of T lymphocytes." Cell **73**(2): 237-247.

de la Roche, M., A. T. Ritter, K. L. Angus, C. Dinsmore, C. H. Earnshaw, J. F. Reiter and G. M. Griffiths (2013). "Hedgehog signaling controls T cell killing at the immunological synapse." Science **342**(6163): 1247-1250.

De Maria, A., A. Ferrazin, S. Ferrini, E. Ciccone, A. Terragna and L. Moretta (1992). "Selective increase of a subset of T cell receptor gamma delta T lymphocytes in the peripheral blood of patients with human immunodeficiency virus type 1 infection." J Infect Dis **165**(5): 917-919.

De Rosa, S. C., J. P. Andrus, S. P. Perfetto, J. J. Mantovani, L. A. Herzenberg, L. A. Herzenberg and M. Roederer (2004). "Ontogeny of gamma delta T cells in humans." J Immunol **172**(3): 1637-1645.

Dechanet, J., P. Merville, A. Lim, C. Retiere, V. Pitard, X. Lafarge, S. Michelson, C. Meric, M. M. Hallet, P. Kourilsky, L. Potaux, M. Bonneville and J. F. Moreau (1999). "Implication of gammadelta T cells in the human immune response to cytomegalovirus." J Clin Invest **103**(10): 1437-1449.

Deusch, K., F. Luling, K. Reich, M. Classen, H. Wagner and K. Pfeffer (1991). "A major fraction of human intraepithelial lymphocytes simultaneously expresses the gamma/delta T cell receptor, the CD8 accessory molecule and preferentially uses the V delta 1 gene segment." Eur J Immunol **21**(4): 1053-1059.

Dieli, F., F. Poccia, M. Lipp, G. Sireci, N. Caccamo, C. Di Sano and A. Salerno (2003). "Differentiation of effector/memory Vdelta2 T cells and migratory routes in lymph nodes or inflammatory sites." J Exp Med **198**(3): 391-397.

Dyer, M. A., S. M. Farrington, D. Mohn, J. R. Munday and M. H. Baron (2001). "Indian hedgehog activates hematopoiesis and vasculogenesis and can respecify

prospective neurectodermal cell fate in the mouse embryo." Development **128**(10): 1717-1730.

Ebert, L. M., S. Meuter and B. Moser (2006). "Homing and function of human skin gammadelta T cells and NK cells: relevance for tumor surveillance." J Immunol **176**(7): 4331-4336.

Egerton, M., R. Scollay and K. Shortman (1990). "Kinetics of mature T-cell development in the thymus." Proc Natl Acad Sci U S A **87**(7): 2579-2582.

El Andaloussi, A., S. Graves, F. Meng, M. Mandal, M. Mashayekhi and I. Aifantis (2006). "Hedgehog signaling controls thymocyte progenitor homeostasis and differentiation in the thymus." Nat Immunol **7**(4): 418-426.

Endoh-Yamagami, S., M. Evangelista, D. Wilson, X. Wen, J. W. Theunissen, K. Phamluong, M. Davis, S. J. Scales, M. J. Solloway, F. J. de Sauvage and A. S. Peterson (2009). "The mammalian Cos2 homolog Kif7 plays an essential role in modulating Hh signal transduction during development." Curr Biol **19**(15): 1320-1326.

Fisher, J. P., M. Yan, J. Heuijerjans, L. Carter, A. Abolhassani, J. Frosch, R. Wallace, B. Flutter, A. Capsomidis, M. Hubank, N. Klein, R. Callard, K. Gustafsson and J. Anderson (2014). "Neuroblastoma killing properties of Vdelta2 and Vdelta2-negative gammadeltaT cells following expansion by artificial antigen-presenting cells." Clin Cancer Res **20**(22): 5720-5732.

Furmanski, A. L., J. I. Saldana, N. J. Rowbotham, S. E. Ross and T. Crompton (2012). "Role of Hedgehog signalling at the transition from double-positive to single-positive thymocyte." European journal of immunology **42**(2): 489-499.

Furmanski, A. L., J. I. Saldana, N. J. Rowbotham, S. E. Ross and T. Crompton (2012). "Role of Hedgehog signalling at the transition from double-positive to single-positive thymocyte." Eur J Immunol **42**(2): 489-499.

Garbe, A. I., A. Krueger, F. Gounari, J. C. Zuniga-Pflucker and H. von Boehmer (2006). "Differential synergy of Notch and T cell receptor signaling determines alphabeta versus gammadelta lineage fate." The Journal of experimental medicine **203**(6): 1579-1590.

Godfrey, D. I., J. Kennedy, T. Suda and A. Zlotnik (1993). "A developmental pathway involving four phenotypically and functionally distinct subsets of CD3-

CD4-CD8- triple-negative adult mouse thymocytes defined by CD44 and CD25 expression." J Immunol **150**(10): 4244-4252.

Goldrath, A. W. and M. J. Bevan (1999). "Selecting and maintaining a diverse T-cell repertoire." Nature **402**(6759): 255-262.

Goodrich, L. V., R. L. Johnson, L. Milenkovic, J. A. McMahon and M. P. Scott (1996). "Conservation of the hedgehog/patched signaling pathway from flies to mice: induction of a mouse patched gene by Hedgehog." Genes Dev **10**(3): 301-312.

Gorlin, R. J. (1995). "Nevoid basal cell carcinoma syndrome." Dermatol Clin **13**(1): 113-125.

Groh, V., R. Rhinehart, H. Secrist, S. Bauer, K. H. Grabstein and T. Spies (1999). "Broad tumor-associated expression and recognition by tumor-derived gamma delta T cells of MICA and MICB." Proc Natl Acad Sci U S A **96**(12): 6879-6884.

Haas, J. D., F. H. Gonzalez, S. Schmitz, V. Chennupati, L. Fohse, E. Kremmer, R. Forster and I. Prinz (2009). "CCR6 and NK1.1 distinguish between IL-17A and IFN-gamma-producing gammadelta effector T cells." European journal of immunology **39**(12): 3488-3497.

Haas, J. D., S. Ravens, S. Duber, I. Sandrock, L. Oberdorfer, E. Kashani, V. Chennupati, L. Fohse, R. Naumann, S. Weiss, A. Krueger, R. Forster and I. Prinz (2012). "Development of interleukin-17-producing gammadelta T cells is restricted to a functional embryonic wave." Immunity **37**(1): 48-59.

Hager-Theodorides, A. L., J. T. Dessens, S. V. Outram and T. Crompton (2005). "The transcription factor Gli3 regulates differentiation of fetal CD4- CD8- double-negative thymocytes." Blood **106**(4): 1296-1304.

Haks, M. C., J. M. Lefebvre, J. P. Lauritsen, M. Carleton, M. Rhodes, T. Miyazaki, D. J. Kappes and D. L. Wiest (2005). "Attenuation of gammadeltaTCR signaling efficiently diverts thymocytes to the alphabeta lineage." Immunity **22**(5): 595-606.

Harfe, B. D., P. J. Scherz, S. Nissim, H. Tian, A. P. McMahon and C. J. Tabin (2004). "Evidence for an expansion-based temporal Shh gradient in specifying vertebrate digit identities." Cell **118**(4): 517-528.

Hathcock, K. S., G. Laszlo, H. B. Dickler, J. Bradshaw, P. Linsley and R. J. Hodes (1993). "Identification of an alternative CTLA-4 ligand costimulatory for T cell activation." Science **262**(5135): 905-907.

Hayday, A. and D. Gibbons (2008). "Brokering the peace: the origin of intestinal T cells." Mucosal Immunol **1**(3): 172-174.

Hayday, A., E. Theodoridis, E. Ramsburg and J. Shires (2001). "Intraepithelial lymphocytes: exploring the Third Way in immunology." Nat Immunol **2**(11): 997-1003.

Hayday, A. C. (2000). "[gamma][delta] cells: a right time and a right place for a conserved third way of protection." Annual review of immunology **18**: 975-1026.

Hayday, A. C. (2009). "Gammadelta T cells and the lymphoid stress-surveillance response." Immunity **31**(2): 184-196.

Hayes, S. M., L. Li and P. E. Love (2005). "TCR signal strength influences alphabeta/gammadelta lineage fate." Immunity **22**(5): 583-593.

He, M., R. Subramanian, F. Bangs, T. Omelchenko, K. F. Liem, Jr., T. M. Kapoor and K. V. Anderson (2014). "The kinesin-4 protein Kif7 regulates mammalian Hedgehog signalling by organizing the cilium tip compartment." Nat Cell Biol **16**(7): 663-672.

Himoudi, N., D. A. Morgenstern, M. Yan, B. Vernay, L. Saraiva, Y. Wu, C. J. Cohen, K. Gustafsson and J. Anderson (2012). "Human gammadelta T lymphocytes are licensed for professional antigen presentation by interaction with opsonized target cells." J Immunol **188**(4): 1708-1716.

Hough, M. R., F. Takei, R. K. Humphries and R. Kay (1994). "Defective development of thymocytes overexpressing the costimulatory molecule, heat-stable antigen." J Exp Med **179**(1): 177-184.

Hui, C. C. and A. L. Joyner (1993). "A mouse model of greig cephalopolysyndactyly syndrome: the extra-toesJ mutation contains an intragenic deletion of the Gli3 gene." Nat Genet **3**(3): 241-246.

Hviid, L., B. D. Akanmori, S. Loizon, J. A. Kurtzhals, C. H. Ricke, A. Lim, K. A. Koram, F. K. Nkrumah, O. Mercereau-Puijalon and C. Behr (2000). "High frequency of circulating gamma delta T cells with dominance of the v(delta)1 subset in a healthy population." Int Immunol **12**(6): 797-805.

Hviid, L., J. A. Kurtzhals, V. Adabayeri, S. Loizon, K. Kemp, B. Q. Goka, A. Lim, O. Mercereau-Puijalon, B. D. Akanmori and C. Behr (2001). "Perturbation and proinflammatory type activation of V delta 1(+) gamma delta T cells in African children with Plasmodium falciparum malaria." Infect Immun **69**(5): 3190-3196.

Ingham, P. W. and A. P. McMahon (2001). "Hedgehog signaling in animal development: paradigms and principles." Genes Dev **15**(23): 3059-3087.

Irvine, D. J., M. A. Purbhoo, M. Krogsgaard and M. M. Davis (2002). "Direct observation of ligand recognition by T cells." Nature **419**(6909): 845-849.

Irving, B. A., F. W. Alt and N. Killeen (1998). "Thymocyte development in the absence of pre-T cell receptor extracellular immunoglobulin domains." Science **280**(5365): 905-908.

Itano, A., D. Kioussis and E. Robey (1994). "Stochastic component to development of class I major histocompatibility complex-specific T cells." Proc Natl Acad Sci U S A **91**(1): 220-224.

Jameson, S. C., K. A. Hogquist and M. J. Bevan (1995). "Positive selection of thymocytes." Annu Rev Immunol **13**: 93-126.

Jensen, K. D., X. Su, S. Shin, L. Li, S. Youssef, S. Yamasaki, L. Steinman, T. Saito, R. M. Locksley, M. M. Davis, N. Baumgarth and Y. H. Chien (2008). "Thymic selection determines gammadelta T cell effector fate: antigen-naive cells make interleukin-17 and antigen-experienced cells make interferon gamma." Immunity **29**(1): 90-100.

Jiang, J. and C. C. Hui (2008). "Hedgehog signaling in development and cancer." Developmental cell **15**(6): 801-812.

Jotereau, F., F. Heuze, V. Salomon-Vie and H. Gascan (1987). "Cell kinetics in the fetal mouse thymus: precursor cell input, proliferation, and emigration." J Immunol **138**(4): 1026-1030.

June, C. H., J. A. Bluestone, L. M. Nadler and C. B. Thompson (1994). "The B7 and CD28 receptor families." Immunol Today **15**(7): 321-331.

Kang, J., A. Volkmann and D. H. Raulet (2001). "Evidence that gammadelta versus alphabeta T cell fate determination is initiated independently of T cell receptor signaling." The Journal of experimental medicine **193**(6): 689-698.

Karhadkar, S. S., G. S. Bova, N. Abdallah, S. Dhara, D. Gardner, A. Maitra, J. T. Isaacs, D. M. Berman and P. A. Beachy (2004). "Hedgehog signalling in prostate regeneration, neoplasia and metastasis." Nature **431**(7009): 707-712.

Kawamoto, H., H. Wada and Y. Katsura (2010). "A revised scheme for developmental pathways of hematopoietic cells: the myeloid-based model." Int Immunol **22**(2): 65-70.

Kindt T, G. R. (2007b). T Cell Maturation, Activation and Differentiation. Kuby Immunology W.H. Freeman and Company**:** p. 245-266.

Kisielow, P., H. Bluthmann, U. D. Staerz, M. Steinmetz and H. von Boehmer (1988). "Tolerance in T-cell-receptor transgenic mice involves deletion of nonmature CD4+8+ thymocytes." Nature **333**(6175): 742-746.

Kisielow, P., H. S. Teh, H. Bluthmann and H. von Boehmer (1988). "Positive selection of antigen-specific T cells in thymus by restricting MHC molecules." Nature **335**(6192): 730-733.

Kogawa, K., S. Nagafuchi, H. Katsuta, J. Kudoh, S. Tamiya, Y. Sakai, N. Shimizu and M. Harada (2002). "Expression of AIRE gene in peripheral monocyte/dendritic cell lineage." Immunol Lett **80**(3): 195-198.

Kondo, M., T. Izumi, N. Fujieda, A. Kondo, T. Morishita, H. Matsushita and K. Kakimi (2011). "Expansion of human peripheral blood gammadelta T cells using zoledronate." J Vis Exp(55).

Korn, T., E. Bettelli, M. Oukka and V. K. Kuchroo (2009). "IL-17 and Th17 Cells." Annu Rev Immunol **27**: 485-517.

Lake, J. P., C. W. Pierce and J. D. Kennedy (1991). "CD8+ alpha/beta or gamma/delta T cell receptor-bearing T cells from athymic nude mice are cytolytically active in vivo." Journal of immunology **147**(4): 1121-1126.

Laky, K., L. Lefrancois, E. G. Lingenheld, H. Ishikawa, J. M. Lewis, S. Olson, K. Suzuki, R. E. Tigelaar and L. Puddington (2000). "Enterocyte expression of interleukin 7 induces development of gammadelta T cells and Peyer's patches." J Exp Med **191**(9): 1569-1580.

Lau, C. I., S. V. Outram, J. I. Saldana, A. L. Furmanski, J. T. Dessens and T. Crompton (2012). "Regulation of murine normal and stress-induced erythropoiesis by Desert Hedgehog." Blood **119**(20): 4741-4751.

Lees, R. K., I. Ferrero and H. R. MacDonald (2001). "Tissue-specific segregation of TCRgamma delta+ NKT cells according to phenotype TCR repertoire and activation status: parallels with TCR alphabeta+NKT cells." Eur J Immunol **31**(10): 2901-2909.

Leung, R. K., K. Thomson, A. Gallimore, E. Jones, M. Van den Broek, S. Sierro, A. R. Alsheikhly, A. McMichael and A. Rahemtulla (2001). "Deletion of the CD4 silencer

element supports a stochastic mechanism of thymocyte lineage commitment." Nat Immunol **2**(12): 1167-1173.

Li, O., P. Zheng and Y. Liu (2004). "CD24 expression on T cells is required for optimal T cell proliferation in lymphopenic host." J Exp Med **200**(8): 1083-1089.

Linsley, P. S., W. Brady, M. Urnes, L. S. Grosmaire, N. K. Damle and J. A. Ledbetter (1991). "CTLA-4 is a second receptor for the B cell activation antigen B7." J Exp Med **174**(3): 561-569.

Liston, A., S. Lesage, J. Wilson, L. Peltonen and C. C. Goodnow (2003). "Aire regulates negative selection of organ-specific T cells." Nat Immunol **4**(4): 350-354.

Lockhart, E., A. M. Green and J. L. Flynn (2006). "IL-17 production is dominated by gammadelta T cells rather than CD4 T cells during Mycobacterium tuberculosis infection." Journal of immunology **177**(7): 4662-4669.

MacDonald, H. R., R. C. Budd and R. C. Howe (1988). "A CD3- subset of CD4-8+ thymocytes: a rapidly cycling intermediate in the generation of CD4+8+ cells." Eur J Immunol **18**(4): 519-523.

Maeurer, M. J., D. Martin, W. Walter, K. Liu, L. Zitvogel, K. Halusczcak, H. Rabinowich, R. Duquesnoy, W. Storkus and M. T. Lotze (1996). "Human intestinal Vdelta1+ lymphocytes recognize tumor cells of epithelial origin." J Exp Med **183**(4): 1681-1696.

Mallick, C. A., E. C. Dudley, J. L. Viney, M. J. Owen and A. C. Hayday (1993). "Rearrangement and diversity of T cell receptor beta chain genes in thymocytes: a critical role for the beta chain in development." Cell **73**(3): 513-519.

Mallis, R. J., K. Bai, H. Arthanari, R. E. Hussey, M. Handley, Z. Li, L. Chingozha, J. S. Duke-Cohan, H. Lu, J. H. Wang, C. Zhu, G. Wagner and E. L. Reinherz (2015). "Pre-TCR ligand binding impacts thymocyte development before alphabetaTCR expression." Proc Natl Acad Sci U S A **112**(27): 8373-8378.

Marigo, V., R. L. Johnson, A. Vortkamp and C. J. Tabin (1996). "Sonic hedgehog differentially regulates expression of GLI and GLI3 during limb development." Dev Biol **180**(1): 273-283.

Markiewicz, M. A., C. Girao, J. T. Opferman, J. Sun, Q. Hu, A. A. Agulnik, C. E. Bishop, C. B. Thompson and P. G. Ashton-Rickardt (1998). "Long-term T cell memory

requires the surface expression of self-peptide/major histocompatibility complex molecules." Proc Natl Acad Sci U S A **95**(6): 3065-3070.

Martin, B., K. Hirota, D. J. Cua, B. Stockinger and M. Veldhoen (2009). "Interleukin-17-producing gammadelta T cells selectively expand in response to pathogen products and environmental signals." Immunity **31**(2): 321-330.

Matise, M. P. and A. L. Joyner (1999). "Gli genes in development and cancer." Oncogene **18**(55): 7852-7859.

McVay, L. D. and S. R. Carding (1996). "Extrathymic origin of human gamma delta T cells during fetal development." J Immunol **157**(7): 2873-2882.

Melichar, H. and J. Kang (2007). "Integrated morphogen signal inputs in gammadelta versus alphabeta T-cell differentiation." Immunol Rev **215**: 32-45.

Melichar, H. J., K. Narayan, S. D. Der, Y. Hiraoka, N. Gardiol, G. Jeannet, W. Held, C. A. Chambers and J. Kang (2007). "Regulation of gammadelta versus alphabeta T lymphocyte differentiation by the transcription factor SOX13." Science **315**(5809): 230-233.

Meneghin, A. and C. M. Hogaboam (2007). "Infectious disease, the innate immune response, and fibrosis." J Clin Invest **117**(3): 530-538.

Michel, M. L., D. J. Pang, S. F. Haque, A. J. Potocnik, D. J. Pennington and A. C. Hayday (2012). "Interleukin 7 (IL-7) selectively promotes mouse and human IL-17-producing gammadelta cells." Proc Natl Acad Sci U S A **109**(43): 17549-17554.

Mo, R., A. M. Freer, D. L. Zinyk, M. A. Crackower, J. Michaud, H. H. Heng, K. W. Chik, X. M. Shi, L. C. Tsui, S. H. Cheng, A. L. Joyner and C. Hui (1997). "Specific and redundant functions of Gli2 and Gli3 zinc finger genes in skeletal patterning and development." Development **124**(1): 113-123.

Mombaerts, P., J. Iacomini, R. S. Johnson, K. Herrup, S. Tonegawa and V. E. Papaioannou (1992). "RAG-1-deficient mice have no mature B and T lymphocytes." Cell **68**(5): 869-877.

Moore, T. A. and A. Zlotnik (1995). "T-cell lineage commitment and cytokine responses of thymic progenitors." Blood **86**(5): 1850-1860.

Morita, C. T., E. M. Beckman, J. F. Bukowski, Y. Tanaka, H. Band, B. R. Bloom, D. E. Golan and M. B. Brenner (1995). "Direct presentation of nonpeptide prenyl

pyrophosphate antigens to human gamma delta T cells." Immunity **3**(4): 495-507.

Morita, C. T., C. Jin, G. Sarikonda and H. Wang (2007). "Nonpeptide antigens, presentation mechanisms, and immunological memory of human Vgamma2Vdelta2 T cells: discriminating friend from foe through the recognition of prenyl pyrophosphate antigens." Immunol Rev **215**: 59-76.

Motoyama, J., T. Takabatake, K. Takeshima and C. Hui (1998). "Ptch2, a second mouse Patched gene is co-expressed with Sonic hedgehog." Nat Genet **18**(2): 104-106.

Nusslein-Volhard, C. and E. Wieschaus (1980). "Mutations affecting segment number and polarity in Drosophila." Nature **287**(5785): 795-801.

O'Brien, R. L. and W. K. Born (2015). "Dermal gammadelta T cells - What have we learned?" Cell Immunol.

O'Brien, R. L., M. P. Happ, A. Dallas, E. Palmer, R. Kubo and W. K. Born (1989). "Stimulation of a major subset of lymphocytes expressing T cell receptor gamma delta by an antigen derived from Mycobacterium tuberculosis." Cell **57**(4): 667-674.

Oettinger, M. A., D. G. Schatz, C. Gorka and D. Baltimore (1990). "RAG-1 and RAG-2, adjacent genes that synergistically activate V(D)J recombination." Science **248**(4962): 1517-1523.

Ohga, S., Y. Yoshikai, Y. Takeda, K. Hiromatsu and K. Nomoto (1990). "Sequential appearance of gamma/delta- and alpha/beta-bearing T cells in the peritoneal cavity during an i.p. infection with Listeria monocytogenes." European journal of immunology **20**(3): 533-538.

Ohteki, T., A. Wilson, S. Verbeek, H. R. MacDonald and H. Clevers (1996). "Selectively impaired development of intestinal T cell receptor gamma delta+ cells and liver CD4+ NK1+ T cell receptor alpha beta+ cells in T cell factor-1-deficient mice." Eur J Immunol **26**(2): 351-355.

Outram, S. V., A. L. Hager-Theodorides, D. K. Shah, N. J. Rowbotham, E. Drakopoulou, S. E. Ross, B. Lanske, J. T. Dessens and T. Crompton (2009). "Indian hedgehog (Ihh) both promotes and restricts thymocyte differentiation." Blood **113**(10): 2217-2228.

Outram, S. V., A. Varas, C. V. Pepicelli and T. Crompton (2000). "Hedgehog signaling regulates differentiation from double-negative to double-positive thymocyte." Immunity **13**(2): 187-197.

Pan, Y., C. Wang and B. Wang (2009). "Phosphorylation of Gli2 by protein kinase A is required for Gli2 processing and degradation and the Sonic Hedgehog-regulated mouse development." Dev Biol **326**(1): 177-189.

Pang, D. J., J. F. Neves, N. Sumaria and D. J. Pennington (2012). "Understanding the complexity of gammadelta T-cell subsets in mouse and human." Immunology **136**(3): 283-290.

Park, H. L., C. Bai, K. A. Platt, M. P. Matise, A. Beeghly, C. C. Hui, M. Nakashima and A. L. Joyner (2000). "Mouse Gli1 mutants are viable but have defects in SHH signaling in combination with a Gli2 mutation." Development **127**(8): 1593-1605.

Parker, C. M., V. Groh, H. Band, S. A. Porcelli, C. Morita, M. Fabbi, D. Glass, J. L. Strominger and M. B. Brenner (1990). "Evidence for extrathymic changes in the T cell receptor gamma/delta repertoire." J Exp Med **171**(5): 1597-1612.

Parmantier, E., B. Lynn, D. Lawson, M. Turmaine, S. S. Namini, L. Chakrabarti, A. P. McMahon, K. R. Jessen and R. Mirsky (1999). "Schwann cell-derived Desert hedgehog controls the development of peripheral nerve sheaths." Neuron **23**(4): 713-724.

Pellicci, D. G., A. P. Uldrich, J. Le Nours, F. Ross, E. Chabrol, S. B. Eckle, R. de Boer, R. T. Lim, K. McPherson, G. Besra, A. R. Howell, L. Moretta, J. McCluskey, M. H. Heemskerk, S. Gras, J. Rossjohn and D. I. Godfrey (2014). "The molecular bases of delta/alphabeta T cell-mediated antigen recognition." J Exp Med **211**(13): 2599-2615.

Perumal, N. B., T. W. Kenniston, Jr., D. J. Tweardy, K. F. Dyer, R. Hoffman, J. Peschon and P. M. Appasamy (1997). "TCR-gamma genes are rearranged but not transcribed in IL-7R alpha-deficient mice." J Immunol **158**(12): 5744-5750.

Petrie, H. T., M. Pearse, R. Scollay and K. Shortman (1990). "Development of immature thymocytes: initiation of CD3, CD4, and CD8 acquisition parallels down-regulation of the interleukin 2 receptor alpha chain." Eur J Immunol **20**(12): 2813-2815.

Petrie, H. T. and J. C. Zuniga-Pflucker (2007). "Zoned out: functional mapping of stromal signaling microenvironments in the thymus." Annu Rev Immunol **25**: 649-679.

Price, M. A. and D. Kalderon (2002). "Proteolysis of the Hedgehog signaling effector Cubitus interruptus requires phosphorylation by Glycogen Synthase Kinase 3 and Casein Kinase 1." Cell **108**(6): 823-835.

Prinz, I., A. Sansoni, A. Kissenpfennig, L. Ardouin, M. Malissen and B. Malissen (2006). "Visualization of the earliest steps of gammadelta T cell development in the adult thymus." Nature immunology **7**(9): 995-1003.

Prinz, I., B. Silva-Santos and D. J. Pennington (2013). "Functional development of gammadelta T cells." Eur J Immunol **43**(8): 1988-1994.

Prockop, S. and H. T. Petrie (2000). "Cell migration and the anatomic control of thymocyte precursor differentiation." Semin Immunol **12**(5): 435-444.

Qureshi, M. H., T. Zhang, Y. Koguchi, K. Nakashima, H. Okamura, M. Kurimoto and K. Kawakami (1999). "Combined effects of IL-12 and IL-18 on the clinical course and local cytokine production in murine pulmonary infection with Cryptococcus neoformans." European journal of immunology **29**(2): 643-649.

Razzaque, M. S., D. W. Soegiarto, D. Chang, F. Long and B. Lanske (2005). "Conditional deletion of Indian hedgehog from collagen type 2alpha1-expressing cells results in abnormal endochondral bone formation." J Pathol **207**(4): 453-461.

Regl, G., G. W. Neill, T. Eichberger, M. Kasper, M. S. Ikram, J. Koller, H. Hintner, A. G. Quinn, A. M. Frischauf and F. Aberger (2002). "Human GLI2 and GLI1 are part of a positive feedback mechanism in Basal Cell Carcinoma." Oncogene **21**(36): 5529-5539.

Ribot, J. C., M. Chaves-Ferreira, F. d'Orey, M. Wencker, N. Goncalves-Sousa, J. Decalf, J. P. Simas, A. C. Hayday and B. Silva-Santos (2010). "Cutting edge: adaptive versus innate receptor signals selectively control the pool sizes of murine IFN-gamma- or IL-17-producing gammadelta T cells upon infection." J Immunol **185**(11): 6421-6425.

Ribot, J. C., A. deBarros, D. J. Pang, J. F. Neves, V. Peperzak, S. J. Roberts, M. Girardi, J. Borst, A. C. Hayday, D. J. Pennington and B. Silva-Santos (2009). "CD27 is a

thymic determinant of the balance between interferon-gamma- and interleukin 17-producing gammadelta T cell subsets." Nature immunology **10**(4): 427-436.

Robey, E. and B. J. Fowlkes (1994). "Selective events in T cell development." Annu Rev Immunol **12**: 675-705.

Robey, E. A., B. J. Fowlkes, J. W. Gordon, D. Kioussis, H. von Boehmer, F. Ramsdell and R. Axel (1991). "Thymic selection in CD8 transgenic mice supports an instructive model for commitment to a CD4 or CD8 lineage." Cell **64**(1): 99-107.

Roessler, E., Y. Z. Du, J. L. Mullor, E. Casas, W. P. Allen, G. Gillessen-Kaesbach, E. R. Roeder, J. E. Ming, A. Ruiz i Altaba and M. Muenke (2003). "Loss-of-function mutations in the human GLI2 gene are associated with pituitary anomalies and holoprosencephaly-like features." Proc Natl Acad Sci U S A **100**(23): 13424-13429.

Rowbotham, N. J., A. L. Furmanski, A. L. Hager-Theodorides, S. E. Ross, E. Drakopoulou, C. Koufaris, S. V. Outram and T. Crompton (2008). "Repression of hedgehog signal transduction in T-lineage cells increases TCR-induced activation and proliferation." Cell cycle **7**(7): 904-908.

Rowbotham, N. J., A. L. Hager-Theodorides, M. Cebecauer, D. K. Shah, E. Drakopoulou, J. Dyson, S. V. Outram and T. Crompton (2007). "Activation of the Hedgehog signaling pathway in T-lineage cells inhibits TCR repertoire selection in the thymus and peripheral T-cell activation." Blood **109**(9): 3757-3766.

Rowbotham, N. J., A. L. Hager-Theodorides, A. L. Furmanski, S. E. Ross, S. V. Outram, J. T. Dessens and T. Crompton (2009). "Sonic hedgehog negatively regulates pre-TCR-induced differentiation by a Gli2-dependent mechanism." Blood **113**(21): 5144-5156.

Russano, A. M., G. Bassotti, E. Agea, O. Bistoni, A. Mazzocchi, A. Morelli, S. A. Porcelli and F. Spinozzi (2007). "CD1-restricted recognition of exogenous and self-lipid antigens by duodenal gammadelta+ T lymphocytes." J Immunol **178**(6): 3620-3626.

Sacedon, R., A. Varas, C. Hernandez-Lopez, C. Gutierrez-deFrias, T. Crompton, A. G. Zapata and A. Vicente (2003). "Expression of hedgehog proteins in the human thymus." J Histochem Cytochem **51**(11): 1557-1566.

Saito, H., D. M. Kranz, Y. Takagaki, A. C. Hayday, H. N. Eisen and S. Tonegawa (1984). "A third rearranged and expressed gene in a clone of cytotoxic T lymphocytes." Nature **312**(5989): 36-40.

Saldana, J. I., A. Solanki, C. I. Lau, H. Sahni, S. Ross, A. L. Furmanski, M. Ono, G. Hollander and T. Crompton (2016). "Sonic Hedgehog regulates thymic epithelial cell differentiation." J Autoimmun.

Sasaki, H., Y. Nishizaki, C. Hui, M. Nakafuku and H. Kondoh (1999). "Regulation of Gli2 and Gli3 activities by an amino-terminal repression domain: implication of Gli2 and Gli3 as primary mediators of Shh signaling." Development **126**(17): 3915-3924.

Satyanarayana, K., S. Hata, P. Devlin, M. G. Roncarolo, J. E. De Vries, H. Spits, J. L. Strominger and M. S. Krangel (1988). "Genomic organization of the human T-cell antigen-receptor alpha/delta locus." Proceedings of the National Academy of Sciences of the United States of America **85**(21): 8166-8170.

Satyanarayana, K., S. Hata, P. Devlin, M. G. Roncarolo, J. E. De Vries, H. Spits, J. L. Strominger and M. S. Krangel (1988). "Genomic organization of the human T-cell antigen-receptor alpha/delta locus." Proc Natl Acad Sci U S A **85**(21): 8166-8170.

Schimmang, T., M. Lemaistre, A. Vortkamp and U. Ruther (1992). "Expression of the zinc finger gene Gli3 is affected in the morphogenetic mouse mutant extra-toes (Xt)." Development **116**(3): 799-804.

Sciammas, R., R. M. Johnson, A. I. Sperling, W. Brady, P. S. Linsley, P. G. Spear, F. W. Fitch and J. A. Bluestone (1994). "Unique antigen recognition by a herpesvirus-specific TCR-gamma delta cell." Journal of immunology **152**(11): 5392-5397.

Scollay, R., J. Smith and V. Stauffer (1986). "Dynamics of early T cells: prothymocyte migration and proliferation in the adult mouse thymus." Immunol Rev **91**: 129-157.

Shah, D. K., A. L. Hager-Theodorides, S. V. Outram, S. E. Ross, A. Varas and T. Crompton (2004). "Reduced thymocyte development in sonic hedgehog knockout embryos." Journal of immunology **172**(4): 2296-2306.

Shibata, K., H. Yamada, M. Nakamura, S. Hatano, Y. Katsuragi, R. Kominami and Y. Yoshikai (2014). "IFN-gamma-producing and IL-17-producing gammadelta T

cells differentiate at distinct developmental stages in murine fetal thymus." J Immunol **192**(5): 2210-2218.

Shimeld, S. M. (1999). "The evolution of the hedgehog gene family in chordates: insights from amphioxus hedgehog." Dev Genes Evol **209**(1): 40-47.

Shinkai, Y. and F. W. Alt (1994). "CD3 epsilon-mediated signals rescue the development of CD4+CD8+ thymocytes in RAG-2-/- mice in the absence of TCR beta chain expression." Int Immunol **6**(7): 995-1001.

Shinkai, Y., G. Rathbun, K. P. Lam, E. M. Oltz, V. Stewart, M. Mendelsohn, J. Charron, M. Datta, F. Young, A. M. Stall and et al. (1992). "RAG-2-deficient mice lack mature lymphocytes owing to inability to initiate V(D)J rearrangement." Cell **68**(5): 855-867.

Silva-Santos, B., K. Serre and H. Norell (2015). "gammadelta T cells in cancer." Nat Rev Immunol **15**(11): 683-691.

Sinclair, C., I. Bains, A. J. Yates and B. Seddon (2013). "Asymmetric thymocyte death underlies the CD4:CD8 T-cell ratio in the adaptive immune system." Proc Natl Acad Sci U S A **110**(31): E2905-2914.

Singer, A., S. Adoro and J. H. Park (2008). "Lineage fate and intense debate: myths, models and mechanisms of CD4- versus CD8-lineage choice." Nat Rev Immunol **8**(10): 788-801.

Sisson, J. C., K. S. Ho, K. Suyama and M. P. Scott (1997). "Costal2, a novel kinesin-related protein in the Hedgehog signaling pathway." Cell **90**(2): 235-245.

Srivastava, M., O. Simakov, J. Chapman, B. Fahey, M. E. Gauthier, T. Mitros, G. S. Richards, C. Conaco, M. Dacre, U. Hellsten, C. Larroux, N. H. Putnam, M. Stanke, M. Adamska, A. Darling, S. M. Degnan, T. H. Oakley, D. C. Plachetzki, Y. Zhai, M. Adamski, A. Calcino, S. F. Cummins, D. M. Goodstein, C. Harris, D. J. Jackson, S. P. Leys, S. Shu, B. J. Woodcroft, M. Vervoort, K. S. Kosik, G. Manning, B. M. Degnan and D. S. Rokhsar (2010). "The Amphimedon queenslandica genome and the evolution of animal complexity." Nature **466**(7307): 720-726.

St-Jacques, B., M. Hammerschmidt and A. P. McMahon (1999). "Indian hedgehog signaling regulates proliferation and differentiation of chondrocytes and is essential for bone formation." Genes & development **13**(16): 2072-2086.

St-Jacques, B., M. Hammerschmidt and A. P. McMahon (1999). "Indian hedgehog signaling regulates proliferation and differentiation of chondrocytes and is essential for bone formation." Genes Dev **13**(16): 2072-2086.

Stamataki, D., F. Ulloa, S. V. Tsoni, A. Mynett and J. Briscoe (2005). "A gradient of Gli activity mediates graded Sonic Hedgehog signaling in the neural tube." Genes & development **19**(5): 626-641.

Stewart, C. A., T. Walzer, S. H. Robbins, B. Malissen, E. Vivier and I. Prinz (2007). "Germ-line and rearranged Tcrd transcription distinguish bona fide NK cells and NK-like gammadelta T cells." European journal of immunology **37**(6): 1442-1452.

Stone, D. M., M. Hynes, M. Armanini, T. A. Swanson, Q. Gu, R. L. Johnson, M. P. Scott, D. Pennica, A. Goddard, H. Phillips, M. Noll, J. E. Hooper, F. de Sauvage and A. Rosenthal (1996). "The tumour-suppressor gene patched encodes a candidate receptor for Sonic hedgehog." Nature **384**(6605): 129-134.

Strauss, W. M., T. Quertermous and J. G. Seidman (1987). "Measuring the human T cell receptor gamma-chain locus." Science **237**(4819): 1217-1219.

Strominger, J. L. (1989). "Developmental biology of T cell receptors." Science **244**(4907): 943-950.

Strominger, J. L. (1989). "The gamma delta T cell receptor and class Ib MHC-related proteins: enigmatic molecules of immune recognition." Cell **57**(6): 895-898.

Sumaria, N., B. Roediger, L. G. Ng, J. Qin, R. Pinto, L. L. Cavanagh, E. Shklovskaya, B. Fazekas de St Groth, J. A. Triccas and W. Weninger (2011). "Cutaneous immunosurveillance by self-renewing dermal gammadelta T cells." J Exp Med **208**(3): 505-518.

Takahama, Y. (2006). "Journey through the thymus: stromal guides for T-cell development and selection." Nature reviews. Immunology **6**(2): 127-135.

Tanaka, Y., C. T. Morita, Y. Tanaka, E. Nieves, M. B. Brenner and B. R. Bloom (1995). "Natural and synthetic non-peptide antigens recognized by human gamma delta T cells." Nature **375**(6527): 155-158.

Tanaka, Y., S. Sano, E. Nieves, G. De Libero, D. Rosa, R. L. Modlin, M. B. Brenner, B. R. Bloom and C. T. Morita (1994). "Nonpeptide ligands for human gamma delta T

cells." Proceedings of the National Academy of Sciences of the United States of America **91**(17): 8175-8179.

Tanimura, A., S. Dan and M. Yoshida (1998). "Cloning of novel isoforms of the human Gli2 oncogene and their activities to enhance tax-dependent transcription of the human T-cell leukemia virus type 1 genome." J Virol **72**(5): 3958-3964.

te Welscher, P., A. Zuniga, S. Kuijper, T. Drenth, H. J. Goedemans, F. Meijlink and R. Zeller (2002). "Progression of vertebrate limb development through SHH-mediated counteraction of GLI3." Science **298**(5594): 827-830.

Tempe, D., M. Casas, S. Karaz, M. F. Blanchet-Tournier and J. P. Concordet (2006). "Multisite protein kinase A and glycogen synthase kinase 3beta phosphorylation leads to Gli3 ubiquitination by SCFbetaTrCP." Mol Cell Biol **26**(11): 4316-4326.

Thayer, S. P., M. P. di Magliano, P. W. Heiser, C. M. Nielsen, D. J. Roberts, G. Y. Lauwers, Y. P. Qi, S. Gysin, C. Fernandez-del Castillo, V. Yajnik, B. Antoniu, M. McMahon, A. L. Warshaw and M. Hebrok (2003). "Hedgehog is an early and late mediator of pancreatic cancer tumorigenesis." Nature **425**(6960): 851-856.

Tough, D. F. and J. Sprent (1998). "Lifespan of gamma/delta T cells." J Exp Med **187**(3): 357-365.

Traxlmayr, M. W., D. Wesch, A. M. Dohnal, P. Funovics, M. B. Fischer, D. Kabelitz and T. Felzmann (2010). "Immune suppression by gammadelta T-cells as a potential regulatory mechanism after cancer vaccination with IL-12 secreting dendritic cells." Journal of immunotherapy **33**(1): 40-52.

Van de Walle, I., G. De Smet, M. De Smedt, B. Vandekerckhove, G. Leclercq, J. Plum and T. Taghon (2009). "An early decrease in Notch activation is required for human TCR-alphabeta lineage differentiation at the expense of TCR-gammadelta T cells." Blood **113**(13): 2988-2998.

Varjosalo, M. and J. Taipale (2008). "Hedgehog: functions and mechanisms." Genes & development **22**(18): 2454-2472.

Vicari, A. P., S. Mocci, P. Openshaw, A. O'Garra and A. Zlotnik (1996). "Mouse gamma delta TCR+NK1.1+ thymocytes specifically produce interleukin-4, are major histocompatibility complex class I independent, and are developmentally related to alpha beta TCR+NK1.1+ thymocytes." Eur J Immunol **26**(7): 1424-1429.

Virts, E. L., J. A. Phillips and M. L. Thoman (2006). "A novel approach to thymic rejuvenation in the aged." Rejuvenation Res **9**(1): 134-142.

Vortkamp, A., M. Gessler and K. H. Grzeschik (1991). "GLI3 zinc-finger gene interrupted by translocations in Greig syndrome families." Nature **352**(6335): 539-540.

Vortkamp, A., M. Gessler and K. H. Grzeschik (1995). "Identification of optimized target sequences for the GLI3 zinc finger protein." DNA Cell Biol **14**(7): 629-634.

Wang, H., G. Sarikonda, K. J. Puan, Y. Tanaka, J. Feng, J. L. Giner, R. Cao, J. Monkkonen, E. Oldfield and C. T. Morita (2011). "Indirect stimulation of human Vgamma2Vdelta2 T cells through alterations in isoprenoid metabolism." J Immunol **187**(10): 5099-5113.

Washburn, T., E. Schweighoffer, T. Gridley, D. Chang, B. J. Fowlkes, D. Cado and E. Robey (1997). "Notch activity influences the alphabeta versus gammadelta T cell lineage decision." Cell **88**(6): 833-843.

Wen, L., D. F. Barber, W. Pao, F. S. Wong, M. J. Owen and A. Hayday (1998). "Primary gamma delta cell clones can be defined phenotypically and functionally as Th1/Th2 cells and illustrate the association of CD4 with Th2 differentiation." Journal of immunology **160**(4): 1965-1974.

Wesch, D., C. Peters, H. H. Oberg, K. Pietschmann and D. Kabelitz (2011). "Modulation of gammadelta T cell responses by TLR ligands." Cell Mol Life Sci **68**(14): 2357-2370.

Wolter, M., J. Reifenberger, C. Sommer, T. Ruzicka and G. Reifenberger (1997). "Mutations in the human homologue of the Drosophila segment polarity gene patched (PTCH) in sporadic basal cell carcinomas of the skin and primitive neuroectodermal tumors of the central nervous system." Cancer Res **57**(13): 2581-2585.

Wu, L., C. L. Li and K. Shortman (1996). "Thymic dendritic cell precursors: relationship to the T lymphocyte lineage and phenotype of the dendritic cell progeny." J Exp Med **184**(3): 903-911.

Wu, Y., W. Wu, W. M. Wong, E. Ward, A. J. Thrasher, D. Goldblatt, M. Osman, P. Digard, D. H. Canaday and K. Gustafsson (2009). "Human gamma delta T cells: a lymphoid lineage cell capable of professional phagocytosis." J Immunol **183**(9): 5622-5629.

Wucherpfennig, K. W., Y. J. Liao, M. Prendergast, J. Prendergast, D. A. Hafler and J. L. Strominger (1993). "Human fetal liver gamma/delta T cells predominantly use unusual rearrangements of the T cell receptor delta and gamma loci expressed on both CD4+CD8- and CD4-CD8- gamma/delta T cells." The Journal of experimental medicine **177**(2): 425-432.

Yang, Y. and X. Lin (2010). "Hedgehog signaling uses lipid metabolism to tune smoothened activation." Dev Cell **19**(1): 3-4.

Zarin, P., G. W. Wong, M. Mohtashami, D. L. Wiest and J. C. Zuniga-Pflucker (2014). "Enforcement of gammadelta-lineage commitment by the pre-T-cell receptor in precursors with weak gammadelta-TCR signals." Proc Natl Acad Sci U S A **111**(15): 5658-5663.

Zeng, X., Y. L. Wei, J. Huang, E. W. Newell, H. Yu, B. A. Kidd, M. S. Kuhns, R. W. Waters, M. M. Davis, C. T. Weaver and Y. H. Chien (2012). "gammadelta T cells recognize a microbial encoded B cell antigen to initiate a rapid antigen-specific interleukin-17 response." Immunity **37**(3): 524-534.

Zhang, W., Y. Zhao, C. Tong, G. Wang, B. Wang, J. Jia and J. Jiang (2005). "Hedgehog-regulated Costal2-kinase complexes control phosphorylation and proteolytic processing of Cubitus interruptus." Dev Cell **8**(2): 267-278.

Zhao, Y., C. Tong and J. Jiang (2007). "Hedgehog regulates smoothened activity by inducing a conformational switch." Nature **450**(7167): 252-258.

Zuklys, S., J. Gill, M. P. Keller, M. Hauri-Hohl, S. Zhanybekova, G. Balciunaite, K. J. Na, L. T. Jeker, K. Hafen, N. Tsukamoto, T. Amagai, M. M. Taketo, W. Krenger and G. A. Hollander (2009). "Stabilized beta-catenin in thymic epithelial cells blocks thymus development and function." J Immunol **182**(5): 2997-3007.